PAGES 265–384

ISSN 0003–2654

The Analyst

A monthly international journal dealing with all branches of analytical chemistry

Vol. 111 No. 3
March
1986

ROYAL SOCIETY OF CHEMISTRY

The Analyst

The Analytical Journal of The Royal Society of Chemistry

Editorial Office: The Royal Society of Chemistry, Burlington House, Piccadilly, London, W1V 0BN. Telephone 01-734 9864. Telex No. 268001

Advertisements: Advertisement Department, The Royal Society of Chemistry, Burlington House, Piccadilly, London, W1V 0BN. Telephone 01-437 8656. Telex No. 268001

The Analyst (ISSN 0003–2654) is published monthly by The Royal Society of Chemistry, Burlington House, London W1V 0BN, England. All orders accompanied with payment should be sent directly to The Royal Society of Chemistry, The Distribution Centre, Blackhorse Road, Letchworth, Herts. SG6 1HN, England. 1986 Annual subscription rate UK £147.00. Rest of World £162.00, USA $285.00. Purchased with *Analytical Abstracts* UK £329.00, Rest of World £361.00, USA $636.00. Purchased with *Analytical Abstracts* plus *Analytical Proceedings* UK £375.00, Rest of World £412.00, USA $726.00. Purchased with *Analytical Proceedings* UK £184.00, Rest of World £202.00, USA $356.00. Air freight and mailing in the USA by Publications Expediting Inc., 200 Meacham Avenue, Elmont, NY 11003.
USA Postmaster: Send address changes to. *The Analyst*, Publications Expediting Inc., 200 Meacham Avenue, Elmont, NY 11003. Second class postage paid at Jamaica, NY 11431. All other despatches outside the UK by Bulk Airmail within Europe, Accelerated Surface Post outside Europe. PRINTED IN THE UK.

Information for Authors

Full details of how to submit material for publication in *The Analyst* are given in the Instructions to Authors in the January issue. Separate copies are available on request.

The Analyst publishes papers on all aspects of the theory and practice of analytical chemistry, fundamental and applied, inorganic and organic, including chemical, physical and biological methods. There is no page charge.

The following types of papers will be considered:

Full papers, describing original work.

Short papers, also describing original work, but shorter and of limited breadth of subject matter; there will be no difference in the quality of the work described in full and short papers.

Communications, which must be on an urgent matter and be of obvious scientific importance. Rapidity of publication is enhanced if diagrams are omitted, but tables and formulae can be included. Communications should not be simple claims for priority: this facility for rapid publication is intended for brief descriptions of work that has progressed to a stage at which it is likely to be valuable to workers faced with similar problems. A fuller paper may be offered subsequently, if justified by later work.

Reviews, which must be a critical evaluation of the existing state of knowledge on a particular facet of analytical chemistry.

Every paper (except Communications) will be submitted to at least two referees, by whose advice the Editorial Board of *The Analyst* will be guided as to its acceptance or rejection. Papers that are accepted must not be published elsewhere except by permission. Submission of a manuscript will be regarded as an undertaking that the same material is not being considered for publication by another journal.

Regional Advisory Editors. For the benefit of potential contributors outside the United Kingdom, a Panel of Regional Advisory Editors exists. Requests for help or advice on any matter related to the preparation of papers and their submission for publication in *The Analyst* can be sent to the nearest member of the Panel. Currently serving Regional Advisory Editors are listed in each issue of *The Analyst*.

Manuscripts (three copies typed in double spacing) should be addressed to:
The Editor, *The Analyst,*
Royal Society of Chemistry,
Burlington House,
Piccadilly,
LONDON W1V 0BN, UK

Particular attention should be paid to the use of standard methods of literature citation, including the journal abbreviations defined in Chemical Abstracts Service Source Index. Wherever possible, the nomenclature employed should follow IUPAC recommendations, and units and symbols should be those associated with SI.

All queries relating to the presentation and submission of papers, and any correspondence regarding accepted papers and proofs, should be directed to the Editor, *The Analyst* (address as above). Members of the Analytical Editorial Board (who may be contacted directly or via the Editorial Office) would welcome comments, suggestions and advice on general policy matters concerning *The Analyst.*

Fifty reprints of each published contribution are supplied free of charge, and further copies can be purchased.

A202 for further information. See page iv.

Determination of Bromide Using A Helium Microwave Induced Plasma with Bromine Generation and Electrothermal Vaporisation for Sample Introduction

Mohamed M. Abdillahi and Richard D. Snook*
Department of Chemistry, Imperial College, London SW7 2AY, UK

A helium microwave induced plasma is utilised for the determination of bromide. The bromide sample solution is either introduced into an oxidation - generation mixture of potassium dichromate - sulphuric acid, or is vaporised electrothermally and then swept into the helium plasma. The microwave induced plasma (MIP) in a TM_{010} cavity excites bromine and the emission measurements are taken at both the Br II 470.5-nm and 478.6-nm lines. The calibration graphs were linear from 5 ng to 50 μg of bromide using the chemical generation technique at both analytical lines, whereas the calibration data from the graphite rod vaporisation sample introduction technique showed a linearity from 5 ng to 10 μg of bromide. Detection limits for both techniques were 1 ng. Fluorine, chlorine and iodine as well as other common anions and cations do not significantly interfere with the measurements, below 100 times the amount determined.

Keywords: *Bromide determination; helium microwave induced plasma; bromine generation; electrothermal vaporisation*

The determination of bromine by an argon microwave induced plasma (MIP) has been recently reported.[1] A continuation of the work revealed that a helium plasma sustained in a TM_{010} cavity at atmospheric pressure provides a more sensitive method for the determination of bromide. The helium MIP has sufficient energy to excite bromine ion emission because of its high ionisation energy of 24.59 eV.[2] This is illustrated in this work, by the fact that the most intense bromine lines in the visible spectrum are the ionic lines at 470.5 and 478.6 nm. Argon plasmas, on the other hand, are unable to excite these bromine ion lines in either the MIP or inductively coupled plasma (ICP) used in our laboratory. Beenakker[2] has used the TM_{010} cavity for both argon and helium plasmas and concluded that halogen atomic and ionic emission is more easily induced in a helium microwave plasma than in an argon microwave plasma; he reported better detection limits for the halogens in the helium plasma. Carnahan and Caruso[3] reported a detection limit of 8 ng of bromine by measuring the emission at the 478.6-nm ion line in a helium MIP by analysing high relative molecular mass halogenated organic compounds. Van Dalen *et al.*[4] stated that the detection limits for bromine are similar in low and atmospheric pressure microwave induced plasmas and reported detection limits of 0.24 and 0.56 μg ml^{-1} using the 470.5-nm Br II line.

This paper presents a method with better detection limits for determining bromine. Bromine is generated from a potassium dichromate - sulphuric acid mixture, after microlitre aliquots of sample solution are added to the generation apparatus. After sufficient time has elapsed to generate bromine, it is then introduced into the plasma. Alternatively, bromide aliquots can be desolvated and vaporised into the microwave induced plasma using an electrothermal vaporisation device. In both sample introduction techniques, the emission intensities of the Br II 470.5- and 478.6-nm lines were measured.

Experimental

Reagents and Instrumentation

The reagents used for the stock solution and the oxidation - generation mixture were of AnalaR grade (BDH Chemicals Ltd., Poole, Dorset). The oxidation mixture was prepared by dissolving 0.05 g of potassium dichromate in 10 ml of concentrated sulphuric acid. Doubly distilled, de-ionised water (Milli-Q water) was used throughout the experiments for preparing both the stock and working solutions. The helium plasma gas was of high-purity research grade (BOC Ltd., Wembley).

The instrumental set-up is shown in Fig. 1 and is similar to that used previously[1] except that the microwave cavity (EMS, Wantage, Berkshire) is a TM_{010} quarter wave modification of the Beenakker cavity. The helium plasma is supported in a quartz tube (6.4 mm o.d.; 1.7 mm i.d.) in the microwave cavity, which is viewed axially by the monochromator (Optica Model CF 2768). Sample introduction into the helium MIP was achieved by using the chemical generation cell as described previously,[1] or a graphite rod electrothermal vaporisation unit.[5]

Procedure

A 10-μl bromide sample solution was added to the generating mixture through the suba-seal septum.[1] The bromine generated, during 1 min, was swept into the helium plasma and the emission measurements were taken at the 470.5- and 478.6-nm lines.

Alternatively, the emission intensity measurements were taken at those wavelengths, after a 10-μl bromide solution was desolvated, and vaporised electrothermally and then swept directly into the microwave induced plasma. Signal registration was achieved using an EMI 9601B nine-stage photomultiplier tube, the output of which was connected across a 22 kohm load to the input of a JJ Lloyd CR450 chart recorder.

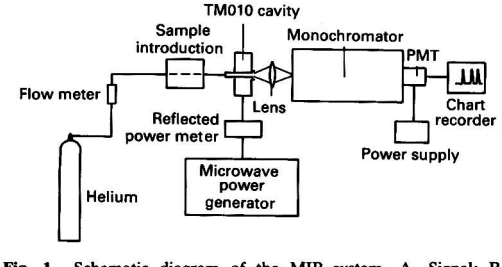

Fig. 1. Schematic diagram of the MIP system. A, Signal; B, background

* Present address: Chelsea Instruments Ltd., 5 Epirus Road, London SW6 7UR.

Results and Discussion

Wavelength Selection

It was found that the Br II 470.5-nm line is twice as intense as the next brightest Br II 478.6-nm line, in agreement with other workers.[6]

Optimisation of the Operating Parameters

The microwave forward power, helium flow-rates, entrance and exit slit widths, photomultiplier voltage, applied voltage to the graphite rod atomiser and the generating solution were optimised using the univariate search method. Using the TM_{010} cavity, the effect of microwave forward power on the emission of Br II lines showed an optimum value of 130 W (Fig. 2). In a previous paper we showed that the argon MIP used for determining bromine[1] required an optimum forward power of 30 W. This fundamental power difference is inherent in the design of the different cavities employed[7] and the nature of the plasma gas used. The physical properties of argon and helium are given in reference 8 (argon: thermal conductivity at 25 °C = 39×10^{-6} cal s^{-1} cm^{-1} $°C^{-1}$, specific heat at 25 °C = 0.13 cal g^{-1}; helium: thermal conductivity at 25 °C = 340×10^{-6} cal s^{-1} cm^{-1} $°C^{-1}$, specific heat at 25 °C = 1.25 cal g^{-1}). The higher thermal conductivity and specific heat mean that helium dissipates more energy and therefore requires higher power to sustain than an argon plasma as was found in the TM_{010} cavity. Varying the helium flow-rates independently of other variables yielded a maximum signal-to-background ratio at 0.43 l min^{-1} (Fig. 3). When the helium plasma gas flow-rate is higher than 0.5 l min^{-1}, the signal to background ratios were gradually reduced and may be attributed to the decrease in residence time of bromine in the plasma, as the intensity of the signal lowers. It was also observed that at lower helium flow-rates, the analyte was not sufficiently swept into the plasma and the peaks tended to be smaller and broader.

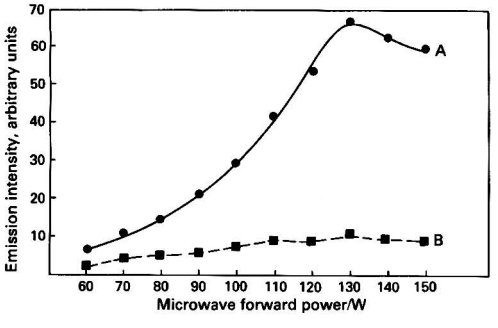

Fig. 2. Effect of microwave forward power on the emission of bromine in a helium MIP. A, Signal; and B, background

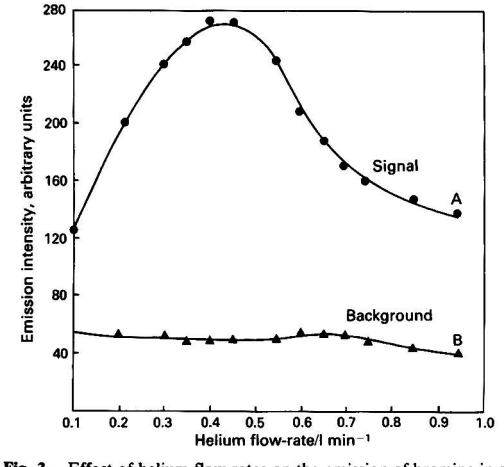

Fig. 3. Effect of helium flow-rates on the emission of bromine in a TM_{010} cavity MIP. A, Signal; and B, background

We have reported[1] that the optimum slit widths for the determination of bromine in an argon plasma using a 3/4 wave Broida cavity was 100 μm. The wide slit widths were used to isolate the molecular (Br_2) band emission, which is much wider than the ionic Br II lines. Optimising the slit widths, an optimum of 10 μm was found for both the entrance and exit slit widths using the Br II 470.5- and 478.6-nm lines. Altering the photomultiplier voltage showed that the best signal-to-background and the highest signal-to-noise ratios were at 1000 V. This differs from the voltage employed in reference 1, because the efficiency of the PMT is worse in the 470–478 nm region than at 291 nm. Optimisation of the generation mixture volume and concentration remain the same as used previously.[1] The bromide sample is being oxidised to bromine and then introduced into the plasma where it is subsequently atomised and excited.

The voltage applied to the graphite rod was varied to determine the optimum peak height for a 10-μl bromide sample solution. Applied voltages of 1 V (60 s), 3 V (5 s) and 8 V (3 s) were found to be the optimum for evaporation, ashing and vaporisation, respectively, of the bromide sample solution before introduction into the helium microwave induced plasma. These are equivalent to temperatures of 105, 300 and 1900 °C, respectively.

Table 1 summarises the optimum conditions.

Table 1. Optimum conditions for the determination of bromide in a helium MIP

Microwave foward power	130 W
Refelected power	0.4 W
Helium flow-rate (generation)	0.43 l min^{-1}
Helium flow-rate (ETV)	0.81 min^{-1}
Entrance and exit slit widths	10 μm
Photomultiplier (EHT)	1000 V
Sample solution volume	10 μl
Wavelengths selected (Br II)	470.5 and 478.6 nm
Graphite rod temperatures:	
Drying	105 °C
Ashing	300 °C
Vaporisation	1900 °C

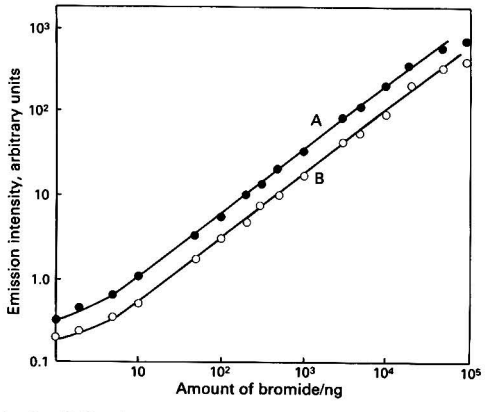

Fig. 4. Calibration graphs of Br II emission at A, 470.5 nm and B, 478.6 nm

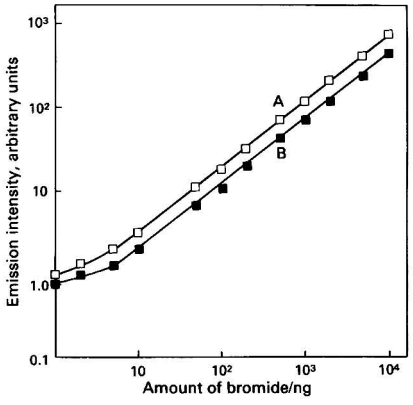

Fig. 5. Response data for Br II emission at A, 470.5 nm and B, 478.6 nm in an atmospheric helium MIP using ETV

Calibration Graphs, Detection Limits and Interferences

Double logarithmic calibration graphs (Figs. 4 and 5) were obtained with respect to bromide in the solution. Fig. 4 illustrates the calibration graphs for Br II emission in the helium MIP at A, 470.5 nm and B, 478.6 nm when the analyte is generated chemically as bromine from the potassium dichromate - sulphuric acid oxidation mixture. The detection limit, defined as the sample concentration that produced a signal-to-noise ratio of two, at both the emission lines was 1 ng of bromide and the log - log calibration graphs were linear in the range from 5 ng to 50 μg with a slope of 0.8. Fig. 5 shows the calibration data for the same emission wavelengths when electrothermal vaporisation was used for the sample introduction technique. The detection limit was 1 ng and the linear dynamic range was from 5 ng to 10 μg of bromide. Although the 470.5-nm line emission is twice as intense as the 478.6-nm line, the linearity of both lines breaks below 5 ng, hence showing no difference in the detection limits or the linearity of the calibration graphs (Figs. 4 and 5).

Possible interference effects of fluorine, chlorine, iodine, sulphate, nitrate, sodium, potassium, iron and mercury were studied. A 1000-fold excess of Na, K, Fe, Hg, SO_4 and NO_3 did not affect the 10 p.p.m. bromine emission signal. However, it seems that the other halogens have slight interference effects if their concentrations are more than 100-fold greater than the 10 p.p.m. bromide solution.

Conclusion

These methods present two sample introduction techniques for the helium microwave induced plasma (MIP) and provide a sensitive, rapid and simple way of determining bromide. The two most intense emission lines for bromine in a helium MIP (470.5 and 478.6 nm) have been evaluated and it was found that both lines exhibit similar behaviour, in terms of detection limits and linear dynamic ranges.

References

1. Abdillahi, M. M., Tschanen, W., and Snook, R. D., *Anal. Chim. Acta*, 1985, **172**, 139.
2. Bennakker, C. I. M., *Spectrochim. Acta, Part B*, 1982, **32**, 173.
3. Carnahan, J. W., and Caruso, J. A., *Anal. Chim. Acta*, 1982, **136**, 261.
4. Van Dalen, H. P. J., Kuwee, B. G., and De Galan, L., *Anal. Chim. Acta*, 1982, **142**, 159.
5. Long, S. E., Snook, R. D., and Browner, R. F., *Spectrochim. Acta, Part B*, 1984, **40**, 553.
6. Tanabe, K., Haraguchi, H., and Fuwa, K., *Spectrochim. Acta, Part B*, 1981, **36**, 119.
7. Mulligan, K. J., Hahn, M. H., and Caruso, J. A., *Anal. Chem.*, 1979, **51**, 1935.
8. Robin, J. P., *Prog. Anal. At. Spectrosc.*, 1982, **5**, 79.

Paper A5/195
Received April 31st, 1985
Accepted September 2nd, 1985

Investigations into the Improvement of the Analytical Application of the Hydride Technique in Atomic Absorption Spectrometry by Matrix Modification and Graphite Furnace Atomisation

Part I. Analytical Results

Klaus Dittrich and Rita Mandry
Karl-Marx-University, Chemistry Section, Analytical Centre, Talstrasse 35, 7010 Leipzig, GDR

Hydride generation AAS is characterised as a very sensitive analytical technique using the commercial AAS-3 hydride system with quartz tube atomisation. Studies of matrix interferences are reported for the trace elements As, Sb, Se and Te. The hydride-forming elements As, Sb, Bi, Se, Te, Ge, Sn and Pb were used as matrices.

Two types of matrix interference can be distinguished: matrix interference in the liquid phase of hydride generation, and matrix interference in the gaseous phase of hydride atomisation. The strong matrix interference in the liquid phase was diminished by matrix modifications and new reagents are characterised. To diminish or avoid matrix interference in the gaseous phase, a new type of graphite tube atomiser was developed. The dimensions of the graphite paper atomiser are comparable to those of commercial quartz tubes, but the heated graphite atomiser volume is very small (comparable to HGA 500 tubes). The analytical applicabilities of both systems were characterised and compared.

The absolute detection limits are between 0.1 and 0.5 ng. The relative detection limits in graphite paper atomisers are 2–1000 times better than in quartz tube atomisers.

Keywords: *Atomic absorption spectrometry; hydride technique; matrix modification; graphite furnace atomisation*

In the last 30 years, atomic absorption spectrometry (AAS) has become one of the most commonly used methods in trace analysis. This development was connected with the introduction of some new techniques, especially atomisation, for example AAS with different flames, AAS with electrothermal atomisation in graphite tubes or graphite rods, AAS with evaporation of solid material by lasers, AAS with sputtering and AAS with the generation of volatile hydrides, called hydride AAS for short. The reasons for all these developments have been to improve the analytical criteria of AAS methods, such as detection ability, accuracy, selectivity, reproducibility and applicability.

The initial development of hydride AAS was carried out by Holak[1] in 1969, but in 1955 Erdey *et al.*[2] generated volatile hydrides for analytical measurements in d.c. arc atomic emission spectrography. Holak used the well known Marsh reaction in AAS. Arsine (AsH_3) was generated by nascent hydrogen (from Zn/H^+), transported by an argon stream and collected in a cold trap (liquid nitrogen). After collection, the trap was rapidly heated to room temperature. The volatile arsine was transported by argon into an air - acetylene flame for atomisation. The absorption was measured at 193.7 nm.

Up to now three distinct operations have been performed in hydride AAS: hydride generation, hydride transportation and hydride atomisation. The procedure of all steps has been changed and improved in the last decade.

Hydride generation. Pollock and West (1972)[3] introduced as the reducing agent Mg - Ti^{3+} - H^+ mixtures and Goulden and Brooksbank (1974)[4] used Al - H^+ for this purpose. As late as 1972 Braman *et al.*[5] introduced BH_4^- - H^+ solutions in atomic emission and Schmidt and Royer[6] transferred this hydride generation reaction system to AAS. The latter system is mostly used today, because the homogeneous reduction reaction is faster than the heterogeneous reduction by M - H^+ systems. In general, 0.5–10% solutions of $NaBH_4$, stabilised by 0.5–2% NaOH, are used. Mostly dilute HCl is used, but HNO_3, citric acid, oxalic acid, tartaric acid and maleic acid can also be used.

Hydride transportation. There are two methods: the direct transfer mode and a collection mode. The latter was necessary for the slowly working M - H^+ reduction systems. Since the introduction of the BH_4^- - H^+ reduction, the direct transfer mode has become possible and useful. Nevertheless, in some instances the collection mode was used for enrichment and concentration, but according to Chapman and Dale[7] this is useful only for the most stable hydrides, such as AsH_3, SbH_3, BiH_3 and SeH_2.

Hydride atomisation. The most intense development has taken place in this field. The air - acetylene flame used at first has disadvantages owing to its high background absorption and sensitivity due to plasma dilution. In 1972, Chu *et al.*[8] introduced the electrically heated quartz tube. Knudson and Christian[9] also used the graphite tube very early. Special flame techniques, the flame-heated quartz tube[6] and the flame-in-tube technique,[10] were introduced in 1974. Today the electrically heated quartz tube is most commonly used, because this technique is simple and for many analytical samples the other techniques including the graphite tube do not give advantages.

The following advantages and disadvantages of hydride AAS can be summarised:

1. In many instances the traces of the analyte can be separated from the sample, which improves the accuracy.
2. The efficiency of sample introduction into the plasma is very high (nearly 100%), which gives good sensitivity.
3. Large solution volumes can be used, in special instances with the collection mode, which gives good sensitivity.
4. The method can be automated and a flow injection mode of operation is possible.
5. Contributions to chemical speciation are possible.[11]

For a long time the first point was the major advantage. However, recently it has become more evident that this is also the reason for the main disadvantage, owing to the existence or occurrence of matrix interferences (see also reference 12). In this paper we present proposals for the systematic

characterisation of matrix interferences, and for avoiding or diminishing such effects.

For this purpose we have used the most complicated conditions: the determination of volatile hydride-forming elements (As, Sb, Se and Te) in volatile hydride-forming matrices (As, Sb, Bi, Se, Te, Ge, Sn and Pb). We have used a new AAS-3 hydride system with a quartz tube atomiser (Carl Zeiss, Jena, GDR) and have also developed a new atomisation system, a long-path graphite tube atomiser, based on a new material, on graphite paper.

In the following paper, some explanations about the causes of matrix interference are given.

Experimental

Apparatus

An AAS-3 atomic absorption spectrometer (Carl Zeiss), a hydride system for AAS-3 (hydride generation system) and quartz tube atomiser (QT) (controlled by computer) (see Fig. 1) and a graphite paper atomiser (GPA) (laboratory constructed) (see Fig. 2) were used.

The graphite paper used had a thickness of about 0.1 mm. A rectangular piece was cut out (92 × 33 mm) and a tube of length 92 mm and diameter 9 mm was formed. The overlap was 3–4 mm. The ends of the tube were stabilised by inner graphite rings (o.d. 8.8 mm; i.d. 7 mm; length 5 mm) and jammed between two water-cooled brass half-rings. To avoid thermal destruction we used four small outer graphite rings (o.d. 9.5 mm, i.d. 9.1 mm, length 1 mm). The tubes were heated by direct resistance heating (0–20 V; 0–200 A). The pyrometrically measured temperatures are shown in Table 1. The medium lifetime of such a tube at atomisation temperatures of about 2000 °C and a heating period of 30 s is about 70–100 heating cycles. The paper was made by EKL (Berlin, GDR). The shielding gas was argon. The outer flow-rate was 20 l h^{-1} and the inner flow-rate was controlled by the hydride system (6–40 l h^{-1}).

For comparison we also used graphite tube cuvettes of the Beckman type (Type 1268) and Carl Zeiss type (AE3).

The light sources were electrodeless discharge lamps for As (9 W), Sb (7 W), Se (8 W) and Te (11 W) (Westinghouse, USA).

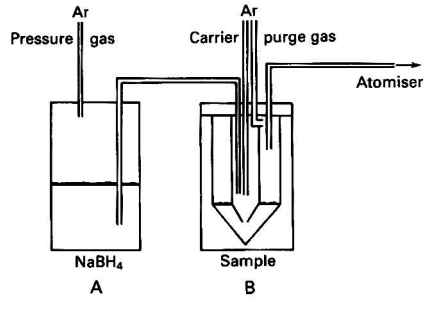

Fig. 1. AAS-3 hydride device (Carl Zeiss, Jena, GDR)

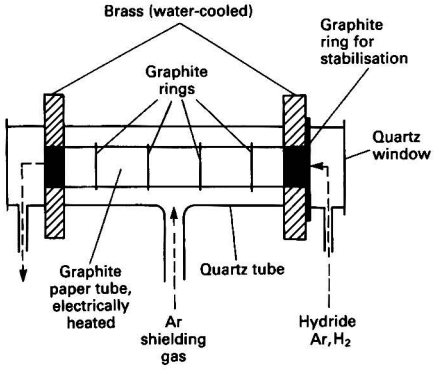

Fig. 2. Graphite paper atomiser (GPA) (laboratory-constructed)

Reagents

Reagents were of analytical-reagent grade from Laborchemie Apolda, GDR.

Stock solutions of As^{3+}, Sb^{3+}, SeO_3^{2-} and TeO_3^{2-} with concentrations of 1 mg ml^{-1} were prepared from As_2O_3, Sb_2O_3, SeO_2 and Te, respectively.

Stock solutions for matrix elements were prepared at concentrations of 50–100 mg ml^{-1} by dissolving the appropriate amounts of As_2O_3, Sb_2O_3, SeO_2, Te, GeO_2, $SnCl_2$ and $Pb(NO_3)_2$ in 1 M hydrochloric or nitric acid.

Procedure

Vessel A (Fig. 1) contains the alkali stabilised solution of sodium tetrahydroborate(III) ($NaBH_4$). Vessel B is for the sample and can be changed rapidly. The system is controlled by different Ar flows using the computer (Fig. 3).

The acidifed sample is placed in vessel B. After initiation, two gas streams [the first purge stream (36 l h^{-1}) and the carrier stream (18 l h^{-1})] purify the system (about 30 s are necessary). In the reaction phase (reduction by $BH_4^- - H^+$), the purge stream is closed and the pressure gas valve is opened

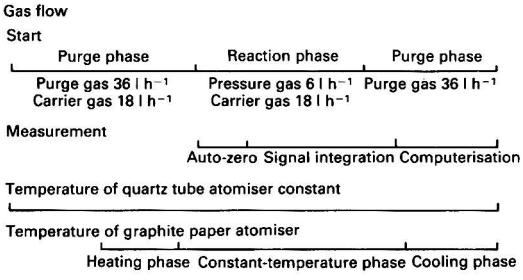

Fig. 3. Scheme of procedure using hydride device

Table 1. Relationship between electrical conditions and the resulting temperatures of the GPA

Potential/V			
Primary	Secondary	Temperature/°C	Heating rate/ °C s^{-1}
110	9.5	1450	100
120	10.2	1600	150
130	11	1700	200
140	12	1800	300
150	13	1900	333
160	14	1980	670
170	14.8	2100	750
180	15.2	2120	1000
190	16.1	2200	1000
200	16.9	2280	1300
210	17.6	2310	1500
220	18.4	2400	1700
230	19.1	2460	2000
240	20.5	2560	2300

(6 l h^{-1}). Depending on the duration of the reaction phase a variable amount of the reagent is transferred from vessel A into vessel B.

After the reaction phase, the second purge (or transportation) phase is initiated. The pressure gas supply is closed and the second purge gas supply is opened. During the reaction phase and the second purge phase, the hydride - hydrogen - argon gas mixture is transported to the atomiser. Every time a small gas stream (6 l h^{-1}) avoids the introduction of air.

The first seconds of the reaction phase are used to auto-zero the instrument. After this, the measuring phase is started (peak-height and -area integration modes are possible). If the system is in operation with the quartz tube atomiser, the tube is heated before to the desired temperature (up to 1000 °C) for all procedures. If the system is operated with the graphite paper atomiser, the graphite tube is heated at the end of the first purge period by resistance heating to the desired temperature (up to 2600 °C). The heating period is completed in 2–3 s. The hold time for the selected temperature is given by the total duration of the reaction and the second purge phases. Subsequently the tube is cooled rapidly by water cooling.

Results and Discussion

Investigations of the Commercial Hydride System (AAS-3, QT)

Analyses of pure dilute solutions of As, Sb, Se and Te

In order to guarantee high sensitivity, it is necessary to optimise the concentration of the acid used, the amount of $NaBH_4$ and the sample volume.

As the sample volume is an independent parameter, two volumes (0.2 and 10 ml) were used for the investigations. It was observed that a concentration of 2 M hydrochloric acid was the best (1 and 3 M HCl led to signal depressions of about 5–10%). The optimum $NaBH_4$ concentration was 3% and the optimum amounts were 0.8 ml for the smaller and 1.3 ml for the larger sample volume. The possibility of the direct introduction of the $NaBH_4$ (introduction time <0.5 s) was also examined. It appeared that the AA signal height and shape were unchanged, but the reagent volumes required were smaller (0.5 and 1.1 ml, respectively).

The analytical results obtained under the optimum conditions are shown in Table 2. Table 2 shows that the absolute reciprocal sensitivities (for 1% absorption, to a first approximation this value is similar to a 3σ detection limit criterion) are one order of magnitude better for the smaller sample volumes. There are two reasons for this: (1) with small sample volumes the reduction is faster owing to the faster mixing and higher concentration of the reagent; the homogeneity of the solution is also more rapidly achieved; and (2) with smaller volumes the amount of $NaBH_4$ required is smaller, which leads to a smaller dilution of hydride by excess of hydrogen. As the larger volume is more than one order of magnitude greater than the small volume used, Table 2 shows that the large volume gives, as expected, better relative reciprocal sensitivity and therefore also better detection limits.

Optimisations of sample volume are possible in both directions, depending on the requirements of specific analytical problems.

Investigation of matrix interferences of volatile hydride-forming matrices

Table 3 shows the systems evaluated and Fig. 4 summarises the results of the investigations. Similarly to our earlier results for the determination of Se and Te,[13] we found in all instances more or less strongly decreased signals. From the results in Fig. 4, it can be concluded that trace analysis is impossible in most instances.

Classification of matrix interferences

Interferences by different matrices have been investigated in hydride generation AAS for many systems. The influence of heavy metals has been frequently described.[12] These metal ions only influence the procedure in the liquid phase of hydride generation. In our case it is possible that the matrix interferences could occur in all three steps of the hydride technique. Table 4 indicates the possible causes of interference.

Possibilities of avoidance of matrix interferences in the liquid hydride generation phase

Many investigators have described methods for decreasing matrix interferences in the liquid phase of hydride generation. A survey of these papers is given in reference 12. Recent publications by Welz and Melcher[14–16] also deal with this problem and have attempted to offer explanations in some instances. Welz and Melcher[17] concluded that the influence of heavy metals does not consist in the simple formation of soluble selenides, such as CuSe and CoSe, but that the true influence is connected with adsorption and destruction of hydrides on surface-active precipitates of the heavy metals formed by reduction. Procedures recommended for avoiding or decreasing matrix interferences have included change of acidity of the solution, formation of complexes (masking) with the matrix interferents, and formation of precipitates of the matrices. Complexation reagents used include EDTA, KI, citric acid, thiosemicarbazide 1,10-phenanthroline, oxalic acid, thiourea and pyridylaldoxime (for details, see reference 12).

Two interesting examples of precipitation reactions should be mentioned. The determination of As in the presence of Se

Table 2. Results of hydride AAS using the AAS-3 with hydride system and quartz tube atomiser (QT)

	Reciprocal sensitivity per 1% *A*			
	Sample volume 0.2 ml		Sample volume 10 ml	
Trace element	Absolute/ng	Relative/ng ml^{-1} (p.p.b.)	Absolute/ng	Relative/ng ml^{-1} (p.p.b.)
As	0.17	0.9	1.6	0.16
Sb	0.11	0.6	0.8	0.08
Se	0.2	1.0	1.8	0.18
Te	0.19	0.95	1.1	0.11

Table 3. Matrix systems investigated

Trace element	Matrix substances
As	Sb, Bi, Se, Te, Ge, Sn, Pb, InSb
Sb	As, Bi, Se, Te, Ge, Sn, Pb, GaAs, InAs
Se	As, Sb, Bi, Te, Ge, Sn, Pb, GaAs, InAs, InSb
Te	As, Sb, Se, Ge, Sn, Pb, GaAs, InAs, InSb

Table 4. Possible causes of matrix interferences in hydride AAS

Step	Interference
Hydride generation	Reduction of matrix (loss of $NaBH_4$); reaction of matrix or reduced matrix with trace amounts of hydride (*e.g.* precipitation); adsorption of hydride on precipitates
Hydride transportation	Decomposition of unstable hydrides on surface (only for hydride-forming matrices)
Hydride atomisation	Relatively unknown; change in atomisation mechanism; molecule formation (only for hydride-forming matrices)

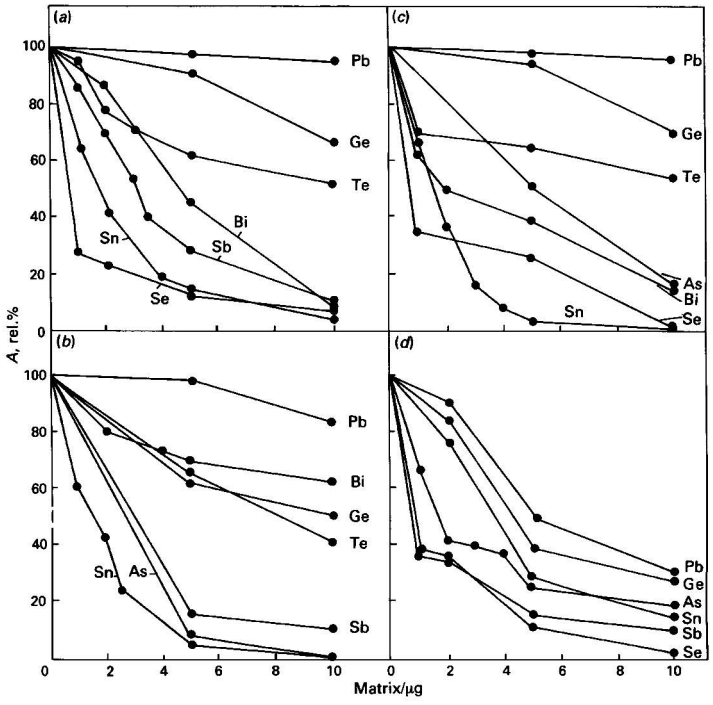

Fig. 4. Interference of hydride-forming matrices on the determination of (*a*) As, (*b*) Se, (*c*) Sb and (*d*) Te, using QT (amount of analyte used, 10 ng)

is actually improved in the presence of Cu^{2+} ions, because these bind the generated H_2Se as soluble CuSe.[17,18] Selenium determinations in the presence of Cu^{2+} ions are improved by the addition of TeO_2, because the simultaneously generated H_2Te forms insoluble CuTe.[19–21] Except for the example of the determination of As in the presence of Se, no other literature information was available for reducing the matrix effects of our analytical combinations. We therefore attempted to obtain appropriate improvements by matrix modification procedures.

Investigation of the influence of Cu^{2+} ions on the determination of As and Sb in the presence of Se and Te. The results of these investigations are illustrated for As in Fig. 5. The effects observed for Sb were the same and are not shown here.

Fig. 5 shows that the influence of the Se matrix is stronger than that of the Te matrix. The general reason for the interference lies in the formation of insoluble compounds such as As_2Se_3, Sb_2Se_3, Sb_2Se_3, As_2Se_3 and Sb_2Te_3, and in the adsorption of these compounds on the surface of elemental Se and Te precipitates. The addition of increasing concentrations of Cu^{2+} ions reduced the depression of both Se and Te on the AA signal. The influence of Cu^{2+} ions is much stronger for the Te matrix than the Se matrix. We assume that this is due to the smaller solubility constant of CuTe compared with CuSe. Particularly with the Se matrix but also for the Te matrix, it is impossible to avoid completely the matrix interference. From this fact we deduce that there are other matrix interferences than those in solution, *e.g.*, in the gaseous phase.

Investigations of the influence of EDTA on the determination of As, Sb, Se and Te in the presence of Bi, Ge, Sn and Pb matrices. The results of these investigations for a trace element to matrix ratio of 1 : 1000 are shown in Table 5.

The amount of EDTA was sufficient to complex the metal ions fully. With the Ge and Pb matrices only small improvements were observed because Pb^{2+} ions do not have a strong

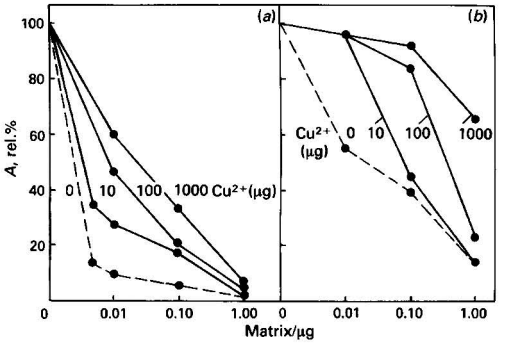

Fig. 5. Influence of the matrix modifier (Cu^{2+}) on the trace determination of As and Sb in the presence of (*a*) Se and (*b*) Te matrix (amount of analyte, 10 ng)

Table 5. Improvement in the determination of As, Sb, Se and Te in the presence of hydride-forming matrices (Bi, Sn, Pb, Ge; 10 μg) achieved by addition of EDTA

Trace element (10 ng)	Improvement factor			
	Bi	Sn	Pb	Ge
As	7	5*	1.05	1.15
Sb	3.3	100*	1.05	1.06
Se	1.3	30*	1.15	1.7
Te	—	1.3*	1.7	1.7

* 5 M HCl.

influence and complex formation between Ge^{2+} ions and EDTA is not high. A successful outcome was achieved for the complexation of Bi^{3+} ions, especially for the determination of Sb and As. Te determinations are impossible in the presence of Bi^{3+} ions, irrespective of the presence or absence of EDTA.

Interference by Sn^{2+} ions, which in most instances is the strongest influence, is diminished by EDTA. The use of a higher concentration of hydrochloric acid (5 M) is advantageous.

Investigation of the influence of citric and tartaric acids on the determination of Se in the presence of Sb and Te matrices. The presence of a 100-fold excess of the complexing reagent (10 μg) improves the analytical results only by a factor of 1.5 (Sb) or 1.4 (Te).

Investigations Using the AAS-3 Hydride Generation Systems Combined with the Graphite Paper Atomiser

As indicated above, only in some instances is it possible to avoid matrix interference using chemical matrix modification. We therefore assumed that very strong matrix interferences occur in the gaseous phase in addition to the solution phase. In order to evaluate such a hypothesis, it is necessary to provide some variation of the temperature of the atomiser. Because further enhancement of the temperature (> 1000 °C) in quartz tube atomisers is impossible, we investigated the use of a graphite tube atomiser.

Characterisation of graphite tubes for hydride atomisation

After the first application of graphite tubes in hydride atomisation by Knudson and Christian,[9] a number of other workers used this technique.[12] In most instances small graphite tubes of the HGA 2100 type (Perkin-Elmer) have been used. This graphite tube is not very useful for hydride atomisation, because the inner volume is small (see Table 6) in relation to the large gas volume produced in the generation reaction (argon - hydrogen - hydride mixture up to 80 ml). The analytical sensitivities achieved are therefore relatively poor. We therefore attempted to develop a new graphite tube atomiser, which avoids this disadvantage, and which has dimensions similar to those of the quartz tube atomiser widely used for this technique. Table 6 shows the dimensions of these different types of atomisers. The Beckman Type 1268 atomiser has the longest path length of the commercial graphite tube atomisers. Its disadvantage is the high energy that is needed (10 V, 1000 A = 10 kW), because the mass of graphite to be heated is very large. The graphite paper atomiser developed in this work has a longer path length (150%) compared with the Type 1268 graphite tube, but the heated graphite volume is only 13%. In comparison with the HGA 500 graphite tube type and AE 3 (Carl Zeiss), the enlargement of the inner dimensions is very high, but the heated graphite volume is only 83%. Depending on the temperature required, a power of 3–4 kW is needed.

Investigation of pure dilute solutions of volatile hydride-forming elements, As, Sb and Te in graphite tube atomisers

The results of these investigations are shown in Table 7. Only with the GPA can the same analytical sensitivities as with the QT be achieved. The results support our assumption that the reason for the relatively infrequent application of graphite tube atomisers in hydride AAS is the poorer analytical sensitivities obtained in normal graphite tube atomisers compared with the QT atomiser.

Investigation of the influence of volatile hydride-forming matrices on the determination of As, Sb, Se and Te using the GPA

The results of this investigation are shown in Fig. 6. The optimum atomisation temperatures were 1850 °C (Se, Te) and 2000 °C (As, Sb). Fig. 6 shows the improvement of the AA signal depression (*i*) using an enhanced atomisation temperature, (*ii*) by chemical matrix modification, using the QT atomiser, and (*iii*) by an enhanced atomisation temperature and chemical matrix modification. It can be seen that the increase in atomisation temperatures available in the GPA gives the best analytical results for the determination of As, Sb and Se in the presence of As, Sb, Bi and Se matrices. Only the effects of a Te matrix on As and Sb determinations, and of all matrices on Te determinations, are not improved by the use of higher temperatures. In all instances the combination of the

Table 6. Dimensions of commercial quartz tube and graphite tube atomisers and of the new developed graphite paper atomiser

Dimensions	QT	Graphite tubes: HGA 500 AE3	Graphite tubes: Beckman 1268	GPA
Length/mm	145	28	63	92
I.d./mm	18	6	9	9
Internal volume/cm³	37	0.8	4.8	5.9
Heated graphite volume/cm³	—	0.6	3.6	0.5

Table 7. Results of hydride AAS using different atomisers (reciprocal sensitivity/ng per 1% *A*). Sample volume, 0.2 ml

Trace element	Quartz tube, AE3	Graphite tube, AE3	Graphite tube, Beckman 1268	Graphite tube, graphite paper
As	0.17	0.35	0.20	0.16
Sb	0.11	0.18	0.14	0.11
Se	0.20	0.32	0.24	0.21
Te	0.19	0.29	0.24	0.20

Table 8. Results of the determination of trace amounts of hydride-forming elements in hydride-forming matrices using GPA at 2000 °C and optimum matrix modification in comparison to QT without matrix modification. Values: reciprocal sensitivities per 0.01 *A**

Trace element	Atomiser	Relative detection limits,* p.p.m. with respect to matrix element: As	Sb	Bi	Se	Te	Ge	Sn	Pb
As	QRA	—	100	400	2600	260	740	1040	4
	GPA	—	5	1	2	0.7	8	30	2
Sb	QRA	180		120	1800	450	45	530	0.4
	GPA	3		3	3	2	4	7	0.4
Se	QRA	600	600	240	—	120	150	600	30
	GPA	120	8	30	—	8	40	120	12
Te	QRA	1100	2900	1900	2900	—	190	390	290
	GRA	230	190	1100	140	—	90	290	190

* Because the 0.01 absorbance is in all instances to a first approximation equal to three times the relative standard deviation it is possible to write detection limits.

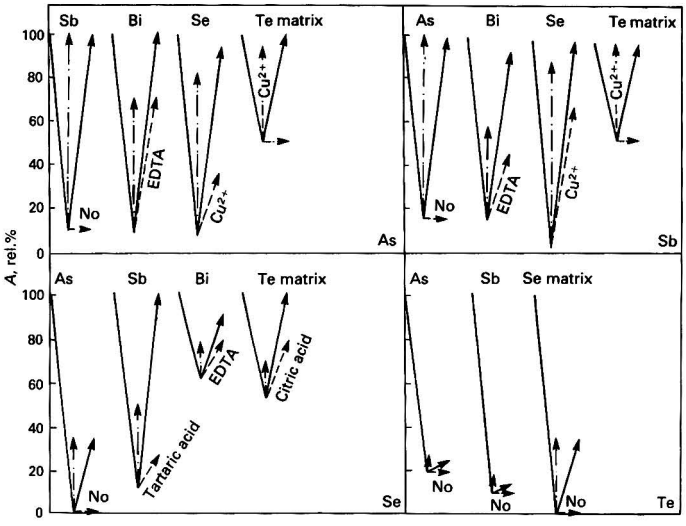

Fig. 6. Improvement of AA signal depressions (—) caused by hydride-forming matrices in QT using chemical matrix modification (– – –) (QT) and enhancement of temperature (1900–2000 °C) (GPA) (–·–·–); sum of improvements (——). Amount of analyte element, 10 ng per 0.2 ml; amount of matrix element, 10 μg per 0.2 ml; EDTA, 1 M; Cu^{2+}, 1 mg per 0.2 ml; citric acid, 5%; and tartaric acid, 5%

Table 9. Results of the determination of As, Sb, Se, Te in thin layers of $A^{III}B^{V}$ semiconductor materials using hydride AAS with GPA. Conditions: layer separation by chemical etching; dimensions of layer, 10 × 10 × 0.0005 mm; sample, 0.25 mg. Values in parentheses are improvement factors relative to QT

Trace element	Relative detection limit/atoms cm^{-3}		
	GaAs	InAs	InSb
As	—	—	9×10^{16} (100)
Sb	2.6×10^{16} (100)	5.6×10^{16} (100)	—
Se	4.8×10^{18} (5)	5.1×10^{18} (5)	4×10^{17} (100)
Te	5.7×10^{18} (5)	6.1×10^{18} (5)	5.4×10^{18} (10)

GPA and chemical matrix modification gave the best results (see Fig. 6 and Table 8).

Table 8 shows the results obtained for the determination of As, Sb, Se and Te in the presence of hydride-forming matrices using the GPA and chemical matrix modification. In all instances significant improvements were achieved, the improvement factors being between 1.5 and 1000.

The combination of GPA and chemical matrix modification has been used for the trace determinations of As, Sb, Se and Te in $A^{III}B^{V}$ semiconductor materials. As shown in Table 9, considerable analytical improvements were obtained in many instances.

Several conclusions can be drawn from these results. In particular, the application of the higher atomisation temperatures in the GPA for hydride AAS is very useful, particularly if volatile hydride-forming elements are present as matrices. Strong matrix interference appears to occur in the gaseous phase in addition to the liquid phase of the QT atomiser for this type of matrix.

Conclusions

Application of the graphite paper atomiser, which allows atomisation temperatures up to 2600 °C is very useful for the determination of trace amounts of hydride-forming elements in the presence of hydride-forming matrices.

The improvement factors for application of the GPA are 1–3 orders of magnitude.

In spite of the strong improvement by high-temperature atomisation, it is necessary to apply matrix modifiers.

The improvements that can be obtained by GPA atomisation and matrix modifications show that matrix interferences occur in different ways in the liquid and gaseous phases.

To explain the reasons, especially for matrix interferences in the gaseous phase, the results of further experiments are given in the following paper.

References

1. Holak, W., *Anal. Chem.*, 1969, **41**, 1712.
2. Erdey, L., Gegus, E., and Koscis, E., *Acta Chim. Hung.*, 1955, **7**, 343.
3. Pollock, E. W., and West, S. J., *At. Absorpt. Newsl.*, 1972, **11**, 104; 1973, **12**, 6.
4. Goulden, P. D., and Brooksbank, P., *Anal. Chem.*, 1974, **46**, 1431.
5. Braman, R. S., Justin, L. L., and Foreback, C. C., *Anal. Chem.*, 1972, **44**, 2195.
6. Schmidt, F. J., and Royer, J. L., *Anal. Lett.*, 1973, **6**, 17.
7. Chapman, J. F., and Dale, L. S., *Anal. Chim. Acta*, 1979, **111**, 137.
8. Chu, R. C., Barron, G. P., and Baumgarner, P. A. W., *Anal. Chem.*, 1972, **44**, 1476.
9. Knudson, E. J., and Christian, G. D., *Anal. Lett.*, 1973, **6**, 1039.
10. Siemer, D. D., and Hagemann, L., *Anal. Lett.*, 1975, **8**, 323.
11. Aggett, J., and Aspell, A. C., *Analyst*, 1976, **101**, 341.
12. Nakahara, T., *Prog. Anal. At. Spectrosc.*, 1983, **6**, 163.

13. Dittrich, K., Vorberg, B., and Wolthers, H., *Talanta*, 1979, **26**, 747.
14. Welz, B., and Melcher, M., *Analyst*, 1984, **109**, 569.
15. Welz, B., and Melcher, M., *Analyst*, 1984, **109**, 573.
16. Welz, B., and Melcher, M., *Analyst*, 1984, **109**, 577.
17. Welz, B., and Melcher, M., "Wissenchaftliche Beiträge der Karl-Marx Universitat, Analytiktreffen 1982, Atomspektroskopie," Karl-Marx-Universität, Leipzig, 1983, p. 165.
18. Welz, B., and Melcher, M., *Anal. Chim. Acta*, 1981, **131**, 131.
19. Kirkbright, G. F., and Taddia, M., *At. Absorpt. Newsl.*, 1979, **18**, 68.
20. Azad, J., Kirkbright, G. F., and Snook, R. D., *Analyst*, 1979, **104**, 232.
21. Bye, R., Engrik, L., and Lund, W., *Z. Anal. Chem.*, 1984, **318**, 25.

Paper A5/82
Received March 5th, 1985
Accepted September 20th, 1985

Investigations into the Improvement of the Analytical Application of the Hydride Technique in Atomic Absorption Spectrometry by Matrix Modification and Graphite Furnace Atomisation

Part II.* Matrix Interferences in the Gaseous Phase of Hydride Atomic Absorption Spectrometry

Klaus Dittrich and Rita Mandry
Karl-Marx-University, Chemistry Section, Analytical Centre, Talstrasse 35, 7010 Leipzig, GDR

Studies of matrix interferences in hydride AAS were carried out in the presence of hydride-forming matrices. It was found that the main interference in most instances occurs in the gaseous phase of hydride atomisation. Thermodynamic calculations, coupled with spectroscopic and thermal investigations, show that the main cause of matrix interferences in the gaseous phase is the formation of diatomic molecules between the trace and matrix elements (*e.g.*, AsSb). Therefore, significant improvements in accuracy and relative sensitivity can be obtained by using graphite tube atomisers, at temperatures >2000 °C.

Keywords: *Atomic absorption spectrometry; hydride technique; matrix modification; graphite furnace atomisation; matrix interferences*

Most papers dealing with matrix interferences in hydride AAS have concerned matrix interferences that occur in the liquid phase of hydride generation.[1] Matrix interferences in the gaseous phase of hydride AAS can only be caused by volatile hydride-forming matrices and are therefore rarely dealt with. Welz and Melcher[2] concluded that the reason for the strong matrix interference of volatile hydride-forming elements using quartz tube atomisers (QT) was the absence of H radicals required for the efficient atomisation of hydrides and hydride-forming matrices.

As shown in Part I,[3] the analytical determinations of "hydride-forming trace elements" in "hydride-forming matrices" are improved very strongly by the use of the graphite paper atomiser (GPA). In this paper we report studies that make a contribution to our knowledge of atomisation mechanisms in hydride AAS and towards the explanation of matrix interferences.

Experimental

Apparatus

An AAS-3 atomic absorption spectrometer (Carl Zeiss, Jena, GDR), a hydride generation system with a quartz tube atomiser (QT) and a graphite paper atomiser (GPA)[3] (laboratory constructed) were used. The light sources were As, Sb, Se and Te electrodeless discharge lamps (Westinghouse, USA).

Reagents

Reagents were of analytical-reagent grade from Laborchemie Apolda, GDR.

Stock solutions of As^{3+}, Sb^{3+}, SeO_3^{2-} and TeO_3^{2-} with concentrations of 1 mg ml^{-1} were prepared from As_2O_3, Sb_2O_3, SeO_2 and Te, respectively.

Stock solutions for matrix elements were prepared at concentrations of 50–100 mg ml^{-1} by dissolving appropriate amounts of As_2O_3, Sb_2O_3, SeO_2, Te, GeO_2, $SnCl_2$ and $Pb(NO_3)_2$ in 1 M hydrochloric or nitric acid.

* For Part I of this series, see p. 269.

Procedure

The procedure described in Part I[3] was followed.

Results and Discussion

Mechanisms of Atomisation in Hydride AAS

Dedina and Rubeška[4] and also Welz and Melcher[5] proposed for the mechanism of atomisation in flames and in quartz tubes a hydrogen radical reaction:

$$AsH_3 \xrightarrow{+H} AsH_2 + H_2 \xrightarrow{+H} AsH + 2H_2 \xrightarrow{+H} As + 3H_2 \quad (1)$$

The required H radicals are generated in flames by combustion processes. Welz and Melcher[5] proposed that the residual oxygen in the argon and in the sample solution produce H radicals in the hot QT by reaction with the excess of hydrogen generated from the tetrahydroborate(III) reaction. Further, they showed that at high temperatures (at about 1000 °C) there are reactions between the SiOH groups of the quartz tube surface and the hydrogen, resulting in the release of H radicals. Thermal dissociation was not excluded but it was assumed that this reaction would lead to dimeric and tetrameric As molecules. Alkman *et al.*[6] proposed that the mechanism of atomisation of AsH_3 in graphite tubes involves thermal destruction to solid As as the first step, followed by evaporation and dissociation steps:

$$AsH_3 \xrightarrow[1000\,°C]{\text{Destruction}} As_{solid} \xrightarrow{\text{Evapo-ration}} As_4 \xrightarrow{\text{Disso-ciation}} As_2 \xrightarrow{\text{Disso-ciation}} As \quad (2)$$

All these proposals were supported by experimental evidence, but not exactly demonstrated.

Equilibria Between Different As Species: Thermodynamic Considerations

The exact determination or calculation of the equilibrium composition of species in complex mixtures of vapours in a QT or GPA is very difficult, because the parameters and total concentrations are themselves not well defined. It is possible to assume the following. A total amount of 0.1–10 ng of arsenic should exist in the forms AsH_3, AsH_2, AsH, As, As_2 and As_4 in a gaseous volume of 10–100 ml of a hydrogen -

argon mixture, because 1 ml of 3% $NaBH_4$ solution produces in the presence of H^+ about 80 ml of hydrogen. The distribution of As species in such a gas mixture is unknown, but it is possible to assume that the total partial pressure of all As species lies between 10^{-9} and 10^{-7} atm.

In connection with investigations concerning epitaxial processes for the production of $A^{III}B^{V-}$ semiconductors (GaAs, GaP),[7-9] calculations and experiments were carried out for the determination of equilibrium compositions. From these results we can suggest that at a total partial pressure of 0.1 atm for As species and at 827 °C in a hydrogen atmosphere, the equilibrium composition is the following: As 2×10^{-4}, AsH_2 2×10^{-3}, AsH_3 7×10^{-3}, As_4 42, As_3 8×10^{-2} and As_2 58%. From these results it can be concluded that (*i*) thermal dissociation of AsH_3 is possible and (*ii*) the main products at 827 °C are As_2 and As_4.

This is clearly the reason for the assumption by some workers that As atoms do not exist at this temperature. The following equation describes the equilibrium $2As_2 \rightleftarrows As_4$ at 1000 °C:

$$K_p = \frac{P^2_{As_2}}{P_{As_4}} = 3 \times 10^{-2} \quad \ldots \quad \ldots \quad \ldots \quad (3)$$

where K_p = equilibrium constant and P = partial pressure. For total partial pressures of As species of 10^{-1}, 10^{-3}, 10^{-5}, 10^{-7}, 10^{-8} and 10^{-9} atm, it is possible to calculate from the equation

$$\frac{4\alpha^2}{(1-\alpha^2)} = \frac{K_p}{P} \quad \ldots \quad \ldots \quad \ldots \quad \ldots \quad (4)$$

the degrees of dissociation (α) at 1000 °C. The values are 0.5, 80, 99, 99.99, 100 and 100%, respectively. This means that at total pressures of $<10^{-3}$ atm As_4 molecules have no practical existence. We have calculated the degree of dissociation of As_2 by the dissociation reaction $2As \rightleftarrows As_2$, using the standard values[12] for As_g, H°_{298} = 68.7 kcal mol^{-1} and S°_{298} = 41.6 cal mol^{-1} k^{-1}, and for As_2, H°_{298} = 45.5 kcal mol^{-1} and S°_{298} = 57.6 cal mol^{-1} K^{-1}, the standard reaction enthalpy and entropy as being ΔH^{OR}_{298} = 91.4 kcal mol^{-1} and ΔS^{OR}_{298} = 25.3 cal mol^{-1} K^{-1} and the free enthalpy as being ΔG^{OR}_{298} = 83.9 kcal mol^{-1}.

Ignoring the dependence of ΔH on temperature, we calculated the following equilbrium constants for this As_2 dissociation:

$$K_p = \frac{P^2_{As}}{P_{As_2}} =$$
$$3 \times 10^{-62}\,(298\text{ K}),\ 1.3 \times 10^{-10}\,(1298\text{ K}) \text{ and } 7 \times 10^{-4}\,(2298\text{ K}) \quad (5)$$

Using equation (4), the degrees of dissociation (α) were calculated for the following total pressures (10^{-1}, 10^{-3}, 10^{-5}, 10^{-7}, 10^{-8} and 10^{-9} atm) at 1025 °C: 1.8×10^{-3}, 1.8×10^{-2}, 1.8×10^{-1}, 1.8, 6 and 18%, respectively; and at 2025 °C: 4.2, 10, 97, 99.9, 100 and 100%, respectively. At 1025 °C at total pressures between 10^{-7} and 10^{-9} atm, dissociation is possible and As atoms exist.

The radical atomisation mechanism proposed by other workers[4,5] is also possible but the following remarks should be made: (a) thermal dissociation is also possible; (b) not all atoms formed react to give molecules (there are also kinetic effects). An increase in temperature to 2025 °C shows that the dissociation to atoms is very high at total pressures up to 10^{-5} atm.

On increasing the temperature from 1000 to about 2000 °C we did not obtain improvements in atomic absorption sensitivity[3] for dilute solutions. This means that the atom concentration at both temperatures is the same. In Table 1, dissociation energies for diatomic species of hydride-forming elements are shown. Columns 1 and 2 in Table 1 show that MH and M_2 species, that is, As_2, Se_2, SeH and AsH molecules, are the most stable in comparison with the other molecules. Therefore we can conclude that at 2025 °C all other species are dissociated and at low partial pressures the same situation exists at 1000 °C.

Mechanism of Atomisation in Gaseous Phases of Complex Composition

The strong depressions of AA signals, which start at 100-fold excesses of typical matrices, were explained by Welz and Melcher[5] by the fact that for the radical mechanism the required H radicals are preferentially consumed by the matrix hydrides. Thus for the trace hydride the degree of atomisation is inefficient or low. Our opinion is that, as shown in the previous section, considerable thermal dissociation of the MH_x molecules occur at 1000 °C.

Depending on the matrix concentration, the partial pressure can be in the range 10^{-5}–10^{-1} atm. Therefore, it is possible to write the following equations:

$$M_{trace} + M_{matrix\ excess} \rightleftarrows M_{trace}\,M_{matrix} + M_{2\ matrix} \quad (6)$$

or, *e.g.*,

$$As + Sb_{excess} \rightleftarrows AsSb + Sb_2 \quad (7)$$

From Table 1, it can be seen that the dissociation energies of such mixed species are of the same order of magnitude as for individual metal molecules. The reaction rate to reach equilibrium should be very high, because the concentration of the matrix is very high. This means that at 1000 °C, most trace species should exist as mixed molecules, because the dissociation energies are similar.

We attempted to calculate the degree of dissociation, for such mixed molecules. For the dissociation energy of AsSb we used the arithmetic mean of the dissociation energies of As_2 (3.9 eV) and Sb_2 (3.1 eV), which is 3.5 eV. As the dissociation energies of the pure substances are very similar to the standard reaction enthalpies for the dissociations, we calculated for the AsSb dissociation energy ΔH^{OR}_{298} = 80.7 kcal mol^{-1}. As the standard entropies for dissociation of the As and Sb molecules are almost identical (As_2, S^{OR}_{298} = 25.3 cal mol^{-1} K^{-2}; Sb_2, S^{OR}_{298} = 24.7 cal mol^{-1} K^{-1}), we used the arithmetic mean in this instance also, *i.e.*, 24.9 cal mol^{-1} K^{-1} for ΔS^{OR}_{298} (AsSb → As + Sb). Using these assumptions, we calculated the following

Table 1. Dissociation energies (E) of diatomic molecules of volatile hydride-forming elements; literature values[10,11] (calculated values in parentheses)

Molecule	*E*/eV	Molecule	*E*/eV	Molecule	*E*/eV	Molecule	*E*/eV	Molecule	*E*/ev	Molecule	*E*/eV	Molecule	*E*/eV	Molecule	*E*/eV	Molecule	*E*/eV
AsH	2.8	As_2	3.9	AsSb	3.5	AsSe	3.0	AsTe	2.5	AsBi	3.0	AsPb	(2.2)	(AsSn)	—	(AsGe)	—
SbH	(2.6)	Sb_2	3.1	SbBi	2.5	(SbGe)	—	(SbSn)	—	SbPb	(1.9)	SbSe	3.0	SbTe	2.7		
BiH	2.5	Bi_2	2.0	(BiGe)	—	(BiSn)	—	(BiPb)	1.4	BiSe	2.9	BiTe	2.4				
GeH	3.2	(Ge_2)	2.8	(GeSn)	—	(GePb)	—	GeSe	5.0	GeTe	4.2						
SnH	2.5	Sn_2	2.0	(SnPb)	—	SnSe	4.1	SnTe	3.6								
PbH	1.8	Pb_2	1.0	PbSe	3.0	PbTe	2.5										
SeH	3.2	Se_2	3.4	SeTe	3.0												
TeH	(2.7)	Te_2	2.7														

equilibrium constants for the dissociation of AsSb at several temperatures: 298 K, 1.9×10^{-54}; 1298 K, 7.8×10^{-9}; and 2298 K, 6.4×10^{-3}. It is now possible to calculate the ratio of partial pressures, P_{As}/P_{AsSb}, for Sb in a large excess (>100) for the temperatures 1298 and 2298 K.

In Table 2, the ratio of the partial pressures and the degrees of dissociation are shown for different total partial pressures of antimony. At 1025 °C only the mixed diatomic molecules (in addition to Sb_2 molecules) exist, and at 2025 °C up to Sb partial pressures of 10^{-3} atm only the free atoms exist. If we compare the results of these calculations with our previous experimental results (reference 3, Table 8), then the same tendency is evident.

It can be concluded that the formation of stable, mixed diatomic molecules is the main reason for the depression of AA signals in the gaseous phase. An exact agreement is impossible, because at such high Sb partial pressures at both temperatures high concentrations of Sb_2 molecules are also present. It is clear, however, that, if it was possible to take this factor into account, agreement of the calculated values with the experimental results would be improved. Exact calculations of all the equilibria in this and other analogous systems have not been carried out to date, but it is intended to persue such studies in the future.

Dependence of the Determination of As and Sb on the Atomisation Temperature Used in Hydride AAS

The results of these investigations are shown in Fig. 1. We investigated the dependence of the AA signals on atomisation temperature in the absence and presence of some matrices.

At first in the absence of matrix elements both elements gave, in both the QT and the GPA at very different temperatures, almost the same analytical sensitivity. The small improvement in the GPA is experimentally significant, but is very difficult to explain. One reason could be the different inner diameters of the tubes used.[3] There is one difference between the Sb and As determinations: at 1600 °C the As AA signal is significantly reduced. The reason for this is probably the higher stability of the As_2 molecule (E_D = 3.9 eV) in comparison with the Sb_2 molecule (E_D = 3.1 eV). At lower temperatures both signals are decreased in the GPA. Because it was impossible to measure the temperature exactly, these results have not been included. This could, however, be explained by the assumption that there are two types of atomisation reaction, radical and thermal.

It can be seen in Fig. 1 that in the presence of matrices we have the strongest depression in the QT at 900 °C. Increasing the temperature to 1900–2000 °C decreases the matrix interference in all instances, and in some instances, *viz.*, Sb in As, and As in Sb, Se and Bi, it is removed entirely. At lower temperatures in the GPA a strong matrix interference is again observed. These experimental results support our opinion about matrix interferences in the gaseous phase of hydride AAS and our calculations in the previous section of this paper. Of course, this is only indirect evidence for the existence of mixed diatomic molecules.

Spectroscopic Investigations of the Composition of the Vapour in Hydride AAS

These experiments were designed to detect spectroscopically the proposed mixed molecules in the hot vapour of the QT in

Table 2. Dependence of ratios of partial pressures and degrees of dissociation (α) on Sb partial pressure; $P_{Sb}/P_{As} > 100$; $P_{As} < 10^{-7}$ atm

Ratio α, %	Temperature/°C	Partial pressure of Sb/atm		
		10^{-5}	10^{-3}	10^{-1}
P_{As}/P_{AsSb}	1025	7.8×10^{-4}	7.8×10^{-6}	7.8×10^{-8}
α, %	1025	7.8×10^{-2}	7.8×10^{-4}	7.8×10^{-6}
P_{As}/P_{AsSb}	2025	6.4×10^{2}	6.4	6.4×10^{-2}
α, %	2025	99.8	86.4	6.0

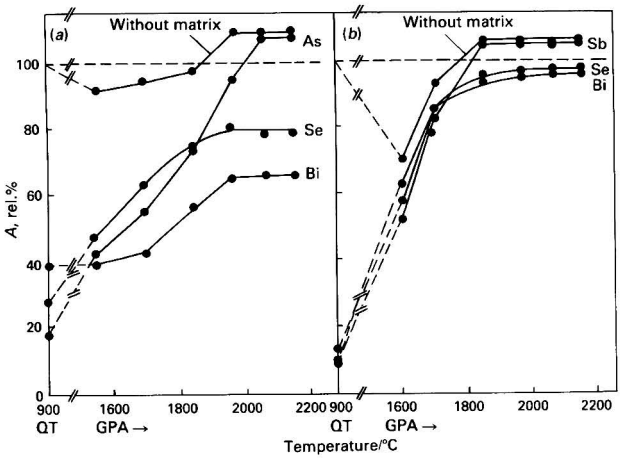

Fig. 1. Dependence of (*a*) Sb and (*b*) As determination on atomisation temperature in the presence and absence of hydride-forming matrices. Amount of analyte element, 10 ng; amount of matrix element, 10 μg. QT = Quartz tube atomiser; GPA = graphite paper atomiser

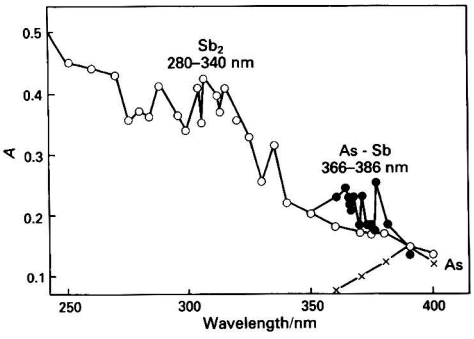

Fig. 2. Molecular absorption spectra in hydride AA with QT atomisation, using Sb or As alone and in combination. Measurement: point by point. Amounts: ×, As, 0.5 mg per point; ○, Sb, 1.0 mg per point; and ●, As - Sb, 0.5 and 1.0 mg per point

order to confirm the accuracy of our hypothesis regarding interferences. Unfortunately, the spectroscopic properties of such molecules are unknown. In general, it can be anticipated that the absorption coefficients of such molecules will be small.

For these reasons, high concentrations of the elements under investigation, As and Sb, were chosen and a deuterium continuum lamp was used as the light source. The results are shown in Fig. 2. For antimony alone, the spectrum was obtained in the spectral range between 250 and 400 nm. Using the QT as the atomiser we observed absorption bands of the Sb_2 molecule. This is also evidence in support of the thermal mechanism, because such high amounts of SbH_3 cannot be decomposed by small amounts of hydrogen radicals. On the other hand, this result is also evidence for the very fast recombination of atoms to molecules under these conditions of high concentration.

In the range between 360 and 400 nm, the absorption spectra of As alone and As - Sb mixtures was measured. It can be seen that absorption bands of the SbAs molecule are present, consistent with those described in the literature.[10]

Similar measurements using the GPA at 2000 °C did not lead to similar characteristic spectra. We therefore believe that this is direct evidence for the existence of such mixed diatomic molecules at 1000 °C in the QT.

Conclusions

Thermodynamic calculations of the system As - H_2 - Ar show that thermal dissociation of AsH_3 is in principle possible at temperatures below 1000 °C.

Further, the thermodynamic calculations show that mixed molecules of the AsSb type exist at low temperatures and that they can be dissociated at higher temperatures. This means that the main reason for matrix interferences in hydride AAS in the presence of hydride-forming matrices consists in this type of molecule formation.

The conclusion in the preceding paragraph was supported by experimental results: measurement of the dependence of the AA signals on the temperature and the spectroscopic detection of AsSb in hydride vapours.

From these results and those in Part I,[3] the matrix interferences of hydride-forming matrices can be classified as follows.

(a) Interferences that involve only molecule formation in the gaseous phase, As in Sb and Sb in As.

(b) Interferences that include both molecule formation in the gaseous phase and chemical reaction and adsorption in the liquid hydride generation phase, As, Sb and Se in Bi, Se, Ge, Sn and Pb.

(c) Main interferences determined by chemical reaction and adsorption in the liquid phase, Te in As, Sb, Bi, Se, Ge, Sn and Pb and As, Sb and Se in Te.

For the analytical determination of hydride-forming elements in the presence of hydride-forming matrices the graphite paper atomiser can be recommended.

References

1. Nakahara, T., *Prog. Anal. At. Spectrosc.*, 1983, **6**, 163.
2. Inui, T., Terada, S., Tamura, H., and Ichinose, N., *Fresenius Z. Anal. Chem.*, 1984, **318**, 502.
3. Dittrich, K., and Mandry, R., *Analyst*, 1986, **111**, 269.
4. Dedina, J., and Rubeška, I., *Spectrochim. Acta, Part B*, 1980, **35**, 119.
5. Welz, B., and Melcher, M., *Analyst*, 1983, **108**, 213.
6. Akman, S., Genc, Ö., and Balkis, T., *Spectrochim Acta, Part B*, 1982, **37**, 903.
7. Murray, J. J., Papp, C., and Pottie, R. F., *J. Chem. Phys.*, 1973, **58**, 2569.
8. Gentner, J. L., Bernardt, C., and Cadoret, R., *J. Cryst. Growth*, 1982, **56**, 332.
9. Ban, V. S., and Ettenberg, M., *J. Phys. Chem. Solids*, 1973, **34**, 1119.
10. Rosen, B., *Editor*, "International Tables of Selected Constants, No. 17, Spectroscopic Data Relative to Diatomic Molecules," Pergamon Press, Oxford, 1970.
11. Krasnova, K. S., "Molekulyarnye Postoianye Regragnitscheskich Soedinenii," Khimiya, Leningrad, 1979.
12. "Termitscheskiye Konstanty Weschtschestw," No. 3, Academy of Sciences of the USSR, Moscow, 1968.

Note: Reference 3 is to part I of this series.

Paper A5/114
Received March 27th, 1985
Accepted September 20th, 1985

Method for Improving the Sensitivity and Reproducibility of Hydride-forming Elements by Atomic Absorption Spectrometry

Nicolaos E. Parisis and Aubin Heyndrickx
Department of Toxicology, State University of Ghent, Hospitaalstraat 13, 9000 Ghent, Belgium

The positive effect of oxygen on the atomisation of hydride-forming elements at temperatures above 800 °C is indicated. Several different materials of construction for gas transport tubing were tested and their influence on the transportation of hydrides and on radical production was studied in order to ascertain their operating efficiency. Silanised glass and FEP tubing gave the highest sensitivity and reproducibility and silicone-rubber and nylon tubing the lowest. The combination of the above, together with the use of 2 M nitric acid as a rinsing agent for the reaction vessel, allows the convenient use of peak areas for the measurement of arsenic, selenium, bismuth, antimony and tin signals at levels of a few nanograms.

Keywords: *Atomic absorption spectrometry; hydride generation; oxygen - argon carrier gas; silanised glass tubing*

The atomisation mechanism for volatile hydride-forming elements in a heated quartz tube was generally thought to involve thermal decomposition. However, in the last few years, some workers have proposed a new mechanism in order to explain the increased sensitivity obtained in their experiments.

First, Dedina and Rubeska[1] suggested that hydride atomisation is caused by free radicals (H·, OH·) generated in the reaction zone of a hydrogen - oxygen flame burning in the T-shaped quartz tube of the system. Welz and Melcher,[2] in studies of the selenium interference with trivalent and pentavalent arsenic, found that the only theory that would explain the results was that selenium, which is volatilised earlier than arsenic, increases the deficiency of radicals so that for the arsenic that appears later there remains an insufficient number of radicals to cause atomisation to the same extent as in the absence of selenium. Moroever, arsenic has a considerably smaller effect on selenium than *vice versa*.

Recently, the same workers in another study[3] concluded that these radicals are formed in a reaction with oxygen at low temperatures (above 600 °C) and in a "clean" environment the concentration of radicals is well above the equilibrium concentration because their formation is a much faster process than the recombination. They found a significant enhancing effect of oxygen on the sensitivity of volatile hydride-forming elements at temperatures around 700–800 °C; they established that this cannot be due to a temperature increase in the gas phase (effective temperature) of the atomiser.

In this work, several investigations have been performed with a commercially available hydride system and an electrically heated quartz cell atomiser. The influence of different purge gases, gas transfer tubing and reaction flasks on the sensitivity of hydride-forming elements was studied.

Experimental

Apparatus

The instrument used was a Perkin-Elmer Model 372 atomic absorption spectrometer, equipped with an external electrodeless discharge lamp (EDL) power supply. Perkin-Elmer electrodeless discharge lamps were used for all elements. Results are shown on a four-digit electronic display. A simple diagram of the apparatus is shown in Fig. 1.

The hydride-generation device is a Perkin-Elmer MHS-20 mercury - hydride system. The volatilised hydrides are atomised in an electrically heated quartz tube (165 × 14 mm i.d.) closed at both ends by quartz windows. The quartz tube can be heated to 1000 °C by eight insulated heating wires. This atomisation device, mounted in the sample compartment of the spectrometer, is connected with an electronic system that allows one to select the required duration of purge and reaction, between sample and reagent solution, and controls the temperature to within ±20 °C by using an Ni - NiCr thermocouple and a feedback system.

Piston stroke pipettes of capacity 10, 25 and 50 µl (Assipette No. 100) and pipette tips from Assistent, Sondheim/Rhön, FRG, were used.

Tubing

Nylon tubing. From Perkin-Elmer (gas supply hose, 079873), 40 cm × 4 mm i.d.

Silicone-rubber tubing. From Perkin-Elmer (transfer hose, 094140), 40 cm × 4 mm i.d.

Soda-glass tubing. Made in our department from commercially available material, 44 cm × 4.5 mm i.d.

PTFE tubing. FEP (fluorinated ethylene - propylene) tubing from Rudolf Brand, Wertheim, FRG, 40 cm × 5.7 mm i.d.

Procedure

Table 1 gives the important operating parameters for the instrument, lamps and hydride system used for the determinations.

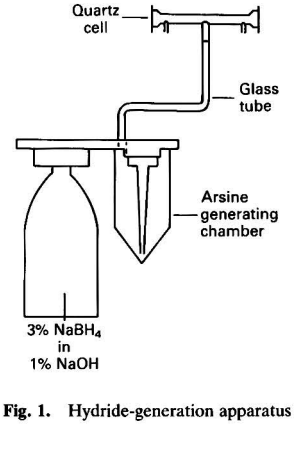

Fig. 1. Hydride-generation apparatus

Table 1. Operating parameters

Element	EDL power/W	Wavelength/ nm	Slit width/ nm	MHS-20 Purge I/ s	MHS-20 Reaction/ s	MHS-20 Purge II/ s
As(III)	8	193.7	0.7	40	4	20
Se(IV)	6	196.0	0.2	48	4	20
Bi(V)	8	223.1	0.2	25	4	30
Sb(III)	8	217.6	0.2	30	4	50
Sn(IV)	8	224.6	0.2	20	4	40

Other conditions were as follows: measuring mode, integrated peak area; reading time, 20 s; background correction, none; quartz cell temperature, 880 ± 20 °C; reaction volume, 10 ml; standard dilution liquid, 1.5% *m/V* H_2SO_4 [except for Sn(IV), 0.75% *m/V* H_2SO_4]; inlet pressure, 250 kN m^{-2}; and hydride-generating reagent, 3.92 ± 0.03 ml of 3% $NaBH_4$ in 1% NaOH, 18–22 °C.

For all the measurements, 10 ml of 1.5% *m/V* H_2SO_4 and an appropriate aliquot of the standard solution (10–50 µl) are added to the polypropylene reaction flasks before attachment to the system. When the start button of the control unit is activated, the purge gas flows through the reaction flask for a pre-selected time (purge I) at a flow-rate of 1000 ml min^{-1}, and purges the air from the system. Immediately after, the gas flow-rate is reduced to 400 ml min^{-1} and a pre-selected amount of tetrahydroborate solution flows through a capillary and the immersion tube into the bottom of the reaction vessel for a pre-selected time (reaction time). At the end of the reaction time, a second selected purge time (purge II) follows at a flow-rate of 1000 ml min^{-1}, in order to remove all gases from the system.

During all the experiments, after each determination of a blank or standard, the reaction vessel was rinsed with 2 M nitric acid (3 × 5 ml) and doubly distilled water (3 × 5 ml). This treatment, as emphasised by Moody and Lindstrom[4] and Reamer *et al.*,[5] is necessary in order to remove all traces of analyte from the walls of the hydride-generation chamber. In this way, the reproducibility of the results and the stability of the base line were greatly improved.

Background correction is usually essential for graphite furnace atomic absorption. However, in hydride systems this is generally not so because the analyte is separated from the sample matrix and only very few elements form hydrides and enter the quartz cell atomiser.[6] Volatile organic compounds, which could eventually interfere, are decomposed during preliminary ashing of the sample. Background correction could improve the precision of the results for arsenic and selenium owing to the small absorption (0.010 and 0.040 A s for arsenic and selenium, respectively) from the oxygen present in the purge gas. However, this absorption phenomenon is also the same for the blank. This, together with the instability of the deuterium hollow-cathode lamp at wavelengths less than 200 nm, which increases the base-line noise and the detection limit and influences the precision of low-level measurements dramatically, compared with measurements made using the electrodeless discharge lamp alone, does not permit its use.

Reagents

Sodium tetrahydroborate(III) solution, 3% *m/V.* Dissolve 30 g of analytical-reagent grade sodium tetrahydroborate(III) powder (Merck) and 10 g of analytical-reagent grade sodium hydroxide pellets (UCB) in 400 ml of doubly distilled water, dilute to 1 l and filter. Store in a refrigerator at 4 °C, where it remains stable for at least 1 week.

Sulphuric acid working solution, 1.5% *m/V.* The solution is obtained by diluting the appropriate volume of 96% *m/V* Suprapur sulphuric acid (Merck) to 1 l.

Nitric acid rinsing solution, 2 M. Prepared by diluting the appropriate volume of 65% *m/V* analytical-reagent grade nitric acid (Merck) to 1 l.

Stock standard solutions of As^{3+}, Sb^{3+} and Bi^{5+}, 1000 mg l^{-1}. Baker atomic spectral standards. Working standard solutions were prepared fresh daily by dilution with doubly distilled water.

Stock standard solution of Se^{4+}. Prepared by diluting Titrisol solution (Merck) containing 1000 g of selenium (as SeO_2) to 1 l with doubly distilled water. Aliquots were diluted with 1.5% *m/V* hydrochloric acid to obtain appropriate working standard solutions.

Stock standard solution of Sn^{4+}. Prepared by diluting a Titrisol solution (Merck) containing 1000 g of tin ($SnCl_4$) to 1 l with 10% *m/V* hydrochloric acid. A 50-µl volume of this solution was further diluted to 50 ml, and 1 ml further to 5 ml, both with 10% *m/V* hydrochloric acid, to obtain a 0.2 µg ml^{-1} working standard solution.

Carrier Gases

High-purity argon.
High-purity 99% argon + 1% oxygen (Cargal 1).
High-purity nitrogen.

These gases were used to purge the system and were obtained from L'Air Liquide, Afdeling Precigaz, Liège, Belgium.

Results and Discussion

Effect of Gas Transport Tubing

Different kinds of plastic and glass transfer tubing were tested in order to study their influence on the determination of 10 ng of As(III) by using the peak area as a measuring mode. In the first part of the experiments, nitrogen was the carrier gas for the hydrides. Silicone-rubber and nylon tubing gave identical results. The reproducibility was very low and the blank values were unstable. This is the main reason why other workers (see Table 4) have found it difficult to use peak areas, especially at analyte levels of 10 ng.

The use of glass tubing did improve the sensitivity and reproducibility but the base line remained unstable. A repeated number of blank determinations returned the absorbance values to the zero level. This indicates that a portion of the hydride was not atomised the first time but was absorbed on the surface of the reaction vessel or the gas transfer tubing, or both. This portion of the hydride was atomised when the repeated number of blank determinations was carried out. This is possibly the main reason for the low reproducibility of the standards.

Subsequently, the glass tubing was silanised in the following manner. It was thoroughly cleaned, dried and filled with a 5% *m/V* dimethyldichlorosilane solution in toluene. The organic solvent was allowed to evaporate at room temperature in a fume-cupboard for 2 h. Finally, the tube was emptied, heated for 1 h in an oven at 110 °C and a nitrogen stream was blown through it for 5 min. As is known, dimethyldichlorosilane reacts with the surface hydroxy groups and deactivates the

Table 2. Precision of replicate analyses of 10 ng of As(III)

Gas transfer tubing	Carrier gas	Peak height, A (mean ± standard deviation)	Peak area/A s: Mean ± standard deviation/ A s	Peak area/A s: No. of analyses	Peak area/A s: Relative standard deviation, %
Silicone-rubber*	N_2	0.062 ± 0.004	0.265 ± 0.029	10	10.9
Glass	N_2		0.323 ± 0.023	10	7.1
FEP	N_2		0.382 ± 0.013	10	3.4
Silanised glass	N_2		0.385 ± 0.013	10	3.4
Silicone-rubber	Ar	0.063 ± 0.003	0.414 ± 0.019	10	4.6
FEP	Ar		0.479 ± 0.011	10	2.3
Silicone-rubber	99% *V/V* Ar - 1% *V/V* O_2		0.688 ± 0.021†	10	3.0
Glass	99% *V/V* Ar - 1% *V/V* O_2		0.710 ± 0.017	10	2.4
Silanised glass	99% *V/V* Ar - 1% *V/V* O_2	0.082 ± 0.002	0.726 ± 0.011‡	10	1.5
FEP	99% *V/V* Ar - 1% *V/V* O_2		0.728 ± 0.009‡	10	1.2

* Silicon-rubber and nylon tubing gave similar results.
† After 200–220 determinations.
‡ After 25–30 determinations.

glass surface, and this treatment further improved the sensitivity and reproducibility. When not used, the silanised glass tubing was cleaned with 3 × 3 ml of toluene and 3 × 3 ml of methanol, dried with a stream of nitrogen for 5 min and kept in a desiccator; it is well known that moisture destroys the silanised glass surface. After the tubing had been used for more than 500 determinations within a period of 3 weeks, the silanisation process had to be repeated.

When argon was used as the carrier gas, all results were higher than those obtained with nitrogen. This difference could be caused by the lower heat capacity of argon compared with nitrogen, resulting in a higher atomisation temperature when using argon. This is supported by the fact that when nitrogen was used, the cell temperature indicator on the front panel of the controller was frequently switched off during the determination, indicating that the feedback circuit was not able to maintain the temperature at the pre-selected value. This was not so when argon or 99% *V/V* argon - 1% *V/V* oxygen was used.

The results are shown in Table 2.

Effect of 99% *V/V* Argon - 1% *V/V* Oxygen as a Purge Gas

The use of nylon or silicone-rubber tubing together with 99% *V/V* argon - 1% *V/V* oxygen as a purge gas slowly and stably increased the sensitivity, which reached its maximum level after about 200 determinations. The reproducibility was low and memory effects made the method time consuming and impractical. Cleaning the nylon and silicone-rubber tubing with methanol and drying with nitrogen destroyed the previously increased sensitivity. As indicated by Reamer *et al.*[5] with radiotracer techniques for hydride generators, plastic materials initially retain or decompose a considerable portion of the generated hydride, but as subsequent reactions are performed, the amount retained or decomposed decreases and larger portions can enter the atomiser, resulting in an increase in sensitivity. It is possible that the available absorption sites on the walls of the 40 cm long plastic tubing are being filled with the metal or the hydride and therefore deactivating the surface towards further hydride absorption. On washing the tubing with methanol it is possible that the surface reverted to its original high absorption characteristics, resulting in a decrease in the signal for the same amount of generated hydride. With glass tubing, better results were obtained, but the memory effects still remained a serious problem.

Silanised glass and FEP tubing gave the most satisfactory results, with a stable base line even if a standard as high as 50 ng of As(III) was determined. A series of five standards of 10 ng of As(III) also did not leave any memory effect.

The probability of free atom formation from the hydride is proportional to the number of collisions with free radicals. This indicates that the atomisation efficiency increases as the number of radicals increases. This is the reason why, when a quartz cell is used that has been cleaned with hydrofluoric acid for 15 min, the peak-area values of a repeatedly determined standard slowly increase and after about 30 determinations the sensitivity reaches its maximum value.

The surface of the quartz cell has an important effect on sensitivity. It probably catalyses the formation of radicals and subsequently the atomisation of hydrides. The quartz cell can be stored in a desiccator and re-used for another day without any decrease in sensitivity.

The replacement of 99% *V/V* argon - 1% *V/V* oxygen with nitrogen does not destroy the sensitivity immediately. The peak area of the first standard has the same value as when 99% *V/V* argon - 1% *V/V* oxygen is used; that for the second standard will be smaller, the third even smaller, and so on. The population of the radicals in the cell was high enough to atomise the first standard completely. However, with the use of nitrogen, the consumption of radicals is greater than its production, with the result that the second standard will not be completely atomised and will give smaller values. As Welz and Melcher[3] suggested, when nitrogen or argon is used, the gas bubbles through the sample solution during the purge time and drives the dissolved air out of the solution. If the purge time is less than 60 s, dissolved oxygen still remains in the sample, and this, together with the hydrogen generated from sodium tetrahydroborate(III) during the reaction time, produces a limited number of radicals in the heated quartz cell. Results obtained with the use of 99% *V/V* argon - 1% *V/V* oxygen are given in Table 2.

The sensitivities attained for the different hydride-forming elements using 99% *V/V* argon - 1% *V/V* oxygen as a purge

Table 3. Precision of replicate analyses using silanised glass tubing and 99% *V/V* argon - 1% *V/V* oxygen

Element (10 ng)	Peak area: Mean ± standard deviation/ A s	No. of analyses	Relative standard deviation, %
As(III)	0.726 ± 0.011	10	1.5
Se(IV)	0.469 ± 0.007	10	1.5
Sb(III)	0.420 ± 0.010	10	2.4
Bi(V)	0.442 ± 0.008	10	1.8
Sn(IV)	0.599 ± 0.015	10	2.5

Table 4. Calculated sensitivities obtained by different recent methods

Element (10 ng)	Sensitivity: Absorbance	Mode	Reference
Se(IV)	0.100	Peak area	7
As(III)	0.070	Peak height	3
As(III)	0.080	Peak height	8
Sb(III)	0.036	Peak height	9
Bi(III)	0.028	Peak height	9
Se(IV)	0.025	Peak height	9
Sn(IV)	0.030	Peak height	9
As(III)	0.100	Peak height	10
Sb(III)	0.001	Peak height	11
Sb(III)	0.017	Peak height	12
Sb(III)	0.045	Peak height	13
Bi*	0.015	Peak height	14
Se(IV)	0.025	Peak height	15

* Not specified.

gas, the operating parameters in Table 1 and silanised glass tubing are listed in Table 3. A comparison with recently reported values in the literature is shown in Table 4.

Effect of Reaction Flask Material

Reamer *et al.*[5] found that glass and polypropylene reaction vessels exhibit the greatest absorption of selenium and silanised glass the least. In our experiments with the same materials, statistically no difference was observed in the peak-area values for 10 ng of selenium. The possible reason is that in this system a 100-fold smaller standard of selenium and a much smaller reaction vessel are used. In addition, the sodium tetrahydroborate(III) solution flows through a capillary into the lowest part of the V-shaped reaction flask, which achieves more complete hydride generation.

Conclusions

Oxygen has an effect on the determination of volatile hydride-forming elements, not only at low quartz cell temperatures, as indicated by Welz and Melcher,[3] but also at temperatures above 800 °C, possibly by accelerating the production of radicals that may take part in the atomisation mechanism of the hydrides. The use of silanised glass or FEP tubing aids the transportation of gases and the maximum sensitivity can be attained after a few determinations. This method permits the use of peak areas as a measuring mode for the routine determination of hydride-forming elements. One of the advantages of peak-area over peak-height values is the smaller dependence on or independence of fluctuations of parameters such as the valence state of the analyte, reaction speed and time, sodium tetrahydroborate(III) concentration, acid concentration, temperature changes of the quartz cell and gas flow-rates.

References

1. Dedina, J., and Rubeska, I., *Spectrochim. Acta, Part B,* 1980, **35**, 119.
2. Welz, B., and Melcher, M., *Anal. Chim. Acta,* 1981, **131**, 17.
3. Welz, B., and Melcher, M., *Analyst,* 1983, **108**, 213.
4. Moody, J. R., and Lindstrom, R. M., *Anal. Chem.,* 1977, **49**, 14, 2264.
5. Reamer, D. C., Veillon, C., and Tokousbalides, P. T., *Anal. Chem.,* 1981, **53**, 245.
6. Dong Soo Lee, *Anal. Chem.,* 1982, **54**, 1682.
7. Lloyd, B., Holt, P., and Delves, H. T., *Analyst,* 1982, **107**, 927.
8. Welz, B., and Melcher, M., *Analyst,* 1984, **109**, 573.
9. Welz, B., and Melcher, M., *Spectrochim. Acta, Part B,* 1981, **36**, 5, 439.
10. Siemer, D., Koteel, P., and Jariwala, V., *Anal. Chem.,* 1976, **48**, 836.
11. Aznárez, J., Palacios, F., Ortega, M. S., and Vidal, J. C., *Analyst,* 1984, **109**, 123.
12. Chapman, J. F., and Dale, L. S., *Anal. Chim. Acta,* 1979, **111**, 137.
13. De Doncker, K., Dumarey, R., Dams, R., and Hoste, J., *Anal. Chim. Acta,* 1983, **153**, 33.
14. Terashima, S., *Anal. Chim. Acta,* 1984, **156**, 301.
15. Verlinden, M., Baart, J., and Deelstra, H., *Talanta,* 1980, **27**, 633.

Paper A5/232
Received June 27th, 1985
Accepted September 20th, 1985

Studies on the Determination of Cadmium in Blood by Furnace Atomic Non-thermal Excitation Spectrometry

Heinz Falk, Erwin Hoffmann and Christian Ludke
Central Institute for Optics and Spectroscopy, Academy of Sciences of GDR, Rudower Chaussee 5, 1199 Berlin, GDR

and John M. Ottaway and David Littlejohn
Department of Pure and Applied Chemistry, University of Strathclyde, Cathedral Street, Glasgow G1 1XL, UK

Cadmium atomic emission can be detected in a FANES low-pressure Ar discharge at atomiser temperatures as low as 140 °C when the analyte is present as $CdCl_2$. Cadmium chloride molecules vaporised at this temperature are dissociated by electron impact in the discharge, giving a substantial Cd atom concentration before thermal dissociation of the molecules becomes feasible. This results in a 100-fold greater tolerance towards chloride matrix chemical interferences than encountered for Cd in ETA-AAS with tube-wall atomisation. However, the determination of cadmium in deproteinised whole blood by FANES is not totally interference free and a standard additions procedure is required to give an accurate determination. The FANES instrument detection limit for Cd was calculated to be 0.04 μg l^{-1}. For the deproteinisation procedure applied, the detection limit for cadmium in whole blood was 0.2 μg l^{-1}.

Keywords: *Atomic emission spectrometry; low-pressure discharge; electrothermal atomisation; electron-impact molecular dissociation; blood matrix interferences*

The determination of cadmium in biological samples by atomic absorption spectrometry with electrothermal atomisation (ETA-AAS) is well established in clinical analysis. However, as with most volatile elements, the measurement of Cd AAS signals is subject to severe chemical and spectral matrix interference effects when conventional tube-wall atomisation procedures are applied. As cadmium has a comparatively low atom appearance temperature, it is not normally possible to ash biological samples at temperatures that allow the complete removal of organic and inorganic matrix constitutents prior to the atomisation stage. Hence, cadmium atom formation tends to be suppressed by the presence of a large excess of chloride salts, and substantial non-specific background absorption invariably occurs. To minimise the influence of these effects in the determination of Cd in whole blood, a variety of regimes has been implemented including the use of matrix matching, matrix modification, platform atomisation and Zeeman-effect background correction.

Stoeppler and Brandt[1] reduced the mass of carbonaceous matter injected into the atomiser tube by deproteinisation of 50–200-μl volumes of whole blood with 1 M HNO_3. Pleban and Pearson[2] simply diluted whole blood with 5% *V/V* HNO_3 for the determination of Cd by Zeeman effect - ETA-AAS using a standard additions procedure. Matrix modification with $(NH_4)_2HPO_4$ was applied by Subramanian and Meranger[3] to determine Cd directly in blood. A similar procedure was reported by Delves and Woodward,[4] but oxygen was added to the atomiser gas flow during the ashing stage to assist removal of the blood matrix. Matrix modification was also used by Hinderberger *et al.*[5] in conjunction with platform atomisation, and Claeys-Thoreau[6] employed platform atomisation and Zeeman-effect background correction for the determination of Cd in blood diluted 1 + 9 with Triton X-100.

It is generally accepted that the mechanism of cadmium atomisation depends on the chemical nature of the sample matrix. When present as the chloride, $CdCl_2$, cadmium atoms are formed by thermal dissociation of gaseous CdCl molecules produced on vaporisation of $CdCl_2$. In the presence of an excess of chloride salts, however, atom formation is impaired, as reported by Barnard and Fishman[7] for solutions containing 1% *m/V* NaCl, KCl, $MgCl_2$ or $CaCl_2$. Similar observations for tube-wall atomisation have been reported by other workers.[8,9] When cadmium is present as an oxy-anion two mechanisms of atom formation are feasible. In an early study, Campbell and Ottaway[10] suggested that CdO was reduced on the graphite surface to produce Cd atoms. Salmon and Holcombe[11] also supported the oxide reduction mechanism and have postulated that metallic Cd is formed on the graphite tube. In contrast, L'vov and Ryabchuk[12] believe that CdO is dissociated in the vapour state. This mechanism was also suggested by Sturgeon and Chakrabarti[13] and has been supported by more recent work by Sturgeon and co-workers.[14,15]

In this work, the atomisation of cadmium from chloride and nitrate matrices has been studied as part of an investigation aimed at the development of a method for the determination of Cd in whole blood by furnace atomic non-thermal excitation spectrometry (FANES). The characteristics of furnace atomisation with non-thermal excitation have been described in recent publications.[16–19] The technique involves conventional electrothermal atomisation of samples in a tube atomiser in which a low-pressure gas discharge is simultaneously generated using the graphite tube as the cathode. The system therefore combines the efficiency of electrothermal vaporisation and atomisation with the high excitation capability of a hollow-cathode type discharge. Although thermal excitation in a conventional electrothermal atomiser allows the measurement of atomic emission signals for many elements with high sensitivity,[20,21] energy levels greater than 4 eV are not significantly populated. In contrast, the FANES source is ideally suited to the excitation of metals and non-metals with high excitation potentials (*e.g.*, cadmium, zinc, selenium and halogens). Hence FANES combines many of the attractive features of ETA-AAS and plasma emission spectrometry, not least of which are sub-μg l^{-1} detection limits and the ease of operation in a simultaneous multi-element mode.

In previous FANES studies, the instrumental features of the system have been described and the analytical characteristics of the source established with respect to analyte detection limits.[16–19] However, to date, the atomiser has been applied to relatively few analytical problems and a primary aim of this work was to assess the suitability of the FANES method for

the determination of a relatively volatile element such as cadmium in a complex matrix such as whole blood. As the FANES atomiser is operated at low pressure and the sample is vaporised into a low-pressure discharge, it was expected that the analytical behaviour of the source would be different to that of a conventional electrothermal atomiser as applied in atomic absorption spectrometry for this analysis. The influence of alkali and alkaline earth metal salts on the vaporisation and atomisation of cadmium in the FANES atomiser has been studied and compared with observations reported in the ETA-AAS literature. The results of the study indicated that the presence of a high-energy discharge assists the dissociation of vapour-phase molecules and for this reason the influence of NaCl, KCl, $MgCl_2$ and $CaCl_2$ on Cd atom production is less pronounced than in a conventional electrothermal atomiser.

Experimental

Instrumentation

The FANES source, which has been decribed in detail in previous publications,[16-19] consisted of a sealed atomiser chamber and power supply unit with separate functions that controlled the heating of the graphite tube and the establishment of the discharge. The atomiser was water cooled, and connected to a mechanical pump for evacuation and an argon gas supply system for purging of the tube and formation of the low-pressure Ar discharge. The FANES atomiser tube was similar in dimensions to that used in the Perkin-Elmer HGA-500 graphite furnace.

With the exception of the discharge pressure (1–20 Torr) and current (15–60 mA), which were set manually, all parameters were under microprocessor control. A series of up to ten temperature stages could be selected via the instrument's microcomputer. At each step in the temperature programme the operator selected a temperature (up to 3000 °C), a linear ramp rate (0–2000 °C s^{-1}) and a hold time. On the basis of the selected temperature and ramp rate, the microprocessor computed the ramp time. The selection of atomiser gas flow-rate at atmospheric pressure, the initiation of the evacuation stage and the establishment of the discharge were also under computer control and the required conditions were selected when compiling the various steps in the atomiser programme.

In this study, the FANES source was operated in conjunction with a laboratory-contructed 1.5-m Rowland circle polychromator equipped with a 2000 grooves mm^{-1} grating. All cadmium atomic emission measurements were made at the Cd 228.8-nm resonance line wavelength with a spectral band pass of 0.017 nm. Emission signals were recorded on a K 201 Jenoptik chart recorder. For atomic absorption measurements, a Cd hollow-cathode lamp was positioned such that the lamp radiation was focused through the FANES atomiser and on to the polychromator entrance slit.

FANES Operational Procedure

The operation of the FANES source is analogous to that used in conventional atomisation. The main difference in the furnace programme occurs prior to and during the atomisation stage. A sample aliquot (typically 10 or 20 µl) was injected into the graphite tube by means of a micropipette and dried and ashed at atmospheric pressure with the injection port lid open and a purge gas flow-rate of 80 l h^{-1} to remove matrix vapours from the atomiser. The injection port lid was then closed, the atomiser evacuated to a pressure of about 10^{-2} Torr, the argon discharge gas pressure established (1–20 Torr) and the discharge formed. This sequence was initiated by selection of the appropriate parameters in the programme step prior to the intended atomisation stage. The conditions of pump-down could be arranged to allow a continuation of the ashing step during the evacuation procedure. As in a conventional atomisation regime, the temperature and ramp rate of the atomisation stage were normally selected to give rapid vaporisation and atomisation of the analyte. In the discharge the analyte atoms were excited and the resulting emission signal detected with the polychromator. When atomic absorption measurements were required with the FANES atomiser, the programme was modified to either prevent formation of a discharge or eliminate the evacuation - discharge sequence entirely.

The optimum atomiser programme devised for the determination of cadmium in blood is given in Table 1. Modified versions of the programme employed in the chloride salt interference studies are indicated in the appropriate section of the text.

Preparation of Whole Blood Samples

To minimise the mass of carbonaceous material atomised in the FANES source a deproteinisation procedure similar to that developed by Stoeppler and Brandt[1] was applied. A 200-µl volume of whole blood was mixed with 200 µl of water or aqueous calibration solution, 50 µl of concentrated nitric acid were added and the mixture was centrifuged for 7 min to produce a clear supernatant solution over the protein precipitate. Volumes of the deproteinised solution (10 or 20 µl) were then injected into the FANES atomiser for the determination of cadmium.

Table 1. FANES programme for the determination of cadmium in deproteinised blood

Step	Temperature/ °C	Ramp rate/ °C s^{-1}	Ramp time*/ s	Hold time/ s	Total step time/ s	Functions	Argon pressure/ Torr	Gas flow-rate/ l h^{-1}
Dry†	150	3	45.0	5	50		760	80
Ash	350	100	2.0	28	30		760	80
Purge‡	35	NP§	6.7	5	11.7		760	80
Evacuate	35	0	0	45	45	E45¶	19	0
Pre-atomisation‖	100	30	2.1	90	92.1		19	0
Atomise	600	600	0.8	9	9.8		19	0
Clean	2000	1000	1.9	3	4.9		760	80

* Calculated from temperature difference and ramp rate selected; for the first step an ambient temperature of 15 °C was assumed.

† Conditions for 10-µl injection volumes.

‡ Additional step used in this application to remove matrix vapour without tube heating.

§ NP implies "no power."

¶ When the "E" function is selected evacuation begins at the start of the step, with discharge on after 45 s in this instance; 30 mA current selected; discharge on until end of atomise step.

‖ Step used to stabilise discharge before atomisation; could have been redued to 20–30 s.

Reagents

Stock solutions of $CdCl_2$, NaCl, KCl, $MgCl_2$ and $CaCl_2$ were prepared by dissolving salts of the highest available purity in distilled water. High-purity nitric acid was used for the deproteinisation of blood samples and for the addition to $CdCl_2$ standard solutions.

Results and Discussion

Vaporisation Characteristics of Cadmium Salts in the FANES Atomiser

It was considered probable that the vaporisation charcteristics of cadmium salts in FANES would be different to those observed in conventional ETA-AAS as atomisation occurs at low pressure and in the environment of a low-pressure discharge. To investigate the influence of both conditions on cadmium atom production in the FANES atomiser, atomic absorption and atomic emission measurements were obtained following vaporisation of cadmium from chloride and nitrate media. In initial experiments, cadmium atomic emission and atomic absorption signals were obtained for the vaporisation of 10-μl volumes of a 100 μg l^{-1} cadmium solution prepared from $CdCl_2$. Emission or absorption signals were obtained for FANES atomisation temperatures in the range 100–1000 °C, at a linear ramp rate of 600 °C s^{-1}. The emission measurements were obtained in the presence of an Ar discharge at 17 Torr, and absorption measurements were made without a discharge at 17 Torr or at atmospheric pressure. At an argon pressure of 17 Torr the maximum cadmium atomic emission and atomic absorption signals were obtained at a similar temperature of about 520 °C as measured with a thermocouple. The first appearance of a cadmium atomic emission signal occurred at a tube temperature of 140 °C. In contrast, however, without the presence of a discharge, atomic absorption signals at 17 Torr were not measured until temperatures above 300 °C. Plots of the relative integrated cadmium atomic emission and atomic absorption signals obtained at 17 Torr for atomisation temperatures in the range 100–1000 °C are illustrated in Fig. 1, together with the corresponding plot for cadmium atomic absorption at atmospheric pressure. The fact that the cadmium emission signal appeared at a considerably lower temperature than the atomic absorption signal at the same pressure suggests that at 17 Torr vaporisation of $CdCl_2$ begins at temperatures as low as 140 °C and that dissociation of gaseous CdCl or $CdCl_2$ molecules by electron impact in the discharge results in the formation of cadmium atoms at atomiser temperatures much lower than would normally be expected. Without the assistance of the discharge, dissociation of vaporised CdCl - $CdCl_2$ molecules is a purely thermal process and at 17 Torr did not occur until the atomiser tube had reached a temperature of approximately 300 °C. At atmospheric pressure significant cadmium atom formation did not occur until about 360–380 °C and the maximum AAS signal was obtained at about 680 °C.

When an excess of chloride salts is present in solution, the vaporisation characteristics of $CdCl_2$ are altered noticeably. Fig. 2 shows the vaporisation curves for cadmium atomic emission obtained at 10 and 17 Torr in the presence of 0.1% *m/V* NaCl and 0.05% *m/V* $MgCl_2$ when the atomiser tube was heated to temperatures in the range 100–1000 °C at a ramp rate of 600 °C s^{-1}. At 17 Torr the first appearance of cadmium atomic emission occurs at about 320 °C, probably because the evaporation of $CdCl_2$ is impaired owing to the occlusion of the cadmium salt in the NaCl - $MgCl_2$ matrix. When the discharge pressure is reduced to 10 Torr, evaporation of the chloride salt matrix occurs at a lower temperature and the first appearance of cadmium atomic emission occurs at 200 °C. Fig. 2 also indicates the vaporisation curve for cadmium in the presence of 0.01% *V/V* HNO_3. Although the cadmium solution was prepared from $CdCl_2$, the presence of an excess of oxy-anion probably ensured the formation of CdO, which has a higher vaporisation temperature than $CdCl_2$. A comparison of the vaporisation curves for $CdCl_2$ and "CdO" in Figs. 1 and 2, respectively, (17 Torr) suggests that the dissociation of the gaseous CdO molecules by electron impact in the discharge is less efficient than dissociation of CdCl or $CdCl_2$ by the same process.

Influence of Chloride Salts on Cadmium Atomic Emission Intensity in FANES

From ETA-AAS studies based on tube-wall atomisation,[9] it is known that a matrix of 0.01% *m/V* NaCl and 0.005% *m/V* $MgCl_2$ causes a 10% depression of the Cd AAS signal. As electron impact in the FANES discharge apparently assists the dissociation of gaseous CdCl - $CdCl_2$ molecules, it was expected that chloride interference effects would be less severe in FANES. Solutions containing 2, 5, 10 and 20 μg l^{-1} of Cd as $CdCl_2$ were prepared in aqueous, 0.01% *V/V* HNO_3 and 0.1% *m/V* NaCl - 0.05% *m/V* $MgCl_2$ solutions. For each solution, 10-μl volumes were injected into the FANES atomiser, dried at 150 °C with a ramp rate of 5 °C s^{-1} and then atomised into the discharge under atomisation conditions of 750 °C and 600 °C s^{-1}. Cadmium atomic emission signals obtained for an Ar pressure of 19 Torr and a discharge current of 30 mA are illustrated in the form of calibration graphs in Fig. 3. No significant difference was observed in the Cd atomic emission intensities obtained for each solution matrix. The slight curvature in the calibration graph observed at 20 μg l^{-1} of Cd was probably due to self-absorption of the Cd line profile.

As there was no apparent interference of 0.1% *m/V* NaCl and 0.05% *m/V* $MgCl_2$ on the Cd atomic emission signal, the interferent concentrations were increased to determine the

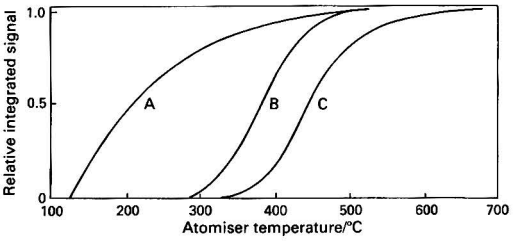

Fig. 1. Relative integrated atomic emission and atomic absorption signals for 10 μl of 100 μg l^{-1} of Cd at different atomisation temperatures. (A) FANES, 17 Torr Ar, 30 mA; (B) AAS, 17 Torr Ar; (C) AAS, 1 atm Ar. Plotted relative to individual maximum signals obtained at 520 °C for A and B and 680 °C for C

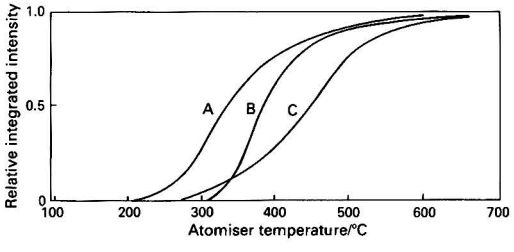

Fig. 2. Relative integrated FANES intensities for 10 μl of 100 μg l^{-1} Cd in different matrix solutions and at different atomisation temperatures. (A) 10 Torr Ar, 30 mA, 0.1% *m/V* NaCl - 0.05% *m/V* $MgCl_2$; (B) 17 Torr Ar, 30 mA, 0.1% *m/V* NaCl - 0.05% *m/V* $MgCl_2$; (C) 17 Torr Ar, 30 mA, 0.01% *V/V* HNO_3. Plotted relative to individual maximum signals at 580 °C for A and 650 °C for B and C

interference-free limit for FANES Cd determinations. Solutions containing 10 μg l^{-1} of Cd and various concentrations of NaCl, KCl, $MgCl_2$ and $CaCl_2$ were prepared, up to levels in excess of the expected concentrations of chloride salts in undiluted whole blood. As shown in Fig. 4, a significant reduction in the Cd atomic emission intensity occurred only at a combined chloride concentration of 1.0% *m/V* NaCl, 1.0% *m/V* KCl, 0.5% *m/V* $MgCl_2$ and 0.5% *m/V* $CaCl_2$, about two orders of magnitude higher than the onset of chloride interference in conventional ETA-AAS.[9]

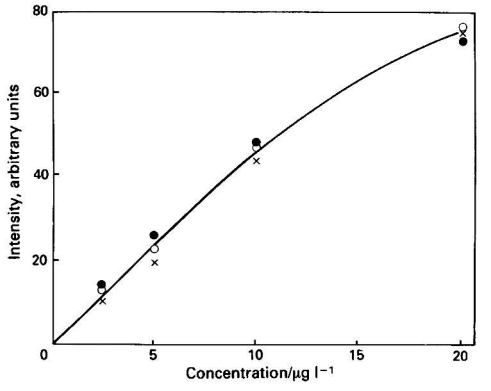

Fig. 3. FANES calibration graphs for Cd in (○) aqueous solution; (×) 0.01% *V/V* HNO_3; and (●) 0.1% *m/V* NaCl - 0.05% *m/V* $MgCl_2$; conditions as indicated in the text

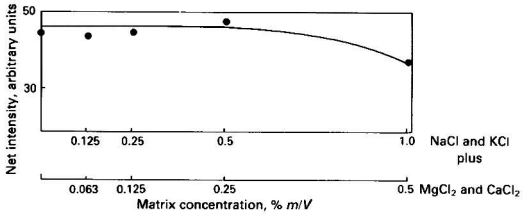

Fig. 4. Effect of various combined concentrations of NaCl, KCl, $MgCl_2$ and $CaCl_2$ on the FANES atomic emission intensity for 10 μl of 10 μg l^{-1} of Cd

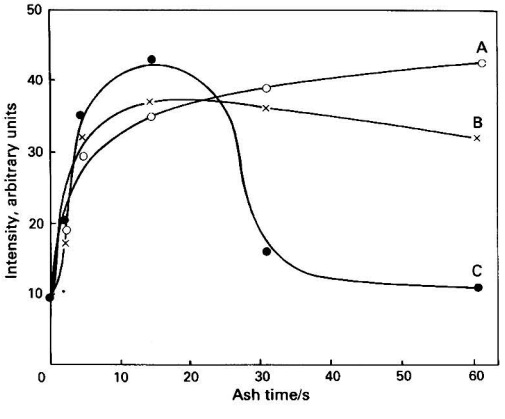

Fig. 5. Influence of ashing time on the FANES atomic emission intensity for 10 μl of 20 μg l^{-1} Cd at ashing temperatures of (A) 300, (B) 350 and (C) 400 °C

Determination of Cadmium in Whole Blood

Although the deproteinisation procedure described previously was used to minimise the mass of carbonaceous material injected into the atomiser, sufficient of the blood matrix remained to merit the inclusion of an ashing step in the analytical programme. Ashing temperatures of 300, 350 and 400 °C were investigated. The Cd atomic emission signals obtained for 10-μl injection volumes of a 20 μg l^{-1} solution after ashing at the above temperatures for 2–60 s are given in Fig. 5. Optimum ashing conditions of 350 °C for 30 s were selected as indicated in Table 1.

The cadmium atomic emission vaporisation curve for a deproteinised blood solution containing 10% *V/V* HNO_3 was obtained and compared with the corresponding curve for an aqueous Cd solution containing the same HNO_3 concentration. The cadmium concentration in both solutions was 20 μg l^{-1} and separate 10-μl injection volumes were dried, ashed and then atomised at a ramp rate of 600 °C s^{-1} to various atomisation temperatures in the range 100–700 °C at 100 °C intervals. Although, as indicated in Fig. 6, there appears to be no significant difference in the vaporisation curves obtained for the two solutions, closer inspection in comparison with the vaporisation curves at 17 Torr in Fig. 2 suggests that the chloride salts present in the deproteinised blood solution may still influence the vaporisation of cadmium even though HNO_3 is present in a large excess.

From the results presented in Figs. 2–6, it was concluded that the chloride and organic constituents of the deproteinised blood sample were unlikely to exert a severe interference on the determination of cadmium by FANES. However, as indicated in Fig. 7, there was a substantial difference in the slopes of the deproteinised blood standard additions graph and the aqueous cadmium calibration graph when both sets of solutions contained an equal concentration of HNO_3. For Cd concentrations in the range 2.5–20 μg l^{-1}, the atomic emission intensity for the deproteinised blood sample was only 20% of the equivalent signal for the HNO_3 solution. The deproteinisation process may not have released all the Cd attached to blood protein, which would result in a lower than expected concentration of the metal in the supernatant liquid injected into the FANES atomiser. However, previous experience with the protein precipitation procedure suggests that at a nitric acid concentration of 10% *V/V* incomplete release of Cd is unlikely. An alternative explanation is that residual organic components and inorganic species, other than chloride salts,

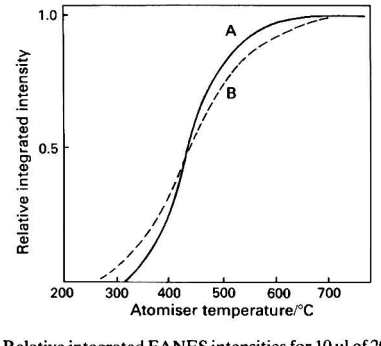

Fig. 6. Relative integrated FANES intensities for 10 μl of 20 μg l^{-1} of Cd in (A) deproteinised whole blood and (B) 10% *V/V* HNO_3 at different atomisation temperatures. Conditions as in text and Table 1; results plotted relative to individual maximum signals at 750 °C

vaporised during the atomisation stage altered the discharge conditions, which may have had an adverse effect on the cadmium atom excitation.

As it was not possible to analyse deproteinised blood samples by direct comparison with cadmium standard solutions prepared in nitric acid, a standard additions procedure was used to determine the Cd concentration of two whole blood samples supplied by the Biochemistry Department at Glasgow Royal Infirmary. The values obtained are given in Table 2, together with the concentrations determined by ETA-AAS at the hospital. Good agreement was achieved between the two techniques. The Cd detection limit of the FANES standard additions procedure was calculated to be 0.2 μg l^{-1} on a 2σ basis. For aqueous solutions containing 10% *V/V* HNO_3 the Cd detection limit was a factor of 5 lower, 0.04 μg l^{-1}. The relative standard deviation of the standard additions procedure was about 10% for the two blood samples analysed. This is a precision of at least a factor of two poorer than would normally be expected for conventional ETA-AAS with manual pipetting. The precision was impaired by the spreading of the nitric acid solution droplets in the tube during the drying sequence, and was also influenced by the blank correction required to take account of the cadmium content of the nitric acid available during this study.

Conclusions

The measurements reported in this work confirmed the widely held opinion that when present as $CdCl_2$, cadmium atom formation proceeds through the dissociation of gaseous CdCl molecules. The dissociation is assisted in the FANES discharge by electron impact and Cd atoms are formed at temperatures as low as 140 °C at 17 Torr. Without the action of the low-pressure discharge, thermal dissociation of CdCl molecules does not occur until around 300 °C at this pressure. Although an excess concentration of alkali and alkaline earth metal chloride salts retards the vaporisation of $CdCl_2$, no significant chemical interferences were encountered until the combined concentrations of NaCl, KCl, etc., had reached 2–3% *m/V*.

In an oxy-anion medium (*e.g.*, HNO_3), it is likely that CdO is formed at some stage in the atomisation process. The vaporisation studies conducted with FANES for Cd in HNO_3 do not prove conclusively that Cd atoms are formed by the dissociation of gaseous CdO molecules. However, at low pressure the volatility of CdO will undoubtedly increase and it is possible that electron impact in the discharge will assist the thermal dissociation of CdO. Additional measurements of both cadmium atomic absorption and atomic emission signals are required in this instance to give a clear indication of the atomisation mechanism in the FANES atomiser.

The chemical interferences encountered in the analysis of deproteinised blood may be due to the action of organic and inorganic constituents (other than chloride salts) on the nature of the discharge. Further fundamental studies of the excitation conditions during atomisation are required in order to assess the influence of the blood matrix in the determination of Cd. Experiments of this nature are in progress. However, the FANES atomiser clearly has potential advantages over conventional ETA-AAS with regard to its tolerance to chloride salt interferences.

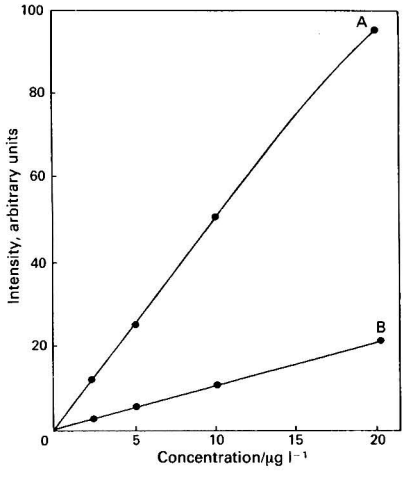

Fig. 7. FANES calibration graphs for Cd in (A) 10% *V/V* HNO_3 and (B) deproteinised whole blood. Conditions as in text and Table 1

Table 2. Determination of cadmium in deproteinised whole blood by FANES and ETA-AAS

	Concentration/μg l^{-1}	
Sample	FANES	ETA-AAS*
1	19.5 ± 2.0	19.6
2	8.5 ± 0.9	8.8

* Samples and values provided by Glasgow Royal Infirmary, Department of Clinical Biochemistry.

This work was made possible by the Cultural Exchange Agreement between the Royal Society in the UK and the Academy of Sciences of the GDR. The authors are extremely grateful for the opportunity for collaborative study and for the financial support provided through the Exchange Scheme. Financial support from the Pye Foundation (for D. L.) is also gratefully acknowledged. The authors thank Dr. G. S. Fell and Dr. D. J. Halls, Department of Clinical Biochemistry, Glasgow Royal Infirmary, for the provision of blood samples.

References

1. Stoeppler, M., and Brandt, K., *Fresenius Z. Anal. Chem.*, 1980, **300**, 372.
2. Pleban, P. A., and Pearson, K. H., *Clin. Chim. Acta*, 1979, **99**, 267.
3. Subramanian, K. S., and Meranger, J. C., *Clin. Chem.*, 1981, **27**, 1866.
4. Delves, H. T., and Woodward, J., *At. Spectrosc.*, 1981, **2**, 65.
5. Hinderberger, E. J., Kaiser, M. L., and Koirtyohann, S. R., *At. Spectrosc.*, 1981, **2**, 8.
6. Claeys-Thoreau, F., *At. Spectrosc.*, 1982, **3**, 188.
7. Barnard, W. M., and Fishman, M. J., *At. Absorpt. Newsl.*, 1973, **12**, 118.
8. Cruz, R. B., and Van Loon, J. C., *Anal. Chim. Acta*, 1974, **72**, 231.
9. Campbell, W. C., and Ottaway, J. M., *Analyst*, 1977, **102**, 495.
10. Campbell, W. C., and Ottaway, J. M., *Talanta*, 1974, **21**, 837.
11. Salmon, S. G., and Holcombe, J. A., *Anal. Chem.*, 1982, **54**, 630.
12. L'vov, B. V., and Ryabchuk, G. N., *Spectrochim. Acta, Part B*, 1982, **37**, 673.
13. Sturgeon, R. E., and Chakrabarti, C. L., *Prog. Anal. At. Spectrosc.*, 1978, **1**, 132.
14. Sturgeon, R. E., Siu, K. W. M., and Berman, S. S., *Spectrochim. Acta, Part B*, 1984, **39**, 213.
15. Sturgeon, R. E., and Berman, S. S., *Anal. Chem.*, 1985, **57**, 1268.

16. Falk, H., Hoffmann, E., and Ludke, Ch., *Spectrochim. Acta, Part B*, 1981, **36**, 767.
17. Falk, H., Hoffmann, E., and Ludke, Ch., *Fresenius Z. Anal. Chem.*, 1981, **307**, 362.
18. Falk, H., Hoffmann, E., Ludke, Ch., Ottaway, J. M., and Giri, S. K., *Analyst*, 1983, **108**, 1459.
19. Eichardt, K., and Falk, H., *Jenaer Rundsch.*, 1983, **28**, 118.
20. Bezur, L., Marshall, J., Ottaway, J. M ., and Fakhrul-Aldeen, R., *Analyst*, 1983, **108**, 553.
21. Giri, S. K., Littlejohn, D., and Ottaway, J. M., *Analyst*, 1982, **107**, 1095.

Paper A5/271
Received July 23rd, 1985
Accepted October 9th, 1985

Alkyl Cyanide Medium for the Determination of Precious Metals by Atomic Absorption Spectrometry

R. Le Houillier and C. De Blois
Ministère de l'Energie et des Ressources, Centre de Recherches Minérales, 2700 Rue Einstein, Sainte-Foy, Québec, Canada G1P 3W8

Concentrations ranging from parts per billion levels up to a few parts per million can be adequately determined for platinum, palladium and gold pre-concentrated in a silver bead, when dissolved in an alkaline cyanide solution, by the use of AAS, with a vanadium buffer to correct for precious metal interference. The same medium is also proposed for the determination of silver, platinum, palladium and rhodium pre-concentrated in a gold bead; however, the rhodium recovery is poor. The difficulty in recovering rhodium is not associated with the medium of the final solution but rather with losses produced by the possible formation of lead rhodium oxide during cupellation and with the acid-insoluble flakes containing lead and rhodium.

Keywords: *Precious metal determination; atomic absorption spectrometry; fire assay pre-concentration; vanadium buffer; alkaline cyanide solution*

Various methods for the determination of noble metals by atomic absorption spectrometry (AAS) and fire assay have been published and reviewed.[1-5] The classical fire assay is an excellent technique for collecting and concentrating in a bead noble metals from rocks, ores, minerals and other matrices prior to AAS determination. When the beads so produced are dissolved in acid, the contents of noble metals such as silver, gold and palladium can be determined by AAS with good precision. Indeed, Kallman and Hobart[6] reported that solutions of 100 ng ml^{-1} of silver and 300 ng ml^{-1} of gold and palladium can be analysed by AAS with a precision of ±1%.

To achieve such results, hydrochloric acid containing a significant amount of gold must be avoided, owing to the possibility of reducing gold in the capillary of the aspirator.[6] Moreover, the solubility of silver chloride in a solution containing less than 25% *V/V* hydrochloric acid is limited. In addition, any precipitation of silver from such a solution containing gold implies a high risk of loss of gold by coprecipitation. Further, silver salts are less soluble in a small volume of hydrochloric acid (25% *V/V*) than in the same volume of an alkaline cyanide solution. For this reason, occlusion of gold and other precious metals in silver salts may be lost, which is responsible for poor recoveries when a certain amount of a silver salt containing precious metals is not solubilised. However, stable complexes of silver, gold, platinum, palladium and, to a certain extent, even rhodium are formed in cyanide solutions. The determination of the noble metals by AAS with the use of such a medium is very attractive as dissolution of silver is more rapid and the risk of losses through coprecipitation is avoided. However, interferences between the noble metals in such a medium have not been thoroughly studied.

In this paper, an alkaline cyanide medium is proposed for the determination of gold, silver, palladium, platinum and rhodium by AAS in rocks, ores and minerals from parts per billion levels up to 3 p.p.m., after pre-concentration of the noble metals by the fire assay procedure. Interferences are reported and a buffer is proposed. The accuracy and precision obtained for the procedure are presented.

Experimental

Standard Solutions

Standard solutions of precious metals were prepared from Specpure (Johnson Matthey Chemicals) chloroammonium salts of rhodium and palladium, platinum sponge and metallic gold. Silver solutions were prepared from pure silver nitrate (Aldrich).

Prepare standard solutions by dissolving weighed amounts of chloroammonium salts of rhodium and palladium in water. Add HCl and dilute with water to obtain a final solution containing 7.5% *V/V* of HCl. Dissolve in the same medium platinum and gold salts produced by dissolution of the pure metals in aqua regia and evaporate a given volume of this solution to dryness. Dissolve the salts in water and dilute with a solution containing 5% *m/V* each of KCN and KOH. Add a solution containing 2% *m/V* of vanadium to obtain a final medium containing 0.5% *m/V* of KCN and KOH and 1% *m/V* of vanadium.

For silver solutions, dissolve silver nitrate in water, then follow the same procedure as above. The KOH is necessary both as a safety measure, owing to the health hazard with cyanide, and to dissolve any lead remaining in the bead.

Buffer Solution

To prepare the buffer solution, dissolve 24.0 g of $NaVO_3$ overnight, without heating, in 400 ml of demineralised water. After filtration through a Whatman No. 44 filter-paper introduce the solution into a 500-ml calibrated flask and dilute to volume. This solution contains 2% *m/V* of vanadium. It is important that the demineralised water be low in oxygen in order to avoid the formation of insoluble vanadium oxide.

Fire Assay

Follow the standard fire assay procedure for collecting and concentrating the noble metals in a bead. Lead was used as the collector throughout the study owing to its technical simplicity. The amount of sample used for fire assay was 15 g. For recovery studies, precious metals in solution are added to 15 g of pure quartz and flux mixture and the whole charge is dried before fusion. In general, the lead button containing the precious metals weighs about 25 g.

Silver as a Collector

As good practice in the fire assay, add silver (10 mg) to collect gold, platinum and palladium in a bead that can be easily dissolved in an acid solution. Conduct the fusion step at 1000 °C but the cupellation must be completed at *ca.* 940 °C when platinoids are present in order to obtain a bead of low

lead content. If the cupellation step is not conducted properly, dissolution of the noble salts in alkaline cyanide solution may be a source of problems, because of lead. For the determination of gold, when only gold is present, the silver bead can be produced at a lower cupellation temperature, *i.e.*, about 870 °C.

Gold as a Collector

Add 5 mg of gold in the fusion step to collect trace amounts of rhodium, platinum and palladium. Perform the fusion at 1000 °C and the cupellation at 940 °C. For silver analysis only, a gold bead obtained after cupellation at 870 °C is adequate.

Bead Treatment

Treat a silver bead containing gold, platinum and palladium or a gold bead containing platinum, palladium and rhodium in a 30-ml beaker with 5 ml of hot dilute hydrochloric acid (1% *V/V*) to dissolve any gangue left on the surface of the bead after cupellation. Such gangue must be eliminated prior to the dissolution of noble metal salts in alkaline cyanide medium in order to avoid precipitation and thus metal losses.[7] Discard the wash solution and treat the bead with 2 ml of hot nitric acid. When no further reaction is observed, add 6 ml of concentrated hydrochloric acid and keep the solution warm for about 10 min, then evaporate the solution to dryness at a low temperature. One advantage of the cyanide dissolution over the use of an acid medium is that if the salts are dried at too high a temperature, precious metal salts may be decomposed to the metallic state. The cyanide dissolution will still allow a good recovery of those precious metals susceptible to such a reaction.

Alkaline Cyanide Dissolution of Noble Metal Salts

Add to noble metal salts 1 ml of 5% *m/V* KCN - 5% *m/V* KOH solution and dilute the solution to 5 ml with water. Just before the AAS measurements, add 5 ml of sodium metavanadate solution containing 2% *m/V* of vanadium to eliminate interferences. This addition is carried out just before the AAS measurements because the final solution has a stability of about 4 h. The final volume of solution is 10 ml and it contains 1% *m/V* of vanadium and 0.5% *m/V* each of KCN and KOH.

Silver and Gold Beads

With a silver bead containing only gold, or *vice versa*, the washing and dissolution procedure is similar to that described above. However, after evaporation to dryness, dissolve the salts in only 0.5 ml of the 5% *m/V* KCN - KOH solution, then dilute to 5 ml. No buffer for interference suppression is needed for silver and gold determinations only. The final volume of solution is 5 ml and it contains 0.5% *m/V* each of KCN and KOH.

Atomic Absorption Measurements

A Varian AA-875 atomic absorption spectrometer, equipped with automatic gas control, an automated background correction system, an air - acetylene burner and an adjustable barrel nebuliser, was used. The wavelengths used to optimise the instrumental parameters with standard solutions are given in Table 1. Table 1 also gives the sensitivities and detection limits (2σ) obtained for Pt, Pd and Rh dissolved in 0.5% *m/V* KCN - KOH - 1% *m/V* vanadium solution. For gold and silver, the analytical values are valid for vanadium-free solutions.

Results and Discussion

Interferences

In general, the addition of KOH to a cyanide solution enhances the absorbance of the noble metals. The greatest increases are observed with platinum and rhodium in 2% *m/V* KOH solution. For 8 μg ml^{-1} of platinum an absorbance increase of 124% is obtained, whereas for 0.8 μg ml^{-1} of rhodium a 40% enhancement is typical. However, at 0.1% *m/V* KOH, a marked decrease in absorbance is encountered for silver; the decrease is less pronounced for gold. The absorbance of these metals is re-established at a higher concentration of KOH (0.5% *m/V*).

Small silver, platinum and palladium absorbance enhancements are observed with increasing concentration of KCN in solution. However, a 54% increase in gold absorbance is obtained in 1% *m/V* KCN solution. KCN interferes differently with rhodium. A maximum 24% decrease in the absorbance of rhodium occurs at approximately 0.4% *m/V* KCN. Increasing the KCN concentration to 2% *m/V* results in a higher absorbance than before the decrease.

Table 1. Instrumental parameters and analytical values

Element	Wavelength/ nm	Slit/ nm	Lamp current/ mA	Background corrector	Sensitivity/ μg ml^{-1}	Detection limit*/ ng g^{-1}
Au	242.8	1.0	4	Yes	0.15	15
Ag	328.1	1.0	3	Yes	0.027	2
Pt	266.0	0.5	10	Yes	0.81	80
Pd	244.8	0.5	5	Yes	0.11	12
Rh	343.5	0.5	5	No	0.065	7

* Detection limits for Au and Ag are valid for 5 ml of final solution compared with 10 ml for all the other elements. These detection limits refer to the original 15-g sample.

Table 2. Interferences detected in 0.5% *m/V* KCN - KOH solution without vanadium buffer

		Change of analyte absorbance, %				
Interferent	Concentration/ μg ml^{-1}	Au, 1.0 μg ml^{-1}	Ag, 1.0 μg ml^{-1}	Pt, 8.0 μg ml^{-1}	Pd, 0.8 μg ml^{-1}	Rh, 0.8 μg ml^{-1}
Au	1500	—	0	−34	0	−32
Ag	2000	0	—	0	0	0
Pt	30	0	0	—	−36	−73
Pd	15	0	0	−40	—	−33
Rh	15	0	0	−56	−22	—

Table 3. Interferent concentrations in 0.5% *m/V* KCN - KOH - 1% *m/V* vanadium solution for which vanadium buffer is efficient

Analyte	Concentration/ μg ml^{-1}	Interferent concentration/μg ml^{-1}				
		Ag	Au	Pt	Pd	Rh
Au	1.0	2000	—	30	15	15
Ag	1.0	—	2000	30	15	15
Pt	8.0	1500	500	—	50	5
Pd	0.8	1500	1000	20	—	20
Rh	0.8	1500	200	10	10	—

Most of the important absorbance changes of the noble metals mentioned above are markedly decreased when a solution containing the same amounts of both KCN and KOH is used. For example, silver, gold and palladium give an almost constant absorbance when solutions containing 0–1% *m/V* of both KCN and KOH are used. However, rhodium and platinum still show an absorbance increase. Nevertheless, this is not a problem as the final solution of noble metals is always adjusted to contain 0.5% *m/V* KCN - KOH. Interferences encountered between precious metals dissolved in alkaline cyanide solutions containing 0.5% *m/V* KCN - KOH are presented in Table 2. No change in analyte absorbance is observed for gold and silver with the concentrations of interferent and analyte reported. The worst situation occurs between platinum and rhodium.

It is worth mentioning that, for 1 μg ml^{-1} of lead in solution, no interference with gold, silver, platinum, palladium or rhodium is observed with the concentration of each analyte reported in Table 2.

Interferences are eliminated in such alkaline cyanide solutions by the addition of sodium metavanadate. Table 3 reports the analyte and interferent concentrations for which a buffer solution containing 1% *m/V* of vanadium eliminates the change in analyte absorbance associated with the action of such interferents.

It is worth mentioning that 0.15–1% *m/V* of vanadium in solution increases the absorbance of 1 μg ml^{-1} of rhodium and platinum by 74 and 135%, respectively. However, vanadium has no releasing action on the absorbance of the same concentration of palladium. When only silver and gold are present in a sample, the addition of vanadium can be omitted as there is no significant interference.

Procedure Testing

Typical fire assay beads resulting from the complete decomposition of 15 g of pure quartz, to which a single addition of different amounts of a precious metal were added in solution, were analysed by AAS. Table 4 gives the over-all recovery obtained with a silver bead. No results are given for rhodium as it is known that silver is not a recommended collector for rhodium.

Table 5 gives the recoveries of palladium, platinum and rhodium obtained when 5 mg of gold was used as a collector. Palladium gives the best recovery. Gold and platinum have recoveries that tend to be high, between 0.5 and 3 μg (33–200 p.p.b.). Rhodium shows the worst recovery. For a 5-mg gold bead, the amount of gold in solution exceeds the limit for which vanadium buffer is efficient. However, from 200 to 500 μg ml^{-1} of gold in solution, the decrease in rhodium absorbance is only 4%, which does not explain the decrease in recovery. It is important to note that the recovery reported refers to both fire assay and AAS analyses. The over-all recovery of rhodium is poor and is associated with incomplete dissolution of rhodium from the gold bead. Small flakes recovered from the dissolution of a 5-mg gold bead containing 5 μg of rhodium were analysed and lead and rhodium were found to be the main constituents, as identified by electron probe X-ray microanalysis. A preliminary X-ray diffraction study indicated that the structure of the flake is similar to that of lead rhodium oxide, which would explain why such flakes are not dissolved by acids or alkaline cyanide solutions.

A dark grey coating of the gold beads with high rhodium contents was observed. Such a coating is rich in lead and rhodium, as shown by electron probe X-ray microanalysis.

Table 4. determination of gold, palladium and platinum in a 10-mg silver bead. Cupellation temperature, 940 °C. Each determination was performed four times

Element	Added/ μg	Found/ μg	Recovery, %
Au	0.5	0.6 ± 0.2	120
	1.0	1.2 ± 0.2	120
	2.5	2.4 ± 0.3	96
	5.0	5.5 ± 0.5	110
	10.0	10.3 ± 0.8	103
	15.0	15.0 ± 0.1	100
Pd	0.5	0.5 ± 0.1	100
	1.0	1.1 ± 0.1	110
	2.5	2.4 ± 0.2	96
	5.0	5.0 ± 0.1	100
	10.0	10.0 ± 0.3	100
	15.0	15.2 ± 0.2	101
Pt	1.5	1.6 ± 0.5	106
	3.0	3.8 ± 0.5	127
	7.5	7.2 ± 0.5	96
	10.0	9.4 ± 0.6	94
	20.0	20.0 ± 1.4	100
	30.0	27.6 ± 1.5	92

Table 5. Determination of palladium, platinum and rhodium in a 5-mg gold bead. Cupellation temperature, 940 °C. Each determination was performed four times

Element	Added/ μg	Found/ μg	Recovery, %
Pd	0.5	0.48 ± 0.04	96
	1.0	1.03 ± 0.04	103
	2.5	2.35 ± 0.18	94
	5.0	4.6 ± 0.4	92
	10.0	10.2 ± 0.5	102
	15.0	20.0 ± 0.5	100
Pt	1.5	1.8 ± 0.4	120
	3.0	3.8 ± 0.4	127
	7.5	7.3 ± 0.4	97
	12.5	11.0 ± 1.0	88
	15.0	14.8 ± 2.0	99
	25.0	24.7 ± 0.5	99
Rh	0.5	0.43 ± 0.05	86
	1.0	0.30 ± 0.08	30
	2.5	0.73 ± 0.05	29
	5.0	1.03 ± 0.08	21

Table 6. Determination of silver in a 10-mg gold bead. Cupellation temperature, 870 °C. Each determination was performed four times

Ag added/ μg	Ag found/ μg	Recovery, %
2.4	2.1 ± 0.5	87.5
4.8	4.2 ± 0.5	87.5
15.0	14.3 ± 0.6	95.3

Table 7. AAS determination of precious metals pre-concentrated in a 5-mg gold bead from blends of standards and a pure quartz. Each determination was performed four times

	Taken, p.p.b.				Found, p.p.b.			
Blend	Ag	Pd	Pt	Rh	Ag†	Pd	Pt	Rh
3.0 g SARM-7* + 12 g quartz ..	84	306	748	48	—	329 ± 16	822 ± 31	35 ± 5
5.0 g SARM-7 + 10 g quartz ..	140	510	1247	80	130 ± 85	511 ± 12	1289 ± 38	64 ± 8
7.5 g SARM-7 + 7.5 g quartz ..	210	765	1870	120	258 ± 61	784 ± 24	1747 ± 98	99 ± 5
15.0 g SARM-7	420	1530	3740	240	—	1530 ± 90	3640 ± 100	170 ± 10

* SARM-7, standard prepared by National Institute for Metallurgy, Republic of South Africa.
† A 10-mg gold bead was produced after cupellation at 870 °C.

Table 8. Determination of precious metals in blends of standards and a pure quartz by fire assay and AAS; a 10-mg silver bead was produced after cupellation at 940 °C. Each determination was performed four times

	Taken, p.p.b.			Found, p.p.b.		
Blend	Au	Pd	Pt	Au	Pd	Pt
3.0 g SARM-7 + 12 g quartz ..	62	306	748	63 ± 9	319 ± 26	786 ± 114
5.0 g SARM-7 + 10 g quartz ..	103	510	1247	89 ± 16	517 ± 6	1152 ± 156
7.5 g SARM-7 + 7.5 g quartz ..	155	765	1870	140 ± 15	765 ± 13	1818 ± 61
15.0 g SARM-7	310	1530	3740	310 ± 71	1538 ± 18	3270 ± 160
7.5 g SU-1A* + 7.5 g quartz ..	—	185	205	80 ± 18	205 ± 12	211 ± 50
4.0 g PTA-1* + 11 g quartz ..	—	—	813	63 ± 24	—	767 ± 183
1.0 g MA* + 14 g quartz	1186	—	—	1265 ± 84	—	—

* SU-1A, PTA-1 and MA, standards prepared by the Canada Centre for Mineral and Energy Technology.

From these findings, it appears that the recovery of rhodium by fire assay is a problem that needs more study. During this investigation, it was noticed that when the gold to platinum ratio in a bead is approximately 10, the recovery of rhodium is about 85%, *i.e.*, better than that without platinum. Recovery studies conducted with rhodium already in solution gave excellent results, and indicated that the rhodium recovery problem lies in the fire assay procedure and the acid digestion step.

Determination of silver in a gold bead can be conducted without vanadium buffer as precious metals do not interfere. Further, the cupellation temperature must be decreased in order to minimise silver losses. Therefore, silver determinations must be conducted on a bead produced at a lower cupellation temperature. Table 6 shows the silver recovery obtained from an analysis performed in a 0.5% *m/V* KCN - KOH solution.

The detection limit of silver determined by AAS is of the order of a few parts per billion. However, silver contamination from the fluxes used in a fire assay often occurs, and it is not recommended to determine silver in the parts per billion range using fire assay as a pre-concentration and separation method. In this work the silver contamination was 1.9 μg (128 ng g^{-1}) and this value was subtracted from the amount found.

Standard and Quartz Blend Analysis

The whole method applied to blends of standards and a pure quartz give the results presented in Tables 7 and 8. In Table 7, the precious metal content of a 5-mg gold bead, produced at a cupellation temperature of 940 °C, was determined in 0.5% *m/V* KCN - KOH - 1% *m/V* vanadium solution. Silver results obtained from a 10-mg gold bead produced at a cupellation temperature of 870 °C are also given. The silver determination was conducted without vanadium in solution.

When only gold, platinum and palladium are to be determined, a silver collection is adequate. Results obtained with a silver bead are given in Table 8 and show that the recovery of precious metals is generally good. However, the platinum recovery decreases at high platinum concentrations in the silver bead, and can be improved by using a gold collector.

Conclusion

The acid decomposition of precious metal beads produced by fire assay and the dissolution of the noble metal salts in alkaline cyanide solution is an attractive procedure for the determination of gold, silver, palladium, platinum and rhodium at parts per billion levels in rocks, ores and minerals. Lengthy separation methods are not required as interferences are corrected by the vanadium buffer added to the cyanide solution. This method offers several advantages over existing methods by eliminating the possible precious metal losses by coprecipitation in HCl solution by formation of stable complexes. Further, it facilitates the rapid dissolution of significant amounts of silver in a small volume of cyanide solution, in contrast to hydrochloric acid.

This method is as simple as the others, but safety precautions relating to the use of cyanide must be rigorously followed.

Finally, the determination of rhodium presents no difficulties once it is in solution. However, the recovery of rhodium by fire assay and by acid decomposition of the bead has to be improved. The flakes observed after acid dissolution of a gold bead containing rhodium has not, to our knowledge, been reported elsewhere.

The authors thank A. Tremblay, N. Rhéaume and P. Plourde for their contributions to the experiments.

References

1. Beamish, F. E., and Van Loon, J. C., "Analysis of Noble Metals," Academic Press, New York, 1977.
2. Gupta, J. G., *Miner. Sci. Eng.*, 1973, **5**, 207.
3. Beamish, F. E., and Van Loon, J. C., *Miner. Sci. Eng.*, 1972, **4**, No. 4, 3.
4. Mallett, R. C., *Miner. Sci. Eng.*, 1970, **2**, No. 3, 28.
5. Moloughney, P. E., *Talanta*, 1977, **24**, 135
6. Kallmann, S., and Hobart, E. W., *Talanta*, 1970, **17**, 845.
7. Le Houillier, R., and Rhéaume, N., *Can. Metall. Q.*, 1984, **23**, 427.

Paper A5/205
Received June 10th, 1985
Accepted September 23rd, 1985

Interferences of Antimony(V) in the Differentiation of Antimony(III) from Antimony(V) by Extraction with Ammonium Tetramethylenedithiocarbamate Using Graphite Furnace Atomic Absorption Spectrometry

Etsuro Iwamoto,* Yasuhiko Inoike, and Yuroku Yamamoto†
Department of Chemistry, Faculty of Science, Hiroshima University, Hiroshima 730, Japan
and Yasuhisa Hayashi
Department of Chemistry, Joetsu University of Education, Joetsu 943, Japan

Procedures for the preparation of antimony sample solutions for the differentiation of antimony(III) from antimony(V) by extraction with ammonium tetramethylenedithiocarbamate (ammonium pyrrolidinedithiocarbamate, APDC) were examined. It was found that, when APDC is added to the antimony(V) solution of pH less than *ca.* 3, the antimony(V) - APDC complex is partially co-extracted with antimony(III) over the pH range 3.5–10. Further, the mixing of antimony(III) solution with acidic antimony(V) solution, prepared by oxidising antimony(III) potassium tartrate solution, leads to the incomplete extraction of antimony(III). A standard procedure for removing the interferences was established.

Keywords: *Antimony(III) determination; antimony(V) interference; ammonium tetramethylene dithiocarbamate; graphite furnace atomic absorption spectrometry; extraction*

Although the combination of solvent extraction with atomic absorption spectrometry (AAS) is very effective for the selective determination of mg l^{-1} levels of arsenic(III) and arsenic(V)[1–3] or antimony(III) and antimony(V),[3–5] much care is needed in the treatment of such small amounts of those elements. Compared with arsenic, antimony is much more subject to the influence of many parameters associated with the extraction of antimony(III) and antimony(V) because of their hydrolysis reactions.

A critical examination of the variables involved in the extraction - spectrophotometric determination of antimony as the ternary chloro complex of Brilliant Green has been reported[6]: a hydrolysis side-reaction gives products that do not form extractable ion association systems with the dye. Al-Sibaai and Fogg[7] used an extraction - spectrophotometric procedure with Brilliant Green and found that dilute standard antimony solutions (4 mg l^{-1}) prepared by dissolving antimony potassium tartrate in water and diluting the solution with water are stable over a period of 50 d, but similar dilute standard antimony solutions containing hydrochloric acid deteriorated rapidly. It was suggested that the effective loss of antimony could be caused by the formation of one or more soluble hydrolysed species but not by adsorption of antimony on the walls of the containers.

Ammonium tetramethylenedithiocarbamate (ammonium pyrrolidinedithiocarbamate, APDC) forms complexes with antimony that can be extracted into organic solvents such as isobutyl methyl ketone (IBMK) and nitrobenzene, and these have been used effectively for the selective determination of antimony(III) and antimony(V).[3–5] However, only a few developments of precise analytical procedures concerning, especially, the preparation of standard sample solutions have been made and some problems concerning the partial extraction of antimony(V) in the pH range 2–10 and interference from antimony(V) for extraction of antimony(III) have remained. In this work, the extraction behaviour of the APDC - antimony system was studied. Dichloromethane (DCM) and IBMK were selected as solvents in place of nitrobenzene because of their lower boiling-points.

* To whom correspondence should be addressed.
† Present address: Fukui Institute of Technology, Gakuen 3-618, Fukui 910, Japan.

Experimental

Reagents

All solutions were prepared from analytical-reagent grade chemicals and de-mineralised water, and were stored in polyethylene bottles.

Stock antimony(III) solution, 10 mg l^{-1}. Prepared by dissolving 2.742 g of antimony potassium tartrate in water, diluting to 1000 ml with water, taking 10 ml of this stock solution and diluting to 1000 ml with water; no acid being added.

Stock antimony(V) solution, 10 mg l^{-1}. (A) Prepared by oxidising the stock antimony(III) solution with potassium permanganate, by taking 5 ml of the 1000 mg l^{-1} antimony (III) solution, adding about 2 ml of sulphuric acid and 4 ml of 1% potassium permanganate solution and heating at *ca.* 80 °C for 30 min, adding hydrogen peroxide to remove the excess of permanganate and manganese dioxide produced, and diluting to 500 ml with 4 M hydrochloric acid. (B) Prepared by dissolving 2.778 g of potassium pyroantimonate $\{K[Sb(OH)_6].4H_2O\}$ in water, diluting to 1000 ml with water to give a 1000 mg l^{-1} solution and diluting 10 ml of this stock solution to 1000 ml with 4 M hydrochloric acid.

APDC solution, 1% *m/V*.

Buffer solution, pH 5.2. Prepared by mixing 1 M acetic acid and 1 M sodium acetate in suitable proportions.

Sodium tartrate solution, 1% *m/V*.

Apparatus

Atomic absorption measurements were made with a Nippon Jarrell-Ash Model AA-1 EW atomic absorption spectrometer equipped with a Model FLA-10 electrothermal atomiser and a Model HU-10 furnace. Peak heights were recorded with a Yanaco Model YR-110 chart recorder. A Hamamatsu TV antimony hollow-cathode lamp (L-223) was used as the light source. The background was checked by using a deuterium lamp. Samples were placed in the carbon tube with a Type 4700 Eppendorf pipette. An Iwaki Model KM shaking apparatus was used for solvent extraction.

General Procedure

Preparation of sample solution

Based on a critical examination of the experimental parameters, the following procedure is recomended. Place *ca.* 80 ml of water and an aliquot of sample solution containing antimony(III) and/or antimony(V) in a 100-ml calibrated flask. Add 2 ml of sodium tartrate solution, stir for 30–60 s, add 2–4 drops of methyl orange and then 2 M sodium hydroxide solution to adjust the pH of the sample solution to 4–5 and dilute to 100 ml.

Antimony(III) determination

Place an aliquot of sample solution containing not more than 1 μg of antimony(III) in a separating funnel. Add 2 ml of APDC solution and 5 ml of acetate buffer solution. Dilute the mixture to 25 ml with water, the pH of the resulting solution being 5–6. Shake the funnel for 5 min with 10 ml of DCM or IBMK, allow it to stand for 30 min and separate the organic phase. Inject 20 μl of the organic phase with a micropipette into the carbon tube. Pass argon through the furnace at a flow-rate of 3 l min^{-1}, then atomise the sample with the following heating sequence: dry for 30 s at 30 A (*ca.* 300 °C), ash for 30 s at 70 A (*ca.* 700 °C) and atomise for 7 s at 230 A (*ca.* 2300 °C). Record the absorption signal at 217.6 nm. Run a reagent blank using the same instrumental settings and subtract the result from the analytical value.

Total antimony determination

Place an aliquot of a sample solution containing not more than 1 μg of antimony in a separating funnel and add 2 ml of APDC solution and 3 ml of 1 M hydrochloric acid. Dilute the mixture to 25 ml with water, the pH of the resulting solution being *ca.* 1. Carry out the extraction and measure the atomic absorption as for antimony(III).

The amount of antimony(V) is calculated from the difference between the total antimony and antimony(III).

Results and Discussion

Partial Extraction of Antimony(V) above pH 3.5

The differentiation of antimony(III) from antimony(V) with APDC extraction is based on the principle that antimony(V) is not extracted above pH 3.5.[3–5] However, it was found that when APDC is added to the antimony(V) solution at a pH below 3, followed by addition of the buffer solution, antimony(V) is partly extracted above pH 3.5.

The effect of the acidity of the 0.1 mg l^{-1} antimony(V) solution to which APDC is added on the extraction of antimony(V) for the APDC - DCM system is shown in Fig. 1. The 0.1 mg l^{-1} standard solution was prepared by diluting the 10 mg l^{-1} stock solution and adjusting the acidity with sodium hydroxide solution. The extraction, in which 10 ml of the standard solution (0.1 mg l^{-1}) were taken, was carried out at pH 5.2 and antimony was determined in the organic phase. The degree of extraction increased with increasing acidity, although antimony(V) was not extracted when APDC was added above pH 3. The behaviour was independent of the acid (hydrochloric, sulphuric and nitric acid) used to adjust the pH and organic solvents (DCM and IBMK). Stock solution B of antimony(V) gave the same result as stock solution A. Further, in tests lasting up to 12 d, the extractability of antimony(V) from each sample solution prepared from 10 mg l^{-1} stock solutions A and B using 4, 1 and 0.01 M acids was found to be unchanged, within experimental error.

As antimony at low acidity tends to be adsorbed on the walls of glass containers, an attempt was made to check the amount of antimony adsorbed. The relative distribution of antimony(V) on extraction at pH 5.2 is given in Table 1 for pH 1.4 and 4 solutions of antimony(V). The percentage values for the separating funnel refer to the amount of antimony adsorbed and present in small amounts of solvents adhering to the walls of the funnel after draining the organic and aqueous phases. Each concentration of antimony(V) was determined according to the procedure for the total antimony determination. As there is virtually no difference in the percentages for the separating funnel between the pH 1.4 and 4 solutions, it can be concluded that the non-extraction for the pH 4 solution is not due to adsorption.

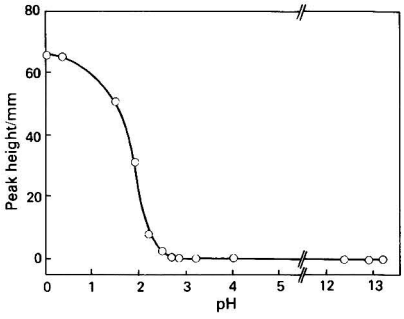

Fig. 1. Effect of pH of the antimony(V) solution to which APDC is added on extraction at pH 5.2. Sb(V), 1 μg

Table 1. Distribution of antimony(V) in extraction at pH 5.2

	Distribution, %	
	pH 1.4*	pH 4*
Organic phase	39	2
Separating funnel	12	13
Aqueous phase	49	84

* pH values of the antimony(V) solution (0.1 mg l^{-1}).

The above observations show clearly that a certain species of antimony(V) forms a complex which is extractable into the organic phase with APDC and the chloride anion is not responsible for its formation. Fig. 2 shows the distribution of species present using 10^{-5} M antimony(V) at 25 °C.[8] It is interesting that the pH dependence of the extractability in Fig. 1 is very similar to that of the formation of $Sb(OH)_5$ in Fig. 2. It seems likely that $Sb(OH)_5$ forms a complex which is extractable in organic solvents with APDC whereas $Sb(OH)_6^-$ does not, and once the complex has been formed below pH 3 it is stable at pH values higher than this.

Interference from Antimony(V) for the Determination of Antimony(III)

In the absence of antimony(V), antimony(III) is completely extracted with APDC over a wide acidity range, from 4 M to pH 10.[3–5] However, it was found that the extraction of antimony(III) is subject to interference from the presence of antimony(V), depending on the conditions of mixing of the antimony(III) solution with the antimony(V) solution.

Procedures for the preparation of sample solutions containing antimony(III) and antimony(V) are given in Table 2. The effect on extraction of the concentration of antimony(V) and the acidity of antimony(V) solutions in procedures I and II is shown in Fig. 3, where stock solution A was used for antimony(V). Evidently, the extraction of antimony(III) is subject to interference from antimony(V) in stock solution A and the degree of interference increases with increasing acidity of the antimony(V) solution and the amount of antimony(V) present. In particular, when antimony(III) was mixed with comparable amounts of antimony(V) in 4 M acid, antimony(III) was not extracted at all. On the other hand, no

Table 2. Procedures for the preparation of sample solutions

Procedure	Stock solution (10 mg l^{-1})	Standard solution (0.1 mg l^{-1})
I	Sb(III) - H_2O, 1 ml	dilution,* 100 ml } mixing → sample solution
	Sb(V) - 4 M HCl, 1 ml → neutralisation†	dilution, 100 ml
II	Sb(III) - H_2O, 1 ml } mixing → neutralisation	dilution, 100 ml → sample solution
	Sb(V) - 4 M HCl, 1 ml	
III	Sb(III) - H_2O, 1 ml	
	Sb(V)-4 M HCl, 1 ml → dilution (*ca.* 80 ml mixing → addition (tartrate) → neutralisation	dilution, 100 ml → sample solution

* Dilution with water.
† Neutralisation with sodium hydroxide using phenolphthalein.
‡ Addition of auxiliary complex reagent (sodium tartrate or sodium citrate).

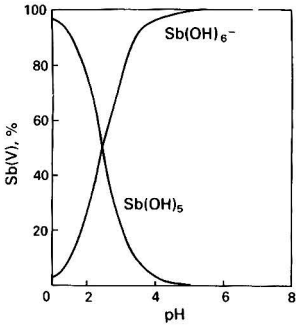

Fig. 2. Distribution of species present at 10^{-5} M Sb(V) in 0.5 M $(CH_3)_4NCl$ at 25 °C. Taken from reference 8

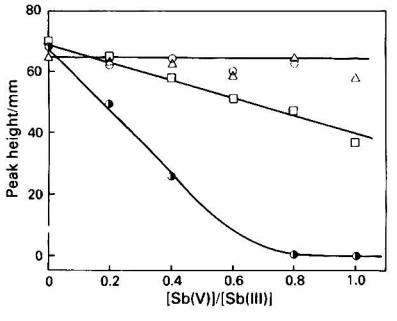

Fig. 3. Effect of amount of antimony(V) and acidity of antimony(V) solution A on the extraction of antimony(III) with APDC - DCM at pH 5.2. Procedure I, ○; procedure II, △, 0.01 M HCl; □, 1 M HCl; ◑, 4 M HCl. Sb(III), 1 μg

interference was found for antimony(V) in stock solution B. This differs from the behaviour in the partial extraction of antimony(V) discussed in the preceding section. Sulphuric acid produced the same behaviour as hydrochloric acid and the use of methyl orange as an indicator also gave the same results. An increase in the amount of APDC did not increase the degree of extraction of antimony(III), showing that the amount present was sufficient.

Although the antimony(III) standard solution prepared from antimony potassium tartrate is very stable at the 1000 mg l^{-1} level in aqueous solution, at low concentrations oxidation of antimony(III) to antimony(V) may take place.[9] Sun *et al.*[10] reported that with the APDC - IBMK system no antimony(III) was extracted at pH 6 in the absence of tartaric acid, which was added as a stabilising agent, but an equivalent

Table 3. Recovery tests on antimony(III) and antimony(V). Dichloromethane was used as the solvent

Antimony added/μg l^{-1}		Antimony found/μg l^{-1}		
Sb(III)	Sb(V)	Sb(total)	Sb(III)	Sb(V)
20	80	106	18	88
30	70	104	31	73
40	60	103	41	62
60	40	101	57	44
70	30	106	77	29
80	20	100	83	17
100	0	94	94	0

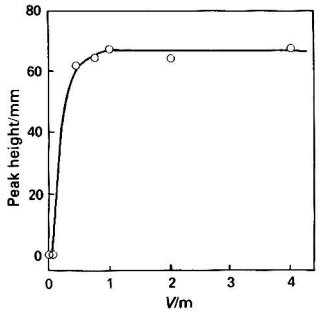

Fig. 4. Effect of volume of 1% sodium tartrate solution on the extraction of Sb(III) at pH 5.2. Sb(III), 1 μg; Sb(V), 1 μg

amount of antimony(V) was found by extraction at pH 1. In these tests lasting up to 6 d at the 1 mg l^{-1} level, the decrease in the degree of extraction at pH 5.2 was less than 10% in the absence of antimony(V). The rate of oxidation appears to depend on the quality of the water used to make the dilutions. Antimony(V) is reported to be hydrolysed rapidly even in 6 M hydrochloric acid.[11] It is also speculated that more complex equilibria of hydrolysis would occur for solution A under acidic conditions, and a certain compound of antimony(V) forms a complex with antimony(III) or adsorbs antimony(III), interfering with the complex formation of antimony(III) with APDC.

An attempt was made to remove this interference by adding auxiliary complexing agents before neutralisation according to procedure III in Table 2. It was found that sodium tartrate and sodium citrate are the most effective: antimony(III) is protected from oxidation or interaction with antimony(V) species by complex formation with tartrate. Fig. 4 shows the effect of the concentration of sodium tartrate solution on the interference of antimony(V) on the extraction of antimony(III) at pH 5.2. At least 2 ml of 1% sodium tartrate are required. The efficiency was independent of standing time for at least 2 h after the addition. EDTA showed no effect.

Addition of the auxiliary reagent to either antimony solution before mixing is equally effective. In our previous studies,[3,4] the antimony(III) solution was prepared according to procedure I. Subramanian and Meranger used ammonium citrate as a buffer solution.[5]

A recovery test on standard samples was carried out according to the standard procedure established here and satisfactory results were obtained, as shown in Table 3.

Although the elucidation of the interference mechanism is beyond our present knowledge, it can be concluded that (i) in order not to extract antimony(V) over the pH range 3.5–10, the pH of the sample solutions must be higher than 3 when APDC is added, and (ii) an auxiliary complexing reagent, tartrate or citrate, is needed to prevent the interference of antimony(V) in the determination of antimony(III) when using an acidic antimony(V) solution prepared from antimony potassium tartrate. Therefore, care must be taken, especially when using the method of standard additions, as unknown and standard solutions are often acidic.

This research was supported in part by a Grant-in-Aid for Scientific Research (Nos. 57470031, 58540363 and 58030061) from the Ministry of Education, Science and Culture, Japan.

References

1. Kamada, T., *Talanta*, 1976, **23**, 835.
2. Yamamoto, Y., and Kamada, T., *Bunseki Kagaku*, 1976, **25**, 567.
3. Chung, C. H., Iwamoto, E., Yamamoto, M., and Yamamoto, Y., *Spectrochim. Acta, Part B*, 1984, **39**, 459.
4. Kamada, T., and Yamamoto, Y., *Talanta*, 1977, **24**, 330.
5. Subramanian, K. S., and Meranger, J. C., *Anal. Chim. Acta*, 1981, **124**, 131.
6. Burke, R. W., and Menis, O., *Anal. Chem.*, 1966, **38**, 1719.
7. Al-Sibaai, A. A., and Fogg, A. G., *Analyst*, 1973, **98**, 732.
8. Baes, C. F., Jr., and Mesmer, R., "The Hydrolysis of Cations," Wiley, New York, 1976, p. 374.
9. Andreae, M. O., Asmode, J.-F., Foster, P., and Van't Dack, L., *Anal. Chem.*, 1981, **53**, 1776.
10. Sun, H.-W., Shan, X.-Q., and Ni, Z.-M., *Talanta*, 1982, **29**, 589.
11. Newmann, H. M., *J. Am. Chem. Soc.*, 1954, **76**, 2611.

Paper A5/314
Received September 9th, 1985
Accepted October 14th, 1985

Photothermal Deflection Spectroscopy and Photoconductivity Studies of Photoelectrochemical Processes at (0001) n-CdS - Electrolyte Interfaces

Robert E. Wagner, Victor K. T. Wong and Andreas Mandelis
Photoacoustic and Photothermal Sciences Laboratory, Department of Mechanical Engineering, University of Toronto, Toronto, Ontario M5S 1A4, Canada

Photothermal deflection spectroscopy (PDS) was used to investigate the manner in which the degree of band bending in a photoelectrochemical cell (PEC), consisting of an illuminated n-CdS (0001) single crystal and a polysulphide electrolyte, affects the non-radiative recombination processes in the semiconductor. The photocurrent was also monitored simultaneously as a complementary energy conversion channel. The results show that PDS can be used successfully as an analytical tool for the understanding and interpretation of photoelectrochemical processes at the photoelectrode - electrolyte interface.

Keywords: *Photothermal deflection spectroscopy; photoconductivity; photoelectrochemical cell; cadmium sulphide electrode; non-radiative process*

Several workers have studied cadmium sulphide and cadmium selenide based photoelectrochemical cells (PEC) in the last decade. The important consideration of stable CdS photoelectrodes during a photoelectrochemical experiment has been successfully addressed by Ellis and co-workers in a series of publications.[1-5] The authors have found that sulphide or polysulphides in aqueous solution quench the photoanodic dissolution of the CdS reaction:

$$\underset{\text{(photoanode)}}{\text{CdS}} \xrightarrow{\hbar\omega} \text{Cd}^{2+}\text{(aq.)} + \text{S(s)} + 2\text{e}^- \qquad (1)$$

The single crystalline CdS photoelectrode has been important technologically, because when used in a PEC, it can form a simple device for sustained conversion of visible optical energy into electricity. The relatively large band gap energy of CdS compared with CdSe and other compound semiconductors renders the former semiconductor more attractive for applications where large open-circuit photovoltages are desired.

The analytical methods conventionally used to study photoelectrochemical effects at semiconductor electrode - electrolyte interfaces include photocurrent and photopotential measurements[1-5] as a function of the wavelength of the exciting radiation (*i.e.*, photoaction spectra); differential capacitance measurements of the interface[2]; emission photoluminescent spectra from the electrode surface following radiative deexcitation of carriers[3-5]; electroluminescent spectra[6]; voltammetric studies[7]; and/or combinations of these techniques.[1-6] The recent development of photoacoustic spectroscopy (PAS) as an analytical electrochemical technique[8,9] has allowed the use of the photoacoustic effect[10] in optical spectra acquisition of metal oxide and semiconductor interfaces. The main advantage of PAS over other conventional spectroscopies lies in its ability to measure the non-radiative pathway of the deexcitation manifold, *i.e.*, carrier recombination processes and other heat-generating mechanisms in electrochemical systems. The non-radiative deexcitation component is the main energy loss mechanism in such systems and is detrimental to their quantum and energy efficiency enhancement.[11] From the experimental point of view, PAS cannot be used easily to monitor electrode - electrolyte processes *in situ* owing to the remote positioning of the transducer - detector system. For this reason, photothermal deflection spectroscopy (PDS) has been recently applied to the investigation of electrochemical interface phenomena.[12,13] PDS is a spectroscopic tool that utilises the mirage effect, the fact that the path of a laser beam, in a given medium, will be bent if the beam encounters a refractive index gradient in its propagation path. This refractive index gradient may be induced by temperature or concentration gradients. This technique therefore can yield solid electrode spectroscopic information[14] through probing the electrolyte portion close to the electrode surface, as well as information concerning chemical changes in the electrolyte owing to interfacial chemical reactions.[15]

In this work we have exploited the dependence of the PDS signal on the non-radiative quantum efficiency of the CdS photoelectrode deexcitation manifold to monitor *in situ* the non-radiative mechanism, simultaneously with the photogenerated current at the junction betwen a (0001)-oriented CdS electrode and a stable polysulphide electrolyte. In this fashion, PDS proved to be a valuable channel of information complementary to the conventional analytical methods, aiding in the establishment of a more complete picture of the electrode deexcitation process pathways at the electronic level.

Experimental

The material used in these experiments was a 1 cm × 1 cm × 0.2 cm low-resistivity (ρ = 20 ohm cm) n-CdS crystal from Eagle-Picher (Miami, OK), oriented with the optic axis perpendicular to the surface (0001) plane. The crystal was etched prior to mounting in the PEC in a solution consisting of 95% *V/V* of 3 M HCl and 5% *V/V* of a 30% hydrogen peroxide solution in water. The crystal was etched for 20 s and then rinsed in distilled water. Subsequently, the crystal had one of its faces coated with a 0.5 mm thick layer of liquid In - Ga amalgam and ohmic contact was assured by allowing diffusion of the In - Ga into the CdS for 3 h at 350 °C. Further, the sample was epoxied on to an acrylic backing, which was chosen for its durability and resistance to electrolyte penetration. The completed working electrode (WE) consisted of the CdS crystal with one face bare and exposed to the electrolyte and the other face contacting a copper lead via the In - Ga amalgam. The metallised face of the WE was insulated from the electrolyte by the acrylic backing and epoxy. In between some of the experiments the WE was immersed in cyclohexane, in order to remove any trace amounts of sulphur that may have formed on the surface during experimentation.[16]

Platinum foil was chosen for the counter electrode (CE), covered with Pt black in order to increase the effective surface area available for the cathodic reaction. The CE was

positioned very close to the WE (*ca.* 5 mm) to decrease the solution resistance. A Fischer saturated calomel electrode (SCE) was employed as the reference electrode (RE).

Mott - Schottky plots were obtained from n-CdS in 1 M each of NaOH, Na_2S and S. This polysulphide solution was found to optimise the stability and reproducibility of the differential capacitance measurements required for the Mott - Schottky plots. Optical absorption spectra of the polysulphide solution were taken with a Cary 17D spectrophotometer. It was thus found that the 1 + 1 + 1 M solution would absorb most light with energies above the CdS band gap at *ca.* 510 nm.[1,17] In order to reduce this absorption a 1 M NaOH - 1 M Na_2S - 0.05 M S electrolyte was used for the subsequent photoelectrochemical experiments and was found to give satisfactory results.

The PEC was made of Teflon and had a screw-on lid, which supported a fused-silica UV grade window for entry of the exciting radiation into the cell. Two more windows made of Crown glass were located on opposite sides of the PEC to allow the passage of the 2-mW, 632.8-nm He - Ne laser probe beam used for PDS measurements. The laser - PEC assembly was mounted on stages, which allowed four degrees of freedom in the beam path movement, two translations and two rotations. The probe beam was further focused with its waist above the CdS electrode surface, using a 15 cm focal length lens. Fig. 1 shows an overview of the experimental apparatus. The source of UV - visible radiation was an Oriel Corp. Model 6141 1000-W Xe arc lamp in series with an Instruments S.A. H-20 monochromator with a concave holographic grating for wavelength selection. The He - Ne probe beam deflection was measured with a United Detector Technology (UDT) Model 431 Position Monitor connected to a UDT SC/25 light position detector. An optical filter with a 5% transmittance for wavelengths below 590 nm was placed over the detector to enhance the signal to noise ratio (SNR). The exciting radiation intensity was modulated by an AMKO OC 4000 mechanical chopper, which also referenced the EG & G Model 5204 lock-in amplifiers used as the PDS and photovoltage signal processors.

External d.c. biases were required for Mott - Schottky plots and PDS - photocurrent measurements. A Stonehart and Associates Model BC 1200 potentiostat was used for the purpose of providing a regulated voltage (potentiostatic mode) between the WE and CE. The a.c. ripple voltage required between the WE and CE for Mott - Schottky plots was supplied from a Krohn - Hite Model 500A generator coupled into the potentiostat. The PEC was operated in the conventional three-lead mode (Fig. 1). Data were collected using software programmed into a D.E.C. DPD-11/23 microcomputer via an A/D conversion board.

Results

Mott - Schottky Analysis

In order to calculate the doping density and flat band potential of n-CdS in the 1 M OH^- - 1 M S^{2-} - 1 M S electrolyte, the space-charge layer capacitance was measured at the semiconductor - electrolyte interface. Using the Mott - Schottky model for the junction, the space-charge layer capacitance C_{sc} can be related to the flat band potential V_{FB} by the equation[18]

$$C_{sc}^{-2} = \frac{2}{q\varepsilon\varepsilon_0 N_D A^2}(V - V_{FB} - kT/q) \quad .. \quad (2)$$

where q is the electronic charge, ε is the dielectric constant of the space-charge layer (= 5.2),[19] ε_0 is the permittivity of vacuum (= 8.85 pF m^{-1}), N_D is the effective donor density, A is the semiconductor electrode area exposed to the electrolyte and V is the applied bias *versus* SCE. The key assumption to the validity of equation (2) is that the whole potential drop takes place in the space-charge region of the semiconductor. Tomkiewicz[20] has shown that this assumption is generally valid at high bias modulation frequencies, where the equivalent electrical circuit of the electrochemical interface can be represented as a single resistor and a capacitor connected in series. Fig. 2 shows the circuit diagram for the experimental apparatus for the Mott - Schottky plot determination. A d.c. bias was applied across the WE and CE, measured with respect to an SCE. A 5-mV r.m.s. a.c. voltage was superimposed over V and the PEC reactance was plotted *versus* the modulation frequency of the a.c. voltage. Following Tomkiewicz,[20] the complex impedance of the cell can be written as

$$Z(\omega) = R_s(\omega) + iX(\omega) = R_s(\omega) - \frac{i}{\omega C_{sc}} \quad .. \quad (3)$$

where $R_s(\omega)$ is the resistance of the space-charge layer and $X(\omega)$ is the cell reactance at angular frequency $\omega = 2\pi f$. A plot of $\log(2\pi X)$ *versus* $\log f$ is shown in Fig. 3(*a*). This graph is a straight line for bias voltages away from the flat band potential. By using the intercepts, s, of curves similar to Fig. 3 with the ordinate for a number of bias voltage values V, the space-charge capacitance was determined for each V from $C_{sc}(V_k) = 10^{-s(V_k)}$. Fig. 3(*b*) shows the combined experimental and theoretical results for the equivalent resistor - capacitor electrical circuit for several capacitor values. A comparison of Fig. 3(*a*) and (*b*) is indicative of the validity of the simple resistor - capacitor representation of the semiconductor - electrolyte interface. Fig. 4 is the Mott - Schottky plot for the interface, from which the V_{FB} value was found to be −1.15 V *versus* SCE.

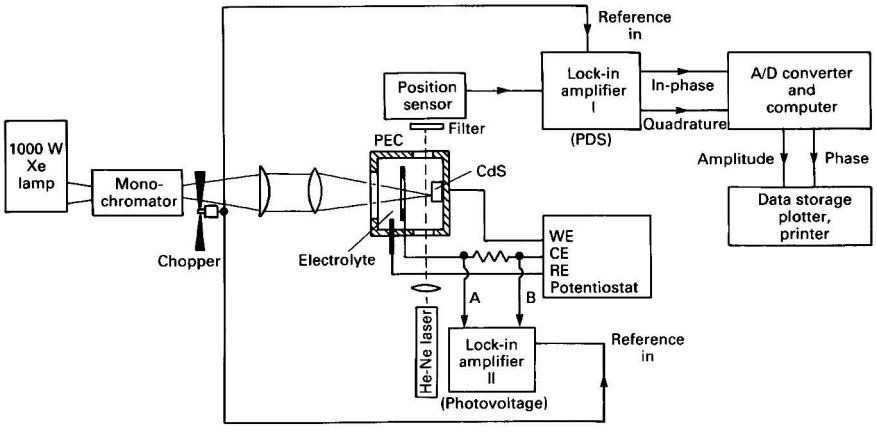

Fig. 1. Experimental apparatus for PDS and photocurrent measurements. See text for details

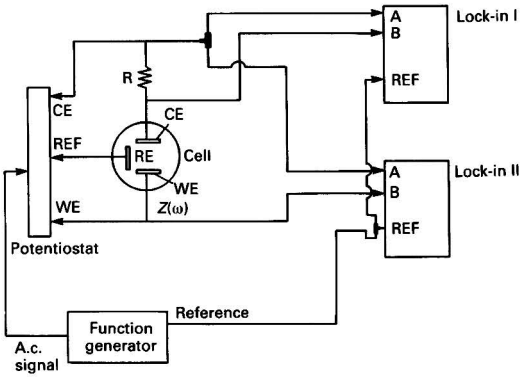

Fig. 2. Experimental apparatus for Mott - Schottky measurements. See text for details

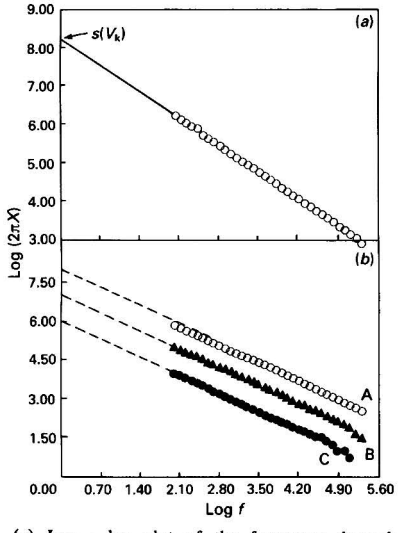

Fig. 3. (*a*) Log - log plot of the frequency dependence of photoelectrochemical cell reactance. WE at −0.75 V *vs.* SCE. (*b*) Log - log plot of the frequency dependence of the capacitance (*C*) of a resistor - capacitor simulation circuit: A, C = 10 nF; B, C = 100 nF; and C, C = 1 μF

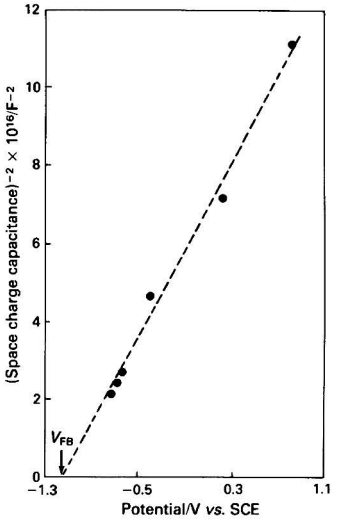

Fig. 4. Mott - Schottky plot of n-CdS in 1 M OH^- - 1 M S^{2-} - 1 M S electrolyte

The donor doping density was also calculated in terms of the slope of the Mott - Schottky plot:

$$N_D = 2/q\varepsilon\varepsilon_o A^2 \left[\frac{\partial}{\partial V}(C_{sc}^{-2})\right] \quad \ldots \ldots (4)$$

From this calculation, the doping density was found to be $N_D = 5.02 \times 10^{14}$ cm^{-3}. The value of V_{FB} found in this work is in good agreement with the range of values −1.52 to −1.20 V *versus* SCE for n-CdS of comparable donor densities calculated previously.[2]

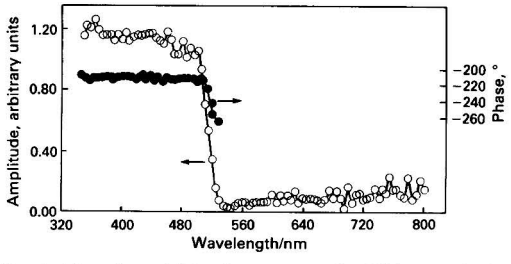

Fig. 5. Photothermal deflection spectrum of n-CdS in water in the open-circuit configuration. Modulation frequency: 25 Hz

PDS, Photovoltage and Photocurrent Spectra

PDS spectra normalised by the Xe lamp spectrum were obtained *in situ* in the PEC with water and with a polysulphide elecrolyte. The PDS spectrum of CdS in water is shown in Fig. 5. Both the amplitude and the phase indicate an energy band gap at *ca.* 510 nm, in excellent agreement with previous spectroelectrochemical work.[2] PDS signal profiles as a function of beam offset distance from a black absorber surface and as a function of chopping frequency were found to be in general agreement with Murphy and Aamodt's work.[21] Some differences in the signal profiles between this work and reference 21 were attributed to our optical *versus* their

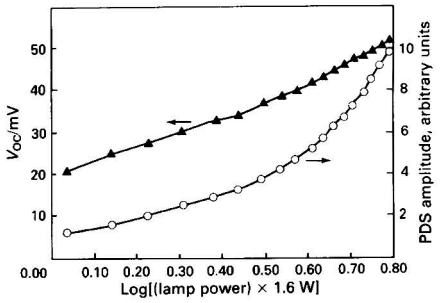

Fig. 6. PDS amplitude and open-circuit photopotential *vs.* Xe lamp light radiant flux (white light) for n-CDs in 1 M OH^- - 1 M S^{2-} - 0.05 M S. Modulation frequency: 15 Hz

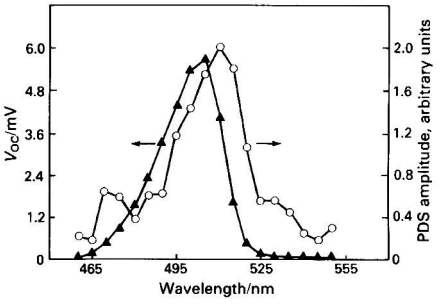

Fig. 7. PDS amplitude and photovoltage spectra of n-CdS in 1 M OH^- - 1 M S^{2-} - 0.05 M S. Modulation frequency: 17 Hz. Signal drop-off above the band gap is due to electrolyte absorption

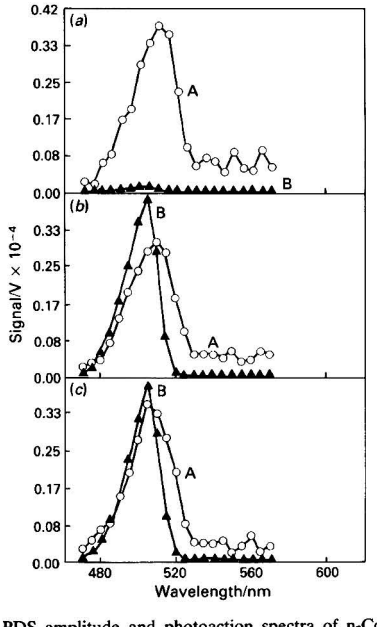

Fig. 8. PDS amplitude and photoaction spectra of n-CdS under different biases *vs.* SCE. (*a*) $V = -1.5$ V; A, PDS; B, photocurrent. (*b*) $V = -0.3$ V; A, PDS; B, photocurrent. (*c*) $V = +0.9$ V; A, PDS; B, photocurrent. Both signal strengths are in volts measured by the lock-in amplifiers. Modulation frequency: 17 Hz

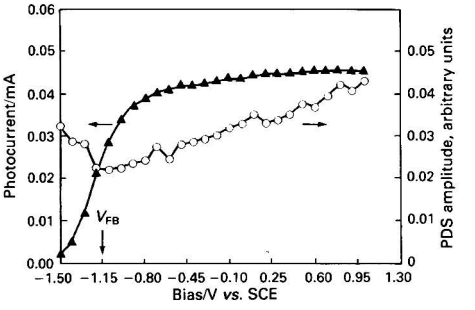

Fig. 9. PDS amplitude and photocurrent - voltage curves for n-CdS irradiated at 505 nm. Modulation frequency: 17 Hz

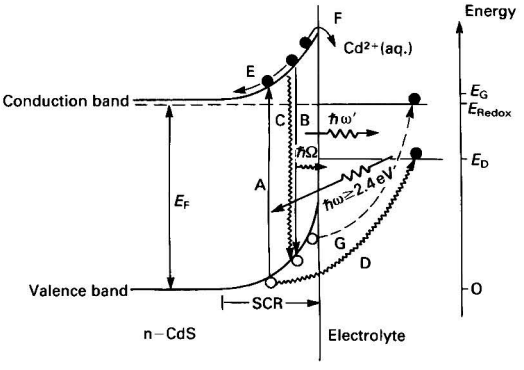

Fig. 10. Energy level diagram of n-CdS - electrolyte interface showing various possible deexcitation pathways. E_D, Activation energy for anodic decomposition; E_{Redox}, energy of electrolyte redox couple; E_G, band gap energy of semiconductor; E_F, Fermi energy of semiconductor; A, band-to-band transition; B, radiative recombination; C, non-radiative recombination; D, photoanodic decomposition; E, anodic carrier separation; F, anodic electrode dissolution; G, electrolyte redox reaction; $\hbar\omega$, incident photon energy; $\hbar\omega'$, luminescent photon energy; $\hbar\Omega$, lattice phonon energy; and SCR, space-charge region

resistive heating and to their tighter focusing of the probe beam.

Fig. 6 shows the measured PDS signal amplitude and open-circuit photopotential for n-CdS in the 1 M OH^- - 1 M S^{2-} - 0.05 M S polysulphide electrolyte as a function of incident optical power as determined by an Oriel Model 7090-2 pyroelectric detector. The monochromator was employed with the grating removed from the lamp light beam path (white light) to enhance the SNR, especially of the PDS signal. Electrode illumination with monochromatic light of 510 ± 4 nm resolution gave PDS and V_{oc} curves similar to those in Fig. 6, but with a poorer SNR. The linear dependence of V_{oc} on the logarithm of the light irradiance has been observed also by Ellis *et al.*[2] and is in agreement with theoretical considerations.[22] The PDS signal amplitude, however, is linear in the logarithm of the irradiance at low power levels and increases more rapidly at higher power levels.

Spectra acquisition in the polysulphide electrolyte was severely hampered at $\lambda < 490$ nm owing to the onset of strong absorption by the electrolyte. For reasons of SNR optimisation CdS spectra taken in the presence of 1 M NaOH - 1 M Na_2S - 0.05 M S electrolyte were not normalised with respect to the absorption spectrum of the electrolyte, as the latter is transparent in the band gap region of interest ($\lambda > 500$ nm), and the semiconductor spectral features are flat below 500 nm (Fig. 5). PDS and photovoltage spectra were obtained simultaneously. Fig. 7 shows PDS and V_{oc} spectra. The PDS

signal is large even at wavelengths below the band gap and appears to be shifted to the right of the open-circuit photovoltage spectrum. The drop-off of both signals on the high energy side is due to absorption of the incident light by the electrolyte. The sub band gap strength of the PDS signal does not appear in V_{oc}. This feature could either be excitonic in nature[23] or surface defect-related.[24] It has also been observed in photoacoustic spectra of n-CdS of the same lot obtained in this laboratory.[25]

PDS and photocurrent spectra were taken under several biases between −1.5 V and +0.9 V *versus* SCE at 0.3-V increments. The wavelength range was between 470 and 570 nm at 8-nm resolution. Fig. 8 shows results under extreme bias conditions and one intermediate value. A PDS spectral shift to longer wavelengths than the photocurrent spectrum, similar to that in Fig. 7, is apparent at all three bias levels and is characteristic of all other such spectra. For all biases shown, the PDS signal strength changes little compared with variations in the photocurrent, which undergoes a dramatic increase when the applied bias becomes positive to the flat band potential. A substantial PDS signal is present at sub-band gap wavelengths, whereas the photocurrent signal is negligible.

Photocurrent - voltage and PDS - voltage measurements were further performed, the WE being illuminated with 505-nm light. The resulting photocurrent and PDS signals were thus monitored as a variable d.c. bias was applied across the WE and CE. Fig. 9 shows the results: the photocurrent increases very rapidly at biases below and around the measured flat band potential, −1.15 V *versus* SCE, and tends to saturation at more positive biases. This behaviour is typical of CdS photoresponse.[2] The PDS signal amplitude anti-correlates with the photocurrent at biases negative to the flat band potential, exhibits a broad minimum around V_{FB} and increases steadily at more positive biases without signs of saturation.

Discussion

The major electronic phenomena occuring at the n-type semiconductor - electrolyte interface on irradiation with band gap or higher energy photons can be summarised as in Fig. 10. The band bending due to the Fermi level mismatch at the interface creates a depletion or space-charge layer, which separates the photocreated electron-hole pairs, thus preventing 100% recombination. For those carriers which eventually recombine (and do not contribute to the anodic photocurrent), both radiative and non-radiative deexcitation processes are the major recombination mechanisms competing for the carrier deactivation. The photoluminescence phenomena observed by Ellis and co-workers[1–5] in n-CdS and other II–VI semiconductors were found to be consistent with radiative deexcitation processes leading to electron-hole recombination at the interface. Non-radiative recombinations would tend to transfer the energy of the photoexcited carriers to lattice phonons resulting in localised heating at the interface. It is expected, therefore, that the PDS signal will be sensitive to the localised surface heating because of the minute variations the latter incurs in the refractive index of the liquid electrolyte adjacent to the heated surface. Assuming an electrochemically stable WE, our photocurrent and PDS results were interpreted as simultaneous monitors of carrier separation *and* non-radiative recombination mechanisms. The photoluminescent deexcitation pathway was not monitored in this work; however, comparisons were made with Ellis and co-workers' results.[4]

The donor-doping density calculated from the Mott - Schottky plot, N_D, can be compared with the theoretical value for an n-type semiconductor:

$$N_D \approx (\rho e \mu_n)^{-1} \quad \ldots \ldots \ldots \quad (5)$$

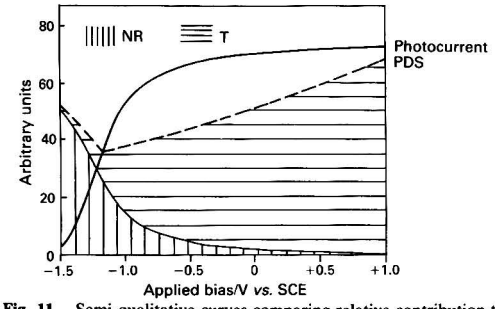

Fig. 11. Semi-qualitative curves comparing relative contribution to PDS signal with photocurrent. Photocurrent, anodic carrier separation; NR, interband non-radiative de-excitation; and T, other thermal processes in n-CdS in polysulphide electrolyte (*e.g.*, space-charge layer carrier separation, electron injection into the working electrode and intraband non-radiative de-excitations). The NR curve is in qualitative agreement with Fig. 5a in Streckert *et al.*[4] Any photodecomposition of electrode was assumed to be negligible

Using ρ = 20 ohm cm and μ_n = 300 cm^2 V^{-1} s^{-1},[26] the theoretical doping density is found to be $N_D \approx 1 \times 10^{15}$ cm^{-3}, a value within a factor of two of the experimental value.

The higher than linear dependence of the PDS signal amplitude on the logarithm of V_{oc} at large radiant fluxes (Fig. 6) is consistent with the enhancement of the PDS signal with respect to the open-circuit photovoltage of Fig. 7, at sub-band gap wavelengths, as all spectra were obtained using the highest power rating of the Xe lamp. The shift of the PDS absorption peak to the right in Fig. 7 is most likely due to surface recombination processes, intra-band gap defects and/or surface states that would provide efficient non-radiative deexcitation pathways[22] detectable by the PDS probe. A systematic study of the PDS signal as a function of controlled surface conditioning of the n-CdS crystal will be necessary to elucidate the particular mechanism(s). For energies around and above 510 nm in Fig. 7 an anti-correlation is apparent between the V_{oc} and PDS signals. At present, we propose that this is due to an increase in the numbers of efficiently separated electron - hole pairs across the space-charge region and therefore an increased value of V_{oc}, while the number of non-radiatively recombining carriers has accordingly decreased with a subsequent decrease in the PDS signal. The maximum value of V_{oc} is seen to occur at *ca.* 503 nm, in agreement with previously reported results[1] within the resolution of our monochromator (8 nm).

In Fig. 8, the PDS spectral shifts to longer wavelengths than the photoaction spectra are consistent with the energy balance mechanism proposed above: at super-band gap energies the efficiently photoseparated electron - hole pairs contribute the electron to the anodic current, while the minority carrier participates in a redox reaction at the semiconductor - electrolyte interface[2] (process G in Fig 10). This mechanism would tend to pull electrons away from the interface towards the CdS bulk, thus decreasing the probability of non-radiative recombination and would be responsible for the anti-correlation of signal observed in Fig. 8 for photon energies above *ca.* 510 nm. Another interesting feature of Fig. 8 is the effect of the bias. At applied bias negative to the flat band potential [Fig. 8(*a*)], band bending is significantly reduced. The decreased electric field across the space-charge layer all but inhibits electron - hole separation, as seen from the greatly decreased photocurrent signal, while the non-radiative deexcitation pathway remains efficient. As the space-charge layer increases with increasing bias positive to the flat bands, the photoseparation mechanism becomes more efficient and the photocurrent signal increases [Fig 8(*b*) and (*c*)]. It is interesting that the PDS signal, associated with the non-radiative component, remains approximately as strong in Fig. 8(*b*) and (*c*) as in Fig. 8(*a*). It must be deduced, therefore, that there is a

significant decrease in the carrier numbers deexciting via pathways other than non-radiative with increasing bias and re-channeling of the excess of carriers to the external circuit. This mechanism is in agreement with the inhibition of the photoluminescent emission observed by Streckert *et al.*[4] at positive biases.

An analysis of Fig. 9 indicates that as the degree of band bending in the CdS space-charge layer is changed, via the applied bias, the predominant heat-generating mechanisms in the WE are altered. For biases at or below −1.2 V, the major source of heat is non-radiative recombination; note that the PDS signal increases and the photocurrent decreases as the voltage decreases from −1.2 V. However, for biases greater than −1.2 V, non-radiative recombination becomes less important as the carrier-separation efficiency increases. At these positive voltages, where a significant photocurrent is present, the dominant heat sources are: (a) carrier separation in the space-charge layer; (b) electron injection and subsequent deexcitation into the valence band from the solution redox couple; and (c) non-radiative transitions of hot electrons in the conduction band.

A semi-qualitative indication as to the relative percentage contribution to the PDS signal from the inter-band non-radiative recombination compared with other current - flow related heating processes, such as those discussed above, is shown in Fig. 11. The non-radiative component anti-correlates with the photocurrent, while the other thermal components correlate with the photocurrent, as expected.[11] The non-radiative component *versus* voltage curve in Fig. 11 agrees well with photoluminescent emission intensity *versus* voltage data from a similar photoelectrochemical experiment with CdS [reference 4, Fig. 5(*a*)]. This correlation between radiative and non-radiative processes is to be expected as they constitute complementary carrier deexcitation pathways to the current-producing electron - hole separation.

Further evidence for assuming that the heat-generation mode in the WE changes nature close to the flat band potential is found when one considers the phase data of the PDS signal for various applied biases. A phase shift of 20° was observed in the region corresponding to the "knee" of the PDS signal *versus* voltage curve in Fig. 9. This phase shift would suggest a fundamental change in the heat generation processes. The various heat generation processes discussed above are expected to take place at different locations relative to the WE - electrolyte interface; a PDS phase shift would indicate a shift in the thermal source location within the WE.

In conclusion, the PDS technique coupled with photoaction spectra has been shown to be capable of monitoring non-radiative recombination and other heat-generating processes at the semiconductor - electrolyte interface and to measure directly the so far little studied non-radiative efficiency of PECs. These observations could be significant in the calculation of PEC efficiency losses and their minimisation through the physical understanding of the interfacial loss mechanisms, for which PDS appears to be a very promising probe.

The authors acknowledge the support of the National Sciences and Engineering Research Council of Canada (NSERC) throughout the duration of this project. They are also grateful to the Institute for Hydrogen Systems (IHS), Mississauga, Ontario, for contributing the PDS apparatus towards the completion of this work. Useful initial discussions on some experimental aspects with Drs. S.-M. Park (Department of Chemistry, University of New Mexico) and M. Weber (Department of Chemistry, University of Toronto) are gratefully acknowledged.

References

1. Ellis, A. B., Kaiser, S. W., and Wrighton, M. S., *J. Am. Chem. Soc.*, 1976, **98**, 6855.
2. Ellis, A. B., Kaiser, S. W., Bolts, J. M., and Wrighton, M. S., *J. Am. Chem. Soc.*, 1977, **99**, 2839.
3. Karas, B. R., and Ellis, A. B., *J. Am. Chem. Soc.*, 1980, **102**, 968.
4. Streckert, H. H., Tong, J.-R., Carpenter, M. K., and Ellis, A. B., *J. Electrochem. Soc.*, 1982, **129**, 772.
5. Streckert, H. H., and Ellis, A. B., *J. Phys. Chem.*, 1982, **86**, 4921.
6. Smiley, P. M., Biagioni, R. N., and Ellis, A. B., *J. Electrochem. Soc.*, 1984, **131**, 1068.
7. Wilson, J. R., and Park, S.-M., *J. Electrochem. Soc.*, 1982, **129**, 149.
8. Masuda, H., Fujishima, A., and Honda, K., *Bull. Chem. Soc. Jpn.*, 1982, **55**, 672.
9. Dohrmann, J. K., and Sander, U., *J. Phys, (Paris)*, 1983, **C6**, 281.
10. Bell, A. G., *Am. J. Sci.*, 1880, **20**, 305.
11. Fujishima, A., Maeda, Y., Honda, K., Brilmyer, G. H., and Bard, A. J., *J. Electrochem. Soc.*, 1980, **127**, 840.
12. Mendoza-Alvarez, J. G., Royce, B. S. H., Sanchez-Sinencio, F., Zelaya-Angel, O., Menezes, C., and Triboulet, R., *Thin Solid Films*, 1983, **102**, 259.
13. Roger, J. P., Fournier, D., and Boccara, A. C., *J. Phys. (Paris)*, 1983, **C6**, 313.
14. Mandelis, A., *J. Appl. Phys.*, 1983, **54**, 3404.
15. Mandelis, A., and Royce, B. S. H., *Appl. Opt.*, 1984, **23**, 2892.
16. Williams, R., *J. Chem. Phys.*, 1959, **32**, 1505.
17. Dutton, D., *Phys. Rev.*, 1958, **112**, 785.
18. Salvador, P., *J. Appl. Phys.*, 1984, **55**, 2977.
19. Van Vechten, J. A., *Phys. Rev.*, 1969, **182**, 899.
20. Tomkiewicz, M., *J. Electrochem. Soc.*, 1979, **126**, 2220.
21. Murphy, J. C., and Aamodt, L. C., *J. Appl. Phys.*, 1980, **51**, 4580.
22. Gerisher, H., *in* Eyring, H., Henderson, D., and Jost, W., *Editors*, "Physical Chemistry: An Advanced Treatise," Volume 9A, Academic Press, New York, 1970, Chapter 5.
23. Thomas, D. G., Hopfield, J. J., and Power, M., *Phys. Rev.*, 1960, **119**, 570.
24. Wasa, K., Tsubouchi, K., and Mikoshiba, N., *Jpn. J. Appl. Phys.*, 1980, **19**, L475.
25. Siu, E., and Mandelis, A., "Fourth International Topical Meeting on Photoacoustic, Thermal and Related Sciences, Montreal, Canada, 1985," Technical Digest, WD 11.1, École Polytechnique, Montreal.
26. Sze, S. M., "Physics of Semiconductor Devices," Wiley, New York, 1969, p. 21.

Paper A5/235
Received July 1st, 1985
Accepted November 10th, 1985

Extraction - Spectrophotometric Determination of Cadmium

Yadvendra K. Agrawal and Tushar A. Desai
Analytical Chemistry Laboratory, Department of Pharmacy, Faculty of Technology and Engineering, M.S. University of Baroda, Kalabhavan, Baroda-390 001, India

A simple and sensitive extraction - spectrophotometric method for the determination of cadmium is described. The binary complex formed between cadmium and *N*-phenylcinnamohydroxamic acid (PCHA) is extracted with chloroform at pH 9.5, and shows maximum absorbance at 380 nm with a molar absorptivity of 3.6×10^3 l mol^{-1} cm^{-1}. The optimum concentration range for measurements is 1.41–11.25 p.p.m. The sensitivity of the method was increased by the addition of 4-(2-pyridylazo)resorcinol (PAR) after extracting cadmium with PCHA at pH 9.5. The Cd - PCHA - PAR complex is reddish orange and shows maximum absorbance at 510 nm with a molar absorptivity of 4.8×10^4 l mol^{-1} cm^{-1}. It obeys Beer's law over the range 0.23–2.25 p.p.m. Various experimental parameters were studied for establishing the optimum conditions for the determination of cadmium. The method had been applied to the determination of cadmium in standard and environmental samples.

Keywords: *Cadmium determination; N-phenylcinnamohydroxamic acid; 4-(2-pyridylazo)resorcinol; extraction; spectrophotometry*

The analytical chemistry of cadmium has developed considerably in recent years especially owing to its toxicity and ubiquity. High concentrations have been found related to industrial activity in some areas.[1] Cd metal itself is not toxic, but most of its compounds have very high toxicity on inhalation. Cadmium and mercury are considered to be two major pollutants for which new and better abatement processes and analytical methods are required. Liquid - liquid extraction is an attractive technique for meeting these challenges.[2]

Dithizone, Cadion, 4-(2-pyridylazo)resorcinol (PAR), etc., have been used for the spectrophotometric determination of cadmium, but the methods are tedious and not selective as many of the common ions interfere.[3–6]

Hydroxamic acids have been widely studied and applied as potential analytical reagents for the separation, detection and determination of various metal ions[7–9] and have also been employed as possible spectrophotometric reagents for metal ions.[10] A few hydroxamic acids have been employed for the extraction and spectrophotometric determination of cadmium.[11–14] Cadmium forms a colourless complex with hydroxamic acid and spectrophotometric determination is possible utilising some chromogenic reagents. The method presented here provides a simple and precise direct determination of yellow cadmium hydroxamate at 380 nm using *N*-phenylcinnamohydroxamic acid (PCHA) in chloroform. The sensitivity of the method was further enhanced by utilising PAR. Moreover, the proposed method also provides a simple and rapid separation of small amounts of cadmium from larger amounts of closely related metal ions. The method has been applied to the determination of cadmium in standard and environmental samples.

Experimental

Apparatus

The spectral measurements were made on VSU 2-P (Carl-Zeiss) spectrophotometer. The pH adjustments were made on Systronics Model 335 digital pH meter, equipped with glass and calomel electrodes.

Chemicals and Reagents

All the chemicals used were of AnalaR and GR grades from BDH Chemicals and E. Merck, respectively, unless stated otherwise.

N-Phenylcinnamohydroxamic acid (PCHA). Freshly synthesised as described elsewhere[15] (m.p. 159 °C; literature[16] m.p., 162 °C). The purity of the reagent was checked by TLC and UV and IR spectroscopy and a 0.10% *m/V* solution was prepared in chloroform.

Standard buffer solutions. Prepared from a mixture of 0.025 M $Na_2B_4O_7$ and 0.1 M NaOH solutions (also form a mixture of 0.05 M $NaHCO_3$ and 0.1 M NaOH solutions) as described elsewhere.[17]

Standard cadmium solution, 4.95×10^4 M. Prepared by dissolving 0.3809 g of $3CdSO_4.8H_2O$ in 1 l of doubly distilled water. The cadmium content was determined titrimetrically.[18]

PAR solution 0.1% *m/V* in 95% *ethanol.*

Extraction Procedure

An aliquot of solution containing 5.62 p.p.m. of Cd(II) (1.0 ml of 4.95×10^{-4} M solution) was transferred into a 60-ml separating funnel and sufficient amounts of distilled water and buffer solution were added to maintain the pH at 9.5 in a total volume of aqueous phase of 10 ml. A 10-ml volume of 0.10% PCHA solution in chloroform was added and the mixture was shaken vigorously for 10–15 min. The phases were allowed to separate and a yellow chloroform layer was collected in a 10-ml calibrated flask after drying over anhydrous sodium sulphate. The absorbance of the yellow chloroform extract was measured at 380 nm against a reagent blank prepared as above but without cadmium.

To enhance the sensitivity of the method, PAR solution was added to the Cd - PCHA extract, and the contents were diluted to 25 ml with ethanol. The absorbance was measured at 510 nm against a reagent blank.

Results and Discussion

Absorption Spectra

The yellow Cd - PCHA complex shows maximum absorbance at 380 nm, while the reagent (PCHA) has maximum absorbance at 290 nm and no absorbance at 380 nm. The Cd - PCHA complex has a molar absorptivity 3.8×10^3 l mol^{-1} cm^{-1}. The Cd - PCHA - PAR extract has maximum absorbance at 510 nm with a molar absorptivity of 4.8×10^4 l mol^{-1} cm^{-1}.

The enhanced sensitivity of PCHA as reflected by an increased molar absorptivity is due to the increase in the length of conjugation by introduction of the side-chain double

bond, –CH=CH– between the R group and the carbon atom of the carbonyl group:

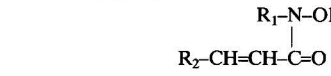

where $R_1 = R_2$ = phenyl.

Effect of pH

The optimum pH for the complete extraction of cadmium with PCHA in chloroform was studied over the range 1.0–10.5. It was observed that the extraction commences at pH 6.0 and is maximum at pH 9.0–9.8 (Table 1); above pH 9.8 the extraction decreases. Hence pH 9.5 was chosen for extraction.

Effect of PCHA Concentration

Extractions were carried out with various amounts of PCHA and it was found that 10 ml of 0.1% PCHA solution in chloroform is adequate for the complete extraction of cadmium. A further excess of PCHA increased the absorbance of the reagent blank. However, for Cd - PCHA - PAR a large excess of PCHA (15 ml of 0.2% PCHA solution in $CHCl_3$) could be used without any difficulty (Tables 2 and 3).

Effect of PAR Concentration

Studies with various concentrations of PAR showed that 2.0 ml of a 0.1% solution of PAR in ethanol was adequate for complete colour development (Table 4). A further excess of PAR increased the absorbance of the reagent blank.

Effect of Shaking Time and Stability

The extraction of cadmium complex is rapid under the conditions recommended in the procedure. A shaking time of 10–15 min is sufficient for the complete extraction of cadmium and the binary Cd - PCHA complex is stable for 3–4 h.

Effect of Solvents

Various solvents were studied for the quantitative extraction of cadmium, *viz.*, chloroform, carbon tetrachloride, toluene, benzene and chlorobenzene. Chloroform was found to be the most suitable (Table 5).

Table 1. Effect of pH on the extraction of the Cd - PCHA complex. Cd(II), 5.62 p.p.m.; PCHA, 10 ml of 0.1% solution in $CHCl_3$; solvent, $CHCl_3$; colour of complex, yellow; λ_{max}, 380 nm. The extraction (E) is given by $E(\%) = 100D/(D + V_{aq.}/V_{org.})$, and the distribution coefficient (D) is calculated from D = concentration of Cd in organic phase/(total Cd taken − Cd extracted into organic phase)

pH	Absorbance	Molar absorptivity/ l mol^{-1} cm^{-1}	E, %
6.0	0.02	4.0×10^2	11
7.0	0.02	4.0×10^2	11
8.0	0.02	4.0×10^2	11
8.5	0.08	1.6×10^3	44
9.0	0.13	2.6×10^3	72
9.5	0.18	3.6×10^3	100
9.8	0.17	3.4×10^3	94
10.0	0.10	2.0×10^3	55
10.5	0.06	1.2×10^3	33

Table 2. Effect of PCHA concentration on the extraction of the Cd - PCHA complex. Cd(II), 5.62 p.p.m.; PCHA, 10 ml of solution in $CHCl_3$; solvent, $CHCl_3$; colour of complex, yellow; $\lambda_{max.}$ 380 nm

Reagent concentration, %	Absorbance	Molar absorptivity/ l mol^{-1} cm^{-1}	E, %
0.05	0.15	3.0×10^3	81
0.10	0.18	3.6×10^3	100
0.15	0.13	2.6×10^3	72
0.20	0.10	2.0×10^3	55

Table 3. Effect of PCHA concentration on the extraction of the Cd - PCHA - PAR complex. Cd(II), 1.124 p.p.m.; PCHA, 10 ml of solution in $CHCl_3$; PAR, 2.0 ml of 0.1% solution in EtOH; solvent, $CHCl_3$ - EtOH (1 + 1); colour of complex, reddish orange; $\lambda_{max.}$, 510 nm

Concentration of PCHA, %	Absorbance	Molar absorptivity/ l mol^{-1} cm^{-1}	E, %
0.03	0.30	3.0×10^4	62
0.05	0.38	3.8×10^4	79
0.10	0.44	4.4×10^4	92
0.20	0.48	4.8×10^4	100
0.25	0.39	3.9×10^4	81

Table 4. Effect of PAR concentration on the extraction of the Cd - PCHA - PAR complex. Cd(II), 1.124 p.p.m.; PCHA, 15 ml of 0.2% solution in $CHCl_3$; PAR, 0.1% solution in EtOH; solvent, $CHCl_3$ - EtOH (1 + 1); colour of complex; reddish orange; $\lambda_{max.}$, 510 nm

Volume of PAR solution/ml	Absorbance	Molar absorptivity/ l mol^{-1} cm^{-1}	E, %
1.0	0.25	2.5×10^4	52
1.5	0.37	3.7×10^4	77
2.0	0.48	4.8×10^4	100
2.5	0.34	3.4×10^4	71
3.0	0.24	2.4×10^4	50

Table 5. Effect of solvents on the extraction of the Cd - PCHA complex. Cd(II), 5.62 p.p.m.; PCHA, 10 ml of 0.1% solution; colour of complex, yellow; $\lambda_{max.}$, 380 nm

Solvent	Absorbance	Molar absorptivity/ l mol^{-1} cm^{-1}	E, %
Chloroform . .	0.18	3.6×10^3	100
Benzene	0.13	2.6×10^3	72
Carbon tetrachloride . .	0.15	3.0×10^3	83
Chlorobenzene	0.10	2.0×10^3	55
Toluene	0.14	2.8×10^3	78

Table 6. Effect of diverse ions on extraction. Cd - PCHA system (I): Cd(II), 5.62 p.p.m.; PCHA, 10 ml of 0.1% solution in $CHCl_3$; solvent, $CHCl_3$; λ_{max}, 380 nm; absorbance, 0.18. Cd - PCHA - PAR system (II): Cd(II), 1.124 p.p.m.; PCHA, 10 ml of 0.2% solution in $CHCl_3$; PAR, 2.0 ml of 0.1% solution in EtOH; solvent, $CHCl_3$ - EtOH (1 + 1); $\lambda_{max.}$, 510 nm; absorbance, 0.48

Ion	Added as	Amount/mg	Absorbance System I	Absorbance System II
Ba^{2+} . .	$BaCl_2$	40	0.18	0.48
Sr^{2+} . .	$SrCl_2$	50	0.18	0.48
Cd^{2+} . .	$CdCl_2$	40	0.18	0.48
Pb^{2+} . .	$Pb(C_2H_3O_2)_2$	50*	0.16	0.47
Be^{2+} . .	$BeSO_4$	50	0.18	0.48
Mg^{2+} . .	$MgSO_4$	50	0.18	0.48
Cu^{2+} . .	$CuSO_4$	50	0.18	0.48
Ni^{2+} . .	$NiCl_2$	50	0.18	0.48
Co^{2+} . .	$CoCl_2$	50	0.18	0.48
As^{3+} . .	As_2O_3	40	0.18	0.48
Ti^{4+} . .	$TiCl_4$	40	0.19	0.48
Zr^{4+} . .	$Zr(NO_3)_4.5H_2O$	30	0.18	0.48
Mo^{6+} . .	$(NH_4)_6Mo_7O_{24}$	30	0.18	0.48
V^{5+} . .	NH_4VO_3	50	0.18	0.48
Hg^{2+} . .	$HgCl_2$	50†	0.17	0.49
Mn^{2+} . .	$MnSO_4$	40*	0.17	0.47
Zn^{2+} . .	$ZnSO_4$	50	0.18	0.48

* Masked with NaF (10 ml of 0.1 M NaF solution).
† Masked with ascorbic acid (10 ml of 0.1 M ascorbic acid).

Table 7. Determination of cadmium in standard and environmental samples

Sample	Certified Cd content, %	Cd found by present method, %	Standard deviation, %	Coefficient of variation, %	Cd found by AAS, %
Copper alloys, BS 2873 C108	0.8	0.79	0.01	1.25	0.80
Magnesium alloy, BS 2901D6	1.5–2.5	2.20	0.02	0.90	2.20
Low-melting solder, BS 219 Grade T (DIN 1707, L-SnPb)	18	17.99 p.p.m.	0.02	0.11	18.0 p.p.m.
Blood (per 100 ml)	—	10.60	—	—	10.58
Urine (μg g^{-1} creatine)	—	10.25	—	—	10.26
Soil*	—	4.80	—	—	4.82
Plant*	—	1.20	—	—	1.20
Industrial effluent†	—	30.00	—	—	30.08
Tobacco‡	—	1.38	—	—	1.40
Waste water§	—	24.96	—	—	24.93

* Samples from G.I.D.C. Makarpura area of Baroda, average of ten samples.
† Samples from Nandeshari Industrial area of Baroda.
‡ Samples from Channi area of Baroda.
§ From Baroda City.

Beer's Law, Molar Absorptivity and Sensitivity

The Cd - PCHA and Cd - PCHA - PAR complexes obey Beer's law from 1.40 to 11.25 and from 0.23 to 2.25 p.p.m. of cadmium, respectively. The molar absorptivities were found to be 3.6×10^3 and 4.8×10^4 l mol^{-1} cm^{-1}, respectively.

Precision and Accuracy

The standard deviation for ten determinations of cadmium (5.62 ppm) was found to be 0.02 p.p.m. and the coefficient of variation was 0.35%.

Stoicheiometry of the Complex

The stoicheiometric composition of the complex was determined by employing the slope ratio method.[19] The stoicheiometry of the Cd - PCHA complex was determined by taking a fixed amount of Cd (1.0 ml of 5×10^{-4} M solution) and gradually increasing the amount of 5×10^{-4} M reagent solution (L_1), keeping the concentration of PAR constant. The slope of the graph of log D_M *versus* $-\log[L_1]$ was found to be 2.0, confirming a metal to ligand (PCHA) ratio of 1:2.

The stoicheiometery of the Cd - PCHA - PAR complex was determined by taking a fixed volume of metal solution (1.0 ml of 5×10^{-4} M solution) and 10 ml of 5×10^{-4} M PCHA in chloroform and gradually increasing the amount of PAR (L_2). The slope of the graph of log D_M *versus* $-\log[L_2]$ was found to be 2.0, confirming a metal to ligand (PAR) ratio of 1:2.

It seems that on addition of PAR to the chloroform extract of cadmium, the PCHA is replaced with PAR.

Effects of Diverse Ions

In order to assess possible analytical applications of the reaction, the effects of diverse ions on the extraction and spectrophotometric determination of Cd(II) were studied by adding a known amount of the ion in question to a solution containing 5.62 p.p.m. of cadmium and following the recommended procedure.

Ba^{2+}, Sr^{2+}, Ca^{2+}, Be^{2+}, Mg^{2+}, Cu^{2+}, Ni^{2+}, Co^{2+}, As^{3+}, Ti^{4+}, Zr^{4+}, Mo^{6+}, V^{5+} and Zn^{2+} do not interfere in the determination of cadmium even at high concentrations. Hg^{2+}, Pb^{2+} and Mn^{2+} interfere; the interference due to Hg^{2+} can be eliminated with ascorbic acid and that due to Pb^{2+} and Mn^{2+} with sodium fluoride (Table 6).

Determination of Cadmium in the Environment

Depending on the concentration of cadmium in environmental samples (soil, plant, waste water, etc.), 20–50 g of material were digested with an excess of perchloric and nitric acids. The mixture was centrifuged and filtered, and the filtrate was evaporated to dryness and the residue dissolved in and diluted to 100 ml with 0.1 M HCl. A 10-ml of sample solution was used for the determination of cadmium. The results are given in the Table 7.

References

1. Forstner, U., and Muller, G., "Schwermetalle in Flussen und Seen als Ausdrucker Umweltverschmutzung," Springer Verlag, Berlin, Heidelberg, New York, 1974, p. 18.
2. Moore, F. L., *Environ. Sci. Technol.*, 1972, **6**, 525.
3. Agrawal, Y. K., and Mehd, G. D., *Rev. Anal. Chem.*, 1982, **6**, 185.
4. Sandell, E. B., and Onishi, H., "Chemical Analysis, Volume 3, Part I, Traces of Metals: General Aspects," Wiley–Interscience, New York, 1978.
5. Watanabe, H., and Ohonori, H., *Talanta*, 1979, **26**, 959.
6. Anderson, R. G., and Nickless, G., *Anal. Chim. Acta*, 1967, **39**, 469.
7. Agrawal, Y. K., *Rev. Anal. Chem.*, 1980, **5**, 3.
8. Agrawal, Y. K., and Patel, S. A., *Rev. Anal. Chem.*, 1980, **4**, 237.
9. Agrawal, Y. K., and Jain, R. K., *Rev. Anal. Chem.*, 1982, **6**, 49.
10. Bass, V. C., and Yoe, J. H., *Talanta*, 1966, **13**, 735.
11. Patke, S. K., *PhD Thesis*, M.S. University of Baroda, 1980.
12. Mehd, G. D., *PhD Thesis*, M.S. University of Baroda, 1982.
13. Rathi, B. N., *PhD Thesis*, M.S. University of Baroda, 1982.
14. Brydon, G. A., and Ryan, D. E., *Anal. Chim. Acta*, 1966, **35**, 190.
15. Bhura, D. C., and Tandon, S. G., *J. Chem. Eng. Data*, 1971, **16**, 106.
16. Tandon, S. G., and Bhattacharya, S. C., *J. Chem. Eng. Data*, 1962, **7**, 553.
17. Dean, J. A., "Lange's Handbook of Chemistry," Twelfth Edition, McGraw-Hill, New York, 1979.
18. Welcher, F. J., "The Analytical Uses of Ethylenediaminetetraacetic Acid," Van Nostrand, New York, 1965.
19. Branko, T. B., and Jerome, O. W., *Anal. Chem.*, 1973, **45**, 1519.

Paper A5/292
Received August 8th, 1985
Accepted September 19th, 1985

Extraction - Spectrophotometric Determination of Manganese with 3-Phenyl-2-mercaptopropenoic Acid

Alvaro Izquierdo, M. Dolors Prat, Núria Garriga and José M. Alegria
Department of Analytical Chemistry, University of Barcelona, Barcelona-28, Spain

An extraction - spectrophotometric procedure for the determination of manganese(II) based on the formation of a chelate with 3-phenyl-2-mercaptopropenoic acid is described. The 1:2 manganese complex is quantitatively extracted into isoamyl alcohol (2-methylbutan-1-ol) in the pH range 6.3–9.4. The extract shows maximum absorbance at 625 nm ($\varepsilon = 7.3 \times 10^3$ l mol^{-1} cm^{-1}) and obeys Beer's law up to 20 μg ml^{-1} of manganese. The method is selective and has been applied successfully to the determination of manganese in standard samples.

Keywords: *Manganese determination; 3-phenyl-2-mercaptopropenoic acid; spectrophotometry; solvent extraction*

3-Aryl-2-mercaptopropenoic acids, characterised by the structure I, are good chelating agents for metal ions. Most of the complexes formed are coloured and readily extractable into oxygen-containing organic solvents, such as alcohols and ketones. In previous papers[1–3] we reported some mercaptopropenoic acids for the extraction and determination of several metal ions. In this work the complex formation of manganese(II) with 3-phenyl-2-mercaptopropenoic acid (PMPA) is described. The green colour ($\lambda_{max.} = 625$ nm) of the extracted complex into isoamyl alcohol (2-methylbutan-1-ol) provides the basis of a spectrophotometric method for the determination of manganese.

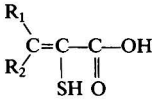

R_1 = aryl; R_2 = alkyl or H

I

The sensitivity of the proposed method is about four times that of the most widely used routine procedure based on the oxidation of manganese(II) to manganese(VII)[4,5] and, although it is lower than those of other reagents such as the heterocyclic azo dyes 4-(2-pyridylazo)resorcinol (PAR) or 1-(2-pyridylazo)-2-naphthol (PAN),[6,7] the method has the advantage of higher selectivity. The most usual interferents in manganese determinations, such as iron and nickel, have been eliminated using masking agents.

The applicability of the method was tested by the determination of manganese in standard samples.

Experimental

Apparatus

A Beckman Acta VII spectrophotometer with 10-mm silica cells, a Perkin-Elmer 4000 atomic absorption spectrophotometer and a Radiometer PHM 64 pH meter equipped with glass - calomel electrodes were used.

Reagents

Analytical-reagent grade chemicals were used throughout without further purification, unless stated otherwise.

Standard manganese solution. A stock solution of manganese(II) chloride (1 g l^{-1} of Mn) was prepared and standardised complexometrically. Working solutions were prepared daily by diluting this stock solution to appropriate concentrations.

3-Phenyl-2-mercaptopropenoic acid (PMPA) solution. A 0.5% PMPA solution in purified isoamyl alcohol was used. The PMPA was synthesised and purified as described previously.[8] This solution was prepared fresh daily.

Buffer solutions. Acetic acid - sodium hydroxide, hydrochloric acid - tris(hydroxymethyl)aminomethane and ammonia - ammonium chloride buffer solutions were used. The ionic strength was adjusted by the addition of sodium nitrate.

Procedures

Determination of manganese

Transfer 10 ml of buffered sample solution containing 10–200 μg of manganese into a 50-ml separating funnel and equilibrate with 10 ml of PMPA reagent in isoamyl alcohol by shaking for 10 min. Collect the organic layer, dry over anhydrous sodium sulphate and measure the absorbance at 625 nm against a reagent blank. Use standard manganese solutions treated in the same way to prepare the calibration graph. The colour is stable for at least 2 h.

Analysis of aluminium alloys

Weigh up to 0.1 g of sample containing 0.1–2 mg of manganese into a 100-ml beaker. Add 5 ml of 10% sodium hydroxide solution in small portions. Evaporate to a syrupy consistency, remove from the hot-plate and carefully add 5 ml of cold water and cool. Add 5 ml of nitric acid (1 + 1) and heat to dissolve the salts and expel the brown fumes. Cool, transfer into a 100-ml calibrated flask, add 1–3 ml of 0.2 M ascorbic acid, depending on the content of iron, and 5–10 ml of 1 M citric acid to prevent the precipitation of aluminium, and adjust the pH to 8.5–9 with ammonia - ammonium chloride buffer solution. Add 1–2 ml of 2 M potassium cyanide solution and dilute to volume. Use 10 ml of this solution to determine manganese as described. Use standard manganese solutions treated in the same way to prepare the calibration graph.

Analysis of stainless steel

Weigh up to 0.025 g of sample, containing 0.1–2 mg of manganese, into a 100-ml beaker. Add 10 ml of a mixture of hydrochloric and nitric acids (1 + 1) and heat gently until decomposition is complete. Add more acid if necessary. Continue the heating to evaporate the excess of acid, cool and transfer into a 100-ml calibrated flask. Add 4–6 ml of 0.5 M

ascorbic acid, 2 ml of 1 M citric acid and neutralise. Add 4–6 ml of 2 M potassium cyanide solution, adjust the pH to 8.5–9.0 and dilute to volume. Extract at once 10 ml of this solution by shaking for 10 min with 10 ml of PMPA reagent in isoamyl alcohol and determine manganese as described. Use standard manganese solutions treated in the same way to prepare the calibration graph.

Analysis of zinc blende

Weigh up to 0.1 g of sample containing 0.1–2 mg of manganese into a 100-ml beaker. Dissolve by heating with hydrochloric acid with the aid of nitric acid. Cool, dilute with distilled water, remove insoluble sulphur residue, if present, by filtration, transfer into a 100-ml calibrated flask and proceed according the method described for steel. The amount of ascorbic acid to be added depends on the content of iron.

Results and Discussion

Characteristics of the Manganese Complex

The green manganese complex formed is soluble in water and in some oxygen-containing organic solvents, such as alcohols and ketones, but is not extractable into non-polar solvents such as benzene or chloroform.

The absorption spectrum of the aqueous solution exhibits a maximum at 625 nm, but its absorbance decreases gradually with time. Organic solutions have similar absorption peaks

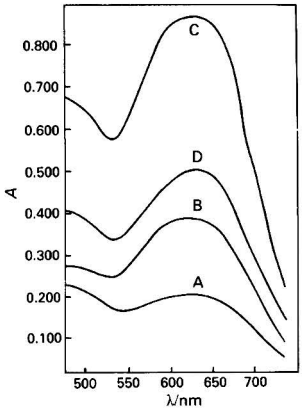

Fig. 1. Absorption spectra of the manganese(II) complex extracted into isoamyl alcohol at different pH values of the aqueous phase. Mn(II), 6.46 μg ml^{-1}. pH, A, 4.32; B, 5.21; C, 7.18; and D, 10.52

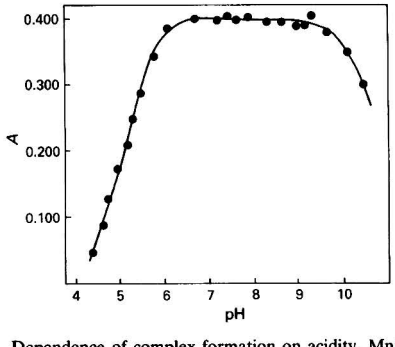

Fig. 2. Dependence of complex formation on acidity. Mn(II), 2.9 μg ml^{-1}

and good stabilities. Under optimum conditions, manganese can be extracted quantitatively from aqueous solutions with PMPA in isoamyl alcohol. The absorption spectra of the manganese complex in isoamyl alcohol are shown in Fig. 1. The curves have a maximum at 625 nm and PMPA has negligible absorption at this wavelength. A maximum and constant absorbance of the organic phase at 625 nm is obtained between pH values of the aqueous phase of 6.3 and 9.4, as shown in Fig. 2. In less or more acidic solutions, the absorbance decreases rapidly. The presence of electrolytes slightly increases the maximum recovery of manganese but no appreciable effect is observed when the ionic strength is >1. A large excess of reagent is necessary for the complete extraction of manganese. The absorbance of the organic phase increases with increasing amount of PMPA up to an 80-fold molar excess. The colour intensity of the complex thus obtained is constant for at least 2 h. Addition of more reagent has no effect on the absorbance but improves the stability of the extracted complex.

A shaking time of 2 min is adequate for the quantitative extraction of manganese under the optimum conditions, the recovery being higher than 99.9%. In the presence of high concentrations of foreign species the colour development is retarded in some instances and therefore a shaking period of 10 min is selected in the recommended procedure. The extraction efficiency was calculated by measuring the manganese concentration of the aqueous phase by atomic absorption spectrometry.

Beer's Law and Precision

The system obeys Beer's law up to a concentration of 20 μg ml^{-1} of manganese. The molar absorptivity at 625 nm is 7.3×10^3 l mol^{-1} cm^{-1}. The limit of detection, expressed as the concentration that gives an absorbance three times greater than the standard deviation of the blank, is 0.06 μg ml^{-1} of manganese. The optimum concentration range, evaluated by Ringbom's method, is 1.4–5.6 μg ml^{-1} of manganese. Ten determinations on standard solutions containing 3.47 μg ml^{-1} gave a relative standard deviation of 0.28%.

Composition of the Complex

The stoicheiometry of the extracted species was studied by the equilibrium shift method. Manganese (3.24 μg ml^{-1}) was extracted at constant pH (5.1) using various concentrations of reagent (2.10–8.10 M). The mercapto acid was introduced in ethanolic medium into the aqueous phase because at this pH the equilibrium was attained very slowly when the reagent was dissolved in the organic phase. The ethanol concentration in the aqueous phase before the extraction was kept constant at 10% *V/V*. The plot of log *D vs.* PMPA concentration was linear with a slope of 2.1, indicating that the metal to ligand ratio was 1:2.

Interferences

The effects of diverse ions on the determination of manganese were examined under the optimum conditions. The tolerance limit was taken as that concentration which does not cause more than a 2% change in the absorbance.

The complexing agents oxalate, tartrate, citrate, phosphate, cyanide and fluoride do not interfere in the determination and were used as masking agents. EDTA inhibits the colour formed by manganese with PMPA.

The interference of most of the ions forming coloured species that absorb near 625 nm under similar experimental conditions can be avoided. Thus, addition of cyanide eliminates the interferences due to Pd(II), Cu(II), Ni(II), Fe(II) and Fe(III) (after reduction with ascorbic acid), whereas Ti(IV) can be masked with fluoride. Certain metal ions, such

Table 1. Results for the determination of manganese in real samples. Each result is the average of five separate determinations

Sample	Composition, %	Mn certified, %	Mn found, %
Stainless steel (NBS 121 d)	Cr 17.4, Ni 11.71, Ti 0.34, Mo 0.16, Cu 0.12, Co 0.10, Si 0.54, C 0.67, P 0.019	1.80	1.81
Duraluminium IV (Hoepfmer Gebr.)	Si 5.63, Cu 1.68, Mg 0.45, Zn 0.41, Fe 0.18, Ni 0.10, Pb 0.05	0.25	0.24
Zinc blende II (Hoepfmer Gebr.)	Zn 48.50, S 31.65, Fe 9.87, Cu 1.61, Pb 1.33, As 0.14	0.61	0.60

as Al(III), Cr(III), Cd(II), Zn(II) and Pb(II), which precipitated at the pH used, cause interference in some instances. This can be overcome by adding citrate or cyanide ions.

Addition of ascorbic acid, potassium cyanide and/or citric acid permits the determination of manganese at the 3.5 μg ml^{-1} level without interference from 500 μg ml^{-1} of copper, nickel, iron, palladium, cadmium, lead, zinc, chromium and aluminium. Of the metals tested, only Co(II) (2 μg ml^{-1}) and V(V) (5 μg ml^{-1}) caused serious interferences.

In samples containing large amounts of some foreign species, a precipitate appeared 10–15 min after the test solution was prepared. In order to obtain good results, the extraction must be carried out immediately.

Applications

To test the validity of the proposed method, manganese was determined in a standard steel sample supplied by the US National Bureau of Standards and in zinc blende and duraluminium samples supplied by Hoepfmer Gebr. (Hamburg, FRG). The results obtained agreed well with the expected values, as shown in Table 1.

References

1. Izquierdo, A., and Calmet, J., *Talanta*, 1977, **25**, 56.
2. Izquierdo, A., Giné, M., and Compañó, R., *J. Inorg. Nucl. Chem.*, 1981, **43**, 617.
3. Izquierdo, A., and Carrasco, J., *Analyst*, 1984, **109**, 605.
4. Cooper, M. D., *Anal. Chem.*, 1953, **25**, 411.
5. Gottschalk, G., *Fresenius Z. Anal. Chem.*, 1965, **212**, 303.
6. Ahrland, S., and Herman, R. G., *Anal. Chem.*, 1975, **47**, 24.
7. Donaldson, E. M., and Inman, W. R., *Talanta*, 1966, **13**, 489.
8. Izquierdo, A., and Garriga, N., *Talanta*, 1985, **32**, 669.

Paper A5/286
Received August 5th, 1985
Accepted October 15th, 1985

Automated Flow Injection Spectrophotometric Determination of Some Phenothiazines Using Iron Perchlorate: Applications in Drug Assays, Content Uniformity and Dissolution Studies

Michael A. Koupparis* and Antonie Barcuchovát
Laboratory of Analytical Chemistry, Department of Chemistry, University of Athens, Athens 106 80, Greece

An automated flow injection determination of some phenothiazine derivatives, based on their oxidation with iron(III) in a strongly acidic medium, is described. Chlorpromazine, promethazine, thioproperazine, promazine, levomepromazine, fluphenazine, trifluoperazine and thioridazine are determined in the range 10–250 μg ml^{-1}. The precision is better than 1% and a measurement rate of 120 per hour can be obtained. The method was evaluated by carrying out an interference study with common excipients and other drugs, a recovery study and by the analysis of commercial formulations, the results of which are compared with those obtained by the official method. The method was applied in content uniformity tests and for monitoring the dissolution of solid dosage forms.

Keywords: *Phenothiazine determination; flow injection analysis; routine assays; content uniformity test; dissolution studies*

Phenothiazine derivatives are one of the most important groups of medicaments, used as antihistamines, tranquillisers, antiemetics, anti-Parkinson drugs, etc. About 30 phenothiazine drugs and 100 formulations are commercially available. The importance of these drugs prompted the development of many methods for their determination, reviewed by Blazek[1] and Fairbrother.[2] Apart from the official methods, based on UV spectrophotometry and non-aqueous titrimetry, two-phase, tetraphenylborate, ammonium reineckate, complexometric and oxidative titrations have also been used. A variety of manual spectrophotometric methods are based on coloured complex formation or oxidation reactions yielding intensely coloured radicals. Individual phenothiazines have been determined using molybdophosphoric acid,[3] molybdoarsenic acid,[4] chloramine-T,[5] Van Urk's reagent[6] and acid dyes[7] as reagents. Other spectrophotometric methods for phenothiazines employ Pd(II),[8] Ce(IV),[9] Fe(III),[10] *N*-bromosuccinimide,[11] etc. A number of chromatographic and polarographic methods have also been proposed.

Despite the large number of manual methods available, automated procedures that can be used for the routine analysis of many samples in governmental and industrial quality control laboratories are limited. A semi-automated method using the Technicon air-segmented continuous flow analyser is based on the dilution and oxidation with $NaNO_2$ (if necessary), and a double extraction and UV determination.[12] Another continuous flow method (unsegmented closed-loop mode) has been proposed by Mottola and Hanna,[9] based on the oxidation of phenothiazines with cerium(IV) to produce transient absorbance peaks due to the intermediate red free radicals.

In recent years, flow injection analysis (FIA) has found wide application in various fields of routine analysis, including pharmaceutical.[13,14] The versatility and simplicity of the FIA technique allow its adaptation at relatively low cost to the different requirements of a variety of analytical problems. The introduction of content uniformity tests (required for all solid formulations with contents equal to or less than 50 mg of drug) increases the workload of quality control laboratories at least ten-fold. This type of analysis, in which a large number of samples of very similar composition have to be analysed, is an attractive field for automated FIA.

Recently FIA was successfully interfaced with dissolution apparatus and the automation of dissolution studies of drug formulations was achieved.[15] Complete tabulated and graphical multi-point time profiles of dissolutions were obtained.

In this paper, the development of an automated FIA method for the determination of some phenothiazines and its application to routine assays, content uniformity tests and dissolution studies are described. The reaction of the phenothiazines with iron(III) in a strongly acidic medium with $HClO_4$ has been found to be suitable for adaptation.

Experimental

Apparatus

A laboratory-constructed automated photometric flow injection analyser,[16] assembled from commercially available components and instruments, was used. This analyser provides for automatic removal of aliquots of samples from the turntable, or manually processed solutions, injection of an accurate adjustable sample volume into the reagent flow stream, measurement of the absorbance peaks of the reaction mixtures and manipulation of the analytical data. The analyser is controlled by a versatile and inexpensive microcomputer (Rockwell AIM 65).

The analytical manifold designed for the determination of phenothiazines, together with the flow-rates of the reagents, is shown in Fig. 1. The $\lambda_{max.}$ for each individual phenothiazine was set on the photometer (Table 1). Because of the use of concentrated $HClO_4$, acid-resistant Vidon tubing in the peristaltic pump of the analyser is preferable to the usual silicone-rubber tubing.

For the automated dissolution studies on solid dosage forms of phenothiazines, the FIA analyser was coupled with a USP rotating basket apparatus as described previously.[15]

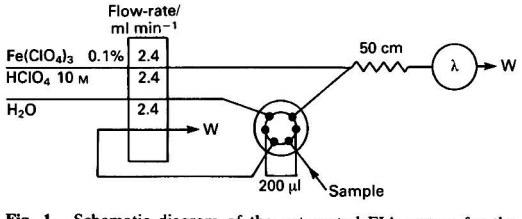

Fig. 1. Schematic diagram of the automated FIA system for the determination of phenothiazines

* To whom correspondence should be addressed.

† On leave from the Department of Physical Chemistry, Faculty of Pharmacy, Charles University, Hradec Králové, Czechoslovakia.

Reagents

All solutions were prepared in de-ionised, distilled water from analytical-reagent grade materials. Pure phenothiazines were obtained directly from the manufacturers and their purity was tested using USP procedures. The formulations analysed and tested were obtained from local commercial sources.

Phenothiazine standard solutions. A 500 μg ml^{-1} stock solution of each phenothiazine was prepared by dissolving 0.1250 g of pure substance in 250 ml of water and stored in amber-coloured bottles in a refrigerator. Working standard solutions, in the range stated in Table 1 for each phenothiazine, were prepared by appropriate dilution of the stock solution.

Iron(III) - perchloric acid solution, 0.10% *m/V*–10 M. Prepared by dissolving 0.500 g of $Fe(ClO_4)_3$ in 500 ml of 10 M $HClO_4$, prepared by appropriate dilution of concentrated 70% *m/V* acid.

Carrier solution. Water.

Dissolution medium. 0.10 M HCl.

$HClO_4$, 0.10 M.

Procedures

Sample preparation

Assays in dosage forms. (*a*) *Tablets.* Not less than 20 tablets were weighed and finely powdered. An accurately weighed portion, equivalent to about 50 mg of the phenothiazine, was transferred into a 100-ml calibrated flask and diluted to volume with water. Using an ultrasonic bath or a mechanical shaker, the powder was completely disintegrated and the solution was filtered. From this sample solution, working solutions were prepared by appropriate dilution, so that their concentration was in the individual phenothiazine working range.

(*b*) *Injections and syrups.* An accurately measured volume was appropriately diluted so that the phenothiazine concentration was in the working range.

(*c*) *Creams.* An accurately weighed portion of the cream, equivalent to about 100 mg of phenothiazine, was transferred into a separating funnel, dissolved in a mixture of 25 ml of diethyl ether and 10 ml of methanol and extracted with three 25-ml portions 0.10 M $HClO_4$. The extractant was diluted to 100 ml with the same medium and further diluted to fall within the working range.

Assays for content uniformity tests. Ten individual tablets were selected, disintegrated and diluted with water in separate calibrated flasks to fall within the working range.

Measurement procedures

The spectrophotometer of the FIA analyser was set at the $\lambda_{max.}$ of the individual phenothiazine, the reagents were pumped and the 100% transmittance was set. Data on the number of standards and samples, the runs per standard and sample and the injection and load time (8 and 15 s, respectively) were provided to the microcomputer's routine program. The determination then proceeded automatically.

Dissolution studies were performed according to a "dissolution" program loaded into the microcomputer's memory. A calibration graph was initially obtained using at least three standards of the phenothiazine examined, prepared in the dissolution medium used (0.1 M HCl) and thermostated at 37 °C. Then a dosage form was placed into a 250-mesh screen basket, immersed and rotating at 60 rev min^{-1}, in a double-wall beaker containing 250 or 900 ml of 0.1 M HCl (for formulations containing less or more than 25 mg, respectively). The dissolution medium was thermostated at 37 ± 0.5 °C.

The filtered dissolution medium was circulated continuously through the sample loop (200 μl) and at pre-set time intervals was injected into the carrier stream. At the end of the experiment the entire dissolution profile was presented on the chart recorder as a series of absorbance peaks *versus* time and also on the computer's printer as a table consisting of time, absorbance, drug concentration and percentage dissolution.

Results and Discussion

From the various oxidants, already used for manual spectrophotometric determinations of phenothiazines, iron(III) was chosen for its mild oxidation power. The formal reduction potential of the Fe(III) - Fe(II) couple does not allow further oxidation of the coloured free radicals to the uncoloured sulphoxides.[17] Using more powerful oxidants, such as Ce(IV), transient redox absorbing products are produced.[9]

Optimisation of the Method

In order to optimise the proposed FIA method, the effects of the various experimental parameters were studied. Of the various acids tested, perchloric was found to be the most suitable. Its mixed solution with iron(III) was uncoloured (in contrast to hydrochloric acid) and had no oxidising action on the free radicals produced (in contrast to nitric acid).

The perchloric acid concentration was found to have a drastic effect on the absorbance peak heights shown in Fig. 2(*a*). A 10 M concentration was chosen as the optimum for high sensitivity. This high acid concentration requires the use of acid-resistant pump tubing.

Various sources of iron(III) reagent were tested. $NH_4Fe(SO_4)_2$ gave turbid solutions at the high acid concentration used and filtration was required. $Fe(NO_3)_3$ showed a considerable decreasing effect on the absorbance peaks at concentrations higher than 0.5% *m/V* because of the oxidising effect of nitrates on the free radicals. $Fe(ClO_4)_3$ was found to be the most suitable and 0.1% *m/V* (2.75×10^{-3} M) was chosen as the optimum. Fig. 2(*b*) shows the effect of $Fe(NO_3)_3$ and $Fe(ClO_4)_3$ concentrations on the absorbance peaks.

The reaction of iron(III) with phenothiazines is very rapid[17] and is completed in a few seconds. The effect of the length of the reaction coil (*L*) is shown in Fig. 2(*c*). An increase in *L*

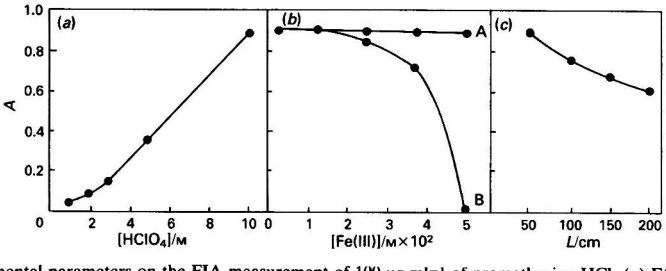

Fig. 2. Effect of experimental parameters on the FIA measurement of 100 μg ml^{-1} of promethazine.HCl. (*a*) Effect of $HClO_4$; [Fe(III)] = 2.5×10^{-2} M, *L* = 50 cm. (*b*) Effect of Fe(III): A, $Fe(ClO_4)_3$; B, $Fe(NO_3)_3$; [$HClO_4$] = 10 M, *L* = 50 cm. (*c*) Effect of reaction coil length; [$HClO_4$] = 10 M, [$Fe(ClO_4)_3$] = 2.75×10^{-3} M

decreases the absorbance peaks, because of increasing sample dispersion, and reduces the sample throughput. A 50-cm reaction coil was chosen as the optimum to ensure high reproducibility of mixing of the sample with the reagents, high sensitivity and a high measurement rate.

Validation of the Method

Typical FIA peaks for the calibration graph of promethazine hydrochloride are shown in Fig. 3, with increasing and decreasing concentrations in order to show the absence of any carry-over effect.

Data relevant to the FIA determination of several phenothiazines in pure solutions are summarised in Table 1. The linearity of the stated calibration graphs was excellent, with correlation coefficients (r) varying from 0.999 to 0.99999. The analytical ranges of the determinations are suitable for both assays of formulations (containing 10–100 mg) and dissolution studies over a wide range of concentrations.

The precision of the measurements varied from 3.3 to 0.4% relative standard deviation (RSD) (n = 10) for the lowest to the highest concentration of the calibration graphs.

The sample throughput is high (120 measurements per hour), assuming a 15-s load time, an 8-s injection time and 7 s for data collection, manipulation and printing.

Interference studies

In order to use the automated FIA method in assays of commercial formulations, common excipients and other additives and drugs coexisting in formulations were tested for possible interference. Synthetic solutions containing 50.0 μg ml^{-1} of promethazine hydrochloride and various amounts of foreign substances were measured. The undissolved material, if any, was filtered before measurement. The recovery results are shown in Table 2. As shown, the only possible interferents are carbopol (carboxypolymethylene), which causes enhancement of the peak height generating coloured aggregates, sodium lauryl sulphate, sodium sulphite, which decreases the peak height because of its reducing action, ascorbic acid, acetylsalicylic acid and codeine phosphate at high concentrations not found in formulations with phenothiazines. All other common excipients showed recoveries varying from 97.9 to 102.2%.

Accuracy

The accuracy of the automated FIA method was examined by performing recovery experiments on solutions prepared from chlorpromazine formulations. A mean recovery of 101.4% was found (range 98.4–105.2%) (Table 3). Similar experiments for promethazine hydrochloride gave an average recovery 101.6%.

The proposed method was also evaluated by analysing commercial formulations of chlorpromazine, promethazine and thioproperazine and comparing the results obtained with those obtained by the official USP methods. A satisfactory agreement between the results was obtained (Table 4) with a mean relative difference of 1.2% (range 0.2–2.8%). The RSD for FIA determinations of these formulations varied from 0.5 to 2.6% (three samples, three measurements per sample).

Content uniformity tests

Fig. 4 shows a typical recorded FIA profile of content uniformity test for Phenergan tablets containing 25 mg of promethazine hydrochloride. Table 5 shows the results of content uniformity tests for chlorpromazine, promethazine and thioproperazine formulations. All the samples examined were found to meet the USP requirements (all the samples examined fell within the limits of 85–115% of the average definition in the individual monograph). The standard deviations of the contents varied from 0.3 to 0.7 mg per tablet (1.6–3.0%).

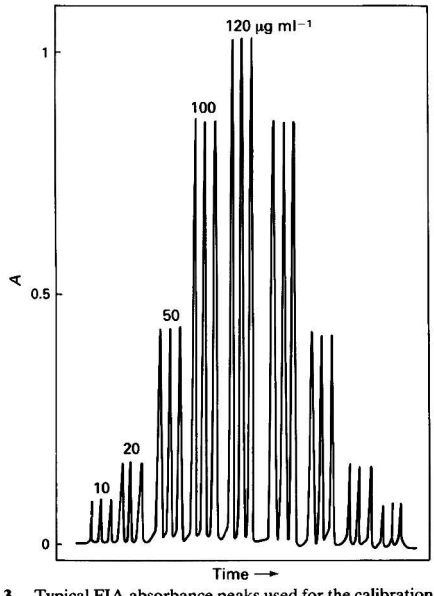

Fig. 3. Typical FIA absorbance peaks used for the calibration graph of promethazine.HCl with increasing and decreasing concentrations of promethazine.HCl

Table 1. Summary of results pertinent to the determination of phenothiazines by automated FIA (200-μl sample volume)

Compound	$\lambda_{max.}$/ nm	Detection limit*/ μg ml^{-1}	Determination range†/ μg ml^{-1}	Sensitivity‡/ mA μg^{-1} ml
Chlorpromazine hydrochloride . .	535	0.6	6–124	8.07
Promethazine hydrochloride . .	515	0.6	6–117	8.53
Promazine hydrochloride	513	0.7	6–128	7.81
Methotrimeprazine (levomepromazine) hydrochloride	560	0.7	7–133	7.50
Thioproperazine bismethanesulphonate	515	1.3	12–248	4.02
Fluphenazine dihydrochloride . .	500	1.6	15–312	3.20
Trifluoperazine dihydrochloride	501	1.2	11–230	4.35
Thioridazine hydrochloride . .	580	1.6	16–318	3.15

* Given as the concentration producing a signal twice the standard deviation of the most dilute standard.
† Given as the concentration range producing absorbance peaks of 0.05–1 A.
‡ Given as the slope of the calibration graph (mA *vs.* concentration).

Table 2. Analytical recovery of promethazine hydrochloride (50 μg ml^{-1}) from various additives used as excipients and from some coexisting drugs

Type	Additive	Concentration ratio, additive to promethazine	Recovery, % ($n = 3$)
Excipients	Galactose	20	98.9
	Glucose	20	100.0
	Lactose	20	97.9
	Sugar	20	100.0
	Starch	20	100.0
	Talc	20	100.0
	Gelatin	20	100.0
	Cellulose	20	100.0
	Cellulose acetate hydroxyphthalate	20	102.1
	Carbopol*	10	124.4
	Carbowax†	20	100.0
	Sodium lauryl sulphate	10	106.4
	Magnesium stearate	20	98.9
	NaCl	20	100.0
	KH_2PO_4	20	100.0
	$CaCl_2$	10	101.0
	Na_2SO_3	25	80.0
	Ethanol	100	102.2
	Formaldehyde	25	101.2
	Phenol	100	102.2
	Na_2EDTA	100	110.2
		25	101.2
Drugs	Ascorbic acid	25	53.6
		1	100.0
	Acetaminophen	100	105.6
		50	100.0
	Phenacetin	100	100.0
	Acetylsalicylic acid	Saturated	110.8
	Caffeine	Saturated	100.0
	Codeine phosphate	100	114.7
		50	101.0

* Carboxypolymethylene.
† Polyethylene glycol 4000.

Table 3. Recovery experiments for chlorpromazine hydrochloride added to sample solutions of commercial formulations

Formulation	Clorpromazine. HCl/ μg ml^{-1} Initially present	Added	Recovered	Recovery, %
Largactil tablets, 25 mg	54.6	25.0	25.5	102.0
	54.6	50.0	49.2	98.4
Largactil tablets, 100 mg	55.2	25.0	24.9	99.6
	55.2	50.0	49.2	98.4
Antistress tablets, 25 mg	54.6	25.0	25.5	102.0
	54.6	50.0	49.2	98.4
Antistress tablets, 100 mg	55.9	25.0	25.8	103.2
	55.9	50.0	50.3	100.6
Solidon tablets, 100 mg	52.2	25.0	25.8	103.2
	52.2	50.0	51.0	102.0
Largactil injection, 5 mg ml^{-1}	59.0	25.0	26.3	105.2
	59.0	50.0	51.9	103.8
			Mean:	101.4

Table 4. Determination of chlorpromazine, promethazine and thioproperazine in commercial formulations by FIA and the official USP method based on extraction and UV spectrophotometry

Type	Formulation (phenothiazine)	Drug/mg Claimed	Found FIA*	Found Official method†	Relative difference (FIA − official method), %
Tablets	Largactil (chlorpromazine)	25	24.5 ± 0.4	24.1 ± 0.5	1.7
		100	99.0 ± 0.5	99.5 ± 0.7	−0.5
	Antistress (chlorpromazine)	25	24.5 ± 0.2	25.0 ± 0.4	−2.0
		100	100.3 ± 0.7	100.7 ± 1	−0.4
	Solidon (chlorpromazine)	100	93.7 ± 0.8	94.2 ± 0.9	−0.5
	Ancholactil (chlorpromazine)	100	98.1 ± 1	97.9 ± 1	0.2
	Phenergan (promethazine)	25	24.3 ± 0.3	24.2 ± 0.5	0.4
	Majeptil (thioproperazine)	10	10.6 ± 0.1	10.9 ± 0.2	−2.8
Cream	Phenergan	2% *m/m*	2.03 ± 0.02	2.05 ± 0.05	−1.0
Syrup, injection	Phenergan	1 mg ml^{-1}	1.13 ± 0.03	1.15 ± 0.04	−1.7
	Largactil	5 mg ml^{-1}	5.29 ± 0.07	5.20 ± 0.2	1.7

* Average for three samples, each measured three times, ± standard deviation.
† Average for three samples, each measured once, ± standard deviation.

Table 5. Content uniformity tests on commercial tablets of some phenothiazines. Ten tablets were analysed; measurements in triplicate

Formulation	Range mg per tablet	Range % of claim	Mean ± SD mg per tablet	Mean ± SD % of claim
Phenergan tablet, 25 mg (promethazine. HCl)	24.3–25.6	97.1–102.5	24.9 ± 0.4	99.5 ± 1.6
Largactil tablet, 25 mg (chlorpromazine. HCl)	23.7–26.0	94.8–104.0	25.0 ± 0.7	100.0 ± 2.8
Majeptil tablet, 10 mg (thioproperazine bismethanesulphonate)	10.2–11.0	102.0–110.0	10.6 ± 0.3	106.0 ± 3.0

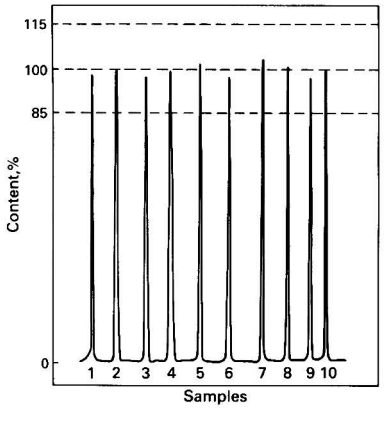

Fig. 4. Typical FIA profile of the content uniformity test on Phenergan tablets (25 mg) (promethazine. HCl). Statistical treatment of contents (mg per tablet): range, 24.3–25.6; mean, 24.9 ± 0.4 (RSD = 1.6%). Only one peak is shown for each individual sample

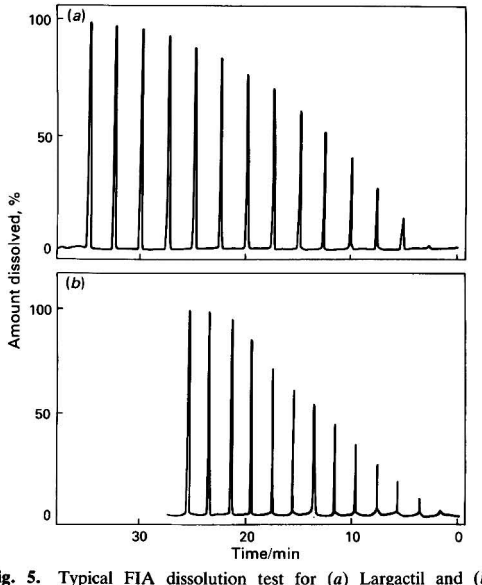

Fig. 5. Typical FIA dissolution test for (*a*) Largactil and (*b*) Phenergan tablets at pH 1.0

Table 6. Dissolution tests on phenothiazine tablets

Injection No.	Time/min	Dissolution, %* Largactil†	Phenergan‡	Majeptil§
1	2	0	2.9	0
2	4	8.0	9.8	0
3	6	18.4	18.1	14
4	8	28.7	26.5	33.2
5	10	39.0	36.8	42.4
6	12	49.0	46.1	51.6
7	14	57.6	55.9	58.5
8	16	65.8	63.7	63.1
9	18	73.5	72.6	65.4
10	20	79.6	86.8	70.1
11	22	84.4	95.1	74.7
12	24	88.5	100.0	81.5
13	26	92.3	100.0	86.1
14	28	95.7		89.4
15	30	98.2		93.1
16	32	99.3		95.3
17	34	99.8		100.0
18	36	100.0		100.0

* Average of three experiments.
† Chlorpromazine.HCl, 100 mg; dissolution medium, 900 ml.
‡ Promethazine.HCl, 25 mg; dissolution medium, 250 ml.
§ Thioproperazine bismethanesulphonate, 10 mg; dissolution medium, 250 ml.

Dissolution tests

Fig. 5 shows typical results for dissolution profiles of Largactil and Phenergan tablets at pH 1.0 (0.1 M HCl). Summarised data are shown in Table 6. An average standard deviation of 2.4% dissolution (range 0–5.7%) ($n = 3$) was obtained in all three instances. Considering the tablet-to-tablet variability, the precision of the proposed technique is excellent.

Conclusions

The proposed automated FIA method is rapid, sensitive, precise and accurate, with a high sample throughput. The set-up time is very short and reagent consumption is low. Interferences from common excipients are limited and the method can be used for the routine analysis of commercial formulations instead of the tedious official methods where separation of the drug is required.

The application of FIA to content uniformity tests should be very useful in meeting the considerably increased workload required to carry out these tests.

The automated performance of dissolution studies of formulations, where a "kinetic" dissolution profile is obtained very easily, should be useful in pharmaceutical technology. The data obtained can be treated to calculate dissolution rate constants.

The authors thank the Greek Ministry of Education for supporting one of the authors (A. B.).

References

1. Blazek, J., *Pharmazie*, 1967, **22**, 129.
2. Fairbrother, J. E., *Pharm. J.*, 1979, **222**, 271.
3. Stan, M., Dorneanu, V., and Ghimicescu, G., *Talanata*, 1977, **24**, 140.
4. Ramappa, P. G., Sanke Gowda, H., and Nayak, A. N., *Analyst*, 1980, **105**, 663.
5. Issa, A. S., Beltagy, Y. A., and Mahrous, M. S., *Talanta*, 1978, **25**, 710.
6. Murty, B. S. R., and Baxter, R. M., *J. Pharm. Sci.*, 1970, **59**, 1010.
7. Matsui, F., and French, F. M., *J. Pharm. Sci.*, 1971, **60**, 287.
8. Mercaldo, D. E., *Ann. N.Y. Acad. Sci.*, 1968, **153**, 403.
9. Mottola, H. A., and Hanna, A., *Anal. Chim. Acta*, 1978, **100**, 167.
10. Istvan, F., Floderer, H., and Valeria, H., *Acta Pharm. Hung.*, 1957, **27**, 152.
11. Taha, A. M., El-Rabbat, N. A., El-Kommos, M. E., and Refat, I. H., *Analyst*, 1983, **108**, 1500.
12. "Drug Autoanalysis Manual," Second Edition, United States Food and Drug Administration, Washington, DC, 1972, method No. 82.
13. Landis, J. B., *in* Munson, J. W., *Editor*, "Pharmaceutical Analysis, Part B," Marcel Dekker, New York, 1984, pp. 217–277.
14. Rios, A., De Castro, M. D., and Valcarcel, M., *J. Pharm. Biomed. Anal.*, 1985, **3**, 105.
15. Koupparis, M., Macheras, P., and Reppas, C., *Int. J. Pharm.*, 1984, **20**, 325.
16. Koupparis, M., and Anagnostopoulou, P., *J. Autom. Chem.*, 1984, **6**, 186.
17. Gasco, M. R., and Carlotti, M. E., *J. Pharm. Sci.*, 1978, **67**, 168.

Paper A5/255
Received July 15th, 1985
Accepted October 9th, 1985

Spectrophotometric Determination of Acetaminophen, Oxyphenbutazone and Salicylamide by Nitration and Subsequent Complexation Reactions

Afaf A. El Kheir
Pharmaceutical Chemistry Department, Faculty of Pharmacy, Zagazig University, Zagazig, Egypt
Saied Belal*
Faculty of Pharmacy, Alexandria University, Alexandria, Egypt
and Mohammad El Sadek and Abdullah El Shanwani
Pharmaceutical Chemistry Department, Faculty of Pharmacy, Zagazig University, Zagazig, Egypt

A simple and sensitive spectrophotometric method for the assay of three antipyretic drugs through their nitration and subsequent complexation with an nucleophilic reagent is proposed. The experimental conditions leading to optimum chromagen stability and intensity were studied. The results of the application of the method to the assay of the test compounds in unit doses were compared statistically with those obtained by official methods, and demonstrated good accuracy and precision.

Keywords: *Antipyretics analysis; phenolic drugs analysis; nitro derivatives; spectrophotometry*

Acetaminophen, oxyphenbutazone and salicylamide tablets are important and widely used analgesic - antipyretic and antirheumatic drugs. Their spectrophotometric determination in dosage forms and biological fluids offers advantages of both sensitivity and simplicity. Most spectrophotometric methods for these compounds were based on the utility of their phenolic hydroxy groups to yield spectrophotometrically useful chromagens through diazo coupling[1-5] or nitrosation reactions.[6-11] The use of nitration has also been reported[12,13] for the determination of acetaminophen; the other two compounds concerned here were not involved.

This work was concerned with the study of the preparation and use of the polynitro derivatives of the investigated drugs as intermediates in their spectrophotometric determination, through interaction with alkaline ketone reagents to form Meisenheimer-type complexes. The aim was to develop a simple and sensitive assay procedure for these drugs.

Polynitro aromatic compounds are known to form various intensely coloured complexes with nucleophiles[14] and other charge-transfer complexes and adducts with electron-rich species.[15] One of these interactions occurs between dinitro or trinitro aromatic compounds with bases, including anions generated from a base and a ketonic compound, forming anionic sigma complexes[16-18] in which the reacting species are linked with a sigma bond.[16] These complexes are more intensely coloured than the original nitro derivatives. This type of interaction has been widely used to determine ketosteroids with dinitrobenzene - acetone - potassium hydroxide,[19] to determine some amines[20] and to detect polynitro aromatic compounds[21,22] and compounds containing an active methylene or a hydrogen α to a carbonyl group.[23-27] It was claimed that test compounds that easily form polynitro derivatives may form an anionic sigma complex. This suggestion was investigated to establish whether the intensely coloured products may be spectrophotometrically useful in determining the parent compounds. The reaction sequences were developed into a spectrophotometric assay of the test drugs.

Experimental

Apparatus

A Pye Unicam SP-400 UV - visible spectrophotometer with 1-cm quartz cells was used.

Materials and Reagents

Acetaminophen, oxyphenbutazone and salicylamide powders. Obtained from Alexandria, El Nile and CID Pharmaceutical Companies, respectively.

Concentrated nitric acid and concentrated sulphuric acid. Prolabo.

Acetone. BDH Chemicals, laboratory-reagent grade.

Potassium hydroxide solution, 10% *m/V*.

Standard ethanolic or methanolic solutions of the drugs.

Procedures

Pure drugs

An accurately weighed amount of the drug (25–100 mg) was transferred into a 100-ml calibrated flask, treated with 2 ml of nitric acid and 2 ml of sulphuric acid (care must be taken during handling of the nitration mixture), left to stand for 10 min, then cooled and diluted to volume with distilled water. A 20-ml aliquot of the solution was diluted with distilled water to 100 ml in a calibrated flask. Aliquots of 0.5–3 ml of the diluted solution were transferred into 25-ml calibrated flasks, treated with 2–3 ml of acetone and 5 ml of potassium hydroxide solution and diluted to volume with distilled water. The absorbance of the resulting colour was measured against a reagent blank at 355 nm (acetaminophen) or 390 nm (oxyphenbutazone or salicylamide).

Construction of calibration graphs

Aliquots of standard alcoholic solutions of the drugs (≡10–20 mg of acetaminophen and 5–10 mg of salicylamide or oxyphenbutazone) were evaporated to dryness in small beakers at about 60 °C. The residues were treated with 2 ml of nitric acid and 2 ml of sulphuric acid, left to stand for 10 min, cooled, transferred quantitatively into 100-ml calibrated flasks and diluted to volume with distilled water. A 1-ml volume of each solution was transferred into a 25-ml calibrated flask and the assay was completed as above.

Application to tablets

Twenty tablets were weighed, powdered, mixed and an amount of the powder (≡ 60 mg of acetaminophen and 20 mg of oxyphenbutazone or salicylamide) was transferred into a small beaker. The powder was subjected to nitration as above and the reaction mixture was transferred into a 100-ml calibrated flask, diluted to volume with distilled water and filtered. A 1-ml volume of the filtrate was transferred into a 25-ml calibrated flask and the assay was completed as above.

* To whom correspondence should be addressed. Present address: College of Medicine and Allied Sciences, King Abdulaziz University, Jeddah, Saudi Arabia.

The concentration of drug was calculated using a regression equation obtained by applying the procedure to serial standard concentrations of the drug. The equation was checked frequently.

Results and Discussion

Nitration of acetaminophen and salicylamide (Schemes 1 and 3) probably results in a dinitro derivative, in spite of the excess of nitric acid used. This was proved by treating the nitro derivative with trimethylamine in a non-aqueous solvent; failure to develop a colour precluded the possibility of formation of a trinitro derivative. This was expected from steric hindrance considerations. On the other hand, oxyphenbutazone, owing to its additional benzene ring (in addition to the *p*-hydroxyphenyl moiety), is able to form a polynitro derivative (probably the tetranitro derivative). This is demonstrated from the more intense colour produced, the red shift

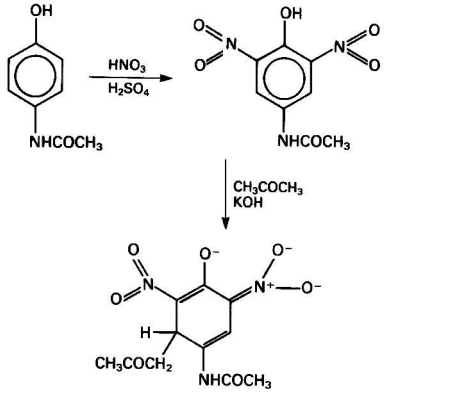

Scheme 1

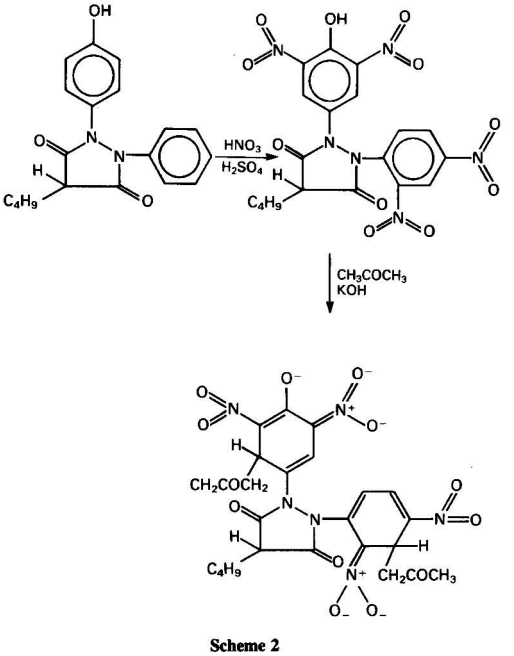

Scheme 2

(with respect to acetaminophen) of $\lambda_{max.}$ and the higher absorptivity of the final complex. Furthermore, treatment of the chloroform extract of oxyphenbutazone nitro derivative with trimethylamine resulted in an intense red colour, which suggests that more than two nitro groups are present in the derivative molecule in acetaminophen and the *p*-hydroxyphenyl moiety (Schemes 1 and 2).

In oxyphenbutazone, it is assumed that the two nitro groups enter the two *ortho* positions (with respect to the OH), whereas in salicylamide (Scheme 3) one nitro group should be directed to the vacant *para* position. In the second benzene ring of the nitro oxyphenbutazone structure, the two entering nitro groups would be *meta* to each other. The optimum volume of nitric acid leading to the maximum final colour intensity was 2 ml. Such a large volume ensured the introduction of a minimum of two groups into the molecule, essential for the electron-acceptor property.

Treatment of the electron-deficient polynitro derivatives with ketones such as acetone in alkaline medium resulted in intensely coloured complexes by interaction with anions such as $CH_3COCH_2^-$ (Schemes 1–3). These complexes are of the Meisenheimer type[15–17] and differ in colour from those obtained by adding only alkalis to the nitro derivatives. The latter colours originate from the formation of alkali metal salts and the generation of quinoid structures.[19] The optimum volume of acetone was 2–3 ml and the optimum volume of alkali was 5 ml of a 10% solution of potassium hydroxide. The absorption curves of the complexes are shown in Fig. 1. The low colour intensities and shorter $\lambda_{max.}$ for the acetaminophen colour may be attributed to the auxochrome ($-NHCOCH_3$) in the *para* position to the OH group, in contrast to the chromophoric (NO_2) group for the salicylamide colour. The intense colour and higher absorptivity in oxyphenbutazone colours may be attributed to complexation in both benzene rings. The coloured complexes are stable for at least 1 h, and give clear aqueous solutions in spite of the poor solubility of the nitro derivatives in cold water.

The calibration graphs obtained obeyed Beer's law in the range 0.2–1, 0.01–0.05 and 0.05–0.30 mg ml^{-1} for acetaminophen, oxyphenbutazone and salicylamide, respectively. Using the least-squares method,[28] the regression equation describing the calibration graphs ($A = a + bC$, where A = absorbance of a 1-cm layer, a = intercept, b = slope and C = concentration in mg-% of the final measured solution) were $A = 0.001 + 0.314C$, $A = 0.001 + 9.60C$ and $A = 0.002 + 0.69C$ for acetaminophen, oxyphenbutazone and salicylamide, respectively.

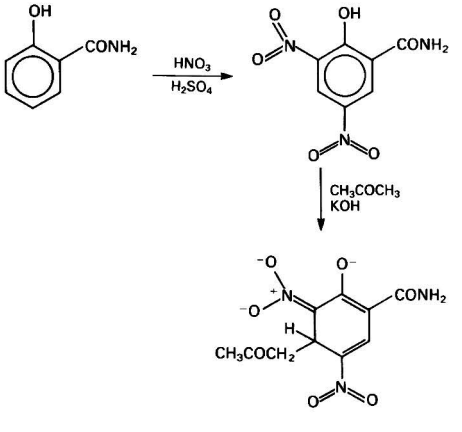

Scheme 3

Table 1. Results for the determination of the investigated drugs in unit doses using the proposed and official methods[29,30]

Compound/preparation	Results, % (mean ± S.D.) Proposed method	Official method	*t*-test	*F*-test
Acetaminophen powder	100.01 ± 0.60			
Acetaminophen tablets (paracetamol tablets)	99.94 ± 1.49	99.46 ± 1.76	0.46 (2.31)	1.666 (6.39)
Salicylamide powder	99.95 ± 0.48			
Salicylamide tablets (Cidal forte tablets)	101.1 ± 1.07	100.90 ± 0.93	0.32 (2.31)	1.324 (6.39)
Oxyphenbutazone powder	99.97 ± 0.43			
Oxyphenbutazone tablets (Tandril tablets)	99.69 ± 0.86	100.1 ± 1.22	0.82 (2.31)	1.33 (6.39)

* Means of five determinations; results are percentages found with respect to the label claim. Figures in parentheses are tabulated values of *t* and *F*.

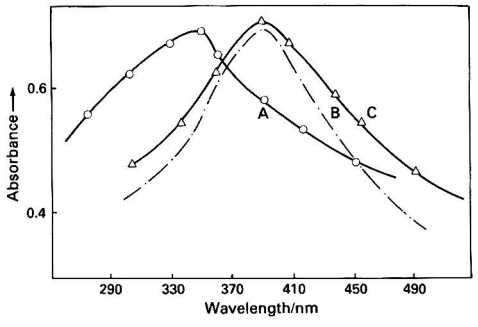

Fig. 1. Absorption graphs for the reaction products obtained from: A, acetaminophen; B, salicylamide; and C, oxyphenbutazone

The validity of the regression equation was tested by analysing commercial tablets using the proposed and official methods[29,30] to analyse unit doses of the test drugs (Table 1). Statistical analysis[31] of the results revealed that a the 95% confidence level, the calculated *t* and *F* values indicate that the proposed method is sufficiently accurate and precise. The proposed method is fairly sensitive, selective and of good reliability owing to the stability of the complex. The results were reproducible. The method could be considered as a general method for determining drug substances having phenolic OH groups. These merits, in addition to the use of simple reagents, suggest its use in drug control laboratories.

References

1. Belal, S., El Sayed, M. A. H., El Walily, A., and Abdine, H., *J. Pharm. Sci.*, 1979, **86**, 750.
2. Sane, R. T., and Amber Dekar, A. B., *Indian Drugs*, 1981, **19**, 115.
3. Hassan, S. M., Walash, M. I., El Sayed, S. M., and Abou Ouf, A. M., *J. Assoc. Off. Anal. Chem.*, 1981, **64**, 1442.
4. Svatek, E., and Hardkava, A., *Cesk. Farm.*, 1966, **15**, 76.
5. Belal, S., El Kheir, A. A., El Shanwani, A. A., *Analyst*, 1985, **110**, 205.
6. Amer, S. M., Ellaithy, M. M., and El Tarrasse, M. F., *Pharmazie*, 1982, **37**, 182.
7. Inamdar, M. C., and Kaji, N. N., *Indian J. Pharm.*, 1969, **31**, 79.
8. Belal, S. F., El Sayed, M. A. H., El Walily, A. M., and Abdine, H., *Analyst*, 1979, **104**, 919.
9. Abou Ouf, A., Walash, M. I., Hassan, S. M., and El-Sayed, S. M., *Analyst*, 1980, **105**, 169.
10. Sanghaiv, M. M., Jivani, N. G., and Mluye, P. D., *India J. Pharm. Sci.*, 1977, **39**, 87.
11. Amer, S. M., Ellaithy, M. M., and El Tarrasse, M. F., *Anal. Lett.*, 1980, **13**, 1625.
12. Hanegraff, C., Chastaigner, N., and DeMonrely, E., *Ann. Pharm. Fr.*, 1969, **27**, 663.
13. Le Pedriel, F., Hangroaff, C., Chastaigner, N., and DeMonrely, E., *Ann. Farm. Fr.*, 1968, **28**, 227.
14. Gold, V., "Advances in Physical Organic Chemistry," Volume 7, Academic Press, New York, 1969, p. 211.
15. Strauss, M. J., *Chem. Rev.*, 1970, **70**, 667.
16. Miller, R. E., and Wyne-Jones, W. F. K., *J. Chem. Soc.*, 1959, 2375.
17. Foster, R., and Mackie, R. K., *J. Chem. Soc.*, 1959, 3508.
18. Foster, R., and Mackie, R. K., *Tetrahedron*, 1961, **6**, 119.
19. Feur, H., "The Chemistry of Nitro and Nitroso Compounds, Part 2," Interscience, New York, 1970, p. 329.
20. Glover, D. J., and Kyser, E. G., *Anal. Chem.*, 1968, **40**, 2055.
21. Anas, S. A. H., and Yallop, H. J., *Analyst*, 1966, **91**, 336.
22. English, F. L., *Anal. Chem.*, 1948, **20**, 745.
23. Zimmermann, W., *Hopper-Seylers Z. Physiol. Chem.*, 1937, **47**, 245.
24. Kimura, M., Obi, N., and Kawazoi, M., *Chem. Pharm. Bull.*, 1972, **20**, 452.
25. Burns, L. B., Stedman, R. J., and Tuckerman, M. M., *J. Pharm. Sci.*, 1977, **66**, 753.
26. Canbeck, T., *Svensk. Farm Tidskr.*, 1950, **54**, 225.
27. Kohashi, K., Tsuruta, Y., Yamaguchi, M., and Ohkura, Y., *Chem. Pharm Bull*, 1979, **27**, 2122.
28. Spiegel, M. R., "Theory and Problems of Probability and Statistics," McGraw-Hill, New York, 1975, pp. 215 and 259–270.
29. "The Pharmacopoeia of Japan," Eighth Edition, Society of Japanese Pharmacopoeia, Tokyo, 1971, p. 674.
30. Davies, O. L., and Goldsmith, P., "Statistical Methods in Research and Production," Fourth Edition, Oliver & Boyd, Edinburgh, 1972, p. 178.
31. "British Pharmacopoeia 1980," Volume 1, HM Stationery Office, London, 1980, pp. 322 and 340.

Paper A5/204
Received June 7th, 1985
Accepted September 25th, 1985

Spectrophotometric and Fluorimetric Methods for the Determination of Indomethacin

C. S. P. Sastry, D. S. Mangala and K. Ekambareswara Rao
Foods and Drugs Laboratories, School of Chemistry, Andhra University, Waltair 530 003, A.P., India

Three spectrophotometric methods and a fluorimetric method are described for the determination of indomethacin in bulk samples and pharmaceutical preparations based on the formation of coloured species with *m*-aminophenol - chloramine-T, resorcinol - sodium hypochlorite or phloroglucinol - hypochlorite reagent and a fluorescent species with *m*-aminophenol - chloramine-T reagent, respectively, under specified experimental conditions. All the methods are simple, sensitive and reproducible to within ±1.7%.

Keywords: *Indomethacin determination; spectrophotometry; fluorimetry*

Indomethacin, [1-(4-chlorobenzoyl)-5-methoxy-2-methylindol-3-yl]acetic acid, is well known for its antipyretic analgesic action and is extensively used in rheumatoid arthritis. The methods reported for the determination of indomethacin include spectrophotometric[1-3] and fluorimetric methods[4] and the official BP procedure.[5] The existing spectrophotometric methods are time consuming, tedious and require some preliminary treatment. This paper describes three simple spectrophotometric (visible region) methods and one fluorimetric method using pairs of reagents, *m*-aminophenol - chloramine-T, resorcinol - hypochlorite, phloroglucinol - hypochlorite or *m*-aminophenol - chloramine-T, under specified conditions.

Experimental

Apparatus

A Systronics Model 105 (Mk. 1) spectrophotometer with 1-cm path length cuvettes, a Perkin-Elmer Model 203 fluorescence spectrophotometer with the sensitivity setting adjusted to 10 and a Systronics Model 305 pH meter were used for absorbance, fluorescence and pH measurements, respectively.

Reagents

All the reagents were of analytical-reagent grade and all solutions were prepared in doubly distilled water. All the pharmaceutical preparations used were available commercially.

Aqueous solutions of *m*-aminophenol (mAP, 0.1% in 0.025 M HCl), phloroglucinol (0.2%), resorcinol (0.2%), chloramine-T (CAT, 0.03 M), sodium hypochlorite (OCl^-, 0.05 M), HCl (2 M) and potassium acid phthalate (0.05 M) were prepared.

Standard drug solution. A 50-mg amount of BP-grade indomethacin (supplied by Themis Chemicals Ltd., Bombay, India) was initially dissolved in 10 ml of 1.25 M NaOH solution and then diluted to 250 ml in a calibrated flask. Working solutions for methods A and D were prepared by suitable dilution of the stock standard solution. The solutions were stable for 2 h.

Sample solution. Twenty capsules were emptied and pulverised and an amount equivalent to 50 mg of indomethacin was taken, dissolved as described above and filtered. The solution was stable for 2 h.

Spectrophotometric Procedures

A. With mAP - CAT reagent

A 15-ml volume of potassium hydrogen phthalate, 3 ml of CAT and 3 ml of mAP solution were placed in a 25-ml calibrated flask. A 1.0–4.0-ml portion of indomethacin (100 μg ml^{-1}) solution and the requisite volume of distilled water were added to make the total volume 25 ml. The pH of the resulting solution was between 4 and 5.0. The absorbance of the coloured species was measured at 490 nm within 3 min against a reagent blank prepared in a similar manner. The indomethacin concentration was calculated from a calibration graph prepared with a standard solution under identical conditions.

B or C. With resorcinol or phloroglucinol - OCl^- reagents

Aliquots of 1.0–4.0 ml of indomethacin solution (200 μg ml^{-1}) were placed in a 25-ml calibrated flask containing 1 ml of 2 M HCl, mixed well (for 1 min), 1 ml of OCl^- was added and the mixture was allowed to stand for 3 min for resorcinol or 2 min for phloroglucinol. A 3-ml volume of resorcinol or phloroglucinol was added after this period and the absorbance of the coloured species was measured at 460 nm after 10 min (the stability periods were as follows: B, resorcinol - OCl^-, 5–20 min; C, phloroglucinol - OCl^-, 10–35 min) against the corresponding reagent blanks prepared in a similar manner. The indomethacin concentration was obtained from calibration graphs obtained under identical conditions.

Fluorimetric Procedure

D. With mAP - CAT reagent

A 0.2–3.0-ml portion of indomethacin (10 μg ml^{-1}) was placed in a 10-ml calibrated flask containing 0.5 ml of 2 M HCl, 2 ml of CAT and 2 ml of mAP solution and diluted to the mark with distilled water. The fluorescence of the solution was measured between 10 and 120 min at excitation and emission wavelengths of 465 and 490 nm, respectively, against the reagent blank prepared in a similar manner. The concentration of indomethacin was calculated from a calibration graph.

Results and Discussion

Of the various combinations of phenols (phenol, catechol, resorcinol, pyrogallol and phloroglucinol), aminophenols (*o*-, *m*-, *p*- and *p*-*N*-CH_3) or phenylenediamines [*o*-, *m*-, *p*-, and *p*-*N*,*N*-$(CH_3)_2$] and oxidising agents [CAT, OCl^-, IO_4^-, IO_3^-, Cr(VI), Fe(III), $S_2O_8^{2-}$, *N*-bromosuccinimide and

Table 1. Optical characteristics, precision and accuracy

Parameter	Method A	B	C	D
Beer's law limits/μg ml^{-1}	4.0 – 16	8.0 – 24	5.5 – 24	0.2 – 3
Molar absorptivity/l mol^{-1} cm^{-1}	5.72×10^3	2.27×10^3	3.18×10^3	—
Sandell's sensitivity/μg cm^{-2} per 0.001 absorbance unit	0.063	0.16	0.11	—
Slope	6.32×10^{-4}	2.41×10^{-4}	3.42×10^{-4}	0.3186
Intercept	-3.49×10^{-3}	3.00×10^{-3}	2.03×10^{-3}	0.1698
Correlation coefficient	0.999	0.998	0.999	0.999
Relative standard deviation, %	1.39	1.65	1.55	1.32
Range of error, % (95% confidence limits)	±1.46	±1.73	±1.62	±1.39

Table 2. Assay and recovery of indomethacin in dosage forms

Capsules	Labelled amount/mg	Amount found/mg: Proposed method A	Proposed method B or C	Proposed method D	Reported method[1]	Recovery, % A	Recovery, % B or C*	Recovery, % D
Idicin (IDPL, Hyderabad)	25	23.44	23.50 (B)	23.52	23.45	97.8	98.4 (B)	98.5
Microcid (Microlabs, Madras)	25	24.23	24.18 (C)	24.30	24.21	98.2	98.2 (C)	98.7
Inobid (Thomis, Bombay)	75	73.32	73.30 (B)	73.36	73.29	97.6	98.6 (B)	99.1

H_2O_2] tried for developing the colour or fluorescence under acidic or alkaline conditions at laboratory temperature, mAP-CAT was found to be superior. Of the other combinations, resorcinol or phloroglucinol and OCl^- were found to be suitable as chromogenic reagents.

The optimum conditions for each method (A–D) were established after a thorough systematic study of the parameters such as acid strength (pH), reagent concentration and order of addition of the reagents.

Potassium hydrogen phthalate solution was found to be necessary only in method A for maintaining the resulting pH between 4 and 5. Even trace amounts of miscible alcohols such as methanol and ethanol were found to quench the fluorescence intensity. The chromophore or fluorophore in methods A–D was partially extractable into butan-1-ol and not extractable into chloroform.

The excitation spectra of the fluorescent species showed three maxima, at 245, 305 and 465 nm. The peaks in the UV region were not considered as the blank interferes.

The optical characteristics such as Beer's law limits, molar absorptivity and Sandell's sensitivity for each method are given in Table 1. The slopes, intercepts and correlation coefficients obtained by linear least-squares treatment[6] of the results for the systems involving indomethacin with the mentioned reagents are also presented in Table 1. The reproducibility of the methods was found by measuring the absorbances (in methods A, B and C) or fluorescence intensity (in method D) of six replicate samples containing a known amount of drug (400 μg per 25 ml in A, B and C and 20 μg per 10 ml in D) and the results obtained are given in Table 1. The accuracy of the methods was further confirmed by adding known amounts of indomethacin to previously analysed

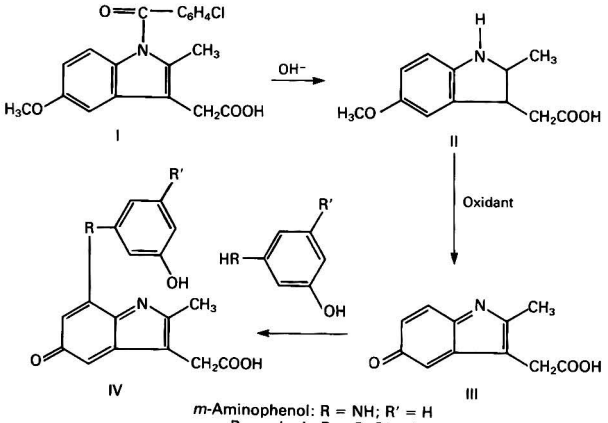

Scheme 1. Reaction mechanism

samples and the recoveries obtained are given in Table 2. The results obtained by the proposed and reported[1] methods for indomethacin in dosage forms are also included in Table 2.

The ingredients usually present in pharmaceutical preparations of indomethacin, such as glucose, lactose, sodium metabisulphite, sodium chloride, magnesium stearate, starch, talc, sodium citrate and other analgesics such as paracetamol, phenacetin and analgin, did not interfere in the proposed methods.

Mechanism

The species reacting with the proposed reagents (Scheme 1) appears to be 5-methoxy-2-methylindol-3-ylacetic acid (**II**), the hydrolysis product of indomethacin (**I**),[7] as the indomethacin sample dissolved only in alkali and not in ethanol produces colour or fluorescence. The failure of tryptophan and indole-3-acetic acid to develop colours with the proposed reagents indicates the necessity to have a 5-OMe group in the indole moiety. Compound **II** reacts initially with the oxidant (CAT or OCl^-) to produce the highly reactive and less stable *p*-benzoquinone monoimine derivative (**III**), as with *p*-phenetidin (*p*-ethoxyaniline).[8] Compound **III** may react further with coupler (*m*-aminophenol, resorcinol or phloroglucinol) to give 7-substituted-**III** such as *p*-*N*-acetylbenzoquinone monoimine and cysteine.[9]

In conclusion, the proposed methods are simple, sensitive, selective and can be used for the routine determination of indomethacin in pharmaceutical preparations.

The authors are grateful to the authorities of Andhra University and also to the Council of Scientific and Industrial Research, New Delhi, for awarding a fellowship to K. E. R.

References

1. Baggi, T. R., Mahajan, S. N., and Rao, G. R., *Indian J. Pharm. Sci.*, 1976, **38**, 101.
2. Sanghavi, N. M., and Kamala, S., *Indian J. Pharm. Sci.*, 1978, **40**, 71.
3. Peterkova, M., Kakac, B., and Matousova, O., *Cesk. Farm.*, 1980, **29**, 73.
4. Garcia, C. R., Lopez, A. A., and Benet, L. Z., *Rev. Soc. Quim.*, 1980, **24**, 68.
5. "British Pharmacopoeia 1980," Pharmaceutical Press, London, 1980, p. 239.
6. Pattergill, M. D., and Sands, D. E., *J. Chem. Educ.*, 1979, **58**, 244.
7. Hajratwala, B. R., and Dawson, J. E., *J. Pharm. Sci.*, 1977, **66**, 27.
8. Davis, D. R., Fogg, A. G., Thorburn Burns, D., and Wragg, J. S., *Analyst*, 1974, **99**, 12.
9. Blair, I. A., Boobis, A. R., Davis, D. S., and Cresh, M., *Tetrahedron Lett.*, 1980, 4947.

Paper A5/254
Received July 15th, 1985
Accepted September 4th, 1985

Spectrofluorimetric Determination of Zinc with Pyrocatechol-1-aldehyde 2-Pyridylhydrazone

Ana M. Afonso, José J. Santana and Francisco García Montelongo
Department of Analytical Chemistry, University of La Laguna, La Laguna, Tenerife, Spain

Pyrocatechol-1-aldehyde 2-pyridylhydrazone was synthesised and its ionisation constants spectrophotometrically determined. A procedure was developed for the spectrofluorimetric determination of 12–250 ng ml^{-1} of zinc in 50% *V/V* ethanol - water medium, acetate-buffered to apparent pH 5.5 ($\lambda_{ex.}$ = 398 nm, $\lambda_{em.}$ = 521 nm), using the above reagent. Interferences were evaluated and the procedure was applied satisfactorily to the determination of zinc in potable tap water.

Keywords: *Zinc determination; spectrofluorimetry; pyrocatechol-1-aldehyde 2-pyridylhydrazone*

Hydrazones have been widely used in the spectrophotometric determination of metal ions[1] but only in recent years have they found application as fluorogenic reagents for metals.[2] Haddad *et al.*[3] determined cobalt fluorimetrically after extraction of its ternary complex with 2-pyridylaldehyde 2-pyridylhydrazone and eosin, and 2-pyridylhydrazones derived from 3-hydroxy-2-pyridylaldehyde, benzyl 2-pyridyl ketone, 2-dipyridyl ketone, salicylaldehyde, β-resorcylaldehyde and 2-hydroxy-1-naphthaldehyde have been used in the fluorimetric determination of Al(III), Ga(III), In(III), Sc(III) and Zn(II).[4–8] Other 2-pyridylhydrazones have been used as substrates for the kinetic and catalytic fluorimetric determination of several metal ions.[9–11]

In this paper the characteristics and analytical properties of pyrocatechol-1-aldehyde 2-pyridylhydrazone (PCAPH) are described, and a rapid and simple method for the spectrofluorimetric determination of 12–250 ng ml^{-1} of zinc based on its fluorescent complex with PCAPH is reported.

Experimental

Apparatus

All fluorescence measurements were made with a Perkin-Elmer MPF-44A recording spectrofluorimeter equipped with a 150-W Osram XBO xenon arc lamp, a DSCU-1 corrected spectra unit (0.5% Rodamine B in ethylene glycol as the reference), a UDR-3 digital read-out, a Selecta Frigitherm ultrathermostat and 1-cm quartz cells. The emission intensity measuring system of the spectrofluorimeter was calibrated daily by using the Perkin-Elmer set of fluorescent polymer blocks. A Radiometer PHM84 digital pH meter with glass and calomel electrodes was also used. pH values in 50% *V/V* ethanol - water were not corrected and are referred to as pH*.

Reagents

Analytical-reagent grade chemicals and de-ionised water were used throughout without further purification.

Pyrocatechol-1-aldehyde 2-pyridylhydrazone. Synthesised by condensation of pyrocatechol-1-aldehyde and 2-pyridylhydrazine.[13] The crude product was washed with diethyl ether until only one spot was revealed by thin-layer chromatography [silica gel G (Merck); benzene - ethanol (9 + 1); iodine vapour as detection agent]. The crystals obtained (yield 85%) melted at 192–194 °C. High-resolution mass spectrometry showed a parent molecular ion (M^+) at *m/z* 229.083 and $C_{12}H_{11}O_2N_3$ as the most probable composition. A 1.0×10^{-2} M solution of the reagent in absolute ethanol was prepared and diluted as required.

Zinc perchlorate standard solution, 0.1 M. Prepared from zinc oxide by perchloric acid treatment and standardised complexometrically. The ionic strength was controlled by adding suitable amounts of 2.5 M sodium perchlorate solution. A pH 4.5 acetic acid - sodium acetate (0.1 M) buffer solution was used as indicated.

Procedure

Determination of zinc

To a solution of zinc (up to 10 ml) containing 0.3–25.5 μg of zinc in a 25-ml calibrated flask add 3 ml of the acetic acid - sodium acetate buffer solution, 2 ml of 2.5 M sodium perchlorate solution, 5 ml of a 4.15×10^{-5} or 1.7×10^{-4} M ethanolic solution of PCAPH (according to the expected zinc concentration, see later) and 7.5 ml of absolute ethanol and dilute to volume with de-ionised water. Measure the fluorescence at 521 nm using excitation at 398 nm, against a reagent blank. Determine the amount of zinc present in the sample from calibration graphs prepared under the same experimental conditions.

If copper is present, add 2 ml of 10^{-2} M sodium thiosulphate solution and a few crystals of ascorbic acid. If aluminium or iron(III) is present, add 0.25 ml of 0.25 M ammonium fluoride solution.

Determination of zinc in potable tap water

Analyse suitable aliquots according to the above method.

Results and Discussion

Characteristics of the Reagent

The infrared spectrum of PCAPH (KBr pellet) was obtained and bands were assigned as follows: phenolic OH (3400 cm^{-1}), –NH– (3250 cm^{-1}), pyridinic –C=N– (1620 cm^{-1}), >C=N– (1286 cm^{-1}) and benzylic >CH– (750 cm^{-1}).

The NMR spectrum (dimethyl sulphoxide-d_6, tetramethylsilane) at 90 MHz was as follows: δ (benzenic moiety) = 6.80 (1H, d, J = 7 Hz, H_6), 7.26 (1H, s, H_4), 7.64 (1H, d, J = 7 Hz, H_5); δ (pyridinic moiety) = 6.95 (1H, s, H_3), 7.08 (1H, s, H_5), 7.44 (1H, s, H_4), 8.09 (1H, s, H_6); δ (benzylic =CH–) = 8.99 (1H, s).

PCAPH is very soluble in ethanol, dimethyl sulphoxide, dimethylformamide and concentrated alkalis, soluble in water and slightly soluble in benzene and diethyl ether. Aqueous ethanolic solutions of the reagent slowly hydrolyse when the pH is less than 1 or higher than 9.

PCAPH behaves as a tribasic substance with protonation of the heterocyclic nitrogen atom and deprotonation of the *meta*- and *ortho*-hydroxy groups. The corresponding ionisation constants were calculated from the variation of the absorbance at different wavelengths with pH by application of the method

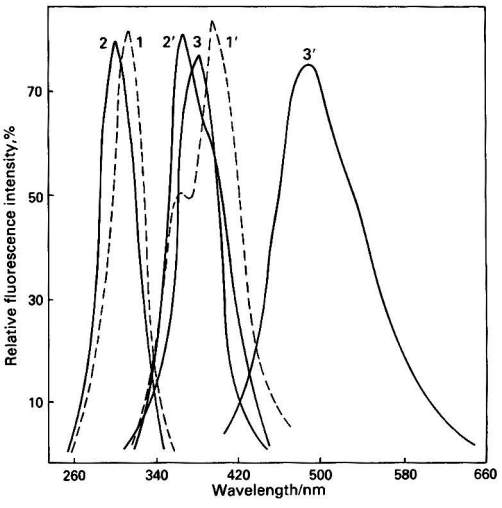

Fig. 1. Corrected excitation (1–3) and emission (1′–3′) spectra of PCAPH in different media. 1,1′ = Neutral medium; 2,2′ = acidic medium; 3,3′ = basic medium. $C_R = 6.0 \times 10^{-5}$ M; solvent = 50% *V/V* ethanol - water

Table 1. Spectral characteristics of the fluorescent complexes of PCAPH

Complex of	pH* ≈ 1†		pH* ≈ 5‡	
	$\lambda_{ex.}$/nm	$\lambda_{em.}$/nm	$\lambda_{ex.}$/nm	$\lambda_{em.}$/nm
Zn(II)	—	—	400	494
Ca(II)	385	440	387	482
Mg(II)	384	438	386	489
Cd(II)	388	440	—	—
Al(III)	405	492	396	490
Ga(III)	400	500	390	486
In(III)	—	—	400	510
La(III)	382	452	376	424

† Perchloric acid.
‡ Acetic acid - sodium acetate buffer solution.

of Hniličová and Sommer.[14] The mean values found were $pK_{a1} = 5.42 \pm 0.06$ and $pK_{a2} = 8.42 \pm 0.04$; pK_{a3} could not be calculated because of the slow hydrolysis of the reagent at higher pH.

The fluorescence maxima of PCAPH at pH* 7.0 ($\lambda_{ex.} = 299$ nm, $\lambda_{em.} = 366$ nm), Fig. 1, show a bathochromic change ($\lambda_{ex.} = 311$ nm, $\lambda_{em.} = 394$ nm) in acidic media, the fluorescence emission intensity increasing as the pH decreases. This may be due to protonation of the ring nitrogen atom, which stabilises its free electron pair and therefore stabilises the corresponding excited states. In ammoniacal media PCAPH also shows a bathochromic change ($\lambda_{ex.} = 380$ nm, $\lambda_{em.} = 490$ nm).

The reactions of PCAPH with 50 metal ions at pH* 1.0 and 5.0 were investigated. Only Cd(II), Mg(II), Ca(II), Ga(III), In(III), Al(III) and La(III) showed fluorescence under UV light. The spectrofluorimetric characteristics of these complexes are given in Table 1.

Reaction with Zinc

With Zn(II) ions PCAPH forms a yellow - green complex with strong yellow fluorescence under UV irradiation. The corrected excitation and emission spectra are shown in Fig. 2; its highest fluorescence emission intensity is at pH* 5–6 (Fig. 3A). A pH 4.5 acetic acid - sodium acetate (0.1 M) buffer solution, which gives pH* 5.5 in the 50% *V/V* ethanol - water medium used, was employed in all subsequent work.

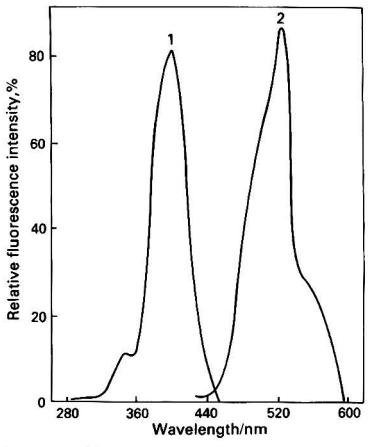

Fig. 2. Corrected (1) excitation and (2) emission spectra of the Zn(II) - PCAPH complex in a 50% *V/V* ethanol - water medium at pH* 5.5 (acetic acid - acetate buffer). $C_{Zn} = 5.3 \times 10^{-6}$ M; $C_R = 1.0 \times 10^{-4}$ M

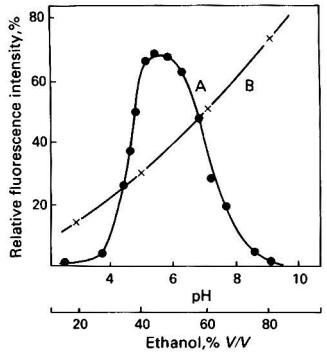

Fig. 3. Effect of (A) pH* and (B) amount of ethanol on the fluorescence intensity of the Zn(II) - PCAPH complex. ($\lambda_{ex.} = 398$ nm, $\lambda_{em.} = 521$ nm)

All fluorescence measurements were made at 25 ± 0.1 °C, at which temperature the fluorescence emission remains stable for at least 1 h. The fluorescence intensity decreases linearly at *ca.* 0.38% °C^{-1} as the temperature increases between 35 and 55 °C. This effect might be due to the easier non-radiative deactivation of the excited singlet state as the temperature increases.

The fluorescence intensity is critically dependent on the concentration of ethanol, increasing steadily with the percentage of ethanol in the medium (Fig. 3B). A 50% *V/V* ethanol - water medium was chosen as the best balance between fluorescence emission and volumes of aqueous solution of sample and reagents to be added.

Several sodium and potassium salts were tested at different concentrations in order to study the influence of the ionic strength on the fluorescence emission. The results show that variations in the ionic strength and the concentration of the electrolyte used to control it do not influence the fluorescence emission. In all subsequent work a 0.2 M ionic strength, adjusted with sodium perchlorate, was used.

Table 2. Interference levels of foreign ions on the spectrofluorimetric determination of 60 ng ml^{-1} of Zn(II) with PCAPH

Tolerance ratio, *m/m*	Ion added
6500	Cl^-
6300	SO_4^{2-}
3300	Mg^{2+}
2800	Ca^{2+}
1000	NO_3^-, F^-, ascorbic acid
800	$S_2O_3^{2-}$
500	CO_3^{2-}
200	I^-, HPO_4^{2-}, $B_4O_7^{2-}$
50	Br^-, SCN^-
15	Mn^{2+}
10	Fe^{3+}
5	As(III), U(VI)
3	Hg(I), Pb(II), Tl(I)
2	Cd(II), Sn(II), La(III), Ag(I), Te(IV), tartrate
1	Mn(VII), Cr(VI), Ce(IV), Zr(IV), V(IV), Se(IV), Au(III), Ru(III), Pd(II), $C_2O_4^{2-}$
0.5	V(V), Th(IV), In(III), Sb(III), Fe(II), Pt(II), Al(III), EDTA, EGTA, DCTA
Strong interference	Mo(VI), Ti(IV), Ga(III), Bi(III), Co(II)

Variation of the order of addition of sample and reagents does not have a marked influence on the fluorescence emission.

The stoicheiometry of the complex was studied under the established experimental conditions by the continuous variations and molar ratio methods. A metal to ligand ratio of 1 : 1 was found.

The effect of the reagent concentration on the fluorescence intensity of solutions containing 35 ng ml^{-1} of zinc(II) was studied under conditions similar to those recommended under Experimental. The fluorescence intensity increases with increasing the reagent concentration up to 5.0×10^{-5} M, and remains constant between 5.0×10^{-5} and 2.5×10^{-4} M. At higher reagent concentrations, the fluorescence decreases markedly, mainly owing to autoabsorption phenomena.

Spectrofluorimetric Determination of Zinc

Under the experimental conditions outlined in the recommended procedure, there is a linear relationship between emitted fluorescence intensity and Zn(II) concentration in the ranges 12–80 and 80–250 ng ml^{-1}, using 5 ml of 4.15×10^{-5} or 1.7×10^{-4} M solutions of the reagent, respectively. The detection limit, as defined by IUPAC,[15] was determined to be 5.5 ng ml^{-1}.

When the developed method was applied to two series of eleven samples containing 35 and 170 ng ml^{-1} of zinc, relative errors of 2.80 and 1.14% (95% confidence limits), respectively, were obtained.

A study of the effect of several ions on the determination of 60 ng ml^{-1} of zinc was carried out by first applying the recommended method to solutions containing a 10 000-fold (*m/m*) ratio of interferent to zinc and, if interference occurred, reducing this ratio until interference ceased. Higher ratios were not tested. The criterion for interference was a variation in the concentration found for zinc of more than ±4% from the value taken. The results are shown in Table 2.

Copper can be tolerated up to a Cu to Zn ratio of 7 when it is masked with thiosulphate and ascorbic acid, Al(III) up to an Al to Zn ratio of 1 and Fe(III) up to an Fe to Zn ratio of 40 in the presence of fluoride as the masking reagent.

The interferences in the proposed method come mainly from ions such as Mg(II), Ca(II) and Al(III), which also form fluorescent complexes with PCAPH as previously shown, and from those giving coloured complexes with the reagent such as Fe(II), Fe(III) and Ni(II).

Table 3. Spectrofluorimetric analysis of potable tap water for zinc

Sample No.	Zn found/ng ml^{-1}* PCAPH (range)	AAS
1	104(102–105)	104
2	277(266–284)	277
3	1295(1258–1319)	1294
4	147(145–149)	147
5	160(158–162)	160
6	271(264–277)	273

* Mean of three determinations.

Applications

The method developed was applied to the determination of zinc in samples of tap water from the distribution systems in several cities of the Canary Islands, collected and preserved as recommended.[16] The results are shown in Table 3, where they are compared with those obtained by the standard AAS method.[17] The zinc concentrations found are well under the tolerance limit set by the Spanish Food Directorate ($\leq$ 1.5 mg l^{-1}).

The authors acknowledge financial support of this work by CAICYT (Spain), grant No. 4122/79.

References

1. Katyal, M., and Dutt, Y., *Talanta*, 1975, **22**, 151.
2. Singh, R. B., Jain, P., and Singh, R. P., *Talanta*, 1982, **29**, 77.
3. Haddad, P. R., Alexander, P. W., and Smythe, L. E., *Talanta*, 1976, **23**, 275.
4. Laserna, J. J., Navas, A., and García Sánchez, F., *Anal. Lett.*, 1982, **14A**, 833.
5. Laserna, J. J., Navas, A., and García Sánches, F., *Anal. Chim. Acta*, 1980, **121**, 295.
6. Laserna, J. J., Navas, A., and García Sánchez, F., *Microchem. J.*, 1982, **27**, 312.
7. Cano, J. M., Trujillo, M. L., and García de Torres, A., *Anal. Chim. Acta*, 1980, **117**, 319.
8. Sommer, L., Maung-Gyee, W. P., and Ryan, D. E., *Scr. Fac. Sci. Nat. Univ. Purkynianae Brun. 2*, 1972, **2**, 115; *Chem. Abstr.*, 1973, **79**, 121493c.
9. García Sánchez, F., Navas, A., and Laserna, J. J., *Anal. Chem.*, 1983, **55**, 253.
10. Rubio, S., Gómez-Hens, A., and Valcárcel, M., *Anal. Lett.*, 1984, **17A**, 651.
11. Rubio, S., Gómez-Hens, A., and Valcárcel, M., *Analyst*, 1984, **109**, 717.
12. Afonso, A. M., Santana, J. J., González, M. P., and García Montelongo, F., *Mikrochim. Acta*, 1984, **II**, 53.
13. Odashima, T., Anzai, P., and Ishii, H., *Anal. Chim. Acta*, 1976, **86**, 231.
14. Hniličková, M., and Sommer, L., *Talanta*, 1966, **13**, 667.
15. Irving, H. M. H. N., Freiser, H., and West, T. S., *Editors*, "IUPAC Compendium of Analytical Nomenclature, Definitive Rules, 1977," Pergamon Press, Oxford, 1978.
16. American Public Health Association, American Water Works Association and Water Pollution Control Federation, "Standard Methods for the Examination of Water and Wastewater," Fourteenth Edition, American Public Health Association, Washington, DC, 1976, p. 38.
17. Reference 16, p. 143.

Paper A5/220
Received June 20th, 1985
Accepted September 20th, 1985

Determination of Theaflavins in Tea Solution Using the Flavognost Complexation Method

Michael Spiro* and William E. Price
Department of Chemistry, Imperial College of Science and Technology, London SW7 2AY, UK

Several aspects of the flavognost method for determining theaflavins (TF) in tea solutions have been quantitatively investigated. Double extraction experiments showed that the partition coefficient of TF between water and isobutyl methyl ketone (IBMK) is 4.1_5 and approximately independent of temperature. The efficiency of the extraction step using 2 volumes of IBMK to 1 volume of tea infusion is then equal to 89%. A structure has been proposed for the green complex formed between the extracted TF and flavognost in a 25% *V/V* IBMK - 75% *V/V* ethanol mixture, and the equilibrium constant for its formation at 25 °C was found to be 0.07_3. The normal analytical procedure thus leaves 4–5% of TF uncomplexed. As only 85% of the TF in a sample of tea solution eventually appears in the form of the green flavognost complex, it is important not to vary the standard analytical procedure.

Keywords: *Theaflavins determination; flavognost; Hilton method; borate complexation; tea solutions*

Theaflavin is an important constituent of black tea. Although present at only 0.5–2% *m/m* in the leaf,[1] it is responsible for much of the attractive red colour of tea infusions and a correlation exists between the market price of a given black tea and its theaflavins (TF) content.[2,3] The latter comprises both theaflavin itself and its mono- and digallates. The earlier method for total TF determination, the solvent-extraction procedure of Roberts and Smith,[1,4] has been criticised on several counts.[5] In many laboratories the determination of TF is now carried out by the simple flavognost method,[6] which was further developed by Hilton.[7,8] Here the TF is extracted by an organic solvent such as isobutyl methyl ketone (IBMK) and is then complexed with 2-aminoethyl diphenylborate (flavognost). The absorbance of the green complex formed is measured spectrophotometrically. It was the purpose of this study to examine several aspects of this method in more detail. It should be mentioned that although individual theaflavins can now be determined by HPLC,[9,10] this method requires prior work-up of samples as well as more expensive equipment, and is less suitable for small or dilute samples.[11]

Experimental

The general procedure involved the infusion of black Kapchorua tea (x g) in 200 cm^3 of distilled water at 80 °C for 30 min to reach partition equilibrium. The pH of the infusion was typically 4.8. Then an aliquot (V cm^3) of the tea solution was removed so as to exclude any leaf, and shaken vigorously for 1 min in a stoppered tube with n times its volume of IBMK (BDH Chemicals, AnalaR grade) (Table 1). The layers were allowed to separate; if the shaking had produced a suspension, separation was achieved by centrifuging for 5 min in a Gallenkamp Junior centrifuge (setting 1). With a clean syringe, 2 cm^3 of the IBMK layer were removed and added to v cm^3 (usually $v = 2$) of an ethanolic 2% *m/V* solution of flavognost (Koch-Light) and $(6 - v)$ cm^3 of absolute ethanol (J. Burrough). The green TF - flavognost complex was allowed 15 min to develop completely before its absorbance (A) was measured in a 1 cm cuvette at 625 nm with a Unicam SP 1800 spectrophotometer. The blank cuvette held a mixture of IBMK - flavognost solution - ethanol $[2 : v : (6 - v)]$. The TF content of the aqueous solution was calculated from Beer's law by the equation

$$[\text{TF}](\text{mmol dm}^{-3}) = fnA \times 9/375 = 0.024fnA \quad (1)$$

where n is the dilution factor in the extraction and f is a molar conversion factor taken as 47.9 for $n = 1.8$ A modified value applies for other values of n, as explained below. The figures 9 and 375 take account of the original conditions[7] in which 9 g of tea leaf were infused in 375 cm^3 of water. The tea employed was Kapchorua (Pekoe Fannings and Dust) whose various size fractions have all been shown to contain 0.022 ± 0.001 mol kg^{-1} of TF.[11]

* To whom correspondence should be addressed.

Table 1. Summary of principal symbols

Symbol	Unit	Significance
x	g	Mass of tea leaf infused in 200 cm^3 of water
V	cm^3	Volume of aliquot of tea infusion removed
n	—	Volume of IBMK/ volume of aqueous aliquot
v	cm^3	Volume of flavognost solution added to 2 cm^3 IBMK layer

Results and Discussion

Effect of Sample and Solvent Temperature

Three sets of experiments were performed to test whether the analytical result depended upon the temperature of either phase in the solvent extraction step. Unsieved Kapchorua Pekoe Fannings tea was employed, and $x = 10$ g, $V = 5$ cm^3, $n = 2$ and $v = 2$ cm^3. In experiments of type A, the hot (80 °C) 5-cm^3 sample of tea solution was added to 10 cm^3 of IBMK that had been pre-heated to 80 °C in the thermostated bath. The mixture was shaken vigorously and returned to the 80 °C bath. The layers separated easily under these conditions and no centrifuging was necessary. In type B experiments, the hot tea sample was shaken with cold (room temperature) IBMK, with all subsequent steps being carried out at room temperature. Analyses of type C were carried out completely at room temperature, the filtered tea liquor having been cooled to 24 °C before a sample was removed. A small amount of tea cream appeared at the interface only. The resulting absorbances of the TF - flavognost complex in duplicate experiments were identical within experimental error: 0.294, 0.293 (type A); 0.294, 0.294 (type B); 0.295, 0.294 (type C). The temperatures of the two phases are therefore not of importance in the procedure. For convenience, in subsequent work the hot tea sample was added to room-temperature IBMK.

Efficiency of the Solvent Extraction Step

Although Hilton has stated[7] that a single IBMK extraction does not exhaustively remove the theaflavins, this point is

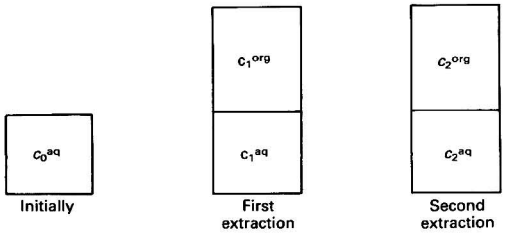

Fig. 1. Schematic illustration of successive extraction steps

normally ignored and has never been quantified. For this reason the partition coefficient (K_p) of TF between water and IBMK has now been determined. This was performed by carrying out two successive extractions as depicted schematically in Fig. 1. The TF concentration in the original tea sample, c_0^{aq}, is reduced to c_1^{aq} after equilibration with n times its own volume of IBMK and to c_2^{aq} after further equilibration with n times its volume of fresh IBMK. The concentration of TF in the two organic layers, c_1^{org} and c_2^{org}, can be determined by complexation with flavognost. Any uncertainty about the exact value of the molar absorptivity of the complex is removed by considering only the ratio

$$c_1^{org}/c_2^{org} = r.$$

From the conservation of mass:

$$c_0^{aq} = c_1^{aq} + nc_1^{org} \quad .. \quad .. \quad .. \quad (2)$$

$$c_1^{aq} = c_2^{aq} + nc_2^{org} \quad .. \quad .. \quad .. \quad (3)$$

If the partition coefficient is the same in both extractions:

$$K_p = c_1^{org}/c_1^{aq} = c_2^{org}/c_2^{aq} \quad .. \quad .. \quad (4)$$

It follows that

$$r = c_1^{org}/c_2^{org} = c_1^{aq}/c_2^{aq} \quad .. \quad .. \quad (5)$$

Hence from equations (3), (4) and (5):

$$r = 1 + nK_p \quad .. \quad .. \quad .. \quad .. \quad (6)$$

whence $K_p = (r-1)/n$.

The theory shows how values of K_p can be evaluated by performing two successive extractions with IBMK. The results of various experiments using unsieved Kapchorua Pekoe Fannings tea and $v = 2$ cm^3 are listed in Table 2. Because the absorbances after the second extractions are small, most K_p values have an attached uncertainty of about ±12%. Within these limits K_p is reproducible and shows no significant variations with the TF concentrations of the infusion (x), the ratio of IBMK to water in the solvent extraction step (n), or the pH of the tea infusion over the range 4.8 (its normal value) down to 2.9 (lemon tea). The mean K_p value over all these experiments is $4.1_5 \pm 0.1_5$.

This result has an important implication for the normal flavognost method based on a single extraction. From equations (2) and (4) it follows that

$$c_0^{aq}/c_1^{org} = n + (1/K_p) \quad .. \quad .. \quad .. \quad (7)$$

Were K_p infinitely large, the extraction would be complete and $c_0^{aq}/(c_1^{org})_{compl.}$ would equal n. As K_p is finite,

$$\frac{c_1^{org}}{(c_1^{org})_{compl.}} = \frac{n}{n + (1/K_p)} = \frac{nK_p}{nK_p + 1} \quad .. \quad (8)$$

which equals 80.6 (± 0.6)% when $n = 1$ and 89.2 (± 0.4)% when $n = 2$. The extraction efficiencies are therefore functions of n. The conversion factor in equation (1) must vary accordingly, and Hilton's value for f of 47.9 obtained with $n = 1$ has to be changed to $47.9 \times (80.6/89.2) = 43.3$ with $n = 2$. This gives

$$[TF](\text{mmol dm}^{-3}) = 0.024 \times 43.3 \times 2A = 2.08A \quad .. \quad (9)$$

Although the extraction is not exhaustive, the partition coefficient has been shown to be independent of various experimental parameters. The flavognost method therefore retains its usefulness for comparing data from different tea infusions provided the same value of n is employed or else the appropriate molar conversion factor f. Calibration of the method must be effected by dissolving a known amount of TF in the aqueous phase and not directly in IBMK.

Table 2. Partition coefficients for theaflavins between aqueous tea infusions and IBMK

x/g	n	A_1 1st extn.	A_2 2nd extn.	K_p
10	2	0.288	0.026	5.0
10	2	0.318	0.034	4.2
10	2	0.300	0.030	4.5
10	2*	0.294	0.031	4.2
20	1	0.83	0.145	4.7
20	2	0.462	0.057	3.6
20	3	0.339	0.029	3.6
10	2†	0.387	0.046	3.7
10	2†	0.380	0.042	4.0
10	2‡	0.373	0.041	4.0_5
10	2§	0.368	0.041	4.0

* Extracted with hot (80 °C) IBMK.

† Tea infusion containing a citric acid (0.32 M) + NaOH (0.11 M) buffer of ionic strength 0.11 M and pH 3 at 80 °C.

‡ Tea infusion containing the same citrate buffer as above, with the sample neutralised with NaOH to pH 4.8 before analysis.

§ Tea infusion containing 0.11 M citric acid (pH 2 at the start of infusion and pH 2.9 at the end).

Stability Constant of the TF - Flavognost Complex

Although the flavognost method depends on the formation of a stable green complex in 25% *V/V* IBMK - 75% *V/V* ethanol, no information has been available on its formula or stability constant. It is well known that boron acids and borates form complexes with organic substances containing *cis*-1,2-dihydroxy groups; with various polyols both 1:1 and 1:2 complexes are formed[12] while only 1:1 complexes are produced with catechols and their derivatives.[13] This latter situation would apply to theaflavin whose only pair of *cis*-1,2-dihydroxy groups is attached to a benzene ring. With a diphenyl-substituted boron compound, such as flavognost, only a 1:1 complex is possible, and so the complexation reaction may be written

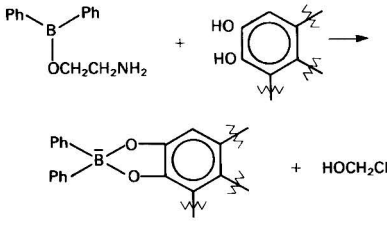

$$+ \ HOCH_2CH_2NH_3^+ \quad .. \quad .. \quad .. \quad (10)$$

The suggested structure of the boron complex follows similar structures proposed by workers in the field,[12,13] and one such structure has received confirmation in a Raman study.[14] Theaflavin gallates, however, also contain 3,4,5-trihydroxybenzoyl groups that could themselves complex with flavognost. A more general reaction scheme should therefore be considered:

$$\underset{c_0-c_x}{TF} + \underset{b_0-mc_x}{mB} \rightleftharpoons \underset{c_x}{\text{complex}} + \underset{c_x}{HOCH_2CH_2NH_3^+} \quad .. \quad (11)$$

where B represents flavognost and b_0 is its initial concentration in the IBMK - ethanol mixture; c_0 is the initial concentration of TF in the same mixture and c_x the equilib-

rium concentrtion of the green complex. Appreciable ion pairing of the two products in equation (10) is unlikely for such dilute solutions in a mainly ethanolic solvent.[15] Provided only one type of complex is formed, its stability constant is thus given by

$$K = \frac{c_x^2}{(c_0 - c_x)(b_0 - mc_x)^m} \quad \ldots \quad (12)$$

It may be noted that $b_0 \gg c_x$.

Experiments were carried out with Kapchorua Pekoe Dust (250–710 μm) and $x = 4$ g, $V = 20$ cm^3, $n = 1$, and six different values of v ranging from 0.1 to 1.5 cm^3 of an ethanolic 1% *m/V* (= 0.0445 M) solution of flavognost. A further 2-cm^3 sample of the IBMK layer was analysed using $v = 2$ cm^3 of an ethanolic 2% *m/V* solution of flavognost to provide a mixture with a sufficient excess of flavognost to convert almost all the TF into the complex. For these experiments the flavognost had been dried *in vacuo* at 100 °C and the ethanol was of AnalaR grade. The mixtures were placed in a thermostated bath at 25 °C for 15 min before the absorbances of the complex were read at 625 nm.

The results are listed in Table 3. The experiment with 2% *m/V* flavognost yielded 89.3 μM as a first approximation for c_0. When this value is inserted into the equilibrium equation (12) with $m = 1$, the K values become constant only at the higher values of b_0. This trend largely disappears when c_0 is increased by several per cent., the best fit being obtained near $c_0 = 94$ μM. All the K values, except that at the lowest concentration, are now in agreement when one makes due allowance for the sensitivity of K to small experimental errors in c_x.

The mean K value is 0.073 with a standard deviation of the mean of 0.003. It can be seen that similar calculations with $m = 2$ and $m = 1/2$ produce K values with pronounced monotonic trends (falling with increasing c_x for $m = 2$, and rising for $m = 1/2$), and these cannot be removed by any reasonable adjustment of c_0.

The following conclusions may now be drawn. (1) The fact that $m = 1$ shows that flavognost complexes only with the *cis*-1,2-dihydroxy group of theaflavin itself but not with the gallate side groups. This point was confirmed by some further complexation experiments carried out with small samples of ungallated theaflavin kindly donated by Mr. A. N. Smith (Unilever Research Laboratories, Colworth). (2) The equilibrium constant is *ca.* 10^3 times greater than that found for $PhB(OH)_2$ complexation with aqueous catechol.[13] Nevertheless, the K value is not sufficiently large for all the extracted TF to be complexed under the normal analytical conditions. If $v = 2$, so that $b_0 = 22.2$ mM in the IBMK - ethanol mixture, and with a typical TF concentration in the mixture of 80 μM, it follows from the above equilibrium constant that $c_x/c_0 \approx 0.96$. A very similar result emerges from the amount by which c_0 had to be increased to yield a constant value of K, as 89.3/94 = 0.95. Incomplete complexation therefore leads to an underestimate by 4–5% in the TF content of the organic phase. To check this conclusion, a set of analyses was carried out on a similar Kapchorua tea solution with $n = 2$, $v = 2$ and using both a 2% *m/V* and a 4% *m/V* solution of flavognost. As expected, the absorbances at 625 nm were consistently 2% greater with the more concentrated flavognost reagent.

Table 3. Equilibrium measurements on the TF - flavognost complex in 25% *V/V* IBMK - 75% *V/V* ethanol at 25 °C

v/cm^3	b_0/mM	c_x/μM	K^* ($m = 1$)	K† ($m = 1$)	10^5K^*/μM^{-1} ($m = 2$)	K^*/μM$^{1/2}$ ($m = 1/2$)
0.1	0.556	35.9	0.046	0.043	10.3	1.04
0.2	1.112	53.2	0.074	0.065	7.74	2.38
0.4	2.225	66.4	0.089	0.074	4.40	4.12
0.6	3.338	74.2	0.112	0.085	3.58	6.34
0.9	5.006	77.3	0.101	0.073	2.11	7.06
1.5	8.344	82.3	0.117	0.070	1.45	10.6

* $c_0 = 89.3$ μM.
† $c_0 = 94.0$ μM.

Conclusions

The solvent extraction step in the Hilton flavognost method has been shown to be 89% efficient if a sample of tea solution is extracted by twice its volume of IBMK. The subsequent complexation of the extracted TF with flavognost is *ca.* 95% complete when 2 cm^3 of the IBMK extract is mixed with 2 cm^3 of 2% *m/V* ethanolic flavognost and 4 cm^3 of ethanol. Overall, only 85% of the TF in a sample of tea solution ultimately appears in the form of the green flavognost complex whose absorbance is measured. The use of an appropriate proportionality constant in the Beer's law equation can overcome this problem provided that a standard analytical procedure is always employed (preferably $n = 2$, $v = 2$ cm^3). The method must be standardised by dissolving a known amount of TF in an aqueous solution and not by dissolving it directly in IBMK.

The authors thank the SERC for the award of a CASE Studentship to W.E.P. and Unilever plc and particularly Dr. D. R. Haisman and Mr. A. N. Smith for their help and support and for supplying the tea leaf and a sample of ungallated theaflavin.

References

1. Roberts, E. A. H., and Smith, R. F., *J. Sci. Food Agric.*, 1963, **14**, 689.
2. Hilton, P. J., and Ellis, R. T., *J. Sci. Food Agric.*, 1972, **23**, 227.
3. Cloughley, J. B., *J. Sci. Food Agric.*, 1980, **31**, 911.
4. Roberts, E. A. H., and Smith, R. F., *Analyst*, 1961, **86**, 94.
5. Collier, P. D., and Mallows, R., *J. Chromatogr.*, 1971, **57**, 19.
6. Nestle's Products Ltd., *Br. Pat.*, 1 034 670, 1966.
7. Hilton, P. J., *in* Snell, F. D., and Ettre, L. S., *Editors*, "Encyclopedia of Industrial Chemical Analysis," Volume 18, Wiley, New York, 1973, p. 455.
8. Hilton, P. J. R., "Tea Research Foundation of Central Africa Annual Report," Mulanje, Malawi, 1972/73, Section 4, p. 80.
9. Hoefler, A. C., and Coggon, P., *J. Chromatogr.*, 1976, **129**, 460.
10. Wellum, D. A., and Kirby, W., *J. Chromatogr.*, 1981, **206**, 400.
11. Price, W. E., and Spiro, M., *J. Sci. Food Agric.*, 1985, **36**, 1303.
12. Conner, J. M., and Bulgin, V. C., *J. Inorg. Nucl. Chem.*, 1967, **29**, 1953.
13. Pizer, R., and Babcock, L., *Inorg. Chem.*, 1977, **16**, 1677.
14. Oertal, R. P., *Inorg. Chem.*, 1972, **11**, 544.
15. Fernández-Prini, R., *in* Covington, A. K., and Dickinson, T., *Editors*, "Physical Chemistry of Organic Solvent Systems," Plenum Press, London, 1973, Appendix 5.1.

Paper A5/230
Received June 26th, 1985
Accepted September 26th, 1985

Micro-determination and Separation of Manganese Using a Liquid Ion Exchanger

Sobhana K. Menon and Yadvendra K. Agrawal
Analytical Chemistry Laboratory, Pharmacy Department, Faculty of Technology and Engineering, M.S. University of Baroda, Kalabhavan, Baroda-390 001, India

A sensitive and selective method for the micro-determination of manganese has been developed involving the extraction of the wine-red manganese - benzohydroxamic acid (BHA) complex with Aliquat 336 liquid ion exchanger, and the optimum conditions have been established. Kinetic and stability studies on the complex were carried out. The extracted metal can be quantitatively eluted with 0.25 M hydrochloric acid, thus rendering the method applicable for the concentration, separation and determination of manganese in samples containing very low levels of the metal.

Keywords: *Manganese determination; spectrophotometry; liquid ion exchanger*

Liquid ion exchangers are extensively used for the pre-concentration, separation and recovery of several metal ions[1-3] and are becoming popular owing to their potential for industrial chemical separations and for the recovery of costly chemicals.[4] The superior extraction ability of liquid ion exchangers can also be utilised for the effective removal of toxic metal ions.[5] The extraction of a coloured species of the metal ion by a liquid ion exchanger permits its direct detection together with its pre-concentration, separation and determination. Interferences can be considerably reduced either by masking before extraction or by removing the interfering ions with a suitable eluant from the liquid ion exchanger phase before the elution of the metal. This method has been adopted for the determination of manganese as reported for the determination of titanium.[6]

Hydroxamic acids have already proved to be very sensitive and selective reagents for the trace determination of metals.[7,8] A few hydroxamic acids have been reported for the determination of manganese[9,10] in basic media. The wine-red complex of manganese with benzohydroxamic acid[10] was found to be extracted instantaneously into Aliquat 336, with a considerable enhancement of the sensitivity; this can be applied to the determination of microgram amounts of manganese and to its separation from closely associated metals by selective elution.

Experimental

Chemicals and Reagents

All chemicals were of analytical-reagent or general-reagent grade from BDH Chemicals and E. Merck, respectively, unless specified otherwise.

Benzohydroxamic acid (BHA). This was prepared as described elsewhere[11] and was further purified by our modified method.[6] A 0.1 M solution in doubly distilled water was prepared.

Manganese standard solution. A stock solution of manganese was prepared by dissolving the requisite amount of $MnSO_4.4H_2O$ in doubly distilled water. The solution was standardised titrimetrically with EDTA[12] and the metal content was found to be 0.703 mg ml^{-1}. The solution was diluted as required.

Liquid Anion Exchangers

Amberlite LA-1 [*N*-dodecyl(trialkylmethyl)amine] (Rohm & Haas, Philadelphia, PA, USA), Aliquat 336 (tricaprylmethylammonium chloride) (Fluka, Buchs, Switzerland) and trioctylamine (Fluka) dissolved in suitable diluents in varying proportions, were used.

Apparatus

A VSU2-P spectrophotometer (Carl Zeiss, Jena, GDR) with matched quartz cells was used for spectral measurements.

pH measurements were made on an Elico digital pH meter equipped with calomel and glass electrodes.

Procedure

A sample solution containing 12–200 μg of the metal was placed in a 60-ml separating funnel and ammonia solution was added so that the basicity of a total volume of 15 ml of aqueous phase was between 0.2 and 0.3 M of ammonia. A 2-ml volume of a 0.1 M solution of BHA was added immediately to the above solution, which was then mixed well and kept for 5 min. The mixture was shaken gently with 15 ml of a 4% solution of Aliquat 336 in xylene for about 1 min after the addition of 5 ml of 2 M ammonium chloride solution. The phases were allowed to separate and the organic extract was dried over anhydrous sodium sulphate and transferred into a 25-ml calibrated flask. To ensure the complete recovery of manganese, the extraction was repeated with 5 ml of the extraction solvent, followed by drying with sodium sulphate and finally dilution of the combined extract to the mark with the solvent. The absorbance was measured at 480 nm against a reagent blank.

To calculate the distribution ratio, D, and the percentage extraction, E, the manganese concentration in the aqueous phase was determined with 4-(2-pyridylazo)resorcinol (PAR).[13] The metal content in the organic phase was determined after elution of the metal from the organic phase as described below.

For the elution of manganese, the organic layer was shaken with 15 ml of 0.25 M hydrochloric acid for 2 min. The two phases were allowed to settle and the aqueous layer was withdrawn carefully. The metal content was determined using PAR. The pH of the solution was adjusted to 7–8 and 5 ml of borate buffer (pH 10) were added together with 5 ml of 0.1 M PAR solution. The solution was diluted to 50 ml and measurements were taken at 500 nm after keeping the mixture for 15 min. The amount of manganese was calculated from a calibration graph.

Results and Discussion

The manganese complex is wine-red and has a fairly wide absorption band at 480 nm. The complex formation is accompanied by a change in the oxidation state of the manganese from +2 to +3, which was accomplished by the oxygen dissolved in the solution. The colour formation will not take place if the mixture of the reagent and manganese ions is

boiled to eliminate the dissolved oxygen. However, on exposure to air or on addition of an oxidising agent such as dilute hydrogen peroxide the wine-red colour appears. The presence of small amounts of hydroxylammonium chloride, which prevents the oxidation of Mn(II), will also inhibit the appearance of the characteristic colour, thereby ensuring the tervalent state of manganese in the complex. The instantaneous extraction of the complex into the liquid anion exchanger shows the anionic nature of the complex.

Effect of Variables on the Extraction

Basicity

The complex formation is most favoured in ammonia solution. Even though the complex will form in sodium or potassium hydroxide solution, the rate of formation is much slower than in ammonia solution. Also, the former bases will cause interferences due to the formation of precipitates of hydroxides with certain metallic ions, whereas precipitates that are soluble in an excess of ammonia are formed in most instances in an ammoniacal medium. The extraction is quantitative about pH 10 and remains constant up to 0.4 M of ammonia. The sensitivity decreases very slowly above 0.5 M of ammonia. Therefore, extractions were carried out at ammonia concentrations around 0.3 M.

Reagent concentration

The absorbance of the manganese complex was constant with the use of excess of the reagent. Extractions with various concentrations of the reagent showed that 1–2 ml of 0.1 M BHA solution was adequate for quantitative extraction of the manganese. The reagent is added immediately after the addition of ammonia solution and mixed well so as to prevent the precipitation of manganese hydroxide, which will delay the colour formation.

Electrolytes

The extraction was carried out in the presence of various concentrations of electrolytes such as NH_4Cl, NaCl, Na_2SO_4, KCl and K_2SO_4 as the separation of the organic and aqueous layers was not clear in the absence of an electrolyte. A 2–4 M solution of NH_4Cl gave satisfactory results. For each extraction, 5 ml of 2 M NH_4Cl solution were used.

Aliquat 336 concentration

The optimum concentration of Aliquat 336 was studied by varying the concentration from 1 to 10% in xylene. The extraction was quantitative from 3% and remained constant up to 8%. A tendency to form emulsions was observed at higher concentrations of the ion exchanger. A 4% solution of the exchanger was used for extraction.

Diluents

Manganese was extracted with 4 and 6% Aliquat 336 solution in various diluents. Equilibration was effected by maintaining the ratio of organic to aqueous phase at 1:1 and the percentage extraction was calculated in each instance (Table 1). The extraction was complete and quantitative with benzene and xylene and a clear separation was obtained. As benzene is highly toxic, xylene was used as the diluent in subsequent work.

Table 1. Effect of various diluents on the extraction (%) of manganese with Aliquat 336

Diluent	Mn extracted, %	
	4% Aliquat 336	6% Aliquat 336
Benzene	99.9	99.9
Toluene	83.5	83.0
Xylene	99.5	99.0
Hexane	55.8	55.3
Chloroform	45.0	45.5
Carbon tetrachloride	51.2	50.8

Type of liquid anion exchanger

Manganese was extracted with three extractants in various diluents (Table 2). Aliquat 336 in benzene or xylene was found to be the best extractant.

Equilibration time and stability

The extraction was very rapid and required only a few seconds for quantitative and complete extraction. The time of shaking was varied from 30 s to 5 min. The extraction was quantitative within 30 s. The complex extracted under optimum conditions was stable for several days.

Optical Properties

The colour system obeyed Beer's law from 0.35 to 9.0 p.p.m. of manganese at 480 nm and the optimum range (Ringbom plot)[14] was 0.5–10 p.p.m. The molar absorptivity was 7.5×10^3 l mol^{-1} cm^{-1}.

Kinetic Study of Colour Formation and Extraction

As the colour formation of the complex and consequently the sensitivity of the extraction depend on time, a study was carried out to follow the rate of the reaction and to evaluate the rate constant. Extractions were carried out at room temperature (30 °C) at regular intervals of 1 min starting from the first to the tenth minute, the time referring to the interval between the time of mixing of the reagent and completion of extraction. The absorbance increased steadily and became constant after the fifth minute, indicating completion of the colour reaction. Therefore, extractions were carried out 5 min after mixing of the reactants. The rate constant was calculated (Table 3) by substituting the values of absorbance and time in the equations for first-and second-order reactions. The rate constant was found to be 0.65 min^{-1} following the first-order reaction.

Table 2. Effect of different liquid anion exchangers on the extraction of manganese

Liquid anion exchanger	Diluent	Extraction, %
Aliquat 336 (4%)	Benzene	99.9
	Xylene	99.5
	Chloroform	45.0
Amberlite LA-1 (4%)	Benzene	81.5
	Xylene	70.8
	Chloroform	41.5
Trioctylamine (4%)	Benzene	72.0
	Xylene	48.3
	Chloroform	32.5

Table 3. Kinetic study of complexation

Time/min	Extraction, %	Rate constant, K^*/min^{-1}
1	62.2	0.69
2	70.8	0.67
3	83.3	0.63
4	92.2	0.63
5	99.0	0.61
6	99.9	∞
7	99.9	∞

* Average rate constant, $K = 0.65$.

Table 4. Effect of diverse ions. Mn taken = 70 μg per 25 ml

Foreign ion	Added as	Tolerance limit/mg
Ag^{+}	$AgNO_3$	15*
Be^{2+}	$BeSO_4$	25
Mg^{2+}	$MgSO_4$	30
Ca^{2+}	$Ca(NO_3)_2$	30
Sr^{2+}	$SrCl_2$	30
Ba^{2+}	$BaCl_2$	29
Sn^{2+}	$Sn(NO_3)_2$	25
Pb^{2+}	$Pb(NO_3)_2$	10†
Cd^{2+}	$CdSO_4$	15†
As^{3+}	As_2O_3	30
Co^{2+}	$CoCl_2$	10*
Cu^{2+}	$CuSO_4$	20*
Hg^{2+}	$HgCl_2$	10†
Ni^{2+}	$NiCl_2$	30*
Zn^{2+}	$ZnSO_4$	2
Ti^{4+}	TiO_2	20
Cr^{3+}	$CrCl_3$	3
Al^{3+}	$AlCl_3$	1.5
V^{5+}	NH_3VO_3	25‡
$Mo_7O_{24}^{6-}$	$(NH_4)_6Mo_7O_{24}$	15§
Zr^{4+}	$Zr(NO_3)_4$	20
U^{6+}	$UO_2(CH_3COO)_2$	10¶
W^{6+}	Na_2WO_4	20
Sb^{3+}	$KSbOC_4H_4O_6.\frac{1}{2}H_2O$	20
Ce^{4+}	$Ce(SO_4)_2.4H_2O$	10

* Masked with 0.1% sodium cyanide solution.
† Masked with 0.5% potassium iodide solution.
‡ Eluted with 0.2 M sodium acetate solution.
§ Stripped with 0.2 M sodium chloride solution.
¶ Stripped with 0.1 M ammonia solution.

Table 5. Determination of manganese in NBS standard samples

Sample	Certified Mn concentration, %	Mn found,* %	Standard deviation, %
Mg alloy	0.44–0.46	0.455	0.002
Steel 14C	0.455–0.470	0.450	0.003
Mn bronze 164	4.65–4.72	4.65	0.01
Si bronze	1.30–1.33	1.31	0.01

* Average of six determinations.

Composition and Stability Constant

The composition of the manganese complex was studied by plotting a graph of the logarithm of the distribution coefficient of the metal [log $D_{(M)}$] against the logarithm of the ligand concentration (log[ligand]).[15] The extraction was carried out by taking a fixed amount of manganese in the presence of (a) a constant amount of Aliquat 336 and varying the concentration of BHA and (b) a constant amount of BHA and varying the concentration of Aliquat 336. In both instances the plot of log $D_{(M)}$ against log[ligand] gave straight lines with slopes of 3 and 1.7, respectively, which indicates that the composition of the complex is manganese : BHA = 1 : 3 and manganese : BHA : Aliquat 336 = 1 : 3 : 2.

It has already been seen that the complex formation is accompanied by a change in the oxidation state of the metal from +2 to +3. The anionic nature of the manganese complex necessitates the reaction with the enol form of the reagent. It has also been established[10,16] that in basic solution a considerable portion of the benzohydroxamic acid exists in the enol form of the two possible structures of the reagent molecule:

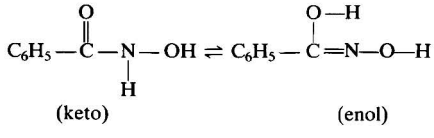

Therefore, the possible structure of the complex is

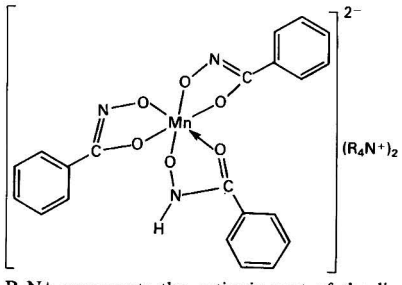

where R_4N^+ represents the cationic part of the liquid ion exchanger. The stoicheiometric proportion of 2 parts of the liquid ion exchanger in the complex shows that there are only two negative charges on the 1 : 3 manganese - BHA complex. This can be explained by assuming that of the three molecules of the reagent reacting with the metal ion, two are in the enol form and one is in the keto form, leaving behind two negative charges on the metal complex, which will form a neutral ion pair by taking up two cationic parts of the liquid ion exchanger.

The stability constant of the complex determined by the spectrophotometric method[17] was 1.175×10^8.

Stripping

After extraction of the manganese into the organic phase, it was stripped with 15 ml of varying concentrations (0.05–5 M) of sulphuric acid, hydrochloric acid, nitric acid, sodium sulphate, sodium chloride, sodium carbonate and sodium hydroxide solutions. The stripping was complete with 0.25 M hydrochloric acid. The metal constant was determined photometrically using PAR.[13]

Effects of Diverse Ions

Manganese was extracted and separated in the presence of a large number of different ions (Table 4). Interference studies were made by measuring the absorbances of the liquid ion exchanger phase and conditions were established for the removal of interfering ions from the organic phase by eluting with suitable solvents. The tolerance limit was set as the amount of foreign ion causing a change in absorbance of ±0.02 unit or ±2% error in the recovery of manganese. Moderate amounts of various metal ions commonly associated with manganese were tolerated, and also most anions. Common anions such as nitrate, chloride, sulphate, acetate, carbonate, thiocyanate, iodide and thiosulphate will not interfere even at very high concentrations, whereas fluoride and cyanide show some interference at higher concentrations (> 5 mg). Up to 20-fold concentrations of zinc and aluminium can be tolerated as their metal hydroxides are soluble in an excess of ammonia. The interference caused by Cu^{2+}, Ni^{2+}, Co^{2+} and Ag^{+} can be masked with 0.1% sodium cyanide solution. A 0.5% solution of potassium iodide can be used to mask Cd^{2+}, Hg^{2+} and Pb^{2+}. Fe^{3+} interferes owing to the precipitation of hydrous iron(III) oxide. This can be overcome by a single selective extraction of Fe^{3+} from 6 M hydrochloric acid with an equal volume of diethyl ether saturated with water prior to the determination of manganese. The interfering ions Fe^{3+}, Co^{2+} and Cu^{2+} can be separated simultaneously from Mn^{2+} by an ion-exchange technique. The separation is effected by the absorption of these ions on Dowex 50W-X8 from 6 M hydrochloric acid, which retains iron, cobalt and copper on the resin column. The effluent contains only manganese and is evaporated to dryness and made alkaline with ammonia solution for further analysis. This method of separation will be extremely useful for the analysis of manganese in standard samples of steel and bronze in which the major constituents are a combination of the above metals in varying proportions.

In certain instances interfering ions can be removed by selective stripping before the recovery of manganese. Thus vanadium, extracted together with manganese, can be stripped first by shaking the organic phase with 10 ml of 0.2 M sodium acetate solution for 5 min. Manganese is subsequently stripped with 0.25 M hydrochloric acid. The extracted molybdenum can be removed by washing the organic phase with 5 ml of 0.2 M sodium chloride solution before the separation of manganese. Uranium can also be separated from manganese by stripping with 5 ml of 0.1 M ammonia solution and manganese can be recovered with 10 ml of 0.25 M hydrochloric acid.

The method is sensitive and reasonably selective. All the interfering ions can either be masked or eluted selectively. The serious interference from iron can also be easily overcome. The interference from iron, cobalt and copper can be easily removed by a simple ion-exchange technique, which makes the method suitable for the analysis of steel and bronze.

Determination of Manganese in Standard Samples

Manganese alloy and ore samples were digested with a mixture of concentrated HNO_3 + $HClO_4$ (1 + 3) and evaporated. The semi-solid mass was heated with concentrated HCl, centrifuged and finally diluted to 250 ml with 0.1 M HCl. An aliquot of this solution was taken and analysed for manganese by the proposed method, and the results are given in Table 5.

We are indebted to UGC, New Delhi, for awarding a Research Associateship to one of us (S. K. M.).

References

1. Green, H., *Talanta*, 1964, **11**, 1561.
2. Asha, R. P., and Khopkar, S. M., *J. Sci. Ind. Res.*, 1971, **30**, 16.
3. Green, H., *Talanta*, 1973, **20**, 139.
4. Moore, F. L., *Environ. Sci. Technol.*, 1972, **6**, 525.
5. McDonald, C. W., and Moore, F. L., *Anal. Chem.*, 1973, **45**, 983.
6. Menon, S. K., and Agrawal, Y. K., *Analyst*, 1984, **109**, 27.
7. Agrawal, Y. K., and Patel, S. A., *Rev. Anal. Chem.*, 1980, **4**, 237.
8. Agrawal, Y. K., *Rev. Anal. Chem.*, 1980, **5**, 3.
9. Dutta, R. L., *J. Indian Chem. Soc.*, 1957, **34**, 311.
10. Dwight, O. M., and John, H. Y., *Talanta*, 1960, **7**, 107.
11. Hauser, E. R., and Renfrow, W. B., Jr., "Organic Synthesis," Wiley, New York, 1944, p. 7.
12. Welcher, F. J., "The Analytical Uses of Ethylenediaminetetraacetic Acid," Van Nostrand, Princeton, NJ, 1958, p. 220.
13. Ahrland, S., and Herman, R. G., *Anal. Chem.*, 1957, **47**, 2422.
14. Ringbom, A., *Fresenius Z. Anal. Chem.*, 1949, **21**, 332.
15. Yoe, J. H., and Jones, A. L., *Ind. Eng. Chem., Anal. Ed.*, 1944, **16**, 111.
16. Plapinger, R. E., *J. Org. Chem.*, 1959, **24**, 802.
17. Harvey, A. E., and Manning, D. L., *J. Am. Chem. Soc.*, 1950, **72**, 4488.

Paper A4/386
Received November 7th, 1984
Accepted September 25th, 1985

Synthetic Inorganic Ion-exchange Materials

Part XLII.* Ion-exchange Selectivity of Divalent Transition Metals and Lead on Titanium Antimonate and Some Chromatographic Separations

R. Chitrakar and M. Abe†
Department of Chemistry, Facultry of Science, Tokyo Institute of Technology, 2-12-1, Ookayama, Meguro-Ku, Tokyo 152, Japan

The equilibrium distribution coefficients of divalent transition metals and lead have been determined on a titanium antimonate (TiSbA) cation exchanger. The selectivity sequence Mn(II) < Ni(II) < Cd(II) < Zn(II) < Co(II) < Cu(II) < Fe(II) < Pb(II) was established for divalent metal ions (10^{-4} M) on TiSbA with different Ti to Sb molar ratios in nitric acid media. Useful separations of lead from transition metals and alkaline earth metals using relatively small columns of TiSbA are discussed.

Keywords: *Titanium antimonate; ion exchanger; chromatographic separation; transition metals; lead*

Many useful inorganic ion-exchange materials have been synthesised during the last two decades that have found many applications in areas of analytical chemistry, radiochemistry, environmental chemistry and biochemistry.[1] Inorganic ion exchangers possessing high selectivities for certain ions or groups of ions[2-5] can be utilised for chromatographic separations of elements. Most investigations with insoluble acid salts of quadrivalent metals have been carried out on zirconium and titanium phoshates of various types.[1] Quadrivalent metal antimonate ion exchangers were studied first by Abe and Ito.[6] Tin(IV) and titanium(IV) antimonates (SnSbA and TiSbA) behaved as cation exchangers with relatively high capacity, and showed unusual selectivities for alkali metal ions in the order Na < K < Rb < Cs ≪ Li on SnSbA,[7] and Na < K < Rb < Li < Cs on TiSbA,[8] while the usual selectivity for alkaline earth metal ions was observed on both exchangers. SnSbA, having a specific selectivity for the lithium ion, has proved a promising ion-exchange material for the selective separation of lithium from sea water.[9]

This paper describes adsorption and chromatographic separations of some divalent transition metals and lead on TiSbA with different Ti to Sb molar ratios. The chromatographic separations of alkaline earth metals from some transition metals and lead are also discussed.

Experimental

Reagents

Antimony pentachloride (Yotsuhata Chemical Co., Japan) and titanium tetrachloride (Wako Chemical Co., Japan) of high purity (> 99% as metal) were used without further purification. Standard solutions of transition metals and lead were prepared by dissolving metals of high purity (> 99.9%) in a minimum amount of nitric acid. For Fe(II) adsorption experiments, all reagents were prepared with nitrogen gas bubbling. Iron(II) nitrate solution was obtained by passing iron(II) sulphate solution through a column of Dowex-1 anion exchanger in the nitrate form in a nitrogen gas atmosphere.

Preparation of TiSbA

Titanium antimonate was synthesised as described previously.[8] A 4 M antimony pentachloride solution was mixed with 4 M titanium tetrachloride solution at different Ti to Sb molar ratios of 60 °C. The mixed solutions (40 ml) were immediately hydrolysed in 960 ml of de-mineralised water at the same temperature. The precipitate obtained was kept in the mother liquor overnight, filtered and washed with cold de-mineralised water using a centrifuge operated at 1000 rev min^{-1} until the pH of the supernatant solution was higher than 1.5. The product obtained was dried at 60 °C for 4 d, ground and sieved to 100–200 mesh and the samples were washed with cold de-mineralised water in order to remove fine adherent particles and conditioned with 1 M HNO_3 until free from Cl^- and Na^+ ions. Finally, the samples were re-washed with de-mineralised water and air dried.

Characterisation of TiSbA

The determination of antimony and titanium by X-ray diffraction and thermal analysis were carried out as described previously.[8]

Distribution Coefficients

The values of the distribution coefficients (K_d) of several metals ions were determined as follows: 0.10 g of TiSbA was equilibrated with 10.0 ml of solution containing 10^{-4} M metal ions in different concentrations of nitric acid with intermittent shaking at 30 °C. The concentrations of metal ions in the solid

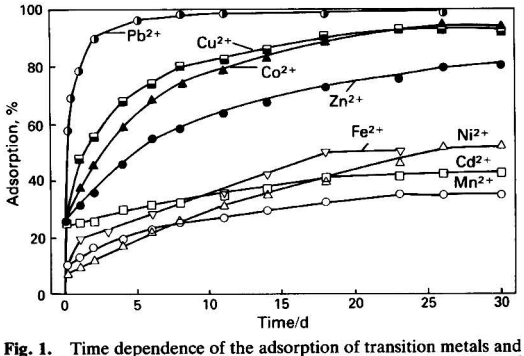

Fig. 1. Time dependence of the adsorption of transition metals and lead on TiSbA. TiSbA (Ti : Sb = 1.6), 0.25 g; initial concentration of metal ions, 10^{-4} M; total volume, 25.0 ml; temperature, 30 ± 0.5 °C; concentration of HNO_3, 0.07 M for Mn(II), Ni(II) and Co(II), 0.1 M for Cu(II), Zn(II) and Cd(II) and 1 M for Pb(II) and Fe(II)

* For Part XLI of this series, see Abe, M., and Furuki, N., *Solvent Extr. Ion Exchange*, in the press.

† To whom correspondence should be addressed.

and the liquid phases were deduced from the concentration relative to the initial concentration in the solution. The K_d values were calculated at equilibrium using the following equation:

$$K_d = \frac{\text{Amount of metal ions in exchanger}}{\text{Amount of metal ions in solution}} \times \frac{\text{Volume of solution (ml)}}{\text{Mass of exchanger (g)}}$$

The concentrations of metal ions were determined by using a Varian Techtron 1100 atomic absorption spectrometer.

Results and Discussion

Characterisation of TiSbA

Among various preparations, titanium antimonates with Ti to Sb molar ratios of 1.1, 1.6, 2.1 and 2.8 were synthesised. The X-ray diffraction and the thermal analysis of all the samples were examined, the results obtained being in good agreement with previous work.[8]

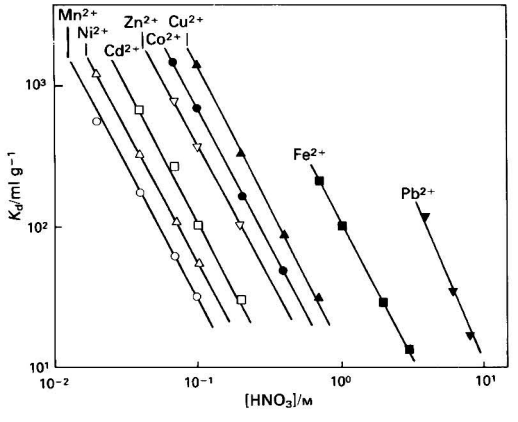

Fig. 2. Distribution coefficients (K_d) of transition metals and lead on TiSbA as a function of concentration of HNO_3. TiSbA (Ti : Sb = 1.6), 0.10 g; initial concentration of metal ions, 10^{-4} M; total volume, 10.0 ml; temperature, 30 ± 0.5 °C

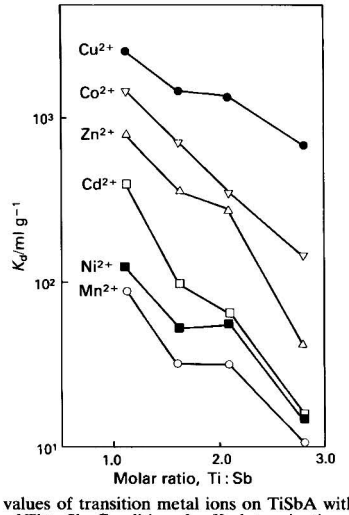

Fig. 3. K_d values of transition metal ions on TiSbA with different molar ratios of Ti to Sb. Conditions for K_d determination as in Fig. 2

Ion-exchange Selectivity

The time dependence of the adsorption of divalent metal ions on TiSbA in nitric acid was measured qualitatively in order to determine the equilibrium distribution coefficients. The time required to attain equilibrium varied among the metal ions studied (Fig. 1). For lithium and caesium ions studied on TiSbA,[8] slow rates of adsorption were also reported. Slow rates of adsorption for divalent transition metal ions were also observed on SnSbA.[10] When reagents prepared without bubbling nitrogen gas through were used in the Fe(II) adsorption experiment, TiSbA (white granules) changed to dark grey; this characteristic dark grey of the SnO_2 exchanger was also noted in Fe(II) sorption experiments.[11,12] However, the dark grey colour of TiSbA was not observed when reagents prepared with nitrogen gas bubbling were used.

After equilibration, log K_d values of metal ions were plotted against log[HNO_3]. A linear relationship with a slope of −2 was obtained for all metal ions studied at different Ti to Sb molar ratios, the result using a Ti to Sb ratio of 1.6 being shown in Fig. 2. This indicated that the adsorption of metal ions on TiSbA proceeded via an ideal ion-exchange mechanism. The selectivity series Mn < Ni < Cd < Co < Zn < Cu < Fe < Pb was established for 10^{-4} M concentrations of divalent metal ions on TiSbA at different Ti to Sb molar ratios in nitric acid. The K_d values of transition metal ions in 0.1 M HNO_3

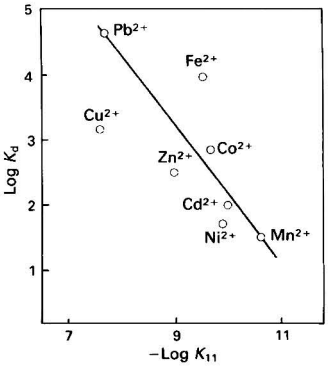

Fig. 4. Plot of log K_d against first hydrolysis constant of cations[18]

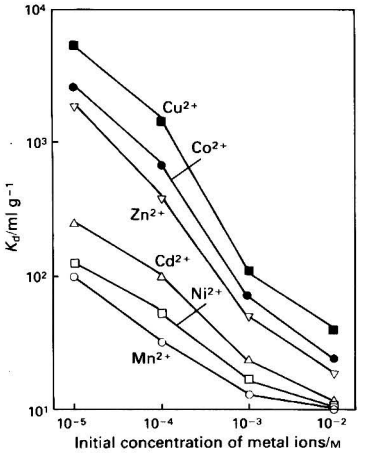

Fig. 5. K_d values of transition metal ions at different concentrations of metal ions. TiSbA (Ti : Sb = 1.6), 0.10 g; total volume, 10.0 ml; HNO_3 concentration, 0.1 M; temperature, 30 ± 0.5 °C

Table 1. Distribution coefficients, K_d, and separation factors, α,* for divalent transition metals and lead on TiSbA and Bio-Rad AG50W-X8[19]

TiSbA

HNO_3/M	Ti:Sb ratio	Parameter	Mn	Ni	Cd	Zn	Co	Cu	Fe†	Pb†
0.1	1.17	K_d	89.1	118.2	396.5	781.1	1392.5	2683.2	117	>10⁴
		α	1.3	3.3	1.9	1.7	1.9			
	1.63	K_d	33.3	53.1	100.0	355.8	699.5	1472.8	93	>10⁴
		α	1.6	1.8	3.5	1.9	2.1			
	2.17	K_d	30.1	60.6	66.2	275.8	346.6	1470.5	131	280
		α	2.0	1.0	4.1	1.2	4.2			
	2.79	K_d	10.1	14.3	14.7	114.3	140.6	681.3	75	140
		α	1.4	1.0	7.7	1.2	4.8			

Bio-Rad AG50W-X8

HNO_3/M	Parameter	Zn	Cu	Ni	Mn	Co	Cd	Pb†
0.1	K_d	1020	1080	1140	1240	1260	1500	35.7
	α	1.05	1.05	1.08	1.01	1.19		

* α is defined by K_d^A/K_d^B.
† K_d value at 1 M HNO_3.

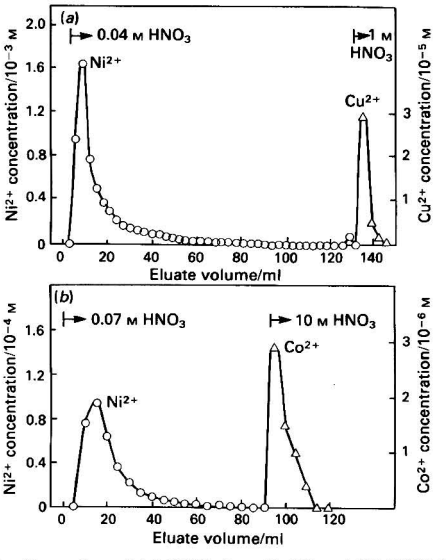

Fig. 6. Separation of (*a*) Ni(II) from Cu(II) and (*b*) Ni(II) from Co(II) with TiSbA using nitric acid. (*a*) Loading, 20 μmol for Ni(II) and 0.2 μmol for Cu(II); flow-rate, 0.20 ml min^{-1}. (*b*) Loading, 2 μmol for Ni(II) and 0.02 μmol for Co(II); flow-rate, 0.15 ml min^{-1}

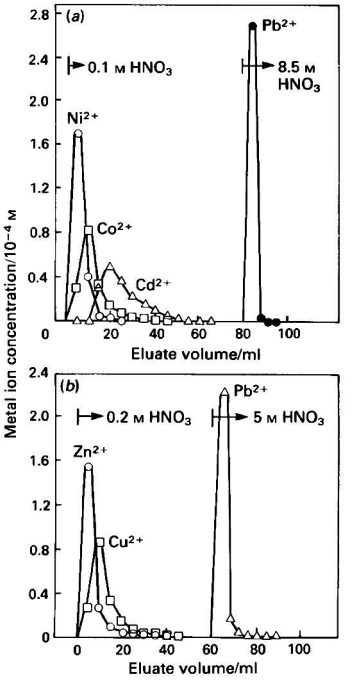

Fig. 7. Separation of (*a*) Ni(II), Co(II) and Cd(II) from Pb(II) and (*b*) Zn(II) and Cu(II) from Pb(II) with a TiSbA column. Pre-treatment of the column: (*a*) 0.1 M HNO_3 and (*b*) 0.2 M HNO_3; loading, 1 μmol of each of metal ion; flow-rate, 0.2 ml min^{-1}

were plotted against the Ti to Sb molar ratios (Fig. 3), the K_d values of Fe(II) and Pb(II) not being included because these metal ions were completely adsorbed in 0.1 M HNO_3. The metal ions showed high K_d values at a Ti to Sb ratio of 1.1 and the values decreased with an increase in the Ti to Sb molar ratio. The exchangeable protons in TiSbA decreased with an increase in the Ti to Sb ratio, causing decreased K_d values of metal ions.

Some inorganic ion exchangers such as C–SbA[1] or MnO_2[13] show size preference selectivity for ions having specific ionic radii, but no such correlation was found between the K_d values and effective ionic radii[14] of metal ions studied on TiSbA. It is known that most ion exchangers exhibit a general selectivity sequence between members of four groups of ions, *i.e.*, polyvalent metals > divalent transition metals > alkaline earth metals > alkali metals.[15] This behaviour is not shown by the insoluble salts of inorganic acids, *e.g.*, zirconium and tin phosphate gels, which exhibit considerable overlap in the selectivity between three groups of the ions.[15] The selectivities of the α- and θ-zirconium phosphates[16,17] for transition metal ions have been reported to be in the order Ni < Co < Mn < Zn < Cu. A slightly different selectivity order was observed on TiSbA at any Ti to Sb molar ratio. The log K_d values of transition metal and lead ions on TiSbA were plotted against the first hydrolysis constants of cations (Fig. 4).[18] The results showed a good correlation except for Fe(II) and Cu(II).

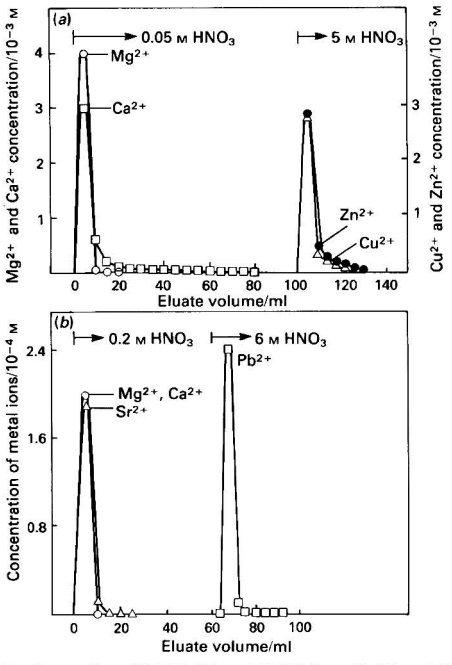

Fig. 8. Separation of (*a*) Mg(II) and Ca(II) from Zn(II) and Cu(II) and (*b*) Mg(II), Ca(II) and Sr(II) from Pb(II) with a TiSbA column. (*a*) Loading, 20 μmol each of Mg(II) and Ca(II), 1 μmol of each of Zn(II) and Cu(II); (*b*) loading, 1 μmol of each metal ion; flow-rate, 0.20 ml min^{-1}; column pre-treated with 0.2 M HNO_3

The distribution coefficients, K_d, and separation factors, α, of metal ions studied on TiSbA at different Ti to Sb ratios are given in Table 1, the values obtained on Bio-Rad AG50W-X8[19] being included for comparison. The separation factors between neighbouring pairs of metal ions on TiSbA are larger than those observed on the organic resins, which show very similar K_d values in nitric or perchloric acid. The separation factor of Pb(II) and the first transition metal ions on resin shows a large value (*ca.* 5) for a low concentration of acid and decreases with increasing concentration (*ca.* 2 in 4 M acid). An improved separation factor was observed between lead and transition metals on Dowex 50W-X8 cation-exchange resin by complex formation with HCl or HBr.[20,21] The separation of Pb(II) from other elements was achieved with 0.6 M HBr on a heated column, which prevented the precipitation of lead bromide.[20,21] The distribution coefficient, K_d, of Pb(II) on Bio-Rad AG50W-X8 is low in hydrochloric acid - acetone, which makes the method less suitable for the separation of small amounts of lead from large amounts of other elements.[22]

An improved separation factor was also obtained on the resin in perchloric acid media and lead could be separated from other metals in 2 M $HClO_4$.[23] Further, a good separation is possible by eluting Pb(II) with 0.5 M HBr in 40% acetone while Zn(II), Cu(II) and Ni(II) are strongly retained on the resin.[24]

The anion-exchange behaviour of bromide complex-forming elements in nitric acid - hydrobromic acid showed that lead could be separated from other elements by preferential elution with HNO_3 - HBr eluent.[25–27]

Some inorganic ion exchangers, *e.g.*, thorium phosphate[28] and cerium phosphate,[29] showed high selectivity for lead. Although lead could be separated from other elements, a long tailing effect could be observed on elution.[28]

On organic ion exchangers, the K_d values of metal ions are usually constant at concentrations below 1 mM at a constant acid concentration. As TiSbA with a Ti to Sb ratio of 1.6 showed a slightly high separation factor between some pairs of metal ions, the concentration dependence of K_d values on the concentration of metal ion on TiSbA was studied at a Ti to Sb ratio of 1.6 in 0.1 M HNO_3. The results are shown in Fig. 5. It was apparent that K_d values of Cu(II), Co(II) and Zn(II) increased considerably compared with those of Mn(II), Ni(II) and Cd(II) at low metal ion loadings. Such a concentration dependence of the K_d values of divalent transition metal ions has also been reported on An-HTDO.[30]

Chromatographic Separation

It is evident from the K_d values that the separation of microamounts of Co(II), Zn(II) and Cu(II) from macro-amounts of Mn(II) and Ni(II) can be achieved on a TiSbA column without the use of a complexing agent. Relatively small columns (2 cm × 0.5 cm i.d.) containing TiSbA (100–200 mesh) with a Ti to Sb ratio of 1.6 were used throughout. A 2-μmol amount of each of Mn(II), Ni(II), Cd(II), Zn(II), Co(II) and Cu(II) were loaded on top of the column and the elution was carried out immediately using nitric acid of different concentrations. The order of elution of metal ions did not coincide with the equilibrium distribution coefficients because Co(II) and Zn(II) could be detected before Cd(II). Such a difference was considered to be due to the slower adsorption process of Co(II) and Zn(II) than Cd(II) on TiSbA. The elution peaks of Mn(II) and Ni(II) were sharp; however, long tails were observed for Cd(II), Zn(II), Co(II), Cd(II) and Zn(II) and the yields were quantitative with incomplete separation. An attempt was made to separate Cu(II) from Mn(II), Ni(II), Co(II), Cd(II) and Zn(II) at lower column loadings and by decreasing the concentration of nitric acid. Although Cu(II) was separated from other metal ions, tailing during elution and low elution yields were encountered. Such behaviour was also reported on an SnO_2 column during an elution experiment with transition metal ions.[12] Low yields were considered to be due to the strong retention of cations to the exchanger particle during the time between feeding and elution periods. The respective yields were 88, 87, 36, 50, 49 and 58% for Mn(II), Ni(II), Cd(II), Zn(II), Co(II) and Cu(II). Coloration of the column during the loading of the metal ions and the elution periods was not observed.

From the elution curve, it seems possible to separate micro-amounts of Co(II) and Cu(II) from macro-amounts of Mn(II) and Ni(II). A 20-μmol amount of Ni(II) and a 0.2-μmol amount of Cu(II) were loaded on to the column and the elutions were carried out with nitric acid. Ni(II) was separated from Cu(II), the respective yields being 99 and 70% [Fig. 6(*a*)]. A similar elution behaviour was observed for the Ni(II) - Co(II) separation with 99% recovery for both metal ions [Fig. 6(*b*)]. The separation of Ni(II) - Cu(II) and Ni(II) - Co(II) can be utilised in Ni - Cu base alloys and steel, where trace amounts of cobalt and copper should be removed.

As the TiSbA showed extremely high selectivity for Pb(II), the separation of Pb(II) from divalent transition metal ions was carried out. The tailing observed for some transition metals in the column experiments could be reduced to some extent if the TiSbA column was pre-treated with dilute nitric acid. Improved recovery for these metal ions was observed with a yield higher than 99%. For separation of Pb(II) from Ni(II), Cd(II) and Co(II), the column was pre-treated with 0.1 M HNO_3 and the metal ions were then eluted with nitric acid of different concentrations [Fig. 7(*a*)]. For separation of Pb(II) from Zn(II) and Cu(II), the exchanger was pre-treated with 0.2 M HNO_3 and the elution was carried out [Fig. 7(*b*)], the yields being 99% for all metal ions. It could be concluded that better yields for transition metal ions could be achieved by pre-treatment of the TiSbA column with dilute nitric acid.

The TiSbA exchanger showed low affinity for alkaline earth metals[8] compared with Zn(II), Co(II) and Cu(II). The separation of micro-amounts of Zn(II) and Cu(II) from macro-amounts of Mg(II), Ca(II) and Sr(II) on a pre-treated column was performed [Fig. 8(*a*)]. Sharp elution peaks were observed with 99% recovery for all metal ions. Separation of Pb(II) from Mg(II), Ca(II) and Sr(II) was achieved with a l-μmol loading of each metal ion [Fig. 8(*b*)] and recoveries were 99% for all the metal ions.

In summary, TiSbA can be utilised for the separation of trace amounts of transition metals from salt solutions of alkaline earth metals. The chromatographic separation can be utilised for the determination of lead in a wide variety of minerals and materials.

References

1. Clearfield, A., *Editor*, "Inorganic Ion Exchange Materials," CRC Press, Boca Raton, FL, 1982.
2. Veselý, V., and Pakárek, V., *Talanta*, 1972, **19**, 219.
3. Abe, M., and Ito, T., *Bull. Chem. Soc. Jpn.*, 1967, **40**, 1013.
4. Abe, M., and Uno, K., *Sep. Sci. Technol.*, 1979, **14**, 355.
5. Abe, M., and Kasai, K., *Sep. Sci. Technol.*, 1979, **14**, 895.
6. Abe, M., and Ito, T., *Kagaku Zasshi*, 1967, **70**, 440.
7. Abe, M., and Hayashi, K., *Solvent Extr. Ion Exchange*, 1983, **1**, 97.
8. Abe, M., Chitrakar, R., Tsuji, M., and Fukumoto, K., *Solvent Extr. Ion Exchange*, 1985, **3**, 149.
9. Abe, M., and Hayashi, K., *Hydrometallurgy*, 1984, **12**, 83.
10. Abe, M., and Furuki, N., *Bull. Chem. Soc. Jpn.*, 1985, **58**, 1812.
11. Donaldson, J. D., and Fuller, M. J., *J. Inorg. Nucl. Chem.*, 1968, **30**, 1083.
12. Donaldson, J. D., Fuller, M. J., and Price, J. M., *J. Inorg. Nucl. Chem.*, 1968, **30**, 2841.
13. Tsuji, M., and Abe, M., *Solvent Extr. Ion Exchange*, 1984, **2**, 253.
14. Shannon, R. D., and Prewitt, C. T., *Acta Crystallogr., Sect. B*, 1969, **25**, 925.
15. Fuller, M. J., *Chromatogr. Rev.*, 1971, **14**, 45.
16. Clearfield, A., and Kalnins, J. M., *J. Inorg. Nucl. Chem.*, 1976, **38**, 849.
17. Allulli, S., Ferragina, C., La Ginestra, A., Massicci, M. A., and Tomassini N., *J. Chem. Soc., Dalton Trans.*, 1977, 1880.
18. Baes, C. F., Jr., and Mesmer, R. E., "The Hydrolysis of Cations," Wiley, New York, 1971.
19. Strelow, F. W. E., Rethemeyer, R., and Bothma, C. J. C., *Anal. Chem.*, 1965, **37**, 106.
20. Fritz, J. S., and Garralda, B. B., *Anal. Chem.*, 1962, **34**, 102.
21. Fritz, J. S., and Greene, R. G., *Anal. Chem.*, 1963, **35**, 811.
22. Strelow, F. W. E., Victor, A. H., Van Zyl, C. R., and Eloff, C., *Anal. Chem.*, 1971, **43**, 870.
23. Strelow, F. W. E., and Sondorp, H., *Talanta*, 1972, **19**, 1113.
24. Strelow, F. W. E., Hanekom, M. D., Victor, A. H., and Eloff, C., *Anal. Chim. Acta*, 1975, **76**, 377.
25. Strelow, F. W. E., and Toerien, F. Von S., *Anal. Chem.*, 1966, **38**, 545.
26. Strelow, F. W. E., *Anal. Chem.*, 1978, **50**, 1359.
27. Strelow, F. W. E., *Anal. Chim. Acta*, 1978, **100**, 577.
28. De, A. K., and Chowdhury, K., *J. Chromatogr.*, 1974, **101**, 73.
29. Alberti, G., Casciola, M., Costantino, U., and Luciani, M. L., *J. Chromatogr.*, 1976, **128**, 289.
30. Abe, M., Tsuji, M., Qureshi, S. P., and Uchikoshi, H., *Chromatographia*, 1980, **13**, 628.

Paper A5/253
Received July 15th, 1985
Accepted November 10th, 1985

Determination of Inorganic and Organomercury Compounds by High-performance Liquid Chromatography - Inductively Coupled Plasma Emission Spectrometry with Cold Vapour Generation

Ira S. Krull* and D. S. Bushee
Barnett Institute of Chemical Analysis and Department of Chemistry, Northeastern University, 360 Huntington Avenue, Boston, MA 02115, USA

and R. G. Schleicher and S. B. Smith, Jr.
Allied Analytical Systems, 590 Lincoln Street, Waltham, MA 02254, USA

An inductively coupled plasma (ICP) emission spectrometer was used as a high-performance liquid chromatographic detector for the determination of mercury compounds. Post-column cold vapour generation was used to obtain improved detection limits. The replacement of the conventional polypropylene spray chamber of the ICP by an all glass chamber is described. A comparison of band broadening indicates that the glass chamber is useful when a severe memory effect is observed with the polypropylene spray chamber. Detection limits ranged from 32 to 62 p.p.b. of mercury for four mercury compounds, based on a signal to noise ratio of 2 : 1. This represents a three to four order of magnitude enhancement over detection limits obtained without cold vapour generation. The approach is linear over three orders of magnitude. A blind, spiked distilled water study illustrates the reproducibility and accuracy of the method.

Keywords: *Mercury determination; high-performance liquid chromatography; inductively coupled plasma; cold vapour generation*

The most common method of mercury speciation in use today is gas chromatography followed by electron-capture detection (GC-ECD). The poor selectivity of the ECD to organomercury species and the time-consuming and elaborate clean-up procedures necessary prior to injection of many samples indicates the need for a simple, more selective approach for the analysis of organomercury and inorganic mercury species.[1,2] Selectivity in gas-chromatographic analysis has been improved by using atomic-absorption and microwave plasma emission detectors.[3-6]

The use of high-performance liquid chromatography (HPLC) for mercury speciation has the advantage of simplified sample preparation. In GC-ECD analysis it is essential to form strong, thermally stable derivatives, whereas it is not necessary to derivatise samples prior to analysis by HPLC.[7] The combination of HPLC with spectroscopic detection provides a simple and selective method of metal speciation.[8-15] In order to obtain practical detection limits with these detectors, it was often necessary to generate a more volatile form of the metal of interest. For mercury, this was carried out by forming the cold vapour derivative of the compounds as they eluted from the HPLC column. Previous reports described relatively complex apparatus for the interface between the HPLC column and the atomic-absorption detector.[8,10] In this paper, a simple interface between an HPLC system and an inductively coupled plasma emission spectroscopic detector is described for the speciation of inorganic and organometallic mercury compounds.

Experimental

Apparatus and Operating Conditions

The chromatographic system consisted of two Laboratory Data Control (LDC) (Riviera Beach, FL, USA) Constametric III pumps with a gradient controller and a Rheodyne Model 7125 injection valve (Rheodyne Corp., Cotati, CA, USA) fitted with a 200-μl loop. The separation[7] was performed on two Waters Resolve columns (Waters Assoc., Milford, MA, USA), 5 μm C_{18} stationary phase, 15 cm × 3.9 mm i.d. placed in series with a mobile phase consisting of 0.06 M ammonium acetate and 0.005% *V/V* 2-mercaptoethanol with a gradient from 15 to 75% of acetonitrile. A flow-rate of 1.0 ml min^{-1} was used for all analyses. The post-column reaction system has been described previously[12] and is shown schematically in Fig. 1. An aqueous solution of 0.5% *m/V* sodium tetrahydroborate(III) in 0.25 M sodium hydroxide solution and a 1.2 M solution of hydrochloric acid served as the two reagents. The reagent flow-rates were 0.5 ml min^{-1}.

An Instrumentation Laboratory Model 200 plasma (Allied Analytical Systems, Waltham, MA, USA), modified for autotune operation, was used to monitor the HPLC effluent at a wavelength of 253.7 nm. The polypropylene nebuliser - spray chamber of the ICP showed a significant memory effect for mercury.[16] An all-glass chamber (Fig. 2) was developed, which replaced the polypropylene nebuliser - spray chamber completely. A short length of 1/16-in Teflon tubing was inserted into each arm. Inlet A of the chamber was used to introduce an argon purge gas at a flow-rate of 0.4 l min^{-1}. For optimum performance, the end of the Teflon tubing was turned upwards to direct the gas towards the plasma torch. The tubing was held in place by the walls of the chamber. The inlet B of the chamber served to introduce the HPLC effluent. The Teflon tube in this arm extended about 1 cm below the

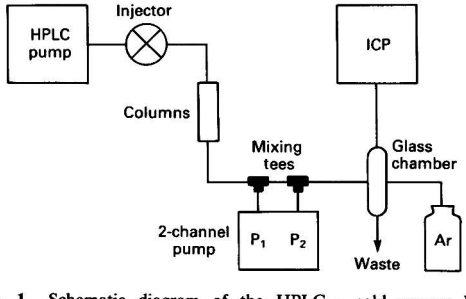

Fig. 1. Schematic diagram of the HPLC - cold vapour ICP instrumentation

* To whom correspondence should be addressed.

glass tube, to prevent the gaseous effluent from travelling back up the glass arm. Just prior to the glass chamber, the effluent had passed through the post-column reactor and was in the form of a gaseous mixture. The mercury compounds, now in their cold vapour form, were swept up into the plasma with the purge gas, by way of outlet C. The chamber was connected to the plasma by means of a short length of Tygon tubing. The aqueous mobile phase flowed to waste through the bottom of the chamber, outlet D. A drain trap was positioned directly below the glass chamber. The ICP peak-height response was monitored on a Honeywell Corp. (Minneapolis, MN) strip-chart recorder, and peak-area data were collected on a Radio Shack TRS-80 Model II computer (Tandy Corp., Fort Worth, TX, USA).

Determination of Cold Vapour Transfer Efficiency

Three aqueous solutions of methylmercury chloride, ethylmercury chloride and mercury(II) chloride (0.97, 0.87 and 1.88 p.p.m. of mercury, respectively) were pumped through the cold vapour generation interface into the ICP. Aliquots of 15 ml of waste were collected from the glass chamber after the signal had stabilised. The waste was collected in 30-ml graduated, plastic cups containing distilled water made basic by the addition of about 90 mg of sodium hydroxide. Three aliquots of waste were collected for each mercury solution, and blank samples were obtained by pumping mobile phase through the system between each mercury solution.

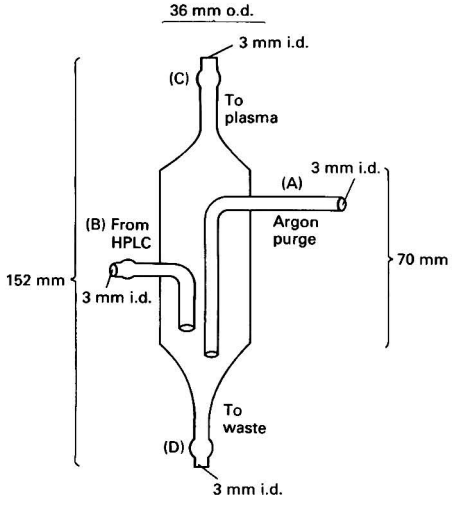

Fig. 2. Schematic diagram of glass sample introduction device

Each waste sample was transferred into a 50-ml plastic bottle and digested overnight with 0.5 ml of 5% potassium dichromate solution and 5 ml of water - hydrochloric acid - nitric acid (4 + 3 + 1). A standard solution of each mercury compound was prepared at the 100–200 p.p.b. of mercury level. The standard solutions of each mercury compound were treated in the same manner as the samples.

The digested waste samples were analysed by direct cold vapour ICP spectrometry using the conventional nebuliser spray chamber assembly. A reducing solution was prepared by adding 50 ml of concentrated sulphuric acid to about 300 ml of distilled water and cooling to room temperature. Sodium chloride (15 g), tin(II) chloride (25 g) and hydroxylammonium chloride (15 g) were then added, and the solution volume was brought to 500 ml with distilled water.[17] Both the sample and reducing solutions were introduced at a flow-rate of 1 ml min^{-1}.

Reagents

All reagents were of analytical-reagent grade and used without further purification. The mercury compounds and sodium tetrahydroborate(III) (98%) were obtained from Alfa Products (Danvers, MA, USA). Mercury standard solutions were prepared fresh daily and were stored in a dark, cool place when not in use. Mobile phase and sodium tetrahydroborate(III) solutions were filtered through 0.45-μm filters (Millipore Corp., Bedford, MA, USA).

Results and Discussion

Evaluation of Glass Chamber

A comparison of band broadening was made between the three sample introduction devices. The band broadening was calculated by the method of Foley and Dorsey.[18] It was not possible to detect mercury easily by flow injection analysis - ICP spectrometry with the conventional nebuliser in the absence of cold vapour generation. In order to include a value for the band broadening for all three devices, it was necessary to use arsenic as the model compound. Arsenic exhibited no substantial absorbance on to either the polypropylene or glass chambers. The conditions for the formation of arsine post-column were similar to those for the formation of the mercury cold vapour and have been described earlier.[12] The results of the flow injection analysis of a solution of 139 p.p.m. of arsenic as arsenite using each introduction device are summarised in Table 1. The conventional nebuliser with hydride generation produced a more symmetrical peak than either of the other configurations. The formation of a sharper peak with hydride generation compared with the response without post-column hydride generation can be explained by considering all open tubing after the hydride generation device as a gas-segmented, open-tubular reactor. The concept of segmentation in flowing streams with air or gas bubbles has been established as effectively suppressing dispersion of sample zones.[19] Of the two interfaces in the hydride formation mode,

Table 1. Band broadening and asymmetry in flow injection analysis (FIA) - ICP. Hydride generation conditions for arsenite: 4% sodium tetrahydroborate(III) solution and concentrated hydrochloric acid introduced at 0.5 ml min^{-1}

Interface	Band broadening* (μl^2)	Relative band broadening	Asymmetry factor*
FIA - ICP with polypropylene nebuliser	17768 ± 434	2.2	1.90 ± 0.08
FIA - hydride generation - ICP with polypropylene nebuliser	8160 ± 347	1.0	1.69 ± 0.06
FIA - hydride generation - ICP with glass chamber	12767 ± 482	1.6	1.8 ± 0.1

* Calculated by the method of Foley and Dorsey.[18] Numbers represent the average ± standard deviation for at least four injections with each interface.

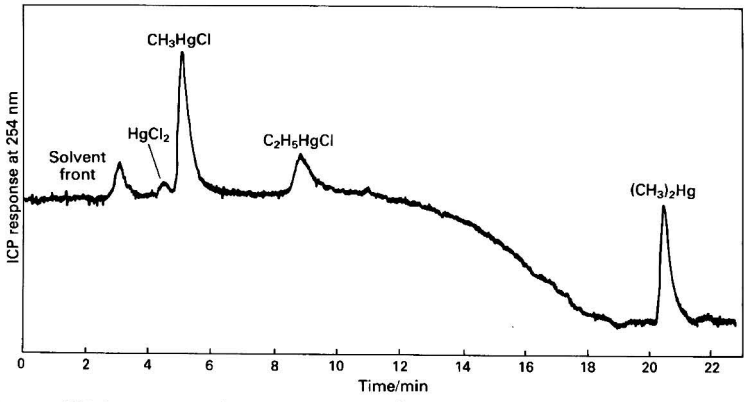

Fig. 3. HPLC - cold vapour ICP chromatogram of mercury species. HPLC on two Waters Resolve columns in series. Gradient elution using (A) 0.06 M ammonium acetate, 0.005% 2-mercaptoethanol; (B) 0.06 M ammonium acetate, 0.005% 2-mercaptoethanol and 75% acetonitrile. Initial [B] = 20%, final [B] = 100%; flow-rate, 1 ml min^{-1}; slope = 5; and injection volume, 200 µl

Table 2. Comparison of HPLC - cold vapour - ICP detection limits (p.p.b. of Hg) for sample introduction devices. Conditions as in Fig. 3

Compound	Conventional nebuliser interface		Glass chamber interface with cold vapour†
	No cold vapour	With cold vapour*	
CH_3HgCl	$>232 \times 10^3$	47 ± 4	37 ± 2
CH_3CH_2HgCl	$>302 \times 10^3$	74 ± 10	62 ± 10
$HgCl_2$	$>409 \times 10^3$	202 ± 30	35 ± 15
$(CH_3)_2Hg$	267 ± 30 p.p.b. Hg	267 ± 21	62 ± 37

* Numbers represent the average ± standard deviation for three injections.

† Numbers represent the average ± standard deviation for at least nine injections. Detection limit values were normalised based on a signal to noise ratio of 2 : 1.

the cross-flow nebuliser produced the least peak band broadening. This indicates that the conventional nebuliser would be satisfactory for most applications involving a post-column volatilisation reaction. The glass chamber interface need only be used when the possibility of strong absorption of analyte on to the walls of the polypropylene spray chamber exists, as with mercury.

Separation of Mercury Compounds

Fig. 3 illustrates the chromatographic separation of the four mercury compounds. The separation was complete in less than 20 min. If only dimethylmercury was of interest in a given sample, it would be possible to elute the dimethylmercury in a much shorter time by using an isocratic system consisting of 75% acetonitrile in the mobile phase. Under these conditions, dimethylmercury eluted in 4.5 min, while the other three mercury compounds eluted as a single peak in the solvent front (Fig. 4).

Detection Limits and Linear Range

The detection limits for the four mercury species were determined using the conventional cross-flow nebuliser without and with cold vapour generation, and also with the glass chamber with cold vapour generation. Detection limits were defined as the minimum concentration of mercury that gave a detector signal twice the peak-to-peak noise on the strip-chart recorder. These results are compared in Table 2. Using the cross-flow nebuliser without post-column cold vapour generation, the methylmercury chloride, ethylmercury chloride and mercury(II) chloride were not detected at or below the indicated levels. More concentrated solutions were not tested because of solubility problems and the extreme toxicity of these compounds at high levels. A three to four order of magnitude enhancement was observed in each instance.

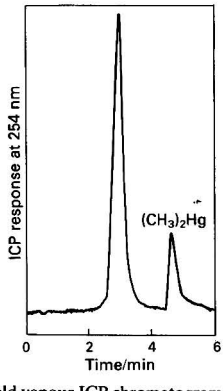

Fig. 4. HPLC - cold vapour ICP chromatogram of dimethylmercury with mercury(II) chloride, methylmercury chloride and ethylmercury chloride eluting in the solvent front. Isocratic mobile phase of 0.06 M ammonium acetate, 0.005% 2-mercaptoethanol and 75% acetonitrile. Other conditions as in Fig. 3

The detectability for dimethylmercury was increased by a factor of four by using post-column cold vapour generation with the glass chamber. The low detection limit observed with the conventional nebuliser was probably due to the inherent volatility of the dimethylmercury before derivatisation.

Calibration graphs for each of the mercury species were linear over three to four orders of magnitude, ranging from the detection limit to the mid-parts per million region. The correlation coefficients for these calibration graphs ranged from 0.9801 to 0.9995.

Stability in Aqueous Solution

The stability of the four mercury compounds in water was studied. Different combinations of the four compounds were dissolved in distilled water at known levels and the responses of these mixtures were compared with those of standards prepared separately. The results in Table 3 indicate that there was no significant interconversion between mercury(II) chloride, methylmercury chloride or ethylmercury chloride. Mixtures 4 and 5 were prepared with dimethylmercury in solution with one of the other mercury compounds. In each instance, the dimethylmercury was not completely recovered. Interconversion between the mercury compounds was clearly evident in mixture 6. The complete disappearance of the two mercury forms originally spiked in the mixture was observed, with the corresponding appearance of a peak for methylmercury chloride. The instability of the dimethylmercury, and its ready conversion into methylmercury chloride when in the presence of other mercury compounds in an aqueous system, led to its exclusion from the blind spiked distilled water study.

Spiked Water Analysis

A series of blind spiked, distilled water samples, with known concentrations of the mercury compounds, were studied by HPLC - cold vapour ICP spectrometry (Table 4). These results indicate a general agreement between the levels of mercury species spiked and the values determined. A linear regression analysis of these results and the actual spiked values gave correlation coefficients of 0.9440, 0.9971 and 0.9869 for mercury(II) chloride, methylmercury chloride and ethylmercury chloride, respectively. The correlation for mercury(II) chloride was not as good as that for the two organomercury species. This was due to the lack of base-line resolution between the mercury(II) chloride and the methylmercury chloride, and could be improved by further optimisation of the chromatographic conditions.

Table 3. Mercury interconversion in aqueous solutions

	Recovery,%†			
Mixture*	$HgCl_2$	CH_3HgCl	C_2H_5HgCl	$(CH_3)_2Hg$
1	96 ± 11	103 ± 4	99 ± 5	§
2	106 ± 11	112 ± 11	§	§
3	§	116 ± 6	107 ± 6	§
4	§	103 ± 3	§	54 ± 7
5	§	‡	77 ± 8	46 ± 6
6	0	‡	§	0

* Mixtures contained between 375 and 675 p.p.b. of mercury and were compared against single standards made up at the same concentration.

† Recovery was determined by HPLC - cold vapour ICP spectrometric analysis of the mixtures immediately following preparation. HPLC - cold vapour ICP conditions as in Fig. 3. Numbers are the average ± standard deviation for at least three injections of each mixture.

‡ Indicates the formation of methylmercury not initially present in the solution.

§ Indicates no addition of this mercury species to the mixture.

Conversion/Transfer Efficiency

The actual amount of derivatised analyte reaching the plasma was studied. All mercury in the waste samples was converted into the inorganic form and then reduced with the tin(II) chloride reagent solution. The concentration of mercury in the waste was determined by direct cold vapour ICP spectrometry as described under Experimental. The amount of mercury found in the waste consists of all the mercury not converted into the cold vapour form or swept into the ICP. All other mercury is assumed to have reached the plasma. The concentrations of mercury(II) chloride, methylmercury chloride and ethylmercury chloride reaching the plasma were 82 ± 2, 77.1 ± 0.5 and 79.3 ± 0.3, respectively. These values represent the mercury that was converted into the cold vapour form and that was transferred successfully to the plasma during HPLC - cold vapour ICP spectrometry, a combination of conversion efficiency and transfer efficiency.

Conclusion

A sample introduction method has been developed that provides for the rapid and direct speciation of low levels of mercury compounds in aqueous systems by HPLC - cold vapour ICP spectrometry. This approach could be used in a number of environmental, biological, industrial and toxicological applications.

We acknowledge the assistance of W. LaCourse, S. Colgan and M. Swartz of Northeastern University in the preparation of various spiked water samples. We appreciate the interest and encouragement of K. Panaro of the Boston District Food and Drug Administration. This work was supported by a research and development contract from Allied Analytical

Table 4. HPLC - cold vapour ICP of blind spiked distilled water. Conditions as in Fig. 3

Mixture No.	Hg species	Hg spiked, p.p.b.	Hg measured, p.p.b.*	Recovery, %*
1	$HgCl_2$	0	ND†	—‡
	CH_3HgCl	290	310 ± 20	107 ± 8
	CH_3CH_2HgCl	179	190 + 20	110 ± 10
2	$HgCl_2$	461	530 ± 60	120 ± 10
	CH_3HgCl	0	ND	—
	CH_3CH_2HgCl	303	290 ± 30	96 ± 9
3	$HgCl_2$	0	ND	—
	CH_3HgCl	572	610 ± 40	107 ± 7
	CH_3CH_2HgCl	242	270 ± 20	111 ± 8
4	$HgCl_2$	248	220 ± 40	90 ± 20
	CH_3HgCl	1090	1040 ± 50	95 ± 5
	CH_3CH_2HgCl	446	510 ± 30	114 ± 4
5	$HgCl_2$	419	380 ± 70	90 ± 20
	CH_3HgCl	537	570 ± 20	106 ± 3
	CH_3CH_2HgCl	0	0	—
6	$HgCl_2$	0	ND	—
	CH_3HgCl	767	780 ± 20	102 ± 2
	CH_3CH_2HgCl	575	580 ± 20	101 ± 3

* Numbers represent the average ± the standard deviation of a minimum of three injections of each mixture.

† ND = not detected.

‡ Indicates no addition of this mercury species to the mixture.

Systems to Northeastern University that allowed us to undertake and complete the work described. This is contribution number 262 from the Barnett Institute of Chemical Analysis and Materials Science at Northeastern University.

References

1. Rodriquez-Vazques, J. A., *Talanta*, 1978, **25**, 299.
2. Hight, S. C., and Capar, S. G., *J. Assoc. Off. Anal Chem.*, 1983, **66**, 1121.
3. Bye, R., and Paus, P. E., *Anal. Chim. Acta*, 1979, **107**, 169.
4. Talmi, Y., *Anal. Chim. Acta*, 1975, **74**, 107.
5. Bzezinska, A., Van Loon, J., Williams, D. Oguma, K., Fuwa, K., and Haraguchi, I. H., *Spectrochim. Acta, Part B*, 1983, **38**, 1339.
6. Sklarew, D. S., Olsen, K. B., and Evans, J. C., Paper presented at the 189th ACS National Meeting, Miami Beach, FL, April 28–May 3, 1965, ANAL. 61.
7. MacCrehan, W. A., and Durst, R. A., *Anal. Chem.*, 1978, **50**, 2108.
8. Holak, W., *Analyst*, 1982, **107**, 1457.
9. Holak, W., *J. Liq. Chromatogr.*, 1985, **8**, 563.
10. Fujita, M., and Takabatake, E., *Anal. Chem.*, 1983, **55**, 454.
11. Holak, W., "Innovative Techniques for the Analysis of Iodine and Methylmercury," 10th Annual Spring Training Workshop, AOAC, Dallas, TX, April 10, 1985.
12. Bushee, D., Krull, I. S., Demko, P., and Smith, S. B., Jr., *J. Liq. Chromatogr.*, 1984, **7**, 861.
13. Krull, I. S., *in* Lawrence, J. F., *Editor*, "Liquid Chromatography in Environmental Analysis," Humana Press, Clifton, NJ, 1984, Chapter 5.
14. Krull, I. S., Panaro, K. W., and Gershman, L. L. *J. Chromatogr. Sci.*, 1983, **21**, 460.
15. Krull, I. S., Bushee, D., Savage, R. N., Schleicher, R. G., and Smith, S. B., Jr., *Anal. Lett.*, 1982, **15A**, 267.
16. Kuldvere, A., *Analyst*, 1982, **107**, 179.
17. Holak, W., *J. Assoc. Off. Anal. Chem.*, 1983 **66**, 1203.
18. Foley, J. P., and Dorsey, J. G., *Anal. Chem.*, 1983, **55**, 730.
19. Frei, R. W., *in* Frei, R. W., and Lawrence, J. F., *Editors*, "Chemical Derivatization in Analytical Chemistry," Volume 1, Plenum Press, New York, 1981, Chapter 4.

Paper A5/226
Received June 24th, 1985
Accepted August 27th, 1985

Examination of Metallochromic Indicators and Water-soluble Reagents for Metals by Planar Electrophoresis

Marie M. Ferris and Michael A. Leonard
Chemistry Department, The Queen's University of Belfast, Belfast BT9 5AG, UK

Water-soluble azo, phthalein, sulphonphthalein and anthraquinone indicators and reagents were subjected to low-voltage electrophoresis on cellulose acetate sheets at pH 2–12. All dyes except low-sulphonated azo dyes yielded one or more sharp bands showing good mobility and resolution over some range of pH values. The performance exceeded that of other possible planar electrophoresis media. The addition of copper, lanthanum, cetyltrimethylammonium or lauryl sulphate ions caused a marked and often beneficial change in behaviour.

Keywords: *Metallochromic indicators; planar electrophoresis; water-soluble dyes*

Electrophoresis is normally regarded as a technique of great value in biochemistry for the separation of protein and similar large molecule ions, but from many years of teaching planar electrophoresis and using it as a research tool, the senior author has been impressed by the excellence of the technique for the examination of comparatively small ions such as hydrophilic dyes. As an undergraduate project we examined the behaviour of a fairly comprehensive set of metallochromic indicators and water-soluble reagents at different pH values and in the presence of charged surfactants and metal ions. Cellulose acetate sheet was the principal medium used, but comparisons were made with paper, polyamide and various thin-layer media. We hope that we have discovered the best conditions under which to examine these various compounds.

There is remarkably little information in the general literature on the planar electrophoresis of dyes, but valuable work that we have noted was that of Criddle *et al.*,[1,2] who separated food dyes at six different pH values on alumina, Kieselguhr, silica gel, cellulose acetate and paper. They commented in depth on the relationship between structure and mobility. Patuska and Trinks[3] also examined synthetic food dyes and Sharma *et al.*[4] have looked at dyes in liquors and beverages as a means of detecting fakes.

Experimental

Apparatus

Electrophoresis was carried out in Shandon equipment consisting of a Vokam power supply operated at 200 V and a simple tank suitable for sheet and plate material. The active electrophoretic distance was 6.5 cm. Contact was made between buffer solution and zone medium with Whatman No. 1 filter-paper rectangles. The zone medium principally used was 14 × 5.7 cm Cellogel sheets (Chemetron, Milan; supplied by J. W. Turner, Liverpool). This was impregnated with buffer solution using the recommended floating technique. Plastic sheet or glass plate thin-layer material was treated with buffer solution by dip or spray procedures, as appropriate. Sample solutions were applied using a Shandon single 5-mm slot applicator.

Materials

Buffer solutions

Initial work on hydrophilic black inks showed that 0.05 M was the optimum buffer concentration. All major buffer components were accordingly of this value, pH adjustment being made with dilute sulphuric acid or sodium hydroxide solution as appropriate. The following buffer solutions were prepared: pH 2.0, sodium dihydrogen phosphate; pH 3.0, sodium hydrogen phthalate; pH 4.0, sodium oxalate; pH 5.0, sodium citrate; pH 6.0, maleic acid; pH 7.0, disodium hydrogen phosphate; pH 8.0, tris(hydroxymethyl)aminomethane; pH 9.0, monoethanolamine; pH 10.0, ethylenediamine; pH 11.0, piperidine; and pH 12.0, disodium hydrogen phosphate.

Sample solutions

These were prepared at a concentration of 1 mg cm^{-3} in water where possible. For dyes showing poor solubility, a few drops of 0.1 M ammonia solution were added, with subsequent reduction of the pH to 7. Most indicators and reagents were obtained from BDH Chemicals and used as received. Sodium alizarin-5-sulphonate was recrystallised Bayer material and sulphonated Alizarin Fluorine Blue (AFBS) was synthesised according to references 5 and 6.

Procedure

Five applications of different dye solutions were made across the cellulose acetate strip at about 30% of the strip length to give a long run towards the anode. The strip was placed in the tank and subjected to the electric field in the usual way as soon as possible.

Results

Ionophoretic mobilities of the indicators and reagents in the buffer solutions described above are given in Table 1. Experiments were repeated in 0.05 M maleic acid - maleate buffer (pH 6.0) with inclusion of 0.02 M copper sulphate, 0.02 M lanthanum nitrate, 0.02 M cetyltrimethylammonium bromide (CTMAB) or 0.02 M sodium lauryl sulphate (SLS). The results are given in Table 2.

Discussion

The cellulose acetate sheets mostly yielded sharp bands with little evidence of tailing or diffusion, especially below pH 10. They were far superior to paper, which gave diffuse bands, cellulose and silica gel, which showed tailing, and polyamide, which gave very low mobilities, presumably owing to excessive hydrogen bonding. Cellulose acetate was the most convenient to impregnate with buffer and gave very little sample diffusion at the origin. A disquieting feature was the way in which, for many compounds, the electrophoretic pattern changed with pH, *e.g.*, Alizarin Fluorine Blue showed one line at all pH values except 8, where three were evident. Hence one cannot be sure whether a multiplicity of lines is due to an impure material, several ionised forms of one compound or some unsuspected complex formation. However, as with most

Table 1. Ionophoretic mobilities of the indicators and reagents in different buffer solutions*

No.	Compound	Ionophoretic mobility × 10^3/cm^2 min^{-1} V^{-1}										
		pH 2	pH 3	pH 4	pH 5	pH 6	pH 7	pH 8	pH 9	pH 10	pH 11	pH 12
1	Eriochrome Blue Black R	—	—	—	—	—	—	−D	0.3T MO	—	0.2T MO	0.5TD MO
2	Arsenazo	3.4	5.9	6.1	5.6	6.7	5.7	6.7	5.8	7.5	*6.3* 7.0	6.6
3	Hydroxynaphthol Blue	1.4D	3.0	1.5D	0.9T *1.6* *2.2*	1.1T *2.0* 3.3T	0.9 *2.0* 3.5T *	0.1T 1.6D 1.8	2.2TD *2.7*	2.0D	*1.7*D 2.6T 3.5T	*0.6*D 2.3T 3.3T
4	Calmagite	—	—	—	—	—	—	—	MO 0.2T 0.6T	MO 0.5T 1.2T *	MOD	0.0T *0.2* 1.4T
5	Fast Sulpon Black F	—	—	—	—	—	—	—	0.2	0.3	—	—
6	Thoron	3.0	5.4	5.6	4.8	6.6	5.2	5.8	5.8	5.8	5.8	6.4
7	Zincon	—	—	—	—	—	—	−D	0.4	0.0T 0.6	0.8D 1.6D	2.2D
8	Eriochrome Black T	—	—	—	—	—	—	—	0.2	—	0.1D	0.0 0.3
9	Solochrome Dark Blue BS (Calcon)	—	—	—	—	—	—	−D	0.1T 0.2D	—	MOD	0.4T MO
10	Acid Alizarin Black SN	—	—	—	—	—	—	—	—	MO 0.4T	—	—
11	HSN (Patton and Reeder's)	—	—	—	—	—	—	—	—	—	—	0.0 0.2
12	Arsenazo III	0.1 2.7T *3.3*	3.0T *3.5*	4.0T *4.7*	4.7	5.3 5.5	6.0	6.3D	6.4T *6.8*	7.2T *7.8* *	7.0T *7.4*	5.0T *5.7*
13	Eriochrome Blue Black SE	*0.5* 2.8T	*0.9*D 2.9T	*0.2* 1.8T	*0.2* 1.9T	0.5 2.5T	0.5D 2.8T	1.1	*3.1* 5.3T	0.7T 1.5T *4.6* *7.5*T *	*4.7* 5.0T 6.0T *	*3.8* 4.9T
14	Eriochrome Blue Black B	—	—	—	—	—	—	—	—	MO 0.1	0.1D	0.1
15	Xylenol Orange	1.8T 2.2T *2.7*	2.6TD 2.9T *3.5*	2.9T 3.4T *4.1* *	3.5T *4.1*	4.7D	4.8T *5.5*	4.0	*4.3* 5.4T	*4.7* 6.1T	*4.4* 5.0T	*4.2* 4.9T
16	Methyl Thymol Blue	1.5T *2.1*	1.8T *2.7*	2.5T *4.0*	2.3T *3.7*	0.6T 2.6T *4.9*	3.1T *5.4*	4.7	0.8T 3.5T *4.1*	1.1T 4.2T 4.6	1.8T 3.7T *3.9*	3.4T 4.7T *4.9*T 5.5 *
17	Calcichrome	0.4 0.8T	1.6	1.3	1.9	4.6	5.4	5.6	6.4	2.9T *6.1* *	2.9T *6.0*	3.0T 6.6
18	Glycine Thymol Blue	0.0 *0.4* 0.8T	*0.9* +4 others	*1.2* +4 others	*1.3* +6 others	*1.7* +5 others	*1.8* +5 others	*1.7* +4 others	*3.2* +7 others	*3.7* +6 others	*4.2* +7 others	*4.8* 3.5TD 4.0T
19	Catechol Violet	1.9	1.4	1.4	0.9	1.4	1.3	1.6	2.8	3.4	4.4	6.5T *6.8*
20	Bromopyrogallol Red	0.4	0.4	0.2	0.4 0.5T	1.5	1.3TD *2.2*	1.2T *2.6*	1.2T 1.9T *2.8* 5.2T *	1.4T *3.2* 5.4T	3.2 5.2	3.0T *3.9* 5.9TD 6.7TD
21	Alizarin Red S	0.2	0.6	*0.2* 1.5T	0.3	0.8T 1.1	0.7T 1.6D	0.0T *2.2* 7.5T	*2.7* 7.6T *	2.3	1.2D 2.4D 6.0T	0.0D 1.9D 2.5D
22	Alizarin Fluorine Blue-5-sulphonate (AFBS)	1.5T *2.5*	3.2	3.9	4.8	5.8	5.2	5.5	6.1D	5.3T *5.8*	6.1	5.0T *6.9*
23	Alizarin-5-sulphonate	0.3T 1.5	1.5	1.1	1.3	1.5	0.0T *2.0*	0.0T *3.7*	4.4 4.9 *	0.0T 5.0	0.0T 0.2T 2.4T *4.2*	0.0T *3.4* *5.2*
24	Pyrogallol Red	0.8	1.0	1.2 4.1T	1.3 2.2T	1.8 2.3T	*2.1* 2.9T 4.2T	*2.8* 3.7T 5.0T 6.4T *	3.8D	3.4	2.9T 5.0D	4.9T 6.5 6.7
25	Alizarin Fluorine Blue	—	1.5	1.3	1.8	1.9	1.4	0.2 *0.8* 1.1T	1.1	1.3D	1.4D	3.0D

Table 1—*continued*

No.	Compound	Ionophoretic mobility × 10^3/cm^2 min^{-1} V^{-1}										
		pH 2	pH 3	pH 4	pH 5	pH 6	pH 7	pH 8	pH 9	pH 10	pH 11	pH 12
26	Thymolphthalein complexone	MO 1.7T 2.3	MO 1.4T 2.0	MO 1.2T 1.7	1.3T *1.6* 	MO 0.7T 2.5	0.2 0.5 0.8T *2.6*	MO 3.8 	0.9T 4.3 	MO 0.5T 1.0T 4.3	0.5T 0.8T *1.4* *	1.4T *1.7* 2.2 2.7T

* Key, —, zero mobility; T = trace; MO = main band has zero mobility; * = pH showing best resolution of bands; D = diffuse. Values in italics refer to principal band(s). A negative sign indicates migration towards the cathode.

Table 2. Ionophoretic mobilities of the indicators and reagents in 0.05 M maleic acid - maleate buffer solution with different additives*

Compound†	Ionophoretic mobility (at pH 6) × 10^3/cm^2 min^{-1} V^{-1}				
	No additive	0.02 M $CuSO_4$	0.02 M $La(NO_3)_3$	0.02 M CTMAB	0.02 M SLS
1	—	—	—	−1.7T *−1.9*	
2	6.7	*5.7*D 6.5T 7.4T	*3.1* 3.5TD 3.9T	0.0 *−1.1* −1.3T	*+2.1* −3.2T
3	1.1T *2.0* 3.3T	0.8T *1.7* 3.4T 5.5T 6.4T 7.2T	0.7T *2.4* 2.7T 3.2T 3.9T	−1.3	
4	—	MO 1.0T	MO 0.9T	−1.6T *−1.8*	
5	—	MO 0.8T	MO 0.3TD	−1.8	
6	6.6	5.2	4.1	−1.1	1.9
7	—	—	MO 3.2T	+0.4T *−1.2*D −2.4	
8	—	—	—	MO −0.3T −1.5T	
9	—	—	—	−2.6	
10	—	MO 0.6TD	0.6D 2.1T	*−2.3* *−2.4*	
11	—	MO 1.8	MO 1.2	−1.2T −1.5T *−1.9*	
12	5.3 5.5	4.3 4.6 5.0	MO 2.2T	−1.2 −1.5	1.7
13	*0.5* 2.5T	0.3T 1.7T *2.7*	0.4T *1.2* 3.2T	−0.4D *−1.1*D −1.6T	
14	—	−D	—	−1.9	
15	4.7D	*1.7*D 2.4T 2.6T *3.2*	1.5 2.0T	*−1.7* −2.0T	0.6T *1.1*
16	0.6T 2.6T *4.9*	0.6T 1.5T 2.1T 2.4T *3.4*	*0.9* *1.6*	*−1.1* −1.2T	
17	4.6	2.5T *4.3*D	2.0T *3.1*D	−0.9	
18	*1.7* +5 others	*0.7* *1.0* 0.3 1.7T 2.7T	*0.8*D 1.7D 2.7T	−1.1T −1.4T *−1.7*	*0.2* 1.7TD 1.8T −0.5
19	1.4	*2.7* 3.2T	1.3	−1.2D	
20	1.5	1.7TD 2.5D 3.5TD	1.7T *3.7* 3.8TD	−1.1	

Table 2—*continued*

Compound†	Ionophoretic mobility (at pH 6) × 10^3/cm^2 min^{-1} V^{-1}				
	No additive	0.02 M $CuSO_4$	0.02 M $La(NO_3)_3$	0.02 M CTMAB	0.02 M SLS
21	0.8T	0.0	0.0	−1.2	
	1.1	0.2T	0.5		
		*2.0*D			
		*2.2*D			
		3.6T			
22	5.8	1.9T	2.5D	−1.1	
		2.4T			
		3.1			
23	1.5	1.3T	MO	*−0.8*	
		2.3	1.7T	*−0.9*	
			3.3		
24	1.8	2.1T	1.4T	−1.1	
	2.3T	*2.9*D	*3.7*D		
		*4.0*D	4.1		
25	1.9	*1.4*	1.2	−0.7	
		1.7T			
26	MO	0.3D	MO	+1.2T	
	0.7T		0.9T	−0.4T	
	2.5		1.7	*−1.4*	

* For key, see Table 1.
† Compounds as in Table 1.

planar chromatographic techniques, careful comparison with pure standards should eliminate ambiguity.

An increase in dye mobility with increasing pH as carboxy and phenolic groups ionised was clearly evident in many instances, such as with Xylenol Orange. For many compounds the mobility remained almost constant between pH 4 and 8 but then increased at higher pH to reflect the pK values of hydroxy groups. Although the mobilities were high at high pH, the sharpness of the bands often deteriorated, and pH 10 was selected as a good compromise. Dyes that had the highest electrophoretic mobilities at all pHs were Arsenazo, Thoron and Arsenazo III. The behaviour of the azo dyes was interesting and followed a well defined pattern. Those with a ratio of number of SO_3^- plus AsO_3H^- groups to number of aromatic moieties of ≤ 1 showed zero or very low mobility at all but very high pH values, whereas those with a ratio >1 showed medium to high mobility at all pHs. Dyes of the former type tend to be poorly soluble at around neutral pH and are not readily amenable to this type of electrophoresis. In contrast, (sulphon)phthaleins and anthraquinone dyes with one or fewer sulphonate groups per aromatic moiety, although often rich in carboxy groups, showed good mobility at pH *ca.* 7. The obviously poor purity of many of these compounds (Glycine Thymol Blue is a bizarre example) illustrates the importance attached to purifying indicators and reagents prior to fundamental studies such as ionisation or stability constant determinations. Electrophoresis of the type described here would be an excellent means of following purification procedures.

The presence of metal ions that are good complex formers with EDTA, *e.g.*, Cu^{2+} and La^{3+}, drastically altered the electrophoretic patterns of the dyes, usually by reducing mobilities, *e.g.*, AFBS, or increasing the number of observed bands, *e.g.*, Hydroxynaphthol Blue. Even some immobile dyes showed movement, *e.g.*, HSN. Such marked changes could greatly assist the comparison of unknowns with standards. However, a proper explanation of this behaviour shown by the metal complexes will require the production of pure dye materials.

The presence of charged surface-active agents caused a marked change of pattern. The cationic agent cetyltrimethylammonium bromide caused most bands to move towards the cathode and, notably, produced extensive and sharp band movement in azo dyes formerly immobile, often with resolution of several bands, *e.g.*, Zincon. However, there seemed to be limited variation in band mobility. Owing to a shortage of cellulose acetate sheets, only a few experiments were carried out with the anionic agent sodium lauryl sulphate. Here, curiously, the mobility of normally highly mobile bands was greatly diminished but the bands remained very sharp and showed good resolution. We feel that high electroosmotic flow is probably the main reason for these phenomena.

Selected dyes were run at pH 11.4 using an anionic buffer based on disodium hydrogen phosphate and a cationic buffer based on piperidine. The mobilities were greater, the bands were sharper and the resolution of the bands were superior in the anionic buffer.

In conclusion, cellulose acetate sheets have been shown to be an excellent medium for the electrophoretic examination of phthalein, sulphonphthalein, anthraquinone and richly sulphonated or arsonated azo water-soluble indicators and reagents. The addition of metal ions or charged surfactants frequently improves separations.

References

1. Criddle, W. J., Moody, G. J., and Thomas, J. D. R., *Nature (London)*, 1964, **202**, 1327.
2. Criddle, W. J., Moody, G. J., and Thomas, J. D. R., *J. Chromatogr.*, 1964, **16**, 350.
3. Patuska, G., and Trinks, H., *Chem. Ztg.*, 1962, **86**, 135.
4. Sharma, V. K., Sharma, I. C., and Tewari, S. N., *Chromatographia*, 1975, **9**, 405.
5. Leonard, M. A., and Murray, G. T., *Analyst*, 1974, **99**, 645.
6. Leonard, M. A., *Analyst*, 1975, **100**, 275.

Paper A5/320
Received September 12th, 1985
Accepted September 24th, 1985

Determination of the Silver Error in the Coulometric Titration of Acids in Various Media

Adam Hulanicki, Stanisław Głąb and Wojciech Jędral
Department of Chemistry, Warsaw University, Warsaw, Poland

The dependence of the silver error in coulometric titrations of acids in a one-compartment cell on the solubility of silver halide has been established. The silver error is proportional to the total solubility of silver and inversely dependent on the current density. Because the main contribution to the total titration error is given by the silver error, it is necessary to choose conditions that produce the minimum value. The silver error is below 0.1% when the current density of the cathodic process is at least 10 mA cm^{-2}. This relationship was tested in solutions of chloride, bromide and iodide in water, methanol, ethanol and acetone. For the aqueous solutions the bromide electrolyte is recommended and, for methanolic solutions, the best results are obtained with chloride ions.

Keywords: *Silver error; coulometric titration; acid determination; non-aqueous solvents*

In coulometric titrations the anode and cathode compartments are commonly separated by a diaphragm to eliminate mutual interferences of electrolysis products formed at both electrodes. To ascertain that such interferences do not occur, special precautions must be taken; however, the decrease in diaphragm permeability increases the cell resistance and makes the generating current stabilisation more difficult. In addition, the increase in applied voltage in the generating circuit may disturb the functioning of the electrochemical indicating system. In addition, some electrolyte flow through the diaphragm occurs, which may influence the titration efficiency and complicate the determination.

Szebelledy and Somogyi[1] introduced the technique of one-compartment coulometric titrations for the determination of acids when the product formed at the anode is insoluble and does not interfere in the the cathodic processes. In this procedure a silver anode is placed in the halide-containing sample solution. A silver halide precipitate is formed at the anode, which should not, in principle, interfere in the determination of acids by the hydroxy ions formed at the cathode.

Lingane and Small[2] and Bishop and Riley[3] stated that bromide is more advantageous than chloride, because of its lower solubility. The solubility of silver halide is not only governed by the solubility product, but also by the formation of soluble halide complexes, which may in turn be reduced at the cathode, decreasing the current efficiency of the generation of hydroxy ions. It has also been observed[4] that the addition of tetraphenylborate anions, which also form sparingly soluble silver salts, improves the results.

Bishop and Riley[3] calculated the silver error from the total charge necessary for the dissolution of silver deposited on the cathode during coulometric titration. For a current density of 30 mA cm^{-2} the error was 0.01% when 0.1 M sodium bromide solution was used as the electrolyte. The experimentally evaluated silver error was taken as a basis for the correction of the results.[5] Because of the increasing importance of coulometric titrations in various solvents the effects of different parameters on the magnitude of the silver error have been studied.

Experimental

Reagents

Doubly distilled water from a quartz still was used in all measurements. Solvents and salts of analytical-reagent grade were used in all experiments. Perchloric acid solutions of approximately 0.01 M were prepared in water and methanol and standardised titrimetrically with sodium carbonate.

Apparatus

A Radelkis Model OH 404 coulometric analyser was used for all coulometric experiments. The generator electrodes were made of platinum foil with a surface area of 0.7, 5 or 20 cm^2. The silver anode had a surface area of about 25 cm^2. The indicator system consisted of a PHM 64 pH meter, G 202 B glass electrode and a K 401 calomel reference electrode, all from Radiometer. Titration end-points were evaluated using Gran's method by plotting $10^{E/S}$ *vs.* Q.

Procedure

The silver error in coulometric titrations of acids was determined in chloride, bromide and iodide solutions in water, methanol, ethanol and acetone (90%). The method followed was that of Bishop and Riley.[3] The platinum electrode was thoroughly cleaned by anodic polarisation in 0.1 M perchloric acid and washing with nitric acid and water.

This electrode was then placed in the coulometric vessel together with the silver anode. After addition of the sample of perchloric acid the electrolysis was performed with the given current density of the cathodic process. The electrolysis was stopped when a charge Q_1, slightly less than that equivalent to the amount of added acid, passed through the solution. At this point the platinum electrode, with the small silver deposit, was removed immediately, washed with water and the amount of silver was anodically stripped in 0.1 M perchloric acid with a 1 mA current using an auxiliary platinum electrode. The potential was measured *versus* a saturated calomel electrode and from the recorded potential *versus* time graph the charge Q_2, necessary for the dissolution of silver, was determined. The silver error was calculated as the charge ratio $Q_2/(Q_1 - Q_2)$.

Results and Discussion

Dependence of the Silver Error on the Solubility of Silver Halide

Satisfactory results for the determination of the acid can be obtained when the current efficiency of base ion formation and/or of direct reduction of hydrogen ion equals 100%. This is disturbed when the silver ions formed at the anode are not completely bound as insoluble precipitate at the electrode surface but enter into solution as free Ag^+ ions, or as soluble complexed species that in turn may be reduced at the cathode.

* Presented at Euroanalysis V, Krakow, Poland, August 26–31, 1984.

Such an interfering process may be formulated as

$$[Ag^+, AgX, AgX_2^-, \ldots, AgX_n^{(n-1)-}] + e^- \rightleftharpoons Ag + nX^- \quad (1)$$

and its extent depends on the total concentration of dissolved silver species. The total silver solubility, S, is

$$S = [Ag^+] + [AgX] + [AgX_2^-] + \ldots + [AgX_n^{(n-1)-}] \quad (2)$$

or after the introduction of respective stability constants

$$S = K_{so}([X^-]^{-1} + \beta_1 + \beta_2[X^-] + \ldots + \beta_n[X^-]^{n-1})$$

$$= K_{so}[X^-]^{-1}(1 + \beta_1[X^-] + \beta_2[X^-]^2 + \ldots + \beta_n[X^-]^n) \quad (3)$$

The term in parentheses is equivalent to the side-reaction coefficient of silver ions under the given conditions. Thus, assuming that the actual concentration, $[X^-]$, of the halide ions equals their total concentration, C_x, the total solubility of silver is

$$S = K'_{so}/C_x \quad (4)$$

where K'_{so} is the conditional solubility product of the corresponding silver halide. From the values of the equilibrium constants of the silver halides (Table 1) it follows that, except for very concentrated halide solutions, the most important term is the constant β_2; however, where available, all constants were used in the calculations.

The silver error was determined using a constant current density of the cathodic process under selected conditions of halide concentration and solvent used. The decrease in halide concentration causes a significant decrease in the silver error [Figs. 1(*a*) and 2(*a*)]. When the total solubility of silver was calculated according to equation (4) a linear dependence on the silver error was found [Figs. 1(*b*) and 2(*b*)]. Some other experimentally determined values of the silver error at a current density of the cathodic process of 1 mA cm^{-2} and for 0.05 M solutions of halide ions are given in Table 2, and these are compared with the calculated values of conditional solubility products, pK'_{so}. Those values of the silver error are reproducible in most solutions. When acetone was used as a solvent a very large scatter of results was observed and a dependence on the electrolysis time was noted. This may be connected with the magnitude of the conditional solubility product of silver halides in acetone, and also with the kinetics of dissolution of the anodic deposit. When in the same solution subsequent determinations were performed, the silver error increased. The data in Table 2 are given for the first and fourth determinations.

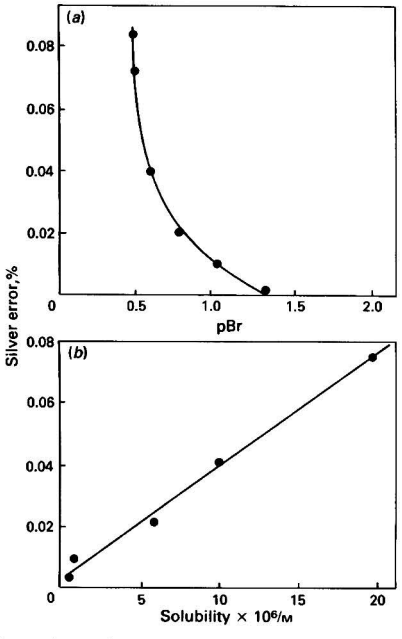

Fig. 1. Dependence of the silver error in coulometric titration of acid in aqueous bromide solutions at a current density of the cathodic process of 25 mA cm^{-2}. (*a*) Dependence on the bromide concentration; and (b) dependence on the calculated molar solubility of silver bromide

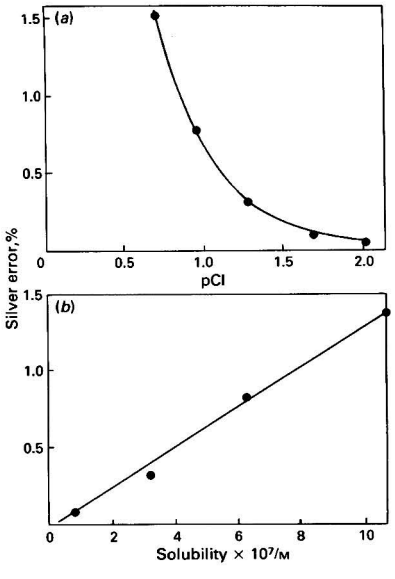

Fig. 2. Dependence of the silver error in coulometric titration of acid in methanolic chloride solutions at a current density of the cathodic process of 1 mA cm^{-2}. (*a*) Dependence on chloride concentration; and (*b*) dependence on calculated molar solubility of silver chloride

Table 1. Equilibrium constants used in calculations of total solubility of silver halides

Solvent	Halide	pK_{so}	Log β_1	Log β_2	Log β_3	Log β_4	Reference
Water	Cl$^-$	9.75	3.4	5.3	5.48		6, 7
	Br$^-$	12.3	4.2	7.1	8.0	8.9	8
Methanol ..	Cl$^-$	13.0		7.9			9
	Br$^-$	15.2		10.9			9
	I$^-$	18.2		14.8			9
Acetone	Cl$^-$	16.4		16.7			9
	Br$^-$	18.7		19.7			9

Table 2. Conditional solubility products for silver halides and the silver error in 0.05 M sodium halide solutions in various solvents. Cathodic current density, 1 mA cm^{-2}

Solvent	Silver error, %			Conditional solubility product for 0.05 M X$^-$		
	Cl^-	Br^-	I^-	Cl^-	Br^-	I^-
Methanol	0.3	1.2	1–7.5	7.7	6.9	6.0
Ethanol	0.4	1.0	1.7–10			
Water	0.6	0.2		7.05	7.8	
Acetone (90%)	2–22	3.7–10		2.3*	1.6*	

* Data for anhydrous acetone.

Table 3. Comparison of the titration error and silver error in the coulometric titration of 0.009660 M perchloric acid in 0.05 M sodium chloride in methanol

	Current density/mA cm^{-2}		
	0.1	1.0	14.6
$HClO_4$ taken/mmol	0.02415	0.0966	0.04830
Q (theoretical)/mC	2330	9320	4660
Q (experimental)/mC	2408	9361	4660
Relative standard deviation, % ($n = 5$)	0.30	0.45	0.43
Titration error, %	+3.35	+0.43	<+0.01
Silver error, %	+3.3	+0.3	<+0.01

Table 4. Comparison of the titration error and silver error in the coulometric titration of 0.01102 M perchloric acid in 0.05 M sodium bromide in water

	Current density/mA cm^{-2}		
	0.5	1.0	10
$HClO_4$ taken/mmol	0.02755	0.0551	0.1102
Q (theoretical)/mC	2658	5317	10633
Q (experimental)/mC	2668	5330	10638
Relative standard deviation, % ($n = 5$)	0.40	0.50	0.45
Titration error, %	+0.38	+0.25	+0.04
Silver error, %	+0.44	+0.21	+0.02

Also, irreproducible results were observed for iodide solutions in alcohols. Here, the first determination also exhibited the smallest error, which increased for the fourth in spite of relatively small values of conditional solubility products. The kinetics of the dissolution and the diffusion of ions may be responsible for those effects.

The data in Table 2 indicate that the best results for acid determination, *i.e.*, the smallest value of the silver error, are obtained in chloride solutions when methanol or ethanol is used as the solvent, whereas they confirm that in water the best electrolyte is bromide.

Dependence of the Silver Error on the Current Density of the Cathodic Process

The next parameter that influences the silver error for determination of acid is the current density at the working electrode. In these experiments the current density was changed from 0.05 to 30 mA cm^{-2} and the results were plotted logarithmically (Fig. 3). For a single system (solvent - halide) a linear dependence was obtained with a slope close to −1. The relative positions of the lines for the systems studied are in accordance with the change of the solubility of the corresponding silver halides. For better results large current densities are advantageous, because the contribution of silver ions in the over-all cathodic process depends on the potential of the cathode. When the current density is small the electrode potential is more positive and corresponds to the reduction of silver ions. When the current is large in comparison with the diffusion current of silver ions at their given concentration, the

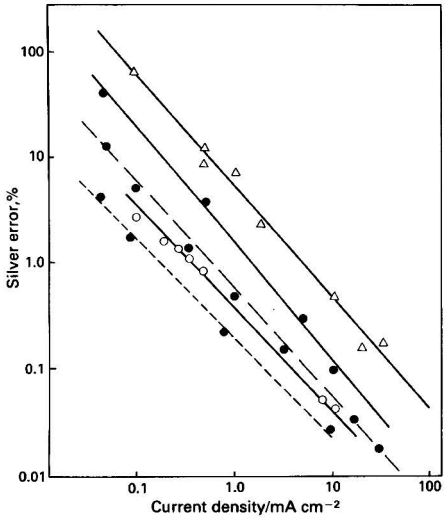

Fig. 3. Dependence of the silver error on current density of the cathodic process for 0.05 M sodium halide in different supporting electrolytes. —, Methanol; — —, ethanol; and - - -, water. ○, Cl; ●, Br; and △, I

cathode potential is more negative, because it is shifted to the potential of solvated protons or solvent reduction. When the current in the coulometric system is higher than the limiting reduction current of silver ions, the absolute amount of reduced silver is constant for a given period of time and is independent of the current density. However, the greater the current density the smaller is the relative contribution of silver reduction in the over-all cathodic process.

Total Titration Error and Total Silver Error

The total error of coulometric titration in a one-compartment cell depends on the silver error, which decreases the current efficiency of titration, on the apparatus error, which is dependent on the error of charge measurement, and on the error of end-point location during titration. For checking the magnitude of the titration error, known samples of perchloric acid were titrated and the total error was compared with the silver error in the same solutions. Such experiments were carried out under the optimum conditions, *i.e.*, in methanolic 0.05 M sodium chloride solutions and in aqueous 0.05 M sodium bromide solutions (Tables 3 and 4). In both systems three different current densities were used. These results indicate that the main source of error in all experiments is the silver error and the difference between the total titration error and the silver error is less than the precision of determinations with the apparatus and experimental procedure used.

Conclusions

It is experimentally evaluated that there is an exact correlation between the solubility of silver halide in the electrolyte solution and the silver error of coulometric titration of acids with the silver anode in the one-compartment coulometric cell. The solubility is dependent on the concentration of the halide used as an electrolyte and on the solvent. The silver error is linearly dependent on the total solubility of silver and inversely dependent on the current density. To obtain silver errors of less than 0.1% the current density of the cathodic process should be at least 10 mA cm^{-2}. Bromide is the best halide for aqueous solutions and chloride for methanolic solutions. Iodide electrolytes and acetone as a solvent are not recommended.

By comparing the total titration error with the silver error it may be stated that the latter gives the main contribution to the total error of determination, indicating the importance of the proper choice of experimental conditions so as to minimise the silver error.

This work was partially supported by the Committee on Analytical Chemistry of the Polish Academy of Sciences.

References

1. Szebelledy, L., and Somogyi, Z., *Fresenius Z. Anal. Chem.*, 1938, **112**, 323.
2. Lingane, J. J., and Small, L. A., *Anal. Chem.*, 1949, **21**, 1119.
3. Bishop, E., and Riley, M., *Analyst*, 1973, **98**, 313.
4. Johansson, G., *Talanta*, 1964, **11**, 789.
5. Bishop, E., and Riley, M., *Analyst*, 1973, **98**, 416 and 426.
6. Davies, C. W., and Jones, A. L., *Trans. Faraday Soc.*, 1955, **51**, 812.
7. Mironov, V. E., *Radiokhimiya*, 1962, **4**, 707.
8. Berne, E., and Leden, I., *Z. Naturforsch.*, 1953, **84**, 719.
9. Luehrs, D. C., Iwamoto, R. I., and Kleinberg, J., *Inorg. Chem.*, 1966, **5**, 201.

Paper A5/233
Received July 1st, 1985
Accepted September 3rd, 1985

Differential-pulse Stripping Voltammetry for the Determination of Soluble Iron in Simulated PWR Coolant

K. Torrance and C. Gatford
Central Electricity Generating Board, Central Electricity Research Laboratories, Kelvin Avenue, Leatherhead, Surrey KT22 7SE, UK

A method has been developed for the determination of dissolved or ionic iron in pressurised water reactor (PWR) coolant using differential-pulse voltammetric stripping (DPVS) following adsorptive accumulation of an iron(III) - catechol complex at a hanging mercury drop electrode. The method does not discriminate between Fe(II) and Fe(III) ions and the total ionic iron is determined in a Tris buffered solution at pH 8 ± 0.1. Interference from the reaction of boric acid in the coolant with the catechol was overcome by limiting the total boron in the analytical solution to ≤ 100 mg l^{-1} and adding mannitol. No interference was observed from ions of common transition metals such as copper, nickel, cobalt and manganese. The effects of pH, catechol concentration, accumulation voltage and time were investigated in simulated coolant solution. The limit of detection was of the order of 0.1 μg l^{-1} and the precision of a single determination based on a standard additions procedure was considered to be in the range 10–15%.

When the results obtained by this technique were compared with those obtained by a spectrophotometric method, good agreement was obtained. The DPVS method for the determination of ionic iron in PWR should prove valuable in corrosion studies and it can complement alternative methods, such as electrothermal atomic absorption, which only gives the total iron in solution.

Keywords: *Iron determination; PWR coolant analysis; adsorptive concentration; differential-pulse voltammetric stripping*

The boric acid solution used as the coolant in the primary circuit of a pressurised water reactor (PWR) contains trace amounts of metals derived from the materials of construction and periodic analysis of the coolant is required to assess the extent of these metals present with a view to adjusting, when necessary, the coolant chemistry. The most abundant metal has been shown to be iron whose concentration can vary widely according to the age and condition of the reactor. In general, the iron content has been reported as <50 μg l^{-1} and at these concentrations the usual method of analysis is electrothermal atomic absorption spectrometry. This technique determines the total rather than the soluble concentration of any element unless a prior separation is used and its sensitivity is such that measurements of iron in the coolant are not very satisfactory below 1 μg l^{-1}. Differential-pulse voltammetric stripping (DPVS) following adsorptive accumulation at a hanging mercury drop electrode has been shown to be suitable for the determination of the low concentrations of soluble nickel and cobalt[1] expected in PWR coolant and the same technique has now been extended to the determination of soluble iron.

Catechol has been used as an adsorption enhancement reagent for the DPVS determination of uranium (VI),[2,3] copper[4] and iron[5] in sea water. In the last application, samples were buffered to pH 6.9 in 10^{-3} mol l^{-1} piperazine-*N*,*N*′-bis-2-ethanesulphonic acid (PIPES), and at this pH a reduction peak, whose current was proportional to the soluble iron concentration, was observed at −0.35 to −0.4 V. The sensitivity and apparent freedom from interference reported for this method of determination for soluble iron suggested that it could be applied to the analysis of PWR coolant.

The difficulty associated with the use of catechol for the determination of iron in PWR coolant is its reaction with borate anions[6] with which it forms complexes in a manner analogous to mannitol. An additional complication is the decrease in the boric acid content throughout the lifetime of a reactor fuel cycle from an initial value of >1000 to a final value of <100 mg l^{-1} of boron. This requires either a variation in analytical reagents corresponding to the decrease in boric acid or an excess sufficient to produce effectively constant analytical conditions throughout. Both these suggestions have their disadvantages and the procedure that was chosen was to dilute all the samples such that the final concentration of boric acid in the analytical solution was the equivalent of ≤ 100 mg l^{-1} of boron. Using this procedure there was no need to vary the volumes of reagents and, further, the effect of borate ion on catechol was immediately reduced. The resulting reduction in the iron concentration in the analytical solution was not expected to be a problem as the accumulation period can be increased to produce a measurable peak current.

Experimental

Reagents

Catechol. Reagent-grade catechol was recrystallised twice from toluene. After drying at 40 °C it was stored in a blackened container. A 0.1 mol l^{-1} ethanolic solution was stable for at least a week when also stored in a blackened container.

Tris buffer solution. Analytical-reagent grade tris(hydroxymethyl)methylamine was recrystallised twice from 3 + 1 ethanol - water. The original concentration of iron in the solid of 0.4–0.6 mg kg^{-1} was reduced to 0.03–0.05 mg kg^{-1} by this procedure. Additional recrystallisation did not improve the purity.

A pH 7.9 (±0.1) buffer solution containing 0.5 mol l^{-1} of Tris was prepared by the addition of isothermally distilled hydrochloric acid to the recrystallised base according to the proportions given by Perrin and Dempsey.[7] Attempts were made to reduce further the iron concentration of this buffer by adsorption on added manganese dioxide but the resulting solution always produced voltammograms with a broad distorted iron(III) reduction peak.

Boric acid. High-purity grade boric acid (Borax Consolidated Ltd.) was used to prepare simulated PWR coolant. No significant amounts of iron were detected in the boric acid at the concentrations (50 and 100 mg l^{-1} of boron) used in the polarographic cell.

Mannitol. Analytical-reagent grade mannitol was prepared as a 0.5 mol l^{-1} solution and was purified by passing through a column of nuclear-grade cation-exchange resin in the

H^+ form. The iron content of the resulting solution was equivalent to 0.03 mg kg^{-1} in the solid mannitol.

Standard iron(III) solution. A standard solution of Fe(III) containing 1000 mg l^{-1} was prepared from analytical-reagent grade iron(III) ammonium sulphate. Working solutions containing 200–1000 μg l^{-1} of Fe(III) were prepared daily as required by sequential dilution. All standard solutions contained 10^{-2} mol l^{-1} of sulphuric acid.

De-ionised water. De-ionised water was prepared by circulating a bulk supply of water continuously through a mixed cation/anion-exchange column such that the conductivity was of the order of 0.06–0.07 μS cm^{-1} at 25 °C.

Storage of reagents. Polythene containers were used exclusively. A cleaning procedure based on that described by Moody and Lindstrom[8] was used in which the bottles were filled with hydrochloric acid (1 + 1), let stand for a week, emptied, rinsed and refilled with nitric acid (1 + 1) and let stand for a further week. The bottles were subsequently rinsed and left filled with de-ionised water.

Polarograph and voltammetric conditions

An EG & G Princeton Applied Research Model 264 polarographic analyser in conjunction with a Model 303 mercury electrode assembly were used in these experiments. The voltammograms were recorded on a Model RE 0089 *X* - *Y* recorder (EG & G Instruments). The standard reference half-cell supplied with the apparatus was replaced by a borosilicate glass tube of the same dimensions but having a crack-junction[1] rather than a ceramic-frit junction as in the original. Nitrogen (99.999%), which was first passed through a gas chromatographic oxygen trap (Phase Separations), was used to de-oxygenate the solutions in the polarographic cell.

The sequence that was followed in most instances was a de-oxygenation period of 12 min, an accumulation period (usually 50 or 100 s) at −0.2 V, then a differential-pulse voltage scan at 5 mV s^{-1} to −0.7 V. In all instances the drop size was set at medium (2.5 mg), the pulse height at 50 mV and the pulse interval at 0.5 s.

Results

Buffer Systems

Voltammograms of the iron(III) - catechol complex were initially investigated in a 0.1 mol l^{-1} ammonium chloride solution whose pH was adjusted over the range 7–9.5 by the addition of isothermally distilled ammonia. Over this range a reduction peak was observed at −0.44 to −0.47 V whose current was proportional to the concentration of Fe(III) and the accumulation period. These experiments indicated that the maximum sensitivity was obtained at about pH 8 and in the presence of boric acid there was a slight increase in peak current with time, which was possibly due to the borate - catechol reaction. In order to optimise the sensitivity, a buffer with a range encompassing pH 8 was required and two such systems were considered. A PIPES buffer at pH 8 was tried but it gave inferior voltammograms to those obtained with a Tris buffer at the same concentration (0.05 mol l^{-1}) and pH. The latter system was then investigated thoroughly.

Effect of pH on the Peak Current and the Sensitivity in Tris Buffer

The effect of pH on a solution containing 100 mg l^{-1} of boron and 1 μg l^{-1} of Fe(III) was investigated in a 0.05 mol l^{-1} Tris buffer whose pH was adjusted over the range 6.6–8.5 by the addition of small volumes of isothermally distilled hydrochloric acid. Catechol was added to the extent of 80 μl of 0.1 mol l^{-1} ethanolic solution per 10 ml of sample. Because a reduction in pH produced a shift (0.1 V per unit of pH) in the positive direction of the voltage of the peak, and thus variations in the base line, it was considered that a measurement of sensitivity [*i.e.*, nA (μg l^{-1})$^{-1}$] at each pH was more applicable than peak height. At each pH, a known addition of 1 μg l^{-1} of Fe(III) was made to the solution above and the change in peak height recorded as a sensitivity. The results in Table 1 show that the optimum sensitivity lies in the range pH 7.4–8, although this range could be extended by ±0.5 unit with only about a 20% loss in sensitivity. The minimum volume of 0.5 mol l^{-1} Tris solution (pH 7.9) required to take the pH of a solution containing 100 mg l^{-1} of boron into the pH range for optimum sensitivity was shown to be 0.5–0.6 ml. In all of the experiments subsequently reported, 1 ml of 0.5 mol l^{-1} Tris solution was added per 10 ml of analytical solution.

Table 1. Effect of pH on peak sensitivity. Current range, 50 nA; accumulation time, 50 s; drop size, medium; pulse amplitude, 50 mV; voltage scan, −0.2 to −0.7 V; pulse interval, 0.5 s

pH	Sensitivity/ nA (μg l^{-1})$^{-1}$
6.54	3.5
7.07	6.3
7.40	8.0
7.74	8.3
8.16	7.8
8.52	6.4

Effect of Catechol Concentration on Peak Current

The effect of varying the catechol concentration in the analytical solution from 10^{-5} to 10^{-3} mol l^{-1} was investigated in a solution containing 100 mg l^{-1} of boron, 2 μg l^{-1} of Fe(III), 1.25×10^{-2} mol l^{-1} of mannitol and Tris buffer at pH 7.8. The peak current gradually increased with addition of catechol up to a catechol concentration of about 2×10^{-4} mol l^{-1} and thereafter it was constant. The catechol concentration used in most of the subsequent experiments was 8×10^{-4} mol l^{-1}.

Mannitol Addition and Peak Current Stability

In the preliminary experiments in the ammonia - ammonium chloride buffer solution there was a slight increase in peak current with time, particularly at pH > 8.5, which was perhaps associated with the reaction of borate anion with catechol. Although this reaction was expected to be much reduced at the pH values in the Tris buffer (7.8–8), where the proportion of free borate will be reduced, it could reduce the over-all accuracy. Mannitol forms stronger complexes with borate anion than does catechol[6] and thus by adding an excess of it over the total boric acid present, the catechol - borate reaction will be reduced and the iron(III) catechol reaction stabilised.

Experiments were carried out on a solution containing 8×10^{-4} mol l^{-1} of catechol, 100 mg l^{-1} of boron and 2 μg l^{-1} of Fe(III) in the presence and absence of mannitol; the mannitol to boron molar ratio was approximately 1.5 : 1. Over a 40-min period there was no significant increase in peak height of the voltammograms measured in the solution containing mannitol whereas there was a 6% increase over the same period for the solution having no mannitol. For all of the experiments reported mannitol was added at 1.25×10^{-2} mol l^{-1} in the analytical solution and no attempt was made to define the minimum mannitol concentration required. For determinations near the limit of detection (*ca.* 0.1 μg l^{-1} of Fe) mannitol could be omitted or its concentration reduced as it introduces 0.1 μg l^{-1} of iron in the analytical solution, but some loss of precision may occur.

Effect of Accumulation Time and Potential

The effect of accumulation time was investigated at two concentrations of iron(III) in the analytical solution, 1.7 and

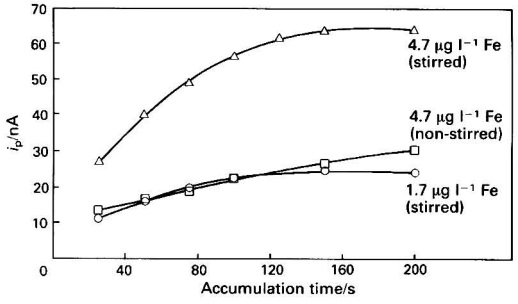

Fig. 1. Effect of accumulation time on peak current

4.7 μg l^{-1} in the presence of 50 mg l^{-1} of boron. The results are shown graphically in Fig. 1, where it can be seen that in stirred solution the onset of non-linearity occurs at *ca.* 120 s for the lower and at *ca.* 100 s for the higher concentration. For analytical purposes it is essential to operate at an accumulation time within the linear region when calibration is made by a standard additions procedure. One method of extending the linear region to solutions of higher concentrations is to use unstirred solution during the accumulation period and the effect of this on the solution containing 4.7 μg l^{-1} was to extend the linearity to times greater than 200 s.

Using accumulation potentials of 0, −0.1 and −0.2 V the peak current of a solution containing 1 μg l^{-1} of Fe(III) decreased by about 6% at the most negative potential. If copper and iron are to be determined simultaneously then it is necessary to use 0 V, but for iron alone a value of −0.2 V is more convenient.

Effect of Iron(II)

A standard solution of iron(II) (100 mg l^{-1}) was prepared by dissolving ammonium iron(II) sulphate in de-ionised water that had been de-aerated with oxygen-free nitrogen. A second standard containing 1000 μg l^{-1} of Fe(II) was prepared from the first by dilution with oxygen-free water. A 10-μl portion of this second standard was added to 10 ml of a de-oxygenated solution containing Tris buffer and catechol. Voltammograms of this solution gave a peak at exactly the same voltage as that found for iron(III). Multiple additions of iron(II) gave the same peak current - concentration dependence as iron(III) and it was concluded that at the voltage used for accumulation of the complex, −0.2 V, the iron(II) ions diffusing to the electrode surface were oxidised to iron(III). Consequently, under the prescribed conditions, the total ionic iron in solution is determined rather than the content of soluble iron(III).

Effect of Some Transition Metal Ions

The effect of transition metal ions, which are known to be present in the primary circuit of a PWR, was investigated. Voltammograms of five portions of a solution containing 1.5 μg l^{-1} of Fe and 50 mg l^{-1} of boron were recorded and the mean peak current was compared with that obtained from five portions of the same solution containing in addition 10 μg l^{-1} each of Cr(VI), Mn(II), Ni(II) and Co(II). No significant difference in the peak currents was observed.

Copper(II) ions form a strong catechol complex that is adsorbed on the electrode and has a reduction peak at about −0.2 V in Tris buffer at pH 7.9. The separation between this peak and that due to iron is *ca.* 200 mV and no interference from peak overlap was observed (see Fig. 2). As the pH of the solution decreases, the iron peak moves closer to that of the copper and interference occurs. At pH 7 van den Berg and Huang[5] found it necessary to mask the copper with EDTA. A

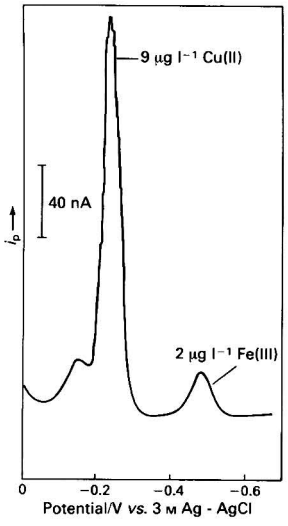

Fig. 2. Voltammogram of Fe(III) - catechol in the presence of Cu(II) in a solution containing 50 mg l^{-1} of boron. Accumulation time, 50 s; accumulation voltage, zero; pulse interval, 0.5 s; scan rate, 5 mV s^{-1}; and pulse height, 50 mV

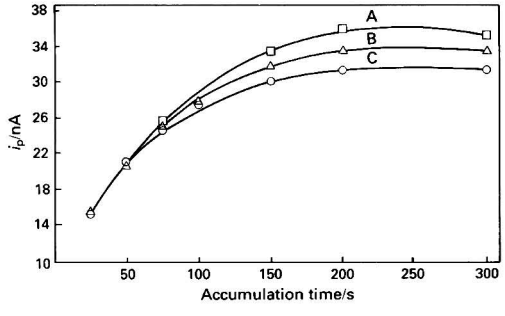

Fig. 3. Effect of copper(II) on accumulation time/peak current of 2 μg l^{-1} of Fe(III). A, 2 μg l^{-1} Fe + 9 μg l^{-1} Cu; B, 2 μg l^{-1} Fe + 4 μg l^{-1} Cu; and C, 2 μg l^{-1} Fe

less obvious form of interference can occur owing to competition between the catechol complexes of copper and iron for adsorption sites on the mercury drop. This type of situation was observed with the nickel and cobalt complexes of dimethylglyoxime.[1] One result of such site competition would be the onset of non-linearity in the peak current - accumulation period relationship at shorter accumulation times. No such effect was observed in a solution containing 2 μg l^{-1} of Fe(III) in the presence of 9 μg l^{-1} of Cu(II) (Fig. 3), although for reasons that are not easy to explain there was a slight increase in sensitivity. This in itself presents no analytical problem as the method of calibration chosen was that of standard additions.

Analytical Procedure, Calibration and Precision

The analytical procedure, which was followed in the calibration and precision tests and also in the analysis of rig samples, was as follows. A known volume of sample, sufficient to give a final concentration of ≤100 mg l^{-1} of boron when diluted to 10 ml, was added to the polarographic cell. De-ionised water was added to make the volume in the cell

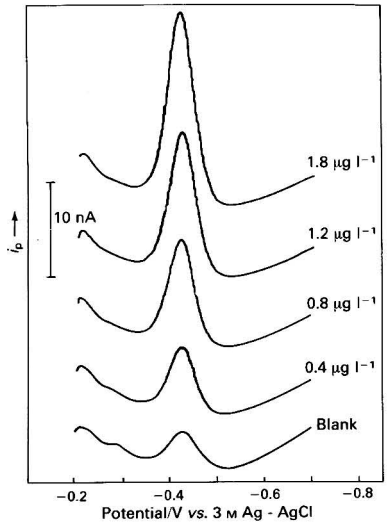

Fig. 4. Voltammograms of Fe(III) - catechol complex from calibration in stirred solution containing 100 mg l^{-1} of boron. Conditions as in Fig. 2, except accumulation voltage, −0.2 V

exactly 8.75 ml followed by 0.25 ml of 0.5 mol l^{-1} mannitol solution. The polarographic cell was transferred to the electrode assembly and the contents of the cell were de-oxygenated for 8 min. At the end of this period 1 ml of 0.5 mol l^{-1} Tris buffer and 80 μl of 0.1 mol l^{-1} catechol solution were added and the solution was de-oxygenated for a further 4 min. The catechol was added at this stage because of its known instability in oxygenated solution. On completion of the de-oxygenation, the voltammetric sequence described previously was followed.

A standard additions procedure was used for the determination of iron in samples but this requires that there is a linear relationship between peak current, i_p, and concentration at a particular accumulation time. The i_p *versus* concentration relationship was investigated in synthetic coolant samples containing 100 mg l^{-1} of boron with iron concentrations in the range 0.2–30 μg l^{-1}. Using a 50-s accumulation period at −0.2 V in stirred solution, voltammograms showed that there was a linear relationship between peak current and concentration up to about 10 μg l^{-1}. A regression analysis for the blank-corrected peak currents for 16 concentrations in the range 0.2–10 μg l^{-1} gave the following equation: i_p (nA) = 8.32c + 1.01 with a regression coefficient r^2 = 0.999, where c is the concentration in μg l^{-1} in the analytical solution. Examples of these voltammograms are given in Fig. 4.

The linearity of the calibration graph can be extended to higher concentrations by accumulating either for a shorter period or without stirring. A calibration was obtained at the same concentration of boron using an accumulation time of 75 s, without stirring, over the range 2–30 μg l^{-1} of iron. A linear relationship was observed up to a concentration in the analytical solution of about 26 μg l^{-1} and regression analysis of the data from 9 concentrations in the range 2–26 μg l^{-1} gave the following equation: i_p (nA) = 4.88c + 3.81 with a regression coefficient r^2 = 0.997. The onset of non-linearity in both calibration graphs occurred at peak currents of about 80–90 nA.

The linearity obtained in these calibration graphs indicated that a standard additions procedure, with a 50-s accumulation period in stirred solution, should be suitable for samples containing up to 6 μg l^{-1} of iron. In unstirred solution, for an accumulation period of 75 s, standard additions calibration can be at sample concentrations up to *ca.* 15 μg l^{-1}. These concentrations are based on samples containing 100 mg l^{-1} of boron and a single standard addition, which will approximately double the peak current.

Table 2. Precision of determinations of peak current in the presence of 50 mg l^{-1} of boron

Concentration of Fe/μg l^{-1}	Accumulation time/s	Mean peak current†/nA	Standard deviation/nA
Blank*	100 (stirred)	1.5	0.2 (13.3%)
1.7	100 (stirred)	18.1	1.0 (5.5%)
4.3	150 (stirred)	23.7	1.0 (4.2%)

* No boric acid present. Accumulation voltage, −0.2 V; voltage scan, −0.2 to −0.7 V.
† Mean of five determinations.

Table 3. Soluble iron determined in samples from PWR rig

Sample	Soluble Fe/μg l^{-1}	Total Fe (on-line)/μg l^{-1}
A	7.3*	8.2
B	2.2†	2.6

* Analysed 90 min after collection.
† Analysed 5 h after collection.

The standard deviations for a single measurement of peak current were obtained from voltammograms of a reagent blank solution (containing no boric acid) and solutions containing 1.7 and 4.3 μg l^{-1} of Fe and 50 mg l^{-1} of boron (see Table 2).

The concentration of iron in the reagent blank solution was determined by standard additions to be 0.13 μg l^{-1}. Taking the statistical limit of detection at the 95% confidence level as 4.65 δ_B, where δ_B is the standard deviation of the blank, gives a limit of detection of 0.08 μg l^{-1} (1.43 × 10^{-9} mol l^{-1}).

Analysis of PWR Rig Samples

The soluble iron content was determined in samples obtained, on two separate occasions, from a rig operating under PWR primary coolant conditions. The results of the voltammetric determinations were compared with those obtained from an on-line total iron monitor based on solubilisation with thioglycollic acid followed by a colorimetric determination using ferrozine. The samples were collected in polythene bottles to which had been added a small volume of hydrochloric acid (*ca.* 1 ml of 5 mol l^{-1} acid per 200 ml of sample) to stabilise the soluble iron. On each occasion, as the boron concentration was about 1100 mg l^{-1}, the sample was diluted 1 + 10 in the polarographic cell. The results are summarised in Table 3.

Sample B was re-analysed 24 h after collection and the soluble iron content was 2.4 μg l^{-1}, indicating very little change on standing at *ca.* pH 2. A recovery test was carried out on this sample by adding to it sufficient Fe(III) to increase the soluble iron by 2 μg l^{-1}; the resulting recovery was 104%.

Discussion

Purity of Reagents and Effect of Other Substances

The iron concentrations in 10 ml of analytical solution resulting from the addition of 1 ml of 0.5 mol l^{-1} Tris and 0.25 ml of 0.5 mol l^{-1} mannitol were 0.1–0.3 and ≤0.1 μg l^{-1}, respectively. Although some variations in the iron concentration of a reagent blank were observed from one batch of reagents to another, in no instance was there <0.1 μg l^{-1}. This relatively high concentration does influence the limit of

detection and should it be necessary to reduce the blank in the analytical solution the simplest alternative to improving the methods of purification would be to reduce the concentration of Tris and mannitol by a factor of two or three. The reduction in Tris will be accompanied by some small loss in sensitivity owing to the lowering of the pH of the analytical solution and the reduction in mannitol could lead to a loss in precision but there could still be an over-all gain in analytical range.

The major interference with the complexing reaction of iron and catechol is from the reaction of borate; this was successfully removed by limiting the boric acid concentration in the analytical solution to *ca.* 10^{-2} mol l^{-1}, buffering the solution to pH 7.8 and adding a molar excess of mannitol. Under these conditions there was insufficient free borate ion to reduce the added catechol concentration of 8×10^{-4} mol l^{-1}. There was no significant interference from the presence of other transition metal ions expected in PWR coolant. Iron(II) ions were not expected to interfere on the basis of either their reduction potential or their complexation with catechol, but it was of interest to note that the bulk concentration of iron(II) ions behaved polarographically in a manner identical with that for the same concentration of iron(III) ions. This ability to detect total soluble iron is particularly important for PWR coolant sample where the main source of iron in solution is derived from magnetite in a hydrogenated boric acid medium such tnat Fe(II) species are predominant. In any batch sampling procedure, the Fe(II) will tend to be oxidised to Fe(III) on exposure to the atmosphere, and therefore the capability of the technique reported here to determine both species as a single entity is a positive advantage.

Calibration and Precision

The sensitivity for iron in the sample, obtained for calibration using a simulated coolant containing 100 mg l^{-1} of boron, was 7.3 nA $(\mu g\ l^{-1})^{-1}$ [equivalent to 4.1 nA per 10^{-8} mol l^{-1} of Fe(III)] for an accumulation period of 50 s in stirred solution. Van den Berg and Huang[5] reported a sensitivity of 5.6 nA per 10^{-8} mol l^{-1} in sea water for an accumulation period of 180 s. The poorer sensitivity was probably due to the high chloride concentration in the sample because when experiments were carried out in simulated sea water using Tris buffer the sensitivities we obtained were comparable to those reported.[5]

The relative standard deviations of the peak currents determined in simulated coolant of 5.5% at 1.7 $\mu g\ l^{-1}$ and 4.2% at 4.3 $\mu g\ l^{-1}$ were comparable to the range 5–7% found for nickel and cobalt by DPVS.[1] The standard deviation of a single determination of the iron concentration, based on the standard additions procedure, will obviously be greater than that obtained for a single determination of peak current as there are three current measurements (blank, sample and sample plus standard addition) to be considered.

The three measurements of peak current that are used in a determination by the standard additions procedure are i_b (peak current of the reagent blank solution), i_s (peak current of the sample solution) and i_{s+a} (the peak current of the sample plus a standard addition). Assuming that the peak currents are proportional to the concentration of the determinand in the analytical solution, then the concentration of the determinand in the latter, C_s, can be expressed as

$$C_s = \frac{C_a (i_s - i_b)}{(i_{s+a} - i_b) - (i_s - i_b)}$$

or

$$C_s = \frac{C_a (i_s - i_b)}{(i_{s+a} - i_s)} \quad \ldots \quad \ldots \quad \ldots \quad (1)$$

where C_a is the increment in concentration caused by the known standard addition. If δ_{i_b}, δ_{i_s} and $\delta_{i_{s+a}}$ are the standard deviation of i_b, i_s and i_{s+a}, respectively, then an expression for the fractional standard deviation of the determinand can be derived from equation (1) by the method of propagation of errors[9] as

$$\left(\frac{\delta_{C_s}}{C_s}\right)^2 = \frac{(\delta_{i_s}^2 + \delta_{i_b}^2)}{(i_s - i_b)^2} + \frac{(\delta_{i_{s+a}}^2 + \delta_s^2)}{(i_{s+a} - i_s)^2} \quad \ldots \quad (2)$$

where δ_{C_s} is the standard deviation of a determination of the sample concentration. Under circumstances where i_b is small relative to i_s, then

$$\left(\frac{\delta_{C_s}}{C_s}\right)^2 \simeq \frac{\delta_{i_s}^2}{i_s^2} + \frac{(\delta_{i_{s+a}}^2 + \delta_{i_s}^2)}{(i_{s+a} - i_s)^2} \quad \ldots \quad \ldots \quad (3)$$

If the increment in concentration caused by the standard addition is made about equal to that of the sample and the assumption is made that the relative standard deviations of i_s and i_{s+a} are equal then equation (3) becomes

$$\left(\frac{\delta_{C_s}}{C_s}\right)^2 \simeq \frac{\delta_{i_s}^2}{i_s^2} + \frac{5\delta_{i_s}^2}{i_s^2} \quad \ldots \quad \ldots \quad \ldots \quad (4)$$

or

$$\frac{\delta_{C_s}}{C_s} \simeq \sqrt{6}\,\frac{\delta_{i_s}}{i_s} \quad \ldots \quad \ldots \quad \ldots \quad \ldots \quad (5)$$

From equation (5) the percentage relative standard deviation of a single determination by the standard additions procedure under these conditions is

$$\frac{100\,\delta_{C_s}}{C_s} \simeq 245\,\frac{\delta_{i_s}}{i_s} \quad \ldots \quad \ldots \quad \ldots \quad (6)$$

On this basis the relative standard deviation of a single determination, from our precision results, would be of the order of 10–15%.

The statistical limit of detection at the 95% confidence level, calculated from the standard deviation of the reagent blank solution, was 0.08 $\mu g\ l^{-1}$ and, as mentioned previously, any reduction in this would largely depend on lowering the iron concentration in the blank. However, these performance statistics are satisfactory for the levels of iron experienced in rig samples and anticipated in PWR coolant samples.

The authors thank Dr. D. Midgley and Dr. C. M. G. Van den Berg for their helpful discussions on certain aspects of this work. This work was carried out at the Central Electricity Research Laboratories of the CEGB Technology Planning and Research Division and is published by permission of the Central Electricity Generating Board.

References

1. Torrance, K., and Gatford, C., *Talanta*, 1985, **32**, 273.
2. Lam, N. K., Kalvoda, R., and Kopanica, M., *Anal. Chim. Acta*, 1983, **154**, 79.
3. Van den Berg, C. M. G., and Huang, Z. Q., *Anal. Chim. Acta*, 1984, **164**, 209.
4. Van den Berg, C. M. G., *Anal. Chim. Acta*, 1984, **164**, 195.
5. Van den Berg, C. M. G., and Huang, Z. Q., *J. Electroanal. Chem.*, 1984, **177**, 269.
6. Connor, J. M., and Bulgrin, V. C., *J. Inorg. Nucl. Chem.*, 1967, **29**, 1953.
7. Perrin, D. D., and Dempsey, B., "Buffers for pH and Metal Ion Control," Chapman and Hall, London, 1974.
8. Moody, J. R., and Lindstrom, R. M., *Anal. Chem.*, 1977, **49**, 2264.
9. Parratt, L. G., "Probability and Experimental Errors in Science," Wiley, London, 1961.

Paper A5/264
Received July 18th, 1985
Accepted October 9th, 1985

Polarography-based Selective Titrations of Carboxylate and Phosphonate Ligands Used in Detergent Formulations

Domenico Perosa, Maria Luisa Zanette, Franco Magno and Gino Bontempelli
Department of Inorganic, Metallorganic and Analytical Chemistry, University of Padua, 35131 Padua, Italy

Monoamperometric titration using dropping-mercury or platinum electrodes with periodic renewal of the diffusion layer of sequestrating agents used in detergent formulations has been performed with some metal ions. The choice of the titrant cations was made on the basis of their polarographic behaviour in comparison with that exhibited by the relevant complexes. Satisfactory results were obtained and are discussed.

Keywords: *Polarography; titrimetry; carboxylate complexes; phosphonate complexes; detergents*

In recent years, the need to reduce the content of polyphosphates in detergents has increased owing to the eutrophication phenomena caused by phosphorus present in waste waters.[1] The consequent reduced use of polyphosphates implies their replacement in detergent formulations by other species that display similar properties. Carboxylate chelating agents such as ethylenediaminetetraacetic acid (EDTA) and nitrilotriacetic acid (NTA) are often employed for this purpose, as they are able to prevent trace amounts of heavy metal ions from catalysing the decomposition of perborates and, at the same time, maintain the cleaning activity (by complexing calcium and magnesium ions) of the reduced content of polyphosphates. More recently, the use of new chelating ligands containing phosphonate groups[2,3] has been proposed, as they combine a high sequestrating power with good stability towards hydrolysis even at high temperatures and extremes of pH[4] (important features for detergent components). Moreover, they exhibit very effective scale inhibition as the "threshold effect" operates for many different precipitating species (*e.g.*, $CaCO_3$ and $CaSO_4$) with a performance much greater than that expected on the basis of mere sequestration.

With the possible use of different complexing agents in detergent formulations, simple and rapid selective methods for their identification and determination are desirable. The analytical procedures reported so far are essentially based either on chromatographic procedures[5,6] or on the formation of complexes with metal ions and subsequent detection by spectrophotometric or electroanalytical measurements.[4,7-9] In this last instance, the potentiometric technique is generally employed, and polarography has surprisingly been neglected although it is characterised by selectivity, detection limits and reproducibility that are at least as good as those of potentiometry. In addition, a complete polarogram is also able to give much qualitative information about the simultaneous presence of different complexes whose reduction processes occur at different potentials depending on the stability constants.

In view of these considerations, we undertook this investigation with the purpose of devising a convenient procedure for the titration of mixtures of sequestrating agents with potential use in detergent formulations; the detection of the end-point and the choice of the optimum experimental conditions are based on the use of polarography. The potential interferences from the presence of the different constituents of detergents (mainly tripolyphosphates) were also considered.

Experimental

Chemicals and Reagents

All chemicals were of analytical-reagent grade, except the phosphonates, which were commercial products (Dequest 2010 and Dequest 2041; Monsanto). These last chemicals were repeatedly crystallised from aqueous acidic solution until a satisfactory purity was obtained as indicated by ion chromatography.[5]

The solvent employed throughout was doubly distilled water and the different buffer media were prepared by adding hydrochloric acid to solutions containing a suitable weak base until the desired pH (in all instances near the value corresponding to half-neutralisation) was monitored by a glass electrode. When necessary, sodium perchlorate was added to these buffer solutions as a supporting electrolyte.

A standard solution of copper ions, prepared by dissolving weighed amounts of pure metallic copper in nitric acid, was used (after suitable dilution) to standardise all the solutions of sequestrating agents. The solution of EDTA standardised in this way was then employed for the standardisation of $Pb(NO_3)_2$ and $FeCl_3$ solutions. In all instances the end-points were detected monoamperometrically, employing either a dropping-mercury electrode (DME) or a platinum microelectrode polarised at a suitable potential.

Apparatus and Procedure

Voltammetric and polarographic experiments were carried out in a three-electrode cell. The working electrode was either a platinum sphere, used with periodic renewal of the diffusion layer,[10] or a DME with mechanical control of the drop time (t = 3 s). The counter electrode was a mercury pool and the potential of the working electrode was probed by a Luggin capillary reference electrode compartment containing an aqueous SCE.

The voltammetric unit employed was a three-electrode system assembled with MP-System 1000 equipment in conjunction with a function generator constructed in these laboratories.[11] The working potentials were monitored with a Keithley 168 Autoranging DMM digital voltmeter and the recording device was a Linseis LY-1800 X - Y recorder.

The volumes of titrant, added from a 5-ml full-scale microburette, were measured to within 0.01 ml and the pH values were read on a Radiometer Model M84 pH meter.

Unless stated otherwise, all the electroanalytical measurements were performed at room temperature and nitrogen, previously equilibrated to the correct vapour pressure, was used for the removal of dissolved oxygen.

All titrations were performed in the concentration range $1 \times 10^{-3} - 5 \times 10^{-3}$ M and the relevant diffusion currents were suitably corrected for dilution.

Results and Discussion

Choice of Samples

To test the potential of the proposed method, two different mixtures of sequestrating agents were analysed.

In the first mixture (sample A), different proportions of EDTA, NTA and Dequest 2041 (ethylenediaminetetramethylenephosphonic acid; EDTMP) were present. This mixture was chosen on the basis of the following considerations: (i) EDTA is often used in detergent formulations to prevent the metal-catalysed decomposition of perborates and optical brightners; (ii) NTA is, at present, the most commonly used allowed replacement for polyphosphates; (iii) EDTMP is, according to Monsanto's suggestions,[4] a very effective sequestrating species suitable for replacing polyphosphates in the future.

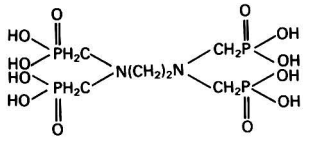

EDTMP

In the second type of mixture examined (sample B), diethylenetriaminepentaacetic acid (DTPA) and Dequest 2010 (1-hydroxyethylidene-1,1-diphosphonic acid; HEDP) were mixed in different proportions. DTPA was chosen because it gives complexes with metal ions characterised by the highest formation constants from aminocarboxylic acids[12] and, consequently, its content in detergents may be kept low. Conversely, HEDP was chosen intentionally in view of the large number of complexes (mono- and polynuclear in nature) formed with several metal ions,[13,14] which are expected to make its determination by titration difficult.

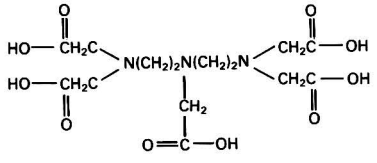

DTPA

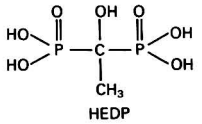

HEDP

Choice of Titrant Cations

The ligands employed can, in principle, be titrated by several cations. Consequently, a preliminary choice must be made by taking into account the following basic criteria: (i) the titrant cation should, with the chosen ligands, be able to give complexes that are much more stable than those formed with other potentially interfering species (*e.g.*, tripolyphosphates), in order to achieve a sharp end-point and a good selectivity; (ii) the cathodic reduction of the metal ion employed should occur at the lowest negative potentials possible so that a sufficiently large potential range is left available for the detection of the reduction displayed by the relevant complex, before the solvent discharge; in this way, the diffusion currents relative to these species can also be exploited for end-point detection, thus making the analysis of mixtures easier; (iii) a cation exhibiting reversible electrode behaviour is to be preferred as a high resolving power of the procedure can be achieved; (iv) cations that are soluble even at high pH should be employed to perform more selective titrations, thus taking advantage of the possibility of changing the pH over a wide range and of the masking effect of hydroxy ions.

In order to satisfy more than one of these requirements simultaneously, Pb^{2+}, Cu^{2+} and Fe^{3+}, exhibiting different features, were employed as titrants.

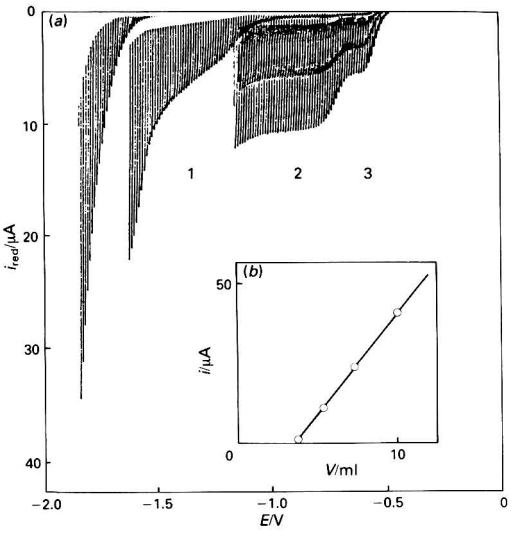

Fig. 1. (*a*) Polarographic curves recorded during the titration of sample A ([EDTA] = [NTA] = [EDTMP] = 5×10^{-3} M) in acetic acid - acetate buffer with Pb^{2+} solution. (1) Pb - EDTA reduction wave; (2) Pb - NTA diffusive reduction wave; (3) mixed wave from the Pb - NTA kinetic reduction and from free Pb^{2+} ions. (*b*) Relevant monoamperometric titration plot. Currents were measured at −0.9 V *vs.* SCE

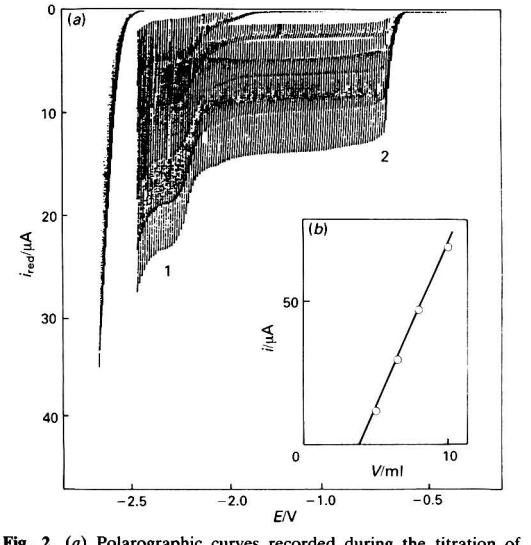

Fig. 2. (*a*) Polarographic curves recorded during the titration of sample A ([EDTA] = [NTA] = [EDTMP] = 5×10^{-3} M) in 6×10^{-2} M NaOH solution with Pb^{2+} solution. (1) Pb - EDTA reduction wave; (2) $HPbO_2^-$ - reduction wave. (*b*) Relevant monoamperometric titration plot. Currents were measured at −0.85 V *vs.* SCE

Titration of Sample A

Inspection of the constants relative to complexes formed by the ligands employed with different metal ions,[4,12,14] and their dependence on pH, suggested the use of Pb^{2+} as a titrant, also in view of its solubility as the hydrogen plumbite ion, $HPbO_2^-$, in basic media.

This cation should make possible, in principle, the titration of EDTA alone at pH values lower than 5, the determination

of the total EDTA and EDTMP content at pH values near 13 and the simultaneous titration of all the three sequestrating agents in an intermediate pH range (7–8). By carrying out titrations with lead ions on solutions of each individual sequestrating agent, and also on mixtures containing a known content of all the three ligands, it is possible to confirm these expectations only in acidic solution (pH 4.8, see Fig. 1) and in basic medium (pH 13, see Fig. 2). Conversely, the total ligand determination at intermediate pH values is precluded by the occurrence of a pre-wave (C.E. in nature[15]) relative to the Pb - NTA complex that takes place at potentials very near to those appropriate for the reduction of free lead ions. This drawback can be overcome, however, by replacing Pb^{2+} with Cu^{2+} (pH 5.2; acetic acid - acetate buffer), the complex of which with NTA is reduced without exhibiting any kinetic complication.

Therefore, the procedure we suggest for determining the individual ligands present in sample A requires the following three monoamperometric titrations: (i) the EDTA content is evaluated by titration with standard Pb^{2+} solution at pH 4.8 (0.1 M acetic acid - acetate ion buffer) employing a polarisation potential of −0.90 V *vs.* SCE for the DME; (ii) the total EDTA and EDTMP content is found at pH 13 (0.1 M NaOH) by titrating with standard Pb^{2+} solution and polarising the DME at a potential of −0.86 V *vs.* SCE; (iii) the total content of EDTA, EDTMP and NTA is determined by using Cu^{2+} as a titrant at pH 5.2 (0.1 M acetic acid - acetate buffer) with the DME polarised at −0.06 V *vs.* SCE. In this way, very satisfactory results are obtained as shown in Table 1, where the reported values are the means of five replicate measurements.

It is worth noting that copper ions cannot substitute lead ions totally in the procedure described as in basic solutions formation of the Cu - NTA complex also partially occurs, owing to the inadequate sequestrating power of ammonia, which must be used to keep Cu^{2+} ions in solution in alkaline media.

Finally, it must be remarked that the proposed procedure is suitable for direct application to the alcohol-insoluble part[16] of a real detergent. In fact, after dissolution of this part in alkaline solution and subsequent filtration to remove zeolites, the only species present in solution able, in principle, to interfere is tripolyphosphate. However, tabulated stability constants[12] and literature reports[8] indicate that this species does not cause overtitration under the experimental conditions adopted (titrant cations and pH values), and we verified this. Further, no problem arises from the very large excess of NTA with respect to EDTA found in real detergents as the two sequestrating agents present at lower concentrations (EDTA and EDTMP) are specifically titrated at suitable pH values.

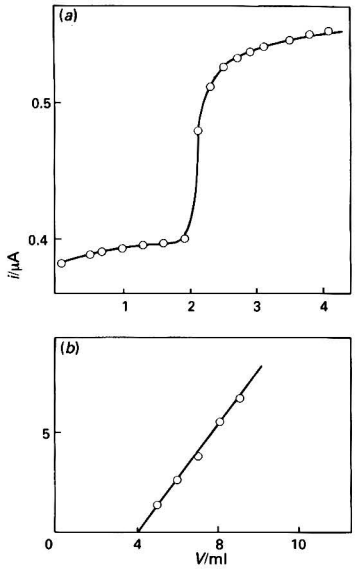

Fig. 3. (*a*) Potentiometric and (*b*) monoamperometric titration plots for a solution of DTPA (2×10^{-3} M) in glycine buffer. Titrant: Fe^{3+} ions

Titration of Sample B

Also in this instance the choice of the titrant cation was made by first considering the formation constants of DTPA and HEDP complexes with different metal ions[12,14] and their dependence on pH. Consequently, the use of the Fe^{3+} ion was studied in view of the high stability of the relevant complexes.

Titrations of solutions containing DTPA alone in acidic medium (pH 2.8, glycine buffer) were satisfactory in that good monoamperometric or potentiometric end-point detection was easily achieved by employing a platinum indicator electrode (see Fig. 3). In contrast, titrations of HEDP gave incorrect results owing to the formation (at any acidic pH value) of different mono- and polynuclear complexes (partially insoluble), the relative concentrations of which appear to depend on the ligand content. Such behaviour is exhibited by HEDP with most metal ions[13,14] and represents the main drawback to devising a suitable procedure for its determination. This is the reason why it is recommended that the complexometric titration of this sequestrating agent is performed with thorium ion[17] (one of the few cations able to give only one complex with HEDP), even though this titrant cannot by employed in all analytical laboratories, its use being restricted by legal provisions.

The use of Pb^{2+} as a titrant at pH 6.7 (triethanolamine buffer) allows this problem to be solved by taking advantage of the very low solubility of the Pb_2(HEDP) complex with respect to the other possible complexes, which leads to its preferential formation during the titration. On the other hand, this titrant when used at pH 6.7 is also suitable for the

Table 1. Typical results obtained in the titration of sample A

	pH 4.8		pH 5.2		pH 13.0	
Sequestrating agent	Pb^{2+} calculated/μmol	Pb^{2+} found*/μmol	Cu^{2+} calculated/μmol	Cu^{2+} found*/μmol	Pb^{2+} calculated/μmol	Pb^{2+} found*/μmol
EDTA	48.8	49.2 ± 0.2	24.5	—	24.5	—
EDTMP	120.0	—	22.6	—	22.6	—
NTA	124.7	—	25.5	—	124.7	—
EDTA + EDTMP + NTA	293.5	—	72.6	72.6 ± 0.1	171.7	—
EDTA + EDTMP	168.8	—	47.1	—	47.1	47.3 ± 0.2

* Mean values of five replicate results.

Table 2. Typical results obtained in the titration of sample B

Sequestrating agent	pH 5.1		pH 6.7	
	Cu^{2+} calculated/μmol	Cu^{2+} found*/μmol	Pb^{2+} calculated/μmol	Pb^{2+} found*/μmol
DTPA	32.0	31.9 ± 0.1	128.0	—
HEDP	135.5	—	54.1	—
DTPA + HEDP	167.5	—	182.1	181.7 ± 0.2

* Mean values of five replicate results.

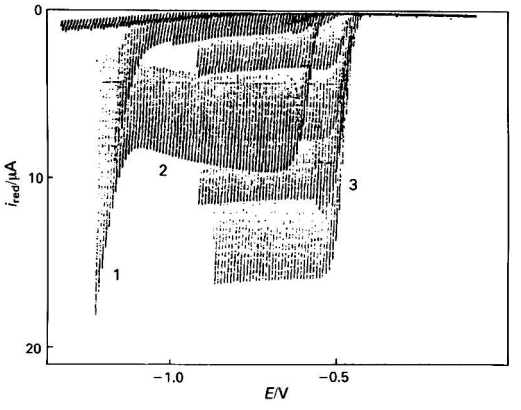

Fig. 4. Polarographic curves recorded during the titration of sample B (DTPA = 5×10^{-3} M; HEDP = 10^{-3} M) in triethanolamine buffer with Pb^{2+} solution. (1) Rising portion of the Pb - DTPA reduction wave; (2) Pb_2(HEDP) reduction wave decreasing with time; (3) reduction wave for free Pb^{2+} ions

quantitative determination of DTPA, so that the total DTPA and HEDP content can be easily evaluated under these experimental conditions, as illustrated in Fig. 4. Before the equivalence point, this monoamperometric titration is not rapid owing to the slow precipitation of the phosphonate complex, which requires that the current measurements be made a few minutes after each titrant addition, thus allowing equilibrium conditions to be reached. It should be noted, however, that the more significant points of this titration are those beyond the equivalence point, which are not affected by this drawback.

The separate contents of the two ligands might be determinable by coupling the mentioned determination with a second monoamperometric titration carried out under the same experimental conditions, but at a working potential corresponding to the Pb - DTPA reduction (beyond −1.2 V; see Fig. 4). However, the slow rate of formation of the Pb_2(HEDP) precipitate again makes it necessary for a slow titration to be carried out (after the equivalence point in this instance). Therefore, it is preferable to determine the DTPA content by employing copper ions as the titrant, owing to the very large difference between the formation constants relative to the two sequestrating agents ($K_{CuDTPA} = 10^{22.5}$ and $K_{Cu_2(HEDP)} = 10^{12.5}$) and to the low stability of the phosphonate complex in acidic solution. At pH 5 (0.1 M acetic acid - acetate buffer), the end-point for the titration of DTPA alone is in fact located correctly by polarising the working electrode corresponding to the nearly contemporaneous reduction of free copper ions and of the poorly formed phosphonate complex.

Consequently, the content of the two sequestrating agents in sample B can be determined by coupling this copper-based determination of DTPA with the over-all titration of DTPA and HEDP performed with Pb^{2+} at pH 6.7 as mentioned above.

Table 2 gives the results obtained with this procedure (means of five replicate measurements).

Again, for the correct application of this procedure to real detergents, the presence of tripolyphosphate must be taken into account. In this instance, the selected pH value (6.7) does not allow their interference to be avoided. This problem can be eliminated, however, by resorting to the well established procedure that employes tin(II) chloride to separate polyphosphate ions by precipitation.[16] On the other hand, Sn^{2+} ions do not give sufficiently stable complexes with DTPA and HEDP, so that they are unable to interfere in the subsequent titration of these sequestrating agents.

Conclusion

The results obtained in this paper clearly indicate that analytical procedures based on polarography are suitable for the qualitative and quantitative determination of sequestrating agents employed in detergent formulations. Of course, better performances are expected from modern and more sophisticated electroanalytical techniques, particularly with regard to detection limits, and in order to verify this, and to evaluate the matrix effect, further work is in progress.

Moreover, it must be remarked that two promising fields of application for this type of electroanalytical detection appear to be flow injection analysis and liquid chromatography. In particular, in the latter instance the information gained can be profitably exploited for enhancing the resolving power of ion chromatography by using voltammetric-type electrochemical detectors, thus maintaining the column separation capability with the selectivity appropriate for voltammetric analysis.

Finally, it is worth comparing the non-equilibrium electroanalytical procedures proposed by us with the equilibrium method (potentiometry) widely used in this field. Potentiometric titrations are indeed easier to carry out even by untrained operators and, moreover, they require simpler apparatus. Notwithstanding this, non-equilibrium methods offer the following significant advantages: (i) they can also be used with non-reversible electrochemical processes; (ii) their response is faster because they do not require equilibrium conditions to be attained; (iii) the linear dependence of the current on the analyte concentration makes possible titrations at lower concentrations; (iv) the relatively more sophisticated apparatus used in monoamperometric titrations enables voltammetric tests to be carried out that provide qualitative information unattainable by potentiometric measurements.

The supply of phosphonate ligands by Carini, Milan, is gratefully appreciated and financial aid from the Italian National Research Council (CNR) and the Ministry of Public Education is acknowledged.

References

1. Chiaudani, G., Gerletti, M., Marchetti, R., Provini, A., and Vighi, M., "Il Problema dell'Eutrofizzazione in Italia," Quaderni dell'Instituto di Ricerca sulle Acque, No. 42, CNR, Rome, 1978.
2. Kabachnik, M. J., Medved, I. Y., Dyatlova, I. M., and Rudomino, M. V., *Russ. Chem. Rev.*, 1974, **43**, 733.
3. Maier, L., *in* "Proceedings of the 1st International Congress on Phosphorus Compounds, Rabat," Inst. Mond. Phosphates, Paris, 1977, p. 195.
4. "Multifunctional Metal Ion Control Agents in Aqueous Solutions," Technical Bulletin No. 53–39(E)ME-1, Monsanto, Brussels, 1983.
5. "Determination of Sequestrating Agents," Application Note No. 44, Dionex, Sunnyvale, CA, 1983.
6. Rudling, L., *Water Res.*, 1971, **5**, 831.
7. King, T. M., and Mitchell, R. S., Special Report No. 7666, Monsanto, St. Louis, MO, 1970.
8. Calapaj, R., Ciraolo, L., Corigliano, F., and Di Pasquale, S., *Analyst*, 1982, **107**, 403, and references cited therein.
9. "Trilon," Technical Bulletin No. IT/P 2840, BASF, Ludwigshafen/Rhein, 1983.
10. Schiavon, G., Mazzocchin, G. A., and Bombi, G. G., *J. Electroanal. Chem.*, 1971, **29**, 401.
11. Magno, F., Bontempelli, G., Mazzocchin, G. A., and Patanè, I., *Chem. Instrum.*, 1975, **6**, 239.
12. Martell, A. E., and Smith, R. M., "Critical Stability Constants," Volume 1, Plenum Press, London, 1974, p. 281.
13. "Dequest 2010-Acide Phosphonique," Technical Bulletin No. 53–34MEI(F), Monsanto, Brussels, 1980.
14. Sillen, L. G., and Martell, A. E., "Stability Constants of Metal Ion Complexes," Supplement 1, Chemical Society, London, 1971, p. 273.
15. Heyrovsky, J., and Kuta, J., "Principles of Polarography," Academic Press, New York, 1966, p. 367.
16. Clinckemaille, G. G., *Anal. Chim. Acta*, 1968, **43**, 520.
17. King, T. M., and Maiec, E. J., Special Report No. 7158, Monsanto, St. Louis, MO, 1968.

Paper A5/86
Received March 7th, 1985
Accepted October 8th, 1985

Sequential Micro-scale Determination of Chlorine (or Bromine) and Sulphur in Organic Compounds

Agostino Pietrogrande and Mirella Zancato
Department of Pharmaceutical Sciences, University of Padua, 35131 Padua, Italy

A comparison is made between the mercurimetric and the potentiometric determination of chlorides. As this comparison indicates the potentiometric titration with silver nitrate has higher accuracy and precision, this procedure has been combined with the bariometric method in order to achieve the sequential determination of halogens and sulphur in the same sample. The results obtained for several samples containing sulphur and chlorine (or bromine) confirm the effectiveness of the proposed method.

Keywords: *Sequential micro-scale determination; organo-chlorine; organo-bromine; organo-sulphur*

Simple and fast methods for the sequential micro-scale determination of halogens and sulphur in the same sample appear to be of practical utility as the presence of these elements in the same molecule is fairly frequently encountered in organic compounds. These methods are expected to offer the advantages not only of a saving of time, but also of requiring the use of small amounts of sample.

In previous studies on this subject, the combustion of the sample (either in a Schöniger flask,[1-4] or in an oxygen stream[5]) was always followed by separate determinations of these elements. The bariometric titration is adopted for sulphur and halogens are determined as halides following different procedures, among which the mercurimetric method is the most widely used. In particular, a simple gravimetric determination was suggested by Hadzija and Kozarac.[6] Some potentiometric titration procedures of considerable interest have also been proposed.[7-10]

This paper describes a convenient method for the sequential determination of halogens and sulphur, based on a combination of potentiometric titration with silver nitrate for halogens and bariometric titration for sulphur, carried out successively directly in the combustion flask. The potentiometric titration of halogens is preferred to the mercurimetric method as higher accuracy and precision are obtained with the former approach.

Experimental

Equipment

The combustion flask[11] (300 ml) was modified in order to avoid the need for transfer of solutions and to make possible the easy titration of small volumes. The titrations were carried out with a Metrohm 636 Titroprocessor connected to a Model 635 automatic burette and a Metrohm EA 246 combined massive electrode.

Procedure

Determination of chlorine by the mercurimetric method

The flask is charged with 5 ml of of 0.2 M sodium hydroxide solution and 0.5 ml of 3% hydrazinium sulphate solution, then 5–7 mg of sample are weighed in and the combustion is performed in the Schöniger flask in the usual way. After 30 min the flask is opened and 50 ml of propan-2-ol are added, carefully washing the stopper, the platinum basket and the inner side of the flask. After the addition of five drops of bromophenol blue (0.5% ethanolic solution), the solution is acidified with $HClO_4$ until a pale green colour persists, then 15 drops of diphenylcarbazone (0.5% ethanolic solution) are added and the titration of halides to a pale violet colour is performed with 0.005 N $Hg(ClO_4)_2$ with magnetic stirring.

Determination of chlorine by the potentiometric method

For the potentiometric titration after combustion, the stopper, the basket and the inner side of the flask are washed with a mixture of 13 ml of propan-2-ol and 12 ml of distilled water. Three drops of methyl red (0.1% ethanolic solution), 0.1 M HNO_3 to a red colour, 3 ml of acetic acid (minimum 96%) and three drops of concentrated nitric acid are added. The electrode and the outlet tube of the burette are inserted to 1 cm above the bottom of the flask and magnetic stirring is started. The "control card operation" (programmed for the "dynamic titration kinetic T at value 3") is inserted and automatic titration with 0.01 M silver nitrate solution is performed. Titration volumes and curves and potential break are printed out. The blank value must be subtracted from the titration volume.

Sequential determination of chlorine (or bromine) and sulphur

The absorption solution consists of 5 ml of distilled water and 1 ml of hydrogen peroxide (30%) and a sample containing not less than 0.7 mg of chlorine (or 1.5 mg of bromine) is weighed in. After the combustion, the stopper, the basket and the inner side of the flask are washed with 16 ml of propan-2-ol, then two drops of Thorin (0.2 % solution) and two drops of methylene blue (0.0125% solution) are added and the titration of sulphates is carried out to a pink colour with 0.01 M barium perchlorate with magnetic stirring. At the end of the titration, 5 ml of 0.2 M NaOH solution and 0.60 ml of hydrazinium sulphate (3% solution) are added. After waiting for 2 min, 5 ml of distilled water and three drops of methyl red (0.1% ethanolic solution) are added and the potentiometric titration of chlorides (or bromides) is performed by following the procedure described above. The blank value must be subtracted from the titration volume. In the titration of bromides, correct values are obtained by subtracting the blank volumes from the second end-point. In this instance it is advisable to "activate" the electrode at the beginning of the analytical series by means of two preliminary titrations on solutions containing about 5 mg of potassium chloride or bromide. The salt must be dissolved in 30–35 ml of water - propan-2-ol (2 + 1), to which all the mentioned reagents are added.

Results and Discussion

A preliminary comparison between the potentiometric and mercurimetric titration procedures was carried out by employ-

ing ten organic compounds characterised by different chlorine contents. The relevant results are reported in Table 1, which indicates a lower accuracy and a higher over-all relative standard deviation, *i.e.*, a lower precision, for the mercurimetric titration method ($s = 0.15\%$) compared with that found for the potentiometric method ($s = 0.08\%$).

The results obtained for organic compounds containing both chlorine (or bromine) and sulphur are reported in Table 2. The solution employed for the absorption of the combustion products in the sequential determination of halogens and sulphur deserves some consideration. Some workers employ an alkaline solution of hydrogen peroxide,[1,3,4] while the use of neutral H_2O_2 has been suggested in other reports.[2,5,12] The aim of this reagent is to reduce free halogens and their related hypohalogenites (formed in the combustion and in the absorption process) to halide ions and, at the same time, to oxidise to sulphate the sulphur dioxide generated in the first of the mentioned processes.

With reference to the standard potentials given in Table 3, it should be noted that an alkaline medium allows the oxidising power of hydrogen peroxide with respect to sulphur dioxide to be maintained, the potential of the H_2O_2 - H_2O and SO_4^{2-} - SO_3^{2-} systems exhibiting the same dependence on pH. Similar arguments can also be employed for the reduction of hypohalogenites. Conversely, such an alkaline medium favours the reduction of halogens to halides owing to the decrease in the potential of the O_2 - H_2O_2 redox couple.

Notwithstanding this, a quantitative reduction to halides is expected to occur also in the weakly acidic medium that originates during the combustion process, owing to the large reducing strength of hydrogen peroxide with respect to halogens and hypohalogenites. Consequently, the alkaline medium appears not to be essential.

In spite of these considerations, and Burns and Maitin[8] have recently suggested the replacement of hydrogen peroxide with hydrazine hydrate, which exhibits a stronger reducing power (see Table 3). The use of this reagent, however, makes the oxidation of sulphur dioxide difficult and consequently Mazzeo-Farina and Mazzeo[3] suggested the elimination of the excess of hydrazine by an extended boiling procedure in the presence of hydrogen peroxide, which is slow and very tedious.

In this investigation, we adopted the bariometric titration recommended by Fritz and Yamamura,[13] which is reported to be strongly affected by the presence in solution of different ions, such as silver or alkali metal ions. Consequently, to allow the correct detection to the end-pont in the bariometric titration, the sulphate determinations were performed before the halide titration and an alkaline absorption solution was not employed.

In conclusion, the recommended procedure involves the absorption of the combustion products (obtained in the Schöniger flask) by a neutral solution of hydrogen peroxide to which propan-2-ol is added at the end of the combustion process and the resulting solution is titrated directly for sulphates. At the end of this titration, hydrazinium sulphate is added to reduce possible residual traces of halogen or hypohalogenite and the solution is then titrated potentiometrically with 0.01 M silver nitrate solution after acidification with nitric acid. Results for halogens and sulphur within ±0.30% error are obtained, which confirm the effectiveness of the method.

Of course, the measured volumes in the potentiometric titrations must be corrected for the chlorine contained in the filter-paper utilised in the combustion (*ca.* 35 μg). The amount of this correction (blank volume) can be easily determined by carrying out a combustion without the sample. No problems with this correction arise when the halogen to be determined is chlorine. Conversely, in the determination of bromine, the presence of chloride ions originating from the filter-paper implies that two distinct end-points are detected. In this instance the difference between these two end-points is greater than that expected on the basis of the amount of chloride ions determined in the independent filter-paper

Table 1. Determination of chlorine

	Chlorine,%				
	Mercurimetry			Potentiometry	
Compound	Theoretical	Found($\bar{x}$)	s,%*	Found ($\bar{x}$)	s,%*
Alprazolam, $C_7H_{13}ClN_4$	11.49	11.70	0.14	11.41	0.07
2-Amino-2′,5-dichlorobenzophenone, $C_{13}H_9Cl_2NO$	26.67	26.46	0.19	26.56	0.08
Benzylisothiourea hydrochloride, $C_8H_{10}N_2S.HCl$	17.49	17.60	0.14	17.64	0.21
Chlordiazepoxide hydrochloride, $C_{16}H_{14}ClN_3O.HCl$	21.11	20.98	0.19	21.00	0.15
p-Chlorobenzoic acid, $C_7H_5ClO_2$	22.65	22.64	0.17	22.68	0.02
1-Chloro-2,4-dinitrobenzene, $C_6H_3ClN_2O_4$	17.50	17.57	0.19	17.44	0.03
Diazepam, $C_{16}H_{13}ClN_2O$	12.46	12.50	0.20	12.36	0.02
Furosemide, $C_{12}H_{11}ClN_2O_5S$	10.73	10.99	0.05	10.79	0.07
Levamisole, hydrochloride, $C_{11}H_{12}N_2S.HCl$	14.74	15.00	0.15	14.71	0.03
Temazepam, $C_{16}H_{13}ClN_2O_2$	11.80	12.00	0.04	11.85	0.10

*s = relative standard deviation (five replicate determinations). Over-all relative standard deviation for mercurimetry, 0.15%; over-all relative standard deviation for potentiometry, 0.08%.

Table 2. Sequential determination of chlorine (bromine) and sulphur

	Halogen,%			Sulphur,%		
Compound	Theoretical	Found ($\bar{x}$)	s,%*	Theoretical	Found ($\bar{x}$)	s,%*
Benzylisothiourea hydrochloride, $C_8H_{10}N_2S.HCl$	17.49	17.65	(0.15)	15.82	15.78	(0.14)
Furosemide, $C_{12}H_{11}ClN_2O_5S$	10.74	10.76	(0.09)	9.68	9.61	(0.14)
Levamisole hydrochloride, $C_{11}H_{12}N_2S.HCl$	14.74	14.84	(0.21)	13.33	13.25	(0.20)
Tetramisole hydrochloride, $C_{11}H_{12}N_2.HCl$	14.74	14.80	(0.13)	13.33	13.18	(0.11)
Zambon 32/C 395, (halogen chlorine)	13.24	13.35	(0.09)	11.97	11.82	(0.14)
Bromocresol purple, $C_{12}H_{16}Br_2O_5S$	29.61	29.51	(0.19)	5.94	5.89	(0.11)
Bromothymol blue, $C_{27}H_{28}Br_2O_5S$	25.60	25.50	(0.18)	5.13	5.07	(0.10)

*s = relative standard deviation (five replicate determinations). Over-all relative standard deviation for halogens, 0.15%; over-all relative standard deviation for sulphur, 0.13%.

Table 3. Standard potentials

Redox couple	E^{0}/V
H_2O_2 - H_2O	+1.77
O_2 - H_2O_2	+0.69
SO_4^{2-} - SO_3^{2-}	+0.15
Cl_2 - $2Cl^-$	+1.39
ClO^- - Cl^-	+1.50
Br_2 - $2Br^-$	+1.05
BrO^- - Br^-	+1.19
NH_2NH_2 - N_2	−0.20

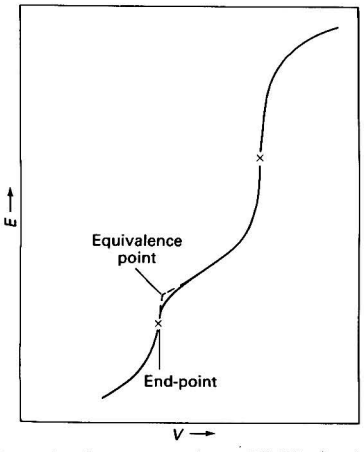

Fig. 1. Comparison between experimental (full line) and theoretical (broken line) generalised potentiometric curves relative to the sequential argentimetric titration of bromide and chloride ions

correction and, at the same time, a negative error of the same order of magnitude is found for bromides if the titration volume relative to the first end-point is used. This result can be explained by considering that the sharp corner expected at the first equivalence point on the basis of theoretical considerations (see Fig. 1) is not found experimentally. In fact, it has a rounded form owing to the coprecipitation of AgBr and AgCl, which occurs near to this point,[14] the bromide concentration being suitably lowered. This roundness, occurring just where the maximum slope should be exhibited by the titration curve, therefore causes the first end-point to be detected with a negative error by the automatic device.

However, as the second end-point always reflects the correct total content of Br^- and Cl^-, the correct value for bromine can be easily found by subtracting "blank volume" from that corresponding to second end-point.

In a previous paper[11] dealing with the sequential potentiometric titration of bromides and chlorides in the same medium as in this work, we reported that the mentioned coprecipitation effect was not appreciable. In that instance, however, comparable concentrations of the two halides were employed, thus making negligible the relative error in the titration data caused by this phenomenon.

Conclusions

The potentiometric procedure allows the chloride determination to be improved with respect to the mercurimetric methods. This result offers the possibility of combining such a potentiometric determination with the bariometric titration of sulphates for the effective sequential micro-scale determination of organo-chlorine (or organo-bromine) and organo-sulphur with satisfactory accuracy and precision.

References

1. Boetius, M., Gutbier, G., and Reith, H., *Mikrochim. Acta*, 1958, 321.
2. Giesselmann, G., and Hagedorn, I., *Mikrochim. Acta*, 1960, 390.
3. Mazzeo-Farina, A., and Mazzeo, P., *Microchem. J.*, 1978, **23**, 137.
4. White, D. C., *Mikrochim. Acta*, 1962, 807.
5. Pella, E., *Mikrochim. Acta*, 1961, 472.
6. Hadzija, O., and Kozarac, Z., *Fresenius Z. Anal. Chem.*, 1975, **277**, 191.
7. Campiglio, A., and Traverso, G., *Mikrochim. Acta*, 1980, **I**, 485.
8. Thorburn Burns, D., and Maitin, B. K., *Analyst*, 1983, **108**, 452.
9. Selig, W., *Microchem. J.*, 1976, **21**, 291.
10. Krijgsman, W., Griepink, B., Mansverld, J. F., and van Oort, W. J., *Mikrochim. Acta*, 1970, 793.
11. Pietrogrande, A., Zancato, M., and Bontempelli, G., *Analyst*, 1985, **110**, 993.
12. Dirscherl, A., and Erne, F., *Mikrochim. Acta*, 1963, 242.
13. Fritz, J. S., and Yamamura, S. S., *Anal. Chem.*, 1955, **27**, 1461.
14. Kolthoff, I. M., Sandell, E. B., Meehan, E. J., and Bruckenstein, S., "Quantitative Chemical Analysis," Macmillan, London, 1969.

Paper A5/151
Received April 25th, 1985
Accepted September 2nd, 1985

SHORT PAPERS

Determination of Trace Amounts of Copper, Lead, Thallium, Cadmium and Zinc in Pure Aluminium by Differential-pulse Anodic-stripping Voltammetry

M. M. Palrecha, A. V. Kulkarni and R. G. Dhaneshwar
Analytical Chemistry Division, Bhabha Atomic Research Centre, Modular Laboratories, Trombay, Bombay 400 085, India

A method for the determination of trace amounts of copper, lead, thallium, cadmium and zinc in pure aluminium metal by differential-pulse anodic-stripping voltammetry, employing a citrate buffer of pH 4.4 as the supporting electrolyte, is described. For the determination of copper, lead + thallium and cadmium, the pre-electrolysis was carried out at −0.80 V *vs.* an Ag - AgCl reference electrode. The overlapping of the lead and thallium anodic peaks was overcome by shifting the reduction potential of lead(II) beyond −1.10 V by chelation with EDTA, while thallium(I) remained uncomplexed and was determined by carrying out deposition at −0.80 V. Copper and bismuth interference, if bismuth is present, can also be eliminated in the presence of EDTA, deposition of copper being carried out at −0.30 V. For the determination of zinc, the pre-electrolysis was carried out at −1.10 V. The effect of intermetallic compound formation between copper and zinc was investigated and the influence of probable impurities in pure aluminium was also studied.

Keywords: *Copper, lead, thallium, cadmium and zinc determination; aluminium analysis; differential-pulse anodic-stripping voltammetry*

There are diverse industrial and technological applications of pure aluminium metal, and the presence of trace impurities alters the the properties of pure aluminium considerably and adversely affects its utility

A number of electrochemical methods have been reported for the determination of various impurities in aluminium. Yoshimura[1,2] analysed high-purity aluminium for trace amounts of copper, lead and zinc using square-wave polarography, however, the dissolution process is tedious and involved. An oscillopolarographic method for the determination of copper, lead, cadmium and zinc was described by Beran *et al.*,[3] but their method does not take account of thallium if present. Neiman and Ponomarenko[4] determined cadmium, indium, lead and copper in high-purity aluminium by inverse voltammetry with a graphite working electrode.

Among different electroanalytical techniques, differential-pulse anodic-stripping voltammetry (DPASV) is the most sensitive and is eminently suitable for analyses at trace and ultra-trace levels. Although the use of a thin mercury film electrode (MFE) in conjunction with DPASV reduces the detection and determination levels of these metals to the p.p.b. and sub-p.p.b. range, it introduces interference effects owing to the formation of intermetallic compounds, particularly between copper and zinc as they are normally present in most matrices.[5]

This paper describes a method for the determination of trace amounts of copper, lead, thallium, cadmium and zinc in high-purity aluminium, taking into consideration two objectives: (i) the development of a procedure for decomposing a relatively large sample (about 2 g) that is simple and does not cause contamination or loss of the sample during its dissolution and (ii) the choice of a suitable supporting electrolyte that prevents the hydrolysis of aluminium(III) in solution and helps to separate interfering metal ions, namely lead(II) and thallium(I).

Experimental

Apparatus

A Model 174A Polarographic Analyser (Princeton Applied Research, USA) was used for the DPASV work. The electrode assembly consisted of a hanging mercury drop electrode (HMDE) (Metrohm, Switzerland), a platinum wire auxiliary electrode and an Ag - AgCl reference electrode. The cell assembly used was described earlier.[6] All the experiments were carried out at 25 °C.

Chemicals

Aristar-grade hydrochloric acid (BDH Chemicals, UK) was used to dissolve aluminium metal. A standard aluminium solution was prepared by dissolving 99.9% pure aluminium metal (Johnson and Matthey, UK). Other chemicals were guaranteed reagents from E. Merck (FRG).

Procedure

About 2.0 g of high-purity aluminium filings were dissolved slowly in 50 ml of 6 M hydrochloric acid in a 200-ml Pyrex beaker. A few drops of 30% hydrogen peroxide and about 0.2 g of ammonium iron(III) sulphate were added slowly to catalyse the dissolution. The mixture was initially boiled gently and then vigorously. After allowing the mixture to cool, a few drops of hydrogen peroxide were added and the mixture was boiled again. This procedure was repeated 2–3 times till the entire mass of aluminium metal had completely dissolved. The solution was then concentrated to a syrupy mass, with frequent stirring to avoid crust formation and bumping. After almost complete removal of hydrochloric acid, 50 ml of distilled water were added to the beaker and stirred to give a clear solution. The solution was then boiled for 5 min, cooled, transferred into a 100-ml calibrated flask and diluted to the mark with distilled water.

The solution thus obtained was further purified by electrolysing it for about 6 h at a mercury pool cathode at a constant potential of −1.20 V *vs.* a saturated calomel electrode and a platinum wire auxiliary electrode. This solution served as the standard aluminium(III) solution to which known amounts of metal solutions under investigation were added.

Forensic samples of aluminium wire were dissolved in the same way.

The pH of the electrolysis solution for DPASV work was maintained at 4.5 ± 0.1. In order that aluminium (III) was not hydrolysed during the pH adjustment, the following pro-

cedure was adopted: a 2-ml aliquot of the standard aluminium solution was taken in a beaker and the pH was adjusted to 2 by adding dropwise 0.01 M sodium hydroxide solution. Then 2.5 ml of 1 M sodium citrate solution were added, the pH was adjusted to 4.5 ± 0.1 and the solution diluted to 10 ml.

Stripping Procedure

After transferring the solution into the electrolysis cell and deaerating it with pure nitrogen (IOLAR grade, Indian Oxygen Ltd., India), pre-electrolysis was carried out for 1 min at −0.80 V *vs.* Ag - AgCl while the solution was being stirred. After the solution had been allowed to rest for 30 s, an anodic scan at 5 mV s^{-1} was applied, keeping the modulation amplitude at 50 mV. The anodic peaks for cadmium, lead + thallium and copper were obtained at −0.54, −0.34 and −0.08 V, respectively. A zinc anodic peak resulted at −0.88 V when the pre-electrolysis potential was kept at −1.10 V (Fig. 1B). A corresponding reagent blank stripping current was also recorded (Fig. 1A) by applying a deposition potential of −0.80 V for cadmium, lead + thallium and copper and −1.10 V for zinc determination. These elements were determined by the method of standard additions to pure aluminium solutions (Fig. 1C).

Results and Discussion

As lead(II) and thallium(I) ions have the same cathodic and anodic peak potentials in most non-complexing and weakly complexing media, they mutually interfere in each other's determination. Dhaneshwar and Zarapkar[6] used EDTA, which preferentially complexes lead(II) and not thallium(I),

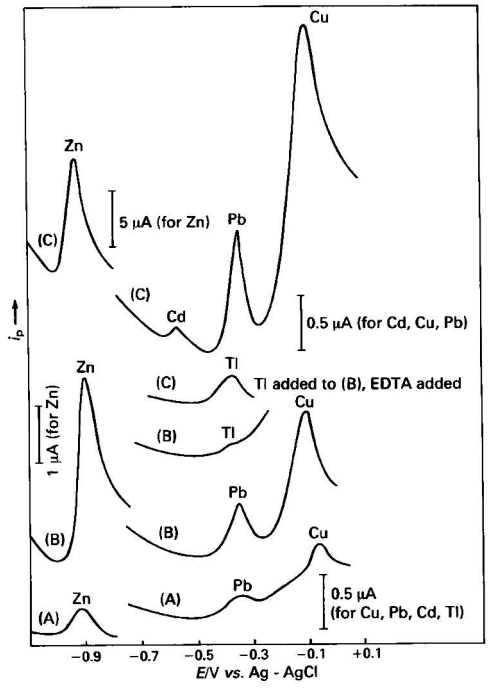

Fig. 1. Differential-pulse anodic-stripping voltammetric polarograms obtained with HMDE (pH 4.4). E_{el} = −1.1 V for Zn and −0.8 V for Cd, Cu, Pb and Tl; electrolysis time = 1 min; rest period = 30 s: voltage scan = 5 mV s^{-1}; pulse height = 50 mV. (A) Blank, 2.5 ml of sodium citrate solution (1 M) + HCl; (B) sample; and (C) standard additions: Cu, 0.574 μg; Pb, 0.5 μg; Cd, 0.045 μg; Tl, 0.5 μg; and Zn, 1.0 μg in 10 ml of sample solution. Polarogram for Tl recorded in EDTA

to determine these metals by ASV in water and silicon. Bonelli *et al.*[7] also complexed cadmium(II) and lead(II) with EDTA to eliminate their interference in the analysis of natural waters for thallium(I).

After recording anodic-stripping peaks for copper, lead + thallium, cadmium and zinc in the citrate buffer (pH 4.4), about 0.5 g of the disodium salt of EDTA was added to the electrolysis cell solution and stirred to give a clear solution. Most of the EDTA was consumed by aluminium(III) to form an Al(III) - EDTA soluble complex. As the metal ions under investigation were present in trace amounts, the excess of EDTA was sufficient to complex them. Owing to strong complexation, the reduction potentials of lead(II) and cadmium(II) shifted to potentials more negative than −1.20 V, while that of thallium(I) remained unchanged as it is not complexed. Hence the pre-electrolysis at −0.80 V and subsequent anodic stripping yielded an anodic peak that corresponded to thallium(I) alone.

Synthetic samples were prepared by adding a number of metal ions to standard aluminium solution. Table 1 lists results for the determination of copper, lead, thallium, cadmium and zinc in synthetic samples to which, in addition to the metal ions under investigation, nickel (0.2), Cr (0.1), iron (1.0) arsenic (0.02), tin (0.1) and antimony (0.02 μg ml^{-1} in the electrolysis solution) were added. None of these elements was found to interfere. However, bismuth(III), if present in a 1 : 1 ratio or more relative to copper, interferes with the copper determination, as the difference in their reduction potentials is only *ca.* 0.1 V. Normally, in high-purity aluminium, bismuth is present in extremely small amounts compared with copper; however, if as much bismuth as copper is present, the addition of EDTA again is helpful in overcoming the interference of bismuth on copper. In the presence of EDTA, copper and bismuth yield separate anodic peaks at −0.07 and +0.03 V, respectively, but the resolution of the peaks is not sufficient to make their determination quantitative. The cathodic peaks of copper(II) and bismuth(III) in the citrate buffer (pH 4.4) containing EDTA occur at −0.20 and −0.55 V, respectively. The pre-electrolysis potential, if kept at −0.30 V, will deposit copper alone, giving rise to a subsequent copper dissolution peak without any interference from bismuth.[8]

There are several reports dealing with the well known copper - zinc intermetallic formation and means of overcoming this interference effect in ASV applications.[5,9,10] Although the copper - zinc intermetallic formation is predominantly noted when using a mercury film electrode (MFE), Copeland *et al.*[5] observed it with even an HMDE, as they observed a slight diminution in zinc stripping current. This diminution was not sufficient to confirm the occurrence of copper - zinc intermetallic formation. During the analysis of

Table 1. Recoveries of Cu, Pb, Tl, Cd and Zn added to synthetic aluminium solution. Al concentration, 4 mg ml^{-1}

Sample No.	Metal	Concentration taken/ μg ml^{-1}	Concentration found/ μg ml^{-1}	Deviation, %
1	Zn	0.1	0.1	—
	Cd	0.045	0.04	11
	Pb	0.05	0.06	20
	Tl	0.051	0.05	2
	Cu	0.029	0.029	—
2	Zn	0.2	0.23	15
	Cd	0.09	0.091	1.1
	Pb	0.102	0.102	—
	Cu	0.057	0.059	3.5
3	Zn	0.4	0.41	2.5
	Cd	0.18	0.18	—
	Pb	0.20	0.19	5
	Tl	0.204	0.21	5
	Cu	0.115	0.108	6

fly ash samples for copper, lead, cadmium and zinc, it was found that the zinc stripping current was affected by a change in the matrix of the sample rather than by intermetallic formation at an HMDE.[11] The presence of Al(III) was found to diminish the zinc peak up to an Al(III) concentration about 70 times the Zn(II) concentration in the solution; a further increase in Al(III) concentration did not affect the zinc current.[11]

In this work, there was no change in the zinc stripping current although copper stripping currents were found to be 25–30% higher when deposition was carried out at −1.10 V (where both zinc and copper were deposited) than when deposited at −0.80 V. This could be attributed to the higher overpotential deposition in relation to copper in the former than in the latter experiment.

By adopting a procedure of depositing cadmium, lead, thallium and copper at −0.80 V and zinc at −1.10 V, reliable results for these elements can be obtained. This also eliminates the possible interference due to irreversible oxidation of cobalt and nickel in the copper determination.

This method was used satisfactorily to analyse various high-purity aluminium metal samples. A typical analysis of aluminium wire for source identification in forensic science is copper 21.0, lead 9, zinc 12 and thallium and cadmium less than 1 p.p.m. The copper concentration obtained by neutron-activation analysis was found to be 19.5 p.p.m.

Conclusion

Copper, lead, thallium, cadmium and zinc in pure aluminium were determined by differential-pulse anodic-stripping voltammetry in citrate buffer of pH 4.4. The dissolution of high-purity aluminium was catalysed by the addition of ammonium iron(III) sulphate, which otherwise was tedious and elaborate. The elements other than zinc were deposited at −0.80 V and zinc was deposited at −1.10 V. The mutual interference of lead and thallium was overcome by carrying out pre-electrolysis at −0.80 V in the presence and absence of EDTA and for copper and bismuth the pre-electrolysis potential was required to be shifted to −0.30 V so that copper alone was deposited.

The authors thank Dr. M. Sankar Das, Head, Analytical Chemistry Division, BARC, for his keen interest and encouragement and Dr. N. Chattopadhyay of CFSL (NAA Unit, Calcutta), BARC, for the neutron-activation analysis determination of copper.

References

1. Yoshimura, W., *Bunseki Kagaku*, 1972, **21**, 4; *Chem. Abstr.*, 1972, **77**, 69753.
2. Yoshimura, W., *Bunseki Kagaku*, 1981, **30**, 347; *Chem. Abstr.*, 1981, **95**, 54158n.
3. Beran, P., Dolezal, J., and Mrazek, D., *J. Electroanal. Chem.*, 1963, **6**, 381.
4. Neiman, E. Ya., and Ponomarenko, G. B., *Zh. Anal. Khim.*, 1973, **28**, 1485; *Chem. Abstr.*, 1974, **80**, 22298g.
5. Copeland, T. R., Osteryoung, R. A., and Skogerboe, R. K., *Anal. Chem.*, 1974, **46**, 2093, and references cited therein.
6. Dhaneshwar, R. G., and Zarapkar, L. R., *Analyst*, 1980, **105**, 386.
7. Bonelli, J. E., Taylor, H. E., and Skogerboe, R. K., *Anal. Chim. Acta*, 1980, **118**, 240.
8. Dhaneshwar, R. G., Kulkarni, A. V., and Zarapkar, L. R., to be published.
9. Neiman, E. Ya., Petrova, L. G., Ignatov, V. I., and Dolgopolova, G. M., *Anal. Chim. Acta*, 1980, **113**, 277.
10. Lazar, B., Nishri, A., and Ben-Yaakov, S., *J. Electroanal. Chem.*, 1981, **125**, 295.
11. Dhaneshwar, R. G., Kulkarni, A. V., and Zarapkar, L. R., paper presented at the Convention of Chemists, Jadhavpur University, October 1984.

Paper A5/57
Received February 13th, 1985
Accepted October 17th, 1985

Determination of Phenolphthalein in Pharmaceutical Preparations Using *N*-Bromosuccinimide

Laila El Sayed, Loris I. Bebawy and Mohmad M. Amer
Analytical Chemistry Department, Faculty of Pharmacy, Cairo University, Kaser El Aini, Cairo, Egypt

Phenolphthalein was determined by direct titration in 0.04 M sodium hydroxide solution with *N*-bromosuccinimide. Micro-elemental analysis and infrared spectroscopy of the reaction product indicated that it was tetrabromophenolphthalein. The method was compared with the US National Formulary method. Amounts of 0.318–11.13 mg of phenolphthalein were determined by this method, the recovery being 100.13 ± 0.72%. The compound was determined in several pharmaceutical formulations. Other laxatives found in combination with it, such as aloin and podophyllin, do not interfere.

Keywords: *Phenolphthalein determination; titrimetry; bromination; laxative determination; N-bromosuccinimide*

Phenolphthalein is used as a laxative (cathartic) in many pharmaceutical formulations and has been determined gravimetrically,[1] iodimetrically,[2,3] polarographically[4,5] and spectrophotometrically.[6,7] The method proposed in this paper is carried out by direct titration of phenolphthalein in 0.04 M sodium hydroxide solution using *N*-bromosuccinimide. The method was used for the determination of phenolphthalein in pharmaceutical preparations.

Experimental

Materials

Authentic samples of phenolphthalein were obtained from BDH Chemicals and its purity was determined by the BP method.[7] *N*-Bromosuccinimide was obtained from E. Merck and its purity was determined iodimetrically.[8]

Pharmaceutical preparations were obtained from the companies indicated in Table 2.

Procedures

Prepare a 0.001 M solution of phenolphthalein by dissolving 31.8 mg in 100 ml of 0.04 M sodium hydroxide solution. Prepare a 0.004 M solution of *N*-bromosuccinimide in distilled water and standardise it iodimetrically. For the determination of phenolphthalein in tablets, grind 20 tablets, mix well, weigh an amount equivalent to one tablet and extract it with 0.04 M sodium hydroxide solution in a 100-ml calibrated flask, using three 15-ml volumes of extractant, then dilute to volume with distilled water. For pills containing phenolphthalein, remove the outer coating, then proceed as described above. For emulsions and chocolate laxatives extracted according to the method of Allen and Johnson[9] dissolve the residue obtained from each extraction in 100 ml of 0.04 M sodium hydroxide solution.

Determine phenolphthalein in authentic samples and pharmaceutical preparations by taking a volume equivalent to 0.318–11.13 mg (1–3.5 μmol) of phenolphthalein and titrate with 0.004 M *N*-bromosuccinimide solution. The end-point is shown by a change in colour from pink to bluish green. Each 1 ml of 0.004 M *N*-bromosuccinimide solution is equivalent to 0.318 mg of phenolphthalein. A microburette may be needed for the titration.

Results

Tables 1 and 2 show the recoveries of authentic phenolphthalein samples and pharmaceutical preparations. The advantages of the method are that it is rapid, accurate and needs only simple equipment. It is also applicable to pharmaceutical preparations and other cathartics found, such as aloin and podophyllin, do not interfere.

Discussion

N-Bromosuccinimide has been widely used as a reagent for the quantitative bromination of phenols,[8] and the mechanism of bromination has been found to be electrophillic substitution reactions that take place in all the available *ortho* and *para* positions.[8] Barakat *et al.*[10] described procedures for the micro-determination of salicylic acid, phenol, vanillin and thymol by direct titration with *N*-bromosuccinimide. However, nothing has been cited in the literature on its use for the determination of phenolphthalein, which possesses two phenolic moieties. In phenolphthalein there are four *ortho* positions available for bromination.

It was found that phenolphthalein reacts with *N*-bromosuccinimide in a molar ratio of 1:4, four bromine atoms being consumed during the titration, as demonstrated by micro-

Table 1. Determination of phenolphthalein by the National Formulary Method and the *N*-bromosuccinimide method

National formulary method[3]			*N*-Bromosuccinimide method		
Taken/ mg	Found/ mg	recovery, %	Taken/ mg	Found/ mg	Recovery, %
10		101.50	0.320	0.317	99.06
15		99.30	0.640	0.639	99.81
25		99.10	0.960	0.953	99.27
50		100.90	1.280	1.274	99.53
100		101.00	1.600	1.580	98.75
150		98.90	3.200	3.180	99.38
—		—	4.800	4.840	100.83
—		—	6.400	6.410	100.16
—		—	8.000	8.140	101.75
—		—	9.600	9.700	101.04
—		—	11.200	11.400	101.79
Mean		100.12			100.13
Standard deviation . .		1.14			1.07
Fiducial limit		±1.19			±0.72

Table 2. Determination of phenolphthalein in some commercial preparations using the direct titrimetric method with *N*-bromosuccinimide

Sample analysis			Control experiment		
	Amount per tablet/mg				
Preparation	Labelled	Found	Standard added/mg	Found/ mg	Recovery, %
Normalin tablet*	50	48.07	50	49.37	98.75
		48.59		50.16	100.30
		48.27		49.84	99.69
			30	29.78	99.20
				30.30	101.00
				29.60	98.60
				Mean ($P = 0.5$):	99.59 ± 0.98
Boldolaxine†	75	78.00	50	50.16	100.30
		79.50		50.78	101.50
		79.50		50.35	100.70
			30	30.30	101.02
				30.40	101.30
				30.56	101.80
				Mean ($P = 0.05$):	101.10 ± 0.61
Alphalaxine tablet†	35	37.22	50	48.59	97.18
		37.83		50.16	100.32
		38.50		48.98	97.96
			30	30.30	101.00
				29.78	99.27
				30.10	100.33
				Mean ($P = 0.05$):	99.34 ± 1.58
Brooklax	130	129.58	50	50.68	101.36
		129.32		50.55	101.10
		129.79		50.16	100.32
			30	29.78	99.27
				30.30	101.00
				30.39	100.30
				Mean ($P = 0.05$):	100.56 ± 0.71
Paragar emulsion†	20 per mg per 15 ml	194.73	32	31.70	99.06
		197.66		32.32	101.00
		197.86		32.32	101.00
				Mean ($P = 0.05$):	100.35 ± 1.17

* Misr Company.
† Kahira Company.

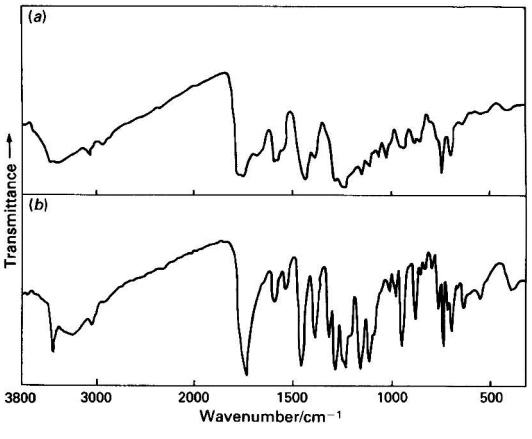

Fig. 1. Infrared spectra of (*a*) phenolphthalein and (*b*) the brominated product

elemental analysis of the product of the reaction. The infrared spectrum of the product (Fig. 1) was characterised by a bromine peak at 740 cm^{-1}. The reaction was carried out in sodium hydroxide medium and the solubility of phenolphthalein increased with increase in alkalinity. The optimum concentration of the sodium hydroxide solution used was 0.04 M, where no fading of colour was observed during the titration. At lower sodium hydroxide concentrations the solubility of the compound was poor. From a statistical comparison of the mean results obtained using the proposed method and the US National Formulary method,[3] with a 95% confidence limit for the difference, it is clear that it lies within the limits that are in agreement with the test of significance

Table 3. Statistical comparison of the results obtained by the proposed direct titrimetric method with that of the National Formulary[3]

	Method of assay	
	National Formulary method	Proposed method
Mean recovery, % ($P = 0.05$)	100.03 ± 1.23	100.13 ± 0.72
No. of determinations	6	11
Variance	1.37	1.14
t	—	0.1786 (2.131)*
F	—	1.202 (3.6)*

* Figures in parentheses indicate theoretical values of *t* and *F* at $P = 0.05$.

(Table 3). Therefore, one can conclude with 95% confidence that there is no significant difference between the accuracy of the two methods.

Other laxatives found in combination with phenolphthalein in pharmaceutical preparations, such as aloin and podophyllin, do not interfere as being anthraquinone glycosides. Emulsions and coloured preparations gave good results (Table 2) using the extraction method of Allen and Johnson.[9] Trials to detect the end-point by potentiometry using two platinum electrodes were carried out, but no sharp inflection in the titration curve was observed.

References

1. Bickford, C. F., and Schoetzow, R. E., *J. Am. Pharm. Assoc.*, 1936, **25**, 1128.
2. Warren, A. T., Logun, J. E., and Thatcher, R., *J. Am. Pharm. Assoc.*, 1950, **39**, 10.
3. "The National Formulary," Fourteenth Edition, American Pharmaceutical Association, 1975, p. 563.
4. Kolthoff, I. M., and Lechmicke, D. I., *J. Am. Chem. Soc.*, 1948, **70**, 1879.
5. Suzuki, M., *J. Electrochem. Soc. Jpn.*, 1954, **22**, 220; *Chem. Abstr.*, 1954, **48**, 134736.
6. Gustafson, J. H., and Benet, L. Z., *J. Pharm. Pharmacol.*, 1974, **26**, 937.
7. "British Pharmacopoeia 1980," HM Stationery Office, London, 1980, p. 342.
8. Mathur, N. K., and Narang, C. K., "The Determination of Organic Compounds with *N*-Bromosuccinimide and Allied Reagents," Academic Press, London, 1975, pp. 54–59.
9. Allen, J., and Johnson, C. A., *J. Pharm. Pharmacol.*, 1962, **14**, 73T.
10. Barakat, M. Z., Fayzalla, A. S., and El-Aassar, S. T., *Analyst*, 1972, **97**, 470.

Paper A5/88
Received March 11th, 1985
Accepted September 16th, 1985

BOOK REVIEWS

Modern Methods for the Determination of Non-Metals in Non-Ferrous Metals

C. Engelmann, G. Kraft, J. Pauwels and C. Vandecasteele. Pp. xiv + 410. Walter de Gruyter. 1985. Price DM190; $76. ISBN 3 11 010342 7; 0 89925 010 6

During the past 10 years, a collaborative exercise sponsored by the Commission of the European Communities has been conducted with the co-operation of a few highly qualified University and industrial laboratories throughout Western Europe. The scope of this exercise has been directed towards the determination of non-metallic impurities in non-ferrous metals with the specific objective of improving the accuracy and precision of analysis. This volume summarises the collective efforts of the contributing laboratories in applying chemical and physico-chemical methods of analysis to the determination of carbon, sulphur, phosphorus, boron, oxygen and nitrogen in a wide range of non-ferrous alloys based on aluminium, copper, lead, nickel, molybdenum, niobium, tantalum, titanium, tungsten and zirconium.

Chapter I outlines the influence of non-metals on various physical properties of non-ferrous alloys including conductivity, hardness, tensile strength, ductility and embrittlement and considers the manner in which these factors can affect production/fabrication. This information will appeal to the practising analyst seeking technical data beyond his/her forté.

Chapter II considers nuclear methods of analysis with specific reference to neutron activation, charged particle activation and photon activation analysis. The theoretical bases for these techniques are discussed in depth and factors that affect accuracy, precision and sensitivity are evaluated.

Chapter III deals extensively with sample preparation—a vital precursor to any method of analysis for trace element determination in alloys based on metals with a high affinity for oxygen and nitrogen—detailing optimum conditions to minimise contamination. Considerable attention is paid to machine tool parameters, compositions and coolants with specific recommendations for the preparation of millings/chippings or solid pieces.

Chapters IV and V consider methods used for the determination of boron and carbon, respectively. Six spectrophotometric methods in addition to flame emission and plasma excitation are described for boron in various matrix applications.

Combustion in air/oxygen provides the most satisfactory means of releasing carbon from non-ferrous matrices, with detector systems utilising coulometry, conductivity, manometry and titrimetry. Choice of flux material is discussed extensively together with the potential contribution to "blank" values derived from crucibles, boats, tubes, combustion gas, etc.

Chapters VI (nitrogen) and VII (oxygen) constitute the bulk of the text. Methods for the determination of both these elements are based predominantly on inert gas or vacuum fusion principles. For nitrogen, chemical methods incorporating Kjeldahl distillation followed by titrimetric or spectrophotometric determination are also included.

Chapters VIII and IX discuss phosphorus and sulphur, respectively, in a brief but succinct manner.

In general, nuclear techniques feature extensively throughout the entire text and tables of collaborative results abound. All individual methods of analysis described contain meticulous working details.

The book is produced in an attractive cover and includes a detailed list of contents supported by an adequate subject index; 661 references are cited in a text that is both easy to read and absorb and is refreshingly free from typographical and publication errors.

M. S. Taylor

Mass Spectrometry in Environmental Sciences

Edited by F. W. Karasek, O. Hutzinger and S. Safe. Pp. xx + 578. Plenum Press. 1985. Price $75. ISBN 0 306 41552 6.

This book consists of a series of reviews by "experts in the subject matter" covering the field of environmental applications of mass spectrometry in some depth. It is laid out starting with a series of seven chapters on the general principles of mass spectrometric techniques such as gas chromatography - mass spectrometry (GC - MS), soft ionisation methods (positive and negative ion chemical ionisation, field desorption), and data retrieval and interpretation. The next two chapters cover the general application of mainly GC - MS in water and air pollution studies followed by the bulk of the book, 16 chapters in 360 pages, containing detailed reviews on the analysis of particular classes of environmental pollutants.

Unlike too many books on mass spectrometric applications, the early chapters do not set out to give a detailed description of a mass spectrometer and how it works, but are rather a series of illustrations of the state of the art around 1980 or so and its use in environmental analysis. This does not detract from the book, as exhaustive monographs of the theory of mass spectrometry are available elsewhere. The unusual chapter on data retrieval is almost wholly concerned with the computer interpretation of spectra using library matching and data enhancement. The techniques described are based on the HP5992 GC - MS - computer system but do provide a description of the various library searching methods used by most manufacturers.

The chapter on water pollution studies by Pellizzari and Bursey is largely devoted to the development of the EPA's general method for the detection and determination of organics in water. The next chapter, on air pollution, gives a much fuller coverage of the methods used to date. In neither chapter does there appear to be a reference to the EPA's priority pollutants guidelines, which is a puzzling omission in a work such as this.

The various in-depth reviews covering particular classes of compounds in general appear to give a comprehensive picture up to 1980. A few later references are given in some chapters but most fall into the period 1975–80. The individual reviews are variable in content and coverage. Thus, Sweetman and

Karasek's chapter on polycyclic aromatic hydrocarbons deals almost exclusively with the mass spectral properties whilst the chapters on polychlorinated biphenyls and dibenzodioxins and dibenzofurans cover not only the mass spectral properties but also the metabolism and breakdown products plus the problems of analysis of interfering compounds in GC - MS. This is illustrated in the chapter on dioxins, which gives a table listing nine possible interfering compounds whose spectra contain ions with the same nominal mass as the molecular ions for TCDD.

The chapters on volatile halocarbons, DDT, organophosphorus compounds, pyrethroids and insect pheromones are also more extensive in their coverage than just a description of mass spectral properties, detailing in addition such aspects as quantitative methods, derivatisation prior to GC - MS and (pheromones) chemical manipulation to determine the positions of any unsaturated bonds.

An Appendix lists a number of chemicals with an indication of the ionisation method used and the page on which it appears.

It is always difficult in a review such as this to publish quickly, and to some extent the work described is dated. Recent introductions such as fast atom bombardment ionisation, target compound analyses using on-line computers and metastable peak monitoring are not discussed. Nevertheless, this book gives a useful and thorough coverage of the field up to 1980 and is sure to find a place on the bookshelves of laboratories carrying out environmental analyses.

N. J. Haskins

FIRST FOLD HERE

THE ANALYST READER ENQUIRY SERVICE
For further information about any of the products featured in the advertisements in this issue, write the appropriate number on the postcard, detach and post.

FOLD HERE

THE ANALYST READER ENQUIRY SERVICE

MAR'86

For further information about any of the products featured in the advertisements in this issue, please write the appropriate number in one of the boxes below.
Postage paid if posted in the British Isles but overseas readers must affix a stamp.

PLEASE USE BLOCK CAPITALS LEAVING A SPACE BETWEEN WORDS *Valid 12 months*

1 NAME

2 COMPANY

PLEASE GIVE YOUR BUSINESS ADDRESS IF POSSIBLE. IF NOT, PLEASE TICK HERE ☐

3 STREET

4 TOWN

5 COUNTY
POST CODE

6 COUNTRY

7 DEPARTMENT/
DIVISION

8 YOUR JOB TITLE/
POSITION

9 TELEPHONE NO

OFFICE USE ONLY REC'D PROC'D

FOLD HERE

Postage will be paid by Licensee

Do not affix Postage Stamps if posted in Gt. Britain, Channel Islands, N. Ireland or the Isle of Man

BUSINESS REPLY SERVICE
Licence No. WD 106

Reader Enquiry Service
The Analyst
The Royal Society of Chemistry
Burlington House, Piccadilly
LONDON
W1E 6WF
England

A201 for further information. See page iv.

ANALAO 111(3) 265–384 (1986) March 1986

The Analyst

The Analytical Journal of The Royal Society of Chemistry

CONTENTS

Typeset and printed by Heffers Printers Ltd, Cambridge, England